Local operator quench induced by two-dimensional inhomogeneous and homogeneous CFT Hamiltonians

Weibo Mao [*1], Masahiro Nozaki[†1,2], Kotaro Tamaoka[‡3] and Mao Tian Tan[§4]

[1]*Kavli Institute for Theoretical Sciences, University of Chinese Academy of Sciences, Beijing 100190, China*
[2]*RIKEN Interdisciplinary Theoretical and Mathematical Sciences (iTHEMS), Wako, Saitama 351-0198, Japan*
[3]*Department of Physics, College of Humanities and Sciences, Nihon University, Sakura-josui, Tokyo 156-8550, Japan*
[4]*Asia Pacific Center for Theoretical Physics, Pohang, Gyeongbuk, 37673, Korea*

Abstract

We explore non-equilibrium processes in two-dimensional conformal field theories (2d CFTs) due to the growth of operators induced by inhomogeneous and homogeneous Hamiltonians by investigating the time dependence of the partition function, energy density, and entanglement entropy. The non-equilibrium processes considered in this paper are constructed out of the Lorentzian and Euclidean time evolution governed by different Hamiltonians. We explore the effect of the time ordering on entanglement dynamics so that we find that in a free boson CFT and RCFTs, this time ordering does not affect the entanglement entropy, while in the holographic CFTs, it does. Our main finding is that in the holographic CFTs, the non-unitary time evolution induced by the inhomogeneous Hamiltonian can retain the initial state information longer than in the unitary time evolution.

---

[*]maoweibo21@mails.ucas.ac.cn

[†]mnozaki@ucas.ac.cn

[‡]tamaoka.kotaro@nihon-u.ac.jp

[§]maotian.tan@apctp.org

Contents

1   Introduction and summary

In recent years, it has come to light that holographic conformal field theories (CFTs), which can be described by semiclassical gravity, possess chaotic properties. To elucidate the mechanism behind holography, a vast literature examining their chaotic properties has been accumulated[1, 2, 3, 4, 5, 6, 7, 8, 9, 10, 11, 12, 13, 14, 15, 16, 17, 18, 19]. One of the main chaotic phenomena observed in holographic CFTs, in which the "size" of local operators grow during time evolution, is known as operator growth. In fact, under time evolution by these maximally chaotic Hamiltonians, the size of these local operators can grow exponentially in time [20, 21, 22].

Some pioneering works on operator growth explored the time dependence of entanglement entropy after a vacuum state has been excited by a local operator before undergoing regular time evolution [23, 24, 25, 26, 27]. In these papers, we similarly start from the vacuum state with the insertion of a single local operator and evolve the system with two-dimensional CFT Hamiltonians. Unlike previous works, we will use spatially inhomogeneous Hamiltonians to either time evolve the system or to regulate the state.

In non-holographic theories such as RCFTs or the free boson CFT, the time dependence of the entanglement entropy of a subsystem A, which we denote S_A, is well-described by the propagation of excitations called quasiparticles. When the subsystem A is half of an infinite system, the entanglement entropy S_A increases by a constant determined by the local operator inserted, at a time that is determined by the motion of these quasiparticles. On the other hand, in 2d holographic CFTs, the entanglement entropy S_A grows logarithmically at late times and so the dependence of S_A on the local operator is hidden by this logarithmic growth. This suggests that the scrambling effect of 2d holographic Hamiltonians hides the information of the local operator inserted[5]. These studies have been generalized in different ways. In [29, 30], the initial states were respectively chosen to be the thermofield double state and the thermal state instead of the vacuum state. In [31, 32], the authors considered the time evolution with two local operators inserted instead of one. Some other studies of local operator quenches can be found in [33, 34, 35]. In this paper, we will explore this scrambling process by using spatially inhomogeneous Hamiltonians instead of the usual uniform Hamiltonian.

The inhomogenous Hamiltonians considered in this paper were originally introduced as inhomogeneous deformations of spin systems with the intention of reducing the systems' dependence on boundary conditions [36, 37, 38, 39]. We consider a family of Möbius Hamiltonians that are parametrized by a parameter θ that controls the spatial inhomogeneity. Setting $\theta = 0$ gives the usual uniform Hamiltonian. On the other hand, sending $\theta \to \infty$ gives the SSD Hamiltonian which is the most inhomogeneous Hamiltonian we consider. These inhomogeneous deformations were subsequently introduced in 2d CFTs [40, 41] which is tantamount to placing these CFTs on curved spacetimes [42]. Currently, these inhomogeneous deformations are used to analytically explore the properties of quantum systems following global quenches and periodic Floquet driving [43, 44, 45, 46, 47, 48, 49, 50, 51, 52, 53, 54, 55, 56, 57, 58]. In addition, the non-equilibrium processes induced by these inhomogeneous quenches can be used to cool systems to the ground state [59, 60, 61, 62, 63, 64] which produces non-local correlations in conformal field theories [65, 66]. This production of non-local correlations was further explored in spin chains in [67]. The generalization of Floquet driving in CFTs with dimensions greater than 2 have been studied in [68]. The relationship between local quenches and Möbius quenches were explored in [69], while the entanglement entropy for quantum quenches in generic inhomogeneous CFTs with open boundary conditions was derived in [70].

In this paper, we consider a Lorentzian time evolution induced by a Hamiltonian H_1, followed by a subsequent Euclidean time evolution induced by a Hamiltonian H_2, and vice versa, in order to explore the effect of the ordering of time evolutions with different signatures on the non-equilibrium process. We also studied the growth of operators induced by homogeneous and inhomogeneous Hamiltonians in both Euclidean and Lorentzian signature

---

[5]In this paper, we will treat the heavy operators as local operator quench in holographic CFTs. If we consider Rényi entropy and treat the light local operator, we can keep some information even at the leading order. See [28], for example.

by investigating the time dependence of entanglement entropy and the energy density. The time-evolved states considered in this paper are

$$\left|\Phi_a(\tilde{t})\right\rangle = \mathcal{N}_a e^{-iH_1\tilde{t}} e^{-\epsilon H_2} \mathcal{O}\left|0\right\rangle,$$
$$\left|\Phi_b(\tilde{t})\right\rangle = \mathcal{N}_b e^{-\epsilon H_2} e^{-iH_1\tilde{t}} \mathcal{O}\left|0\right\rangle,$$

(1.1)

where ϵ denotes the time duration of the Euclidean evolution, $\tilde{t}$ denotes the time duration of the Lorentzian evolution, $\mathcal{N}_{a,b}$ guarantees that the norms of the states are unity, and the Hamiltonians H_i considered in this paper are the undeformed, sine-square deformed, and Möbius Hamiltonians in two-dimensional conformal field theories (2d CFTs) on the circle with circumference L. We assume that the ground state for the undeformed Hamiltonian is equal to that of the deformed Hamiltonian and we denote this ground state by $\left|0\right\rangle$, so $\left|0\right\rangle$ is the ground state of both H_1 and H_2. When H_1 is not equal to H_2, the state $\left|\Phi_a(\tilde{t})\right\rangle$ is different from the state $\left|\Phi_b(\tilde{t})\right\rangle$.

The role of the Euclidean time evolution is to reduce the effect of the local operators on the non-equilibrium processes. To see this, note that the Euclidean time evolution operator can be expanded in terms of the eigenstates of H_2 as $e^{-\epsilon H_2} = \sum_{a=1}^{M} e^{-\epsilon E_a}\left|a\right\rangle\left\langle a\right|$, where E_a and $\left|a\right\rangle$ denote the eigenvalues and eigenstates of H_2 respectively. Here, a labels the eigenstates while E_M is the maximum eigenvalue. Since exponential function e^{-x} is negligible for $x \gg 1$, we approximate the Euclidean time evolution by

$$e^{-\epsilon H_2} = \sum_{a=1}^{M} e^{-\epsilon E_a}\left|a\right\rangle\left\langle a\right| \approx \sum_{a=1}^{\tilde{M}} e^{-\epsilon E_a}\left|a\right\rangle\left\langle a\right|,$$

(1.2)

where $\tilde{M}$ labels the largest eigenvalue such that $\epsilon E_{\tilde{M}} = \mathcal{O}(1)$. Thus, the Euclidean time evolution approximately removes contributions from the high-energy modes with $E_h > E_{\tilde{M}}$. In other words, the Euclidean time evolution effectively reduces the dimension of the Hilbert space of states contributing to the non-equilibrium process. For the states in (1.1), the terms in the expansion in the energy eigenbasis of H_2 with $\left\langle E_h\right|\mathcal{O}\left|0\right\rangle$ in $\left|\Phi_a(\tilde{t})\right\rangle$ and $\left\langle E_h\right| e^{-iH_1\tilde{t}}\mathcal{O}\left|0\right\rangle$ in $\left|\Phi_b(\tilde{t})\right\rangle$ are negligible. Therefore, the local operator is smeared within a region of size $\mathcal{O}(\epsilon)$ as in Fig. 1 and the Euclidean time evolution has reduced the locality of the system.

Once the Lorentzian time evolution is included, the order in which the Lorentzian and Euclidean time evolutions are performed potentially lead to different physics. In $\left|\Phi_a(\tilde{t})\right\rangle$, the local operator state first evolves under Euclidean time evolution before a subsequent Lorentzian time evolution with leads to operator growth. On the other hand, in $\left|\Phi_b(\tilde{t})\right\rangle$, the order of time evolution is swapped; the operator grows during the initial Lorentzian time evolution before it undergoes a subsequent Euclidean time evolution. In the former case, the initial Euclidean time evolution approximately removes the contribution of high-energy modes where the fine-grained information of the local operator might be encoded before the smeared local operator grows under the final Lorentzian time evolution (see the left panel of Fig. 2). Contrast this with the latter case where the local operator grows during the

4
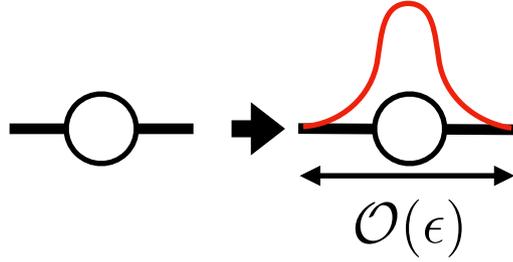
Figure 1: A sketch depicting the smearing of a local operator. After acting $e^{-\epsilon H_2}$ on a state with an insertion of a local operator, the local operator is smeared within a region of size $\mathcal{O}(\epsilon)$. The circle and red curve illustrate the local and smeared local operators respectively.

Lorentzian time evolution before the Euclidean time evolution operator removes the high-energy modes. In this case, during the initial Lorentzian time evolution, the information of the local operator which is encoded in the high-energy modes may spread to the low-energy modes. Consequently, even after the final Euclidean time evolution, the fine-grained information of the local operator might still remain (see the right panel of Fig. 2).

Summary

Let us summarize the main results of this paper below.

Time dependence of the partition function

Since the time dependence of the partition function is determined by that of the two point function for the vacuum state, it is independent of the details of the CFTs. For the Möbius Hamiltonians, the partition functions in the cases considered in this paper are finite. For SSD Hamiltonian, when the excitations created by the local operator hit a spatial point where the Hamiltonian density vanishes, the partition function becomes infinite. This suggests that at the spatial position where the Hamiltonian density vanishes, the corresponding Euclidean time evolution operator does not reduce the Hilbert space to a subspace that only contains the low energy modes.
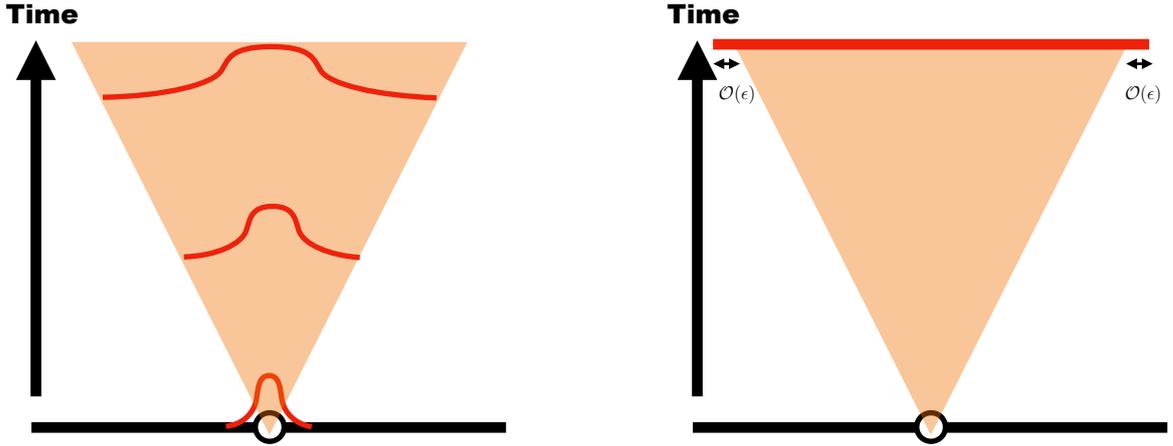
<div align="center">[a] Unitary process   [b] Non-unitary process</div>

Figure 2: Unitary and non-unitary processes. In [a], we smear the local operator, then evolve the system in real time. In [b], we evolve the system in real time before smearing the local operator. The orange region illustrates the space-time region where the local operator is delocalized by the dynamics. In the case of $|\Phi_a\rangle$, the effect of smearing is delocalized during the real time evolution. In the case of $|\Phi_b\rangle$, the effect of smearing is spatially localized.

Time dependence of energy density

We also explored the time dependence of the energy density which is a CFT-independent quantity as well. During both unitary and non-unitary Lorentzian time evolutions, the time dependence of the energy density follows the propagation of excitations with velocities determined by the Hamiltonians. An exception occurs for the non-unitary Lorentzian time evolution. For example, during non-unitary process induced by the SSD time evolution, the energy density at the origin grows quartically in time.

Time dependence of entanglement entropy in two-dimensional conformal field theories

Unlike the partition function and the energy density, the entanglement entropy of a single interval in 2d CFTs depends on the theory under consideration.

Two-dimensional free bosons and rational CFTs: During the inhomogeneous time evolutions in 2d free bosons and rational CFTs (RCFTs), the time ordering of Lorentzian and Euclidean time evolution does not affect the growth of entanglement entropy when it is well-behaved. The time evolution of the entanglement entropy follows the propagation of quasiparticles created by the insertion of the local operators. In the time interval where entanglement entropy deviates from the vacuum entanglement entropy, its value is determined by the local operator that is inserted. For a particular Hermitian sum of vertex operators

<div align="center">6</div>

in the free boson CFT, this value is $\log 2$. For general RCFTs, this value is given by the logarithm of the quantum dimension of the local operator.

Two-dimensional holographic CFTs: In contrast to the 2d free boson CFT and RCFTs, the ordering of the Lorentzian and Euclidean time evolution does affect the growth of entanglement entropy. For Möbius time evolution, the time dependence of entanglement entropy exhibits quantum revivals. In other words, the value of entanglement entropy oscillates periodically in time. During the Lorentzian time evolution induced by the Möbius Hamiltonian, the period of quantum revivals is $L \cosh 2\theta$, while during the time evolution induced by the uniform Hamiltonian, the period is L. Here, L is the system size and θ is the parameter determining the inhomogeneity of the Möbius Hamiltonian. When the entanglement entropy becomes larger than the vacuum entanglement entropy, the deviation between these two quantities depends on the ordering of the Lorentzian and Euclidean time evolution (see Section 5.1 for the details of the analysis.).

Finally, we summarize our findings on the SSD limit, where $\theta \to \infty$. During the real time evolution induced by the uniform Hamiltonian, the time evolution of the entanglement entropy is similar to the Möbius case. There are a few main differences between the Möbius Hamiltonians and the SSD Hamiltonian. Firstly, during unitary time evolution with the uniform Hamiltonian, if the operator is inserted at the origin where the SSD Hamiltonian density is zero, the entanglement entropy becomes infinite in the SSD case. Secondly, during the non-unitary time evolution with the uniform Hamiltonian, the entanglement entropy becomes infinite when the excitations created by the local operator hit the origin. Together with the divergences observed in the partition function, this suggests that the SSD euclidean time evolution does not reduce the dimension of the local Hilbert space at the origin. During real time evolution induced by the SSD Hamiltonian, the entanglement entropy remains constant if the local operator is inserted at the origin where the SSD Hamiltonian density vanishes but changes in time if the local operator is inserted somewhere else. Yet another difference with inhomogeneous Hamiltonian with $\theta \neq \infty$ is the absence of quantum revivals in the entanglement entropy. The time dependence of entanglement entropy is well described by the propagation of quasiparticles created by the local operator (see Section 4.2.), although this quasiparticle picture can not determine the value of the entanglement entropy. If one of the boundaries of the subsystem is at the origin where the SSD Hamiltonian density is zero, the information of the local operator survives longer under the non-unitary real time evolution than during the unitary real time evolution.

Organization of this paper

In Section 2, we present the details of the systems considered in this paper, define entanglement entropy, and present the time evolution of local operators in the Heisenberg picture. In Section 3, the time evolution of the CFT-independent quantities, namely the partition function and the energy density, are presented. In Section 4, we report the time dependence of entanglement entropy in 2d free boson CFT and general RCFTs, and then propose an effec-

7

tive picture describing the time dependence of entanglement entropy in such non-holographic theories. In Section 5, the time dependence of entanglement entropy in 2d holographic CFTs is presented. We conclude the paper in Section 6 where we discuss our findings in this paper.

2 Preliminary

In this section, we will explain the details of the inhomogeneous Hamiltonians and systems considered, how to compute the entanglement entropy in the path-integral formalism, and discuss the real time trajectory, induced by the inhomogeneous Hamiltonians, of the local operator.

2.1 Inhomogeneous Hamiltonians

Here, we will explain the Hamiltonians considered in this paper. The CFT Hamiltonians considered in this paper are undeformed, Möbius, and SSD Hamiltonians defined as

$$H_{\text{inh}} = \int dx f(x) h(x), \tag{2.1}$$

where the envelope function are defined as

$$f(x) = \begin{cases} 1 & \text{for } H \\ 1 - \tanh(2\theta)\cos\left(\frac{2\pi x}{L}\right) & \text{for } H_{\text{Möbius}} \\ 2\sin^2\left(\frac{\pi x}{L}\right) & \text{for } H_{\text{SSD}} \end{cases} . \tag{2.2}$$

For $\theta = 0$, $H_{\text{Möbius}}$ reduces to the undeformed Hamiltonian, H, while for $\theta = \infty$, $H_{\text{Möbius}}$ reduces to the SSD Hamiltonian H_{SSD}. In the SSD limit, where $\theta = \infty$, the deformed Hamiltonian density, $\overline{h}(x) = f(x)h(x)$ vanishes at $x = 0$, while at $x = L/4$ and $x = 3L/4$, the deformed density reduces to the undeformed one. Let us defined the Virasoro generator as

$$L_n = \oint \frac{dz}{2\pi i} z^{n+1} T(z), \overline{L}_n = \oint \frac{d\overline{z}}{2\pi i} \overline{z}^{n+1} \overline{T}(\overline{z}), \tag{2.3}$$

where n are integer numbers, $(z, \overline{z}) = (e^{\frac{2\pi(ix+\tau)}{L}}, e^{\frac{2\pi(-ix+\tau)}{L}}) = (e^{\frac{2\pi w}{L}}, e^{\frac{2\pi \overline{w}}{L}})$, and the chiral and anti-chiral parts of the energy-momentum tensor is defined by $h(x) = T(w) + \overline{T}(\overline{w})$. In terms of Virasoro generators, the inhomogeneous Hamiltonian are given by

$$H_0 = \frac{2\pi}{L}\left(L_0 + \overline{L}_0\right),$$

$$H_{\text{Möbius}} = \frac{2\pi}{L}\left[L_0 + \overline{L}_0 - \frac{\tanh 2\theta}{2}\left(L_1 + L_{-1} + \overline{L}_1 + \overline{L}_{-1}\right)\right], \tag{2.4}$$

$$H_{\text{SSD}} = \frac{2\pi}{L}\left[L_0 + \overline{L}_0 - \frac{1}{2}\left(L_1 + L_{-1} + \overline{L}_1 + \overline{L}_{-1}\right)\right].$$

8

2.2 The systems considered in this paper

We explain the system considered in this paper. We start from the vacuum state with the insertion at the spatial position x of the local operator, and then evolve the systems according to the evolution constructed of the Euclidean and Lorentzian time evolution. More precisely, the systems considered in this paper are

$$
\begin{aligned}
|\Psi_1\rangle = \mathcal{N}_1 e^{-iH_{\text{Möbius}}t_1} e^{-\epsilon H_0} \mathcal{O}(x) |0\rangle \, , \, |\Psi_2\rangle = \mathcal{N}_2 e^{-\epsilon H_0} e^{-iH_{\text{Möbius}}t_1} \mathcal{O}(x) |0\rangle \, , \\
|\Psi_3\rangle = \mathcal{N}_3 e^{-iH_0 t_0} e^{-\epsilon H_{\text{Möbius}}} \mathcal{O}(x) |0\rangle \, , \, |\Psi_4\rangle = \mathcal{N}_4 e^{-\epsilon H_{\text{Möbius}}} e^{-iH_0 t_0} \mathcal{O}(x) |0\rangle \, ,
\end{aligned}
\tag{2.5}
$$

where the normalization constants satisfy with

$$
\begin{aligned}
\mathcal{N}_1^{-2} = \langle 0| \mathcal{O}^\dagger(x) e^{-2\epsilon H_0} \mathcal{O}(x) |0\rangle \, , \mathcal{N}_2^{-2} = \langle 0| \mathcal{O}^\dagger(x) e^{iH_{\text{Möbius}}t_1} e^{-2\epsilon H_0} e^{-iH_{\text{Möbius}}t_1} \mathcal{O}(x) |0\rangle \\
\mathcal{N}_3^{-2} = \langle 0| \mathcal{O}^\dagger(x) e^{-2\epsilon H_{\text{Möbius}}} \mathcal{O}(x) |0\rangle \, , \mathcal{N}_4^{-2} = \langle 0| \mathcal{O}^\dagger(x) e^{iH_0 t_0} e^{-2\epsilon H_{\text{Möbius}}} e^{-iH_0 t_0} \mathcal{O}(x) |0\rangle \, .
\end{aligned}
\tag{2.6}
$$

The inverse normalization constants, $\mathcal{N}_1^{-2}$ ($\mathcal{N}_3^{-2}$), are independent of t_1 (t_0), while $\mathcal{N}_2^{-2}$ ($\mathcal{N}_4^{-2}$) varies with times under the evolution induced by $H_{\text{Möbius}}$ (H_0). Thus, since the normalization constants for $i = 1, 3$ are constant and those for $i = 2, 4$, we call the time evolution for $i = 1, 3$ the unitary one, while we call the time evolution for $i = 2, 4$ the non-unitary one. The systems considered are defined on the spatial circle with the circumference L. The difference between $|\Psi_1\rangle$ ($|\Psi_3\rangle$) and $|\Psi_2\rangle$ ($|\Psi_4\rangle$) is the time ordering of the Euclidean and Lorentzian time evolution. In $|\Psi_{i=1,3}\rangle$, the systems initially follow the Euclidean time evolution, and then undergo Lorentzian time evolution, while in $|\Psi_{i=2,4}\rangle$, the ordering of the time evolution is opposite. For $i = 1, 2$, the time evolution is induced by the inhomogeneous Hamiltonian, while for $i = 3, 4$, it is induced by the uniform Hamiltonian. The density operators associated with the systems in (2.5) are given by

$$
\begin{aligned}
\rho_1 &= \mathcal{N}_1^2 e^{-iH_{\text{Möbius}}t_1} e^{-\epsilon H_0} \mathcal{O}(x) |0\rangle \langle 0| \mathcal{O}^\dagger(x) e^{-\epsilon H_0} e^{iH_{\text{Möbius}}t_1} \, , \\
\rho_2 &= \mathcal{N}_2^2 e^{-\epsilon H_0} e^{-iH_{\text{Möbius}}t_1} \mathcal{O}(x) |0\rangle \langle 0| \mathcal{O}^\dagger(x) e^{iH_{\text{Möbius}}t_1} e^{-\epsilon H_0} \, , \\
\rho_3 &= \mathcal{N}_3^2 e^{-it_0 H_0} e^{-\epsilon H_{\text{Möbius}}} \mathcal{O}(x) |0\rangle \langle 0| \mathcal{O}^\dagger(x) e^{-\epsilon H_{\text{Möbius}}} e^{iH_0 t_0} \, , \\
\rho_4 &= \mathcal{N}_4^2 e^{-\epsilon H_{\text{Möbius}}} e^{-it_0 H_0} \mathcal{O}(x) |0\rangle \langle 0| \mathcal{O}^\dagger(x) e^{iH_0 t_0} e^{-\epsilon H_{\text{Möbius}}} \, ,
\end{aligned}
\tag{2.7}
$$

2.3 Entanglement entropy

In this paper, we will mainly explore the effect on the entanglement dynamics of the time ordering of Euclidean and Lorentzian time evolution by using entanglement entropy. Therefore, let us define the entanglement entropy. To this end, we divide the circle into a single interval, A, and a complement subsystem, $\overline{A}$, and then define a reduced density matrix associated to A by $\rho_{A,i} = \text{tr}_{\overline{A}} \rho_i$. Endpoints of A are X_1 and X_2, and we assume that $X_1 > X_2 > 0$. We will consider the time-dependence of $S_{A,i}$ in only three cases in the following section (See

Fig. [3]):

$$A = \begin{cases} \{x \,|\, 0 \le x \le X_2, X_1 \le x \le L\}, & \text{where } X_2 > L - X_1 > 0 \text{ and } X_1 > \frac{L}{2} > X_2 > 0 \text{ for } (a) \\ \{x \,|\, X_2 \le x \le X_1\}, & \text{where } 0 < X_2 < \frac{L}{2} < X_1 \text{ and } \frac{L}{2} - X_2 > X_1 - \frac{L}{2} \text{ for } (b) \\ \{x \,|\, X_2 \le x \le X_1\}, & \text{where } 0 < X_2 < X_1 < \frac{L}{2} \text{ for } (c) \end{cases} \quad . \tag{2.8}$$
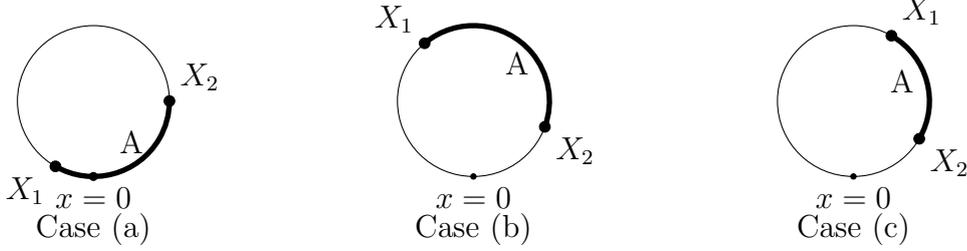
Figure 3: The subsystems considered in this paper. In (a), the subsystem includes only the origin. In (b), the subsystem includes only $x = \frac{L}{2}$. In (c), the subsystem does not contain both the origin and $\frac{L}{2}$. The origin and $\frac{L}{2}$ are the fixed points during the SSD time evolution, as explained in Section 2.4.

We define the n-th moment of the Rényi entanglement entropy as

$$S_A^{(n)} = \frac{1}{1-n} \log \left[\mathrm{tr}_A \rho_A^{(n)} \right]. \tag{2.9}$$

Then, we define entanglement entropy as the Von Neumann limit, where $n \to 1$, of $S_A^{(n)}$,

$$S_A = \lim_{n \to 1} S_A^{(n)} = -\mathrm{tr}_A \left(\rho_A \log \rho_A \right). \tag{2.10}$$

2.3.1 Euclidean path integral

In this paper, we will employ the twist operator formalism suitable for the analytic computation [71, 72]. To do so, we first define the Euclidean Rényi entanglement entropy, a cousin of the Rényi entanglement entropy, and then compute it in the path-integral formalism. Subsequently, we will perform the analytic continuation from Euclidean time to Lorentzian time. Consequently, we explore the time dependence of the entanglement entropy for a single interval. Define the Euclidean density operators as a Euclidean counterpart of the density operators in (2.7),

$$\rho_{1,E} = \mathcal{N}_{E,1}^2 e^{-H_{\text{Möbius}}\tau_1} e^{-\epsilon H_0} \mathcal{O}(x) |0\rangle \langle 0| \mathcal{O}^\dagger(x) e^{-\epsilon H_0} e^{H_{\text{Möbius}}\tau_1} = \mathcal{N}_{E,1}^2 U_{1,\epsilon}^E \mathcal{O}(x) |0\rangle \langle 0| \mathcal{O}^\dagger(x) \tilde{U}_{1,\epsilon}^E,$$

$$\rho_{2,E} = \mathcal{N}_{E,2}^2 e^{-\epsilon H_0} e^{-H_{\text{Möbius}}\tau_1} \mathcal{O}(x) |0\rangle \langle 0| \mathcal{O}^\dagger(x) e^{H_{\text{Möbius}}\tau_1} e^{-\epsilon H_0} = \mathcal{N}_{E,2}^2 U_{2,\epsilon}^E \mathcal{O}(x) |0\rangle \langle 0| \mathcal{O}^\dagger(x) \tilde{U}_{2,\epsilon}^E,$$

$$\rho_{3,E} = \mathcal{N}_{E,3}^2 e^{-\tau_0 H_0} e^{-\epsilon H_{\text{Möbius}}} \mathcal{O}(x) |0\rangle \langle 0| \mathcal{O}^\dagger(x) e^{-\epsilon H_{\text{Möbius}}} e^{H_0 \tau_0} = \mathcal{N}_{E,3}^2 U_{3,\epsilon}^E \mathcal{O}(x) |0\rangle \langle 0| \mathcal{O}^\dagger(x) \tilde{U}_{3,\epsilon}^E,$$

$$\rho_{4,E} = \mathcal{N}_{E,4}^2 e^{-\epsilon H_{\text{Möbius}}} e^{-\tau_0 H_0} \mathcal{O}(x) |0\rangle \langle 0| \mathcal{O}^\dagger(x) e^{\tau_0 H_0} e^{-\epsilon H_{\text{Möbius}}} = \mathcal{N}_{E,4}^2 U_{4,\epsilon}^E \mathcal{O}(x) |0\rangle \langle 0| \mathcal{O}^\dagger(x) \tilde{U}_{4,\epsilon}^E, \tag{2.11}$$

where $\mathcal{N}_{E,i=1\sim4}^2$ guarantee that $\mathrm{tr}\rho_{i,E} = 1$, and they are given by

$$\mathcal{N}_{E,1}^2 = \frac{1}{\langle 0|\,\mathcal{O}^\dagger(x)e^{-2\epsilon H_0}\mathcal{O}(x)\,|0\rangle}, \ \mathcal{N}_{E,2}^2 = \frac{1}{\langle 0|\,\mathcal{O}^\dagger(x)e^{H_{\text{Möbius}}\tau_1}e^{-2\epsilon H_0}e^{-H_{\text{Möbius}}\tau_1}\mathcal{O}(x)\,|0\rangle},$$

$$\mathcal{N}_{E,3}^2 = \frac{1}{\langle 0|\,\mathcal{O}^\dagger(x)e^{-2\epsilon H_{\text{Möbius}}}\mathcal{O}(x)\,|0\rangle}, \ \mathcal{N}_{E,4}^2 = \frac{1}{\langle 0|\,\mathcal{O}^\dagger(x)e^{H_0\tau_0}e^{-2\epsilon H_{\text{Möbius}}}e^{-H_0\tau_0}\mathcal{O}(x)\,|0\rangle}.$$

$$(2.12)$$

In this paper, $\mathcal{O}$ is a primary operator with the conformal dimension $(h_\mathcal{O}, h_\mathcal{O})$. Define an Euclidean reduced density matrix by $\rho_{A,i,E} = \mathrm{tr}_{\overline{A}}\rho_{i,E}$ and then define the Euclidean n-th Rényi and Von Neumann entanglement entropies by

$$S_{A,i,E}^{(n)} = \frac{1}{1-n}\log\left[\mathrm{tr}_A\rho_{A,i,E}^n\right], \quad S_{A,i,E} = \lim_{n\to1}S_{A,i,E}^{(n)} \qquad (2.13)$$

In the twist operator formalism [73, 27], the Euclidean n-th Rényi entanglement entropy for single interval A is given by

$$S_{A,i}^{(n)} = \frac{1}{1-n}\log\left[\frac{\left\langle\mathcal{O}_n^\dagger(x)\tilde{U}_{i,\epsilon}^E\sigma_n(X_1)\overline{\sigma}_n(X_2)U_{i,\epsilon}^E\mathcal{O}_n(x)\right\rangle}{\left\langle\mathcal{O}_n^\dagger(x)\tilde{U}_{i,\epsilon}^EU_{i,\epsilon}^E\mathcal{O}_n(x)\right\rangle^n}\right], \qquad (2.14)$$

where $\langle\cdot\rangle$ denotes the vacuum expectation value, σ_n and $\overline{\sigma}_n$ are the twist and anti-operators with the conformal dimension $\left(h_n, \overline{h}_n\right) = \left(\frac{c(n^2-1)}{24n}, \frac{c(n^2-1)}{24n}\right)$, and $\mathcal{O}_n$ is a primary operator with the conformal dimensions $(nh_\mathcal{O}, nh_\mathcal{O})$ as in [27]. In terms of Heisenberg picture, $S_{A,i,E}^n$ reduces to

$$S_{A,i,E}^{(n)} = \frac{1}{1-n}\log\left[\left\langle\mathcal{O}_{n,i,\epsilon}^{\dagger,H}(x)\sigma_n(X_1)\overline{\sigma}_n(X_2)\mathcal{O}_{n,i,-\epsilon}^H(x)\right\rangle\right] - \frac{n}{1-n}\log\left[\left\langle\mathcal{O}_{i,\epsilon}^{\dagger,H}(x)\mathcal{O}_{i,-\epsilon}^H(x)\right\rangle\right],$$

$$(2.15)$$

where $\mathcal{O}_{n,i,\pm\epsilon}^H(x)$ denote the local operator in the Heisenberg picture. Here, we use the facts that $U_{i,E,\pm\epsilon}|0\rangle = |0\rangle$ and $U_{i,\epsilon}^E\tilde{U}_{i,-\epsilon}^E = U_{i,-\epsilon}^E\tilde{U}_{i,\epsilon}^E = \tilde{U}_{i,\epsilon}^EU_{i,-\epsilon}^E = \tilde{U}_{i,-\epsilon}^EU_{i,\epsilon}^E = \mathbf{1}$. The primary operators in the Heisenberg picture are given by

$$\mathcal{O}_{n,i,\epsilon}^H(x) = U_{i,-\epsilon}^E\mathcal{O}(w_x, \overline{w}_x)\tilde{U}_{i,\epsilon}^E = \left|\frac{dw_\epsilon^{\text{New},i}}{dw_x}\right|^{2nh_\mathcal{O}}\mathcal{O}(w_\epsilon^{\text{New},i}, \overline{w}_\epsilon^{\text{New},i}), \qquad (2.16)$$

where complex coordinates $(w, \overline{w})$ are defined by $(w, \overline{w}) = (\tau + ix, \tau - ix)$, and $(w_x, \overline{w}_x) = (ix, -ix)$. The details of computation on (2.16) and the trajectories of local operators during the evolution considered are reported in Appendix A.1. Consequently, in terms of $(w_{\pm\epsilon}^{\text{New},i}, \overline{w}_{\pm\epsilon}^{\text{New},i})$, the n-th moment of Rényi entanglement entropy is given by

$$S_{A,i,E}^{(n)} = \frac{1}{1-n}\log\left[\frac{\left\langle\mathcal{O}_n^\dagger(w_\epsilon^{\text{New},i}, \overline{w}_\epsilon^{\text{New},i})\sigma_n(w_{X_1}, \overline{w}_{X_1})\overline{\sigma}_n(w_{X_2}, \overline{w}_{X_2})\mathcal{O}_n(w_{-\epsilon}^{\text{New},i}, \overline{w}_{-\epsilon}^{\text{New},i})\right\rangle}{\left\langle\mathcal{O}^\dagger(w_\epsilon^{\text{New},i}, \overline{w}_\epsilon^{\text{New},i})\mathcal{O}(w_{-\epsilon}^{\text{New},i}, \overline{w}_{-\epsilon}^{\text{New},i})\right\rangle^n}\right]$$

$$(2.17)$$

Thus, the contributions from the conformal factors are canceled out. In the following sections, we consider the time dependence of the entanglement entropy in various 2d CFTs.

2.4 Time trajectory of the local operators

We will close this section by exploring the time trajectory, induced by the Möbius and SSD Hamiltonian, of the local operator after performing the analytic continuation. Before performing the analytic continuation, we define the spatial position of the local operator by

$$X_{\pm\epsilon}^{\text{New},i=1,2} = \frac{w_{\pm\epsilon}^{\text{New},i=1,2} - \overline{w}_{\pm\epsilon}^{\text{New},i=1,2}}{2i}. \tag{2.18}$$

Then, we perform the analytic continuation, $\tau_1 = it_1$. Let X_1^f and X_2^f denote 0 and $\frac{L}{2}$. We assume that at $t_1 = 0$, the local operator is inserted at x. During the time evolution induced by the Möbius Hamiltonian, the local operator for $X_1^f < x < X_2^f$ periodically oscillates with time between X_1^f and X_2^f, while for $X_2^f < x < L$ the one does between L and X_2^f (See Fig. 4). During the time evolution induced by H_{SSD}, if the local operator is inserted at either X_1^f or X_2^f, the local operator does not spatially move. Therefore, we call them fixed points. In addition to them, during the SSD time evolution, the local operator spatially moves to X_2^f, and consequently accumulates around X_2^f.

[a] Möbius evolution   [b] SSD evolution
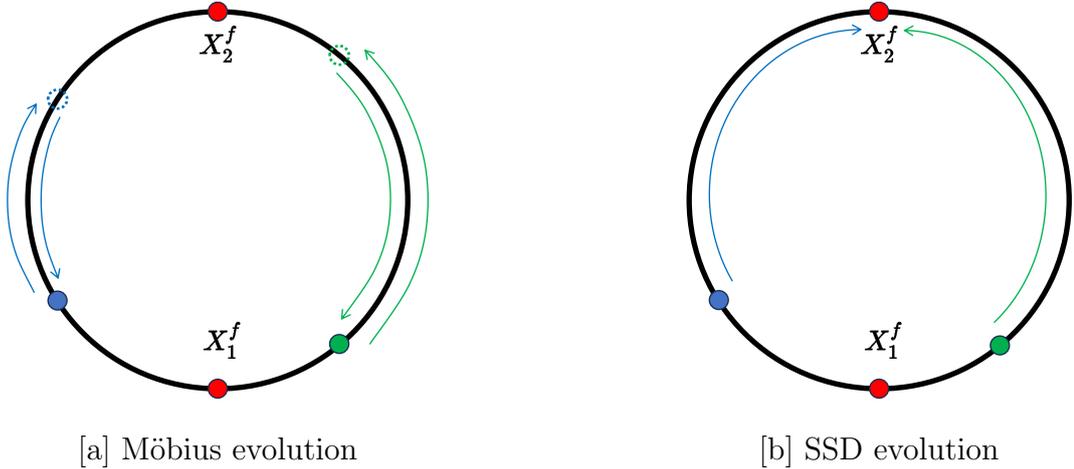
Figure 4: The picture illustrating the spatial trajectory of the operator during the time evolution. Panel [a] illustrates the time evolution of the local operator during the Möbius time evolution, while [b] does it during the SSD time evolution. The initial insertion points of the operator are marked by blue and green, and their trajectories are denoted by blue and green curves. The two fixed points, $X_1^f = 0$ and $X_2^f = L/2$, are marked in red.

3 Universal quantities

In this section, we will explore the time dependence of universal quantities which are independent of the details of the 2d CFTs. First, we present the time dependence of the partition function, and then we will report on the time dependence of the expectation value of the energy density.

3.1 Time-dependence of partition function

Define the partition function as

$$Z_{i=1,\cdots,4} = \mathcal{N}_{E,i=1,\cdots,4}^{-2} \tag{3.1}$$

where Z_0 is the partition function for the vacuum state. Then, we perform the analytic continuation, $\tau_{i=0,1} = it_{0,1}$, and explore the time dependence of the partition functions. Since Z_0 is time-independent and we are focusing on the time dependent piece of the partition function, we redefine the partition function as $\tilde{Z}_i = \frac{Z_i}{Z_0}$.

3.1.1 Möbius case

Let us consider the time dependence of the redefined partition function for the four density operators in (2.7). For general $\theta \neq \infty$, their time dependence is determined by

$$\tilde{Z}_1 = \left(\frac{L}{\pi \sinh\left(\frac{2\pi\epsilon}{L}\right)} \right)^{4h_{\mathcal{O}}} \underset{\frac{\epsilon}{L} \ll 1}{\approx} \frac{1}{(2\epsilon)^{4h_{\mathcal{O}}}} =: \tilde{Z}_1^{(1)},$$

$$\tilde{Z}_2 = \tilde{Z}_1 \times \left[\frac{1}{\chi\overline{\chi}} \right]^{2h_{\mathcal{O}}} \underset{\frac{\epsilon}{L} \ll 1}{\approx} \tilde{Z}_1^{(1)} \times \left[\frac{1}{\chi\overline{\chi}} \right]^{2h_{\mathcal{O}}},$$

$$\tilde{Z}_3 = \left[\frac{\pi}{L \sinh\left(\frac{2\pi\epsilon}{L_{\text{eff}}}\right) \cosh 2\theta \left(1 - \cos\left(\frac{2\pi x}{L}\right) \tanh 2\theta\right)} \right]^{4h_{\mathcal{O}}} \underset{\frac{\epsilon}{L} \ll 1}{\approx} \tilde{Z}_1^{(1)} \times \left(\frac{1}{\left(1 - \cos(\frac{2\pi x}{L}) \tanh(2\theta)\right)} \right)^{4h_{\mathcal{O}}},$$

$$\tilde{Z}_4 = \left[\frac{\pi}{L \cosh 2\theta \sinh\left(\frac{2\pi\epsilon}{L_{\text{eff}}}\right)} \right]^{4h_{\mathcal{O}}} \times \left[\frac{1}{\left(1 - \cos(\frac{2\pi(t_0+x)}{L}) \tanh(2\theta)\right) \left(1 - \cos(\frac{2\pi(t_0-x)}{L}) \tanh(2\theta)\right)} \right]^{2h_{\mathcal{O}}}$$

$$\underset{\frac{\epsilon}{L} \ll 1}{\approx} \tilde{Z}_1^{(1)} \times \left[\frac{1}{\left(1 - \cos(\frac{2\pi(t_0+x)}{L}) \tanh(2\theta)\right) \left(1 - \cos(\frac{2\pi(t_0-x)}{L}) \tanh(2\theta)\right)} \right]^{2h_{\mathcal{O}}} \tag{3.2}$$

where the χ are defined as

$$\chi = \cos^2\left(\frac{\pi t_1}{L_{\text{eff}}}\right) + \sin^2\left(\frac{\pi t_1}{L_{\text{eff}}}\right) \left(\cosh(2\theta) + \sinh(2\theta) \left(-\cos\left(\frac{2\pi x}{L}\right) + i \sin\left(\frac{2\pi x}{L}\right) \right) \right)^2 \tag{3.3}$$

Here, since for $\theta \neq \infty$, $|1 - \cos(A) \tanh 2\theta| > 0$, where A is assumed to be a real parameter, $\tilde{Z}_{i=3,4}$ do not diverge. Additionally, since $|\chi| > 0$ for any $t_1, x, \theta \in \mathbb{R}$, $\tilde{Z}_{i=2}$ does not diverge. Therefore, these partition functions for the Möbius case are well-defined and the Euclidean time evolution induced by the Möbius Hamiltonian. The redefined partition functions, $\tilde{Z}_{i=1,3}$, are independent of time, while $Z_{i=2,4}$ depends on the time. The partition function, $\tilde{Z}_{i=2}$, is a periodic function with the period L_{eff}, while $\tilde{Z}_{i=4}$ is the periodic one with L.

3.1.2 SSD limit

Now, we look closely at the time dependence of the partition functions for the states considered in the SSD limit, where $\theta \to \infty$. Since $\tilde{Z}_{i=1}$ is independent of θ, $\tilde{Z}_{i=1}$ in the SSD limit is the same as that for finite θ. In the SSD limit, the redefined partition function for $i = 3$ reduces to

$$\tilde{Z}_3 = \left(\frac{\csc^2 \left(\frac{\pi x}{L} \right)}{4\epsilon} \right)^{4h_{\mathcal{O}}}. \tag{3.4}$$

Thus, $\tilde{Z}_3$ depends on the insertion point of the local operator. If the local operator is inserted at $x = 0$, $\tilde{Z}_3$ becomes infinite. Since the Hamiltonian density of H_{SSD} vanishes at $x = 0$, and $\mathcal{O}(x = 0)$ commutes with $e^{-\epsilon H_{\text{SSD}}}$, this damping functor, $e^{-\epsilon H_{\text{SSD}}}$, can not keep the state finite. In other words, this suggests that at $x = 0$, the Euclidean time evolution induced by H_{SSD} does not play as a regulator. In the SSD limit, the time dependence of the partition functions for $i = 2, 4$ at the leading other of the small ϵ reduces to

$$\tilde{Z}_2 = \tilde{Z}_1 \times \left[\frac{1}{\left[16 \sin^4 \left(\frac{\pi x}{L} \right) \left(\frac{\pi t_1}{L} \right)^4 - 8 \sin^2 \left(\frac{\pi x}{L} \right) \cos \left(\frac{2\pi x}{L} \right) \left(\frac{\pi t_1}{L} \right)^2 + 1 \right]^2} \right]^{h_{\mathcal{O}}}$$

$$\underset{\frac{\epsilon}{L} \ll 1}{\approx} \tilde{Z}_1^{(1)} \times \left[\frac{1}{\left[16 \sin^4 \left(\frac{\pi x}{L} \right) \left(\frac{\pi t_1}{L} \right)^4 - 8 \sin^2 \left(\frac{\pi x}{L} \right) \cos \left(\frac{2\pi x}{L} \right) \left(\frac{\pi t_1}{L} \right)^2 + 1 \right]^2} \right]^{h_{\mathcal{O}}}, \tag{3.5}$$

$$\tilde{Z}_4 = \left(\frac{1}{2\epsilon \left[\cos \left(\frac{2\pi x}{L} \right) - \cos \left(\frac{2\pi t_0}{L} \right) \right]} \right)^{4h_{\mathcal{O}}},$$

where at $t_0 = nL \pm x$, where n is an integer, $\tilde{Z}_4$ diverges. Here, $\tilde{Z}_4$ is a periodic function of t_0 with a period L. Our interpretation is that when the excitations created by the local operator hit $X = 0$, the spatial point where the Hamiltonian density of H_{SSD} vanishes, the partition function becomes infinite. A possible explanation is that the Euclidean time evolution induced by H_{SSD} does not work as a regulator at the origin. In the large t_1-regime, the t_1 dependence of Z_2 is approximately given by

$$\tilde{Z}_2 \approx \begin{cases} \left(\frac{L^8 \csc^8 \left(\frac{\pi x}{L} \right)}{4096 \pi^8 t_1^8 \epsilon^4} \right)^{h_{\mathcal{O}}} & x \neq 0 \\ \frac{1}{(2\epsilon)^{4h_{\mathcal{O}}}} & x = 0 \end{cases}. \tag{3.6}$$

Thus, when the operator is inserted at $x \neq 0$, the partition function decays with t_1, while when the operator is inserted at $x = 0$, the partition function is independent of time. This suggests that during the SSD time evolution, the local operator at $x = 0$ does not change the entanglement structure.

3.2 Non-unitarity

Let us define the current as the derivative of the partition with respect to time,

$$\mathbf{j}_i = \frac{d \left\langle \Psi_i(t) \middle| \Psi_i(t) \right\rangle}{dt_{a=0,1}}, \tag{3.7}$$

where i labels the states. The symbol t_1 is for $i = 1, 2$, while t_0 is for $i = 3, 4$. For $i = 1, 3$, $\mathbf{j}_i$ vanishes, which means that the time evolution is unitary because the norm of state is conserved. For $i = 2, 4$, $\mathbf{j}_i$ does not vanish. The currents for $i = 2, 4$ are determined by

$$\mathbf{j}_2 = i \left(\frac{2\pi}{L} \right) \sinh \left(\frac{2\pi\epsilon}{L} \right) \tanh 2\theta \left\langle \Psi_2(t) \middle| (L_1 - L_{-1} + \overline{L}_1 - \overline{L}_{-1}) \middle| \Psi_2(t) \right\rangle,$$

$$\mathbf{j}_4 = i \left(\frac{2\pi}{L} \right) \left(\frac{2\tanh 2\theta}{\mathrm{csch}4\theta} \right)^{\frac{1}{2}} \sinh \left(\frac{2\pi\epsilon}{L} \sqrt{2\tanh 2\theta \, \mathrm{csch}4\theta} \right) \left\langle \Psi_4(t) \middle| (L_1 - L_{-1} + \overline{L}_1 - \overline{L}_{-1}) \middle| \Psi_4(t) \right\rangle, \tag{3.8}$$

We can see from (3.8) that for both $|\Psi\rangle_2$ and $|\Psi\rangle_4$, the dissipation of the partition function is determined by $L_1 - L_{-1} + \overline{L}_1 - \overline{L}_{-1}$. In SSD limit, the equations for the current reduce to

$$\mathbf{j}_2 = i \left(\frac{2\pi}{L} \right) \sinh \left(\frac{2\pi\epsilon}{L} \right) \left\langle \Psi_2(t) \middle| (L_1 - L_{-1} + \overline{L}_1 - \overline{L}_{-1}) \middle| \Psi_2(t) \right\rangle,$$

$$\mathbf{j}_4 = 2\epsilon i \left(\frac{2\pi}{L} \right)^2 \left\langle \Psi_4(t) \middle| (L_1 - L_{-1} + \overline{L}_1 - \overline{L}_{-1}) \middle| \Psi_4(t) \right\rangle. \tag{3.9}$$

Non-unitarity of the dynamics for $i = 2, 4$ is due to the time evolution of expectation value of $L_1 - L_{-1} + \overline{L}_1 - \overline{L}_{-1}$.

3.3 Energy density

Above, we explored the global properties of the systems by using the (redefined) partition functions. Here, we will explore the time dependence of a local universal quantity, the energy density. In our calculation, we begin with the calculation of the energy density in the Euclidean path integral, and then perform the analytic continuation to real time. Define the expectation values of chiral and anti-chiral parts of the energy density as

$$\left\langle T_{ww}(w_X, \overline{w}_X) \right\rangle_{i,E} = \mathrm{tr} \left(\rho_{i,E} T_{ww}(w_X, \overline{w}_X) \right) = \frac{\left\langle \mathcal{O}^\dagger (w_\epsilon^{\mathrm{New},i}, \overline{w}_\epsilon^{\mathrm{New},i}) T_{ww}(w_X, \overline{w}_X) \mathcal{O} \left(w_{-\epsilon}^{\mathrm{New},i}, \overline{w}_{-\epsilon}^{\mathrm{New},i} \right) \right\rangle}{\left\langle \mathcal{O}^\dagger \left(w_\epsilon^{\mathrm{New},i}, \overline{w}_\epsilon^{\mathrm{New},i} \right) \mathcal{O} \left(w_{-\epsilon}^{\mathrm{New},i}, \overline{w}_{-\epsilon}^{\mathrm{New},i} \right) \right\rangle},$$

$$\left\langle T_{\overline{w}\overline{w}}(w_X, \overline{w}_X) \right\rangle_{i,E} = \mathrm{tr} \left(\rho_{i,E} T_{\overline{w}\overline{w}}(w_X, \overline{w}_X) \right) = \frac{\left\langle \mathcal{O}^\dagger (w_\epsilon^{\mathrm{New},i}, \overline{w}_\epsilon^{\mathrm{New},i}) T_{\overline{w}\overline{w}}(w_X, \overline{w}_X) \mathcal{O} \left(w_{-\epsilon}^{\mathrm{New},i}, \overline{w}_{-\epsilon}^{\mathrm{New},i} \right) \right\rangle}{\left\langle \mathcal{O}^\dagger \left(w_\epsilon^{\mathrm{New},i}, \overline{w}_\epsilon^{\mathrm{New},i} \right) \mathcal{O} \left(w_{-\epsilon}^{\mathrm{New},i}, \overline{w}_{-\epsilon}^{\mathrm{New},i} \right) \right\rangle}, \tag{3.10}$$

where the energy density is assumed to be defined as the linear combination of T_{ww} and the chiral and anti-chiral parts of the energy density, $T = T_{ww} + T_{\overline{w}\overline{w}}$. We call $\langle T_{ww} \rangle_i$ and $\langle T_{\overline{w}\overline{w}} \rangle_i$

chiral and anti-chiral energy densities, respectively. By performing the conformal map from cylinder to the flat space and using the Ward-Takahashi identity, the the expectation values of energy densities [6] are given by

$$
\begin{aligned}
\langle T_{ww}(w_X, \overline{w}_X) \rangle_{i,E} &= -\frac{c}{24} \left(\frac{2\pi}{L} \right)^2 + h_{\mathcal{O}} \left(\frac{dz_X}{dw_X} \right)^2 \left[\frac{1}{z_X - z_{\epsilon}^{\text{New},i}} - \frac{1}{z_X - z_{-\epsilon}^{\text{New},i}} \right]^2 , \\
\langle T_{\overline{ww}}(w_X, \overline{w}_X) \rangle_{i,E} &= -\frac{c}{24} \left(\frac{2\pi}{L} \right)^2 + h_{\mathcal{O}} \left(\frac{d\overline{z}_X}{d\overline{w}_X} \right)^2 \left[\frac{1}{\overline{z}_X - \overline{z}_{\epsilon}^{\text{New},i}} - \frac{1}{\overline{z}_X - \overline{z}_{-\epsilon}^{\text{New},i}} \right]^2 .
\end{aligned}
\tag{3.12}
$$

3.3.1 Möbius case

First, we will closely look at the time dependence of the chiral and anti-chiral energy densities during the Möbius time evolution. After performing analytic continuations, $\tau_{i=0,1} = it_{0,1}$, at the second order of the small ϵ expansion, they are determined by

$$
\langle T_{ww}(w_X) \rangle_{i=1,\cdot,4} \approx \left(\frac{2\pi}{L} \right)^2 \left[-\frac{c}{24} + \epsilon^2 \mathcal{T}_{i=1,\cdot,4}^{\theta} \right], \quad \langle T_{\overline{ww}}(\overline{w}_X) \rangle_{i=1,\cdot,4} \approx \left(\frac{2\pi}{L} \right)^2 \left[-\frac{c}{24} + \epsilon^2 \overline{\mathcal{T}}_{i=1,\cdot,4}^{\theta} \right],
\tag{3.13}
$$

---

[6] Here, the Ward-Takahashi identity is

$$
\begin{aligned}
\langle T_{zz}(z)\mathcal{O}(z_1, \overline{z}_1)\mathcal{O}(z_2, \overline{z}_2) \rangle &= \sum_{i=1}^{2} \left[\frac{h_{\mathcal{O}}}{(z - z_i)^2} + \frac{1}{z - z_i} \partial_{z_i} \right] \langle \mathcal{O}(z_1, \overline{z}_1)\mathcal{O}(z_2, \overline{z}_2) \rangle , \\
\langle T_{\overline{zz}}(\overline{z})\mathcal{O}(z_1, \overline{z}_1)\mathcal{O}(z_2, \overline{z}_2) \rangle &= \sum_{i=1}^{2} \left[\frac{h_{\mathcal{O}}}{(\overline{z} - \overline{z}_i)^2} + \frac{1}{z - z_i} \partial_{\overline{z}_i} \right] \langle \mathcal{O}(z_1, \overline{z}_1)\mathcal{O}(z_2, \overline{z}_2) \rangle .
\end{aligned}
\tag{3.11}
$$

where functions, $\mathcal{T}_{i=1,\cdots,4}^{\theta}$, $\overline{\mathcal{T}}_{i=1,\cdots,4}^{\theta}$, $D_{i=1,2,\pm}$ and $N_{\pm}$, are defined as

$$\mathcal{T}_{i=1}^{\theta} = \frac{\pi^2 h_{\mathcal{O}}}{L^2 D_+}, \ \overline{\mathcal{T}}_{i=1}^{\theta} = \frac{\pi^2 h_{\mathcal{O}}}{L^2 D_-}, \ \mathcal{T}_{i=2}^{\theta} = \frac{\pi^2 h_{\mathcal{O}} N_+}{L^2 D_+}, \ \overline{\mathcal{T}}_{i=2}^{\theta} = \frac{\pi^2 h_{\mathcal{O}} N_-}{L^2 D_-},$$

$$\mathcal{T}_{i=3}^{\theta} = \frac{\pi^2 \epsilon^2 h_{\mathcal{O}} \left(\tanh 2\theta \cos\left(\frac{2\pi x}{L}\right) - 1\right)^2}{L^2 \sin^4\left[\frac{\pi(t_0 + X - x)}{L}\right]}, \ \overline{\mathcal{T}}_{i=3}^{\theta} = \frac{\pi^2 h_{\mathcal{O}} \left(\tanh 2\theta \cos\left(\frac{2\pi x}{L}\right) - 1\right)^2}{L^2 \sin^4\left[\frac{\pi(t_0 - X + x)}{L}\right]},$$

$$\mathcal{T}_{i=4}^{\theta} = \frac{\pi^2 h_{\mathcal{O}} \left(\tanh 2\theta \cos\left(\frac{2\pi(t_0 - x)}{L}\right) - 1\right)^2}{L^2 \sin^4\left[\frac{\pi(t_0 + X - x)}{L}\right]}, \ \overline{\mathcal{T}}_{i=4}^{\theta} = \frac{\pi^2 h_{\mathcal{O}} \left(\tanh 2\theta \cos\left(\frac{2\pi(t_0 + x)}{L}\right) - 1\right)^2}{L^2 \sin^4\left[\frac{\pi(t_0 - X + x)}{L}\right]},$$

$$D_{\pm} = \left[\frac{1}{2} \left(\sinh^2(2\theta) \cos^2\left(\frac{\pi(x + X)}{L}\right) + \cosh^2(2\theta) \cos^2\left(\frac{\pi(x - X)}{L}\right)\right)\right.$$

$$- \left(\sinh(4\theta) \cos\left(\frac{\pi(x - X)}{L}\right) \cos\left(\frac{\pi(x + X)}{L}\right) + \sin^2\left(\frac{\pi(x - X)}{L}\right)\right)$$

$$+ \frac{1}{2} \cos\left(\frac{2\pi t_1}{L_{\text{eff}}}\right) \left(\cosh^2(2\theta) \left(-\cos^2\left(\frac{\pi(x - X)}{L}\right)\right) - \sinh^2(2\theta) \cos^2\left(\frac{\pi(x + X)}{L}\right)\right)$$

$$+ \frac{1}{2} \cos\left(\frac{2\pi t_1}{L_{\text{eff}}}\right) \left(\sinh(4\theta) \cos\left(\frac{\pi(x - X)}{L}\right) \cos\left(\frac{\pi(x + X)}{L}\right) + \sin^2\left(\frac{\pi(x - X)}{L}\right)\right)$$

$$\left. \pm \sin\left(\frac{2\pi t_1}{L_{\text{eff}}}\right) \sin\left(\frac{\pi(x - X)}{L}\right) \left(\sinh(2\theta) \cos\left(\frac{\pi(x + X)}{L}\right) - \cosh(2\theta) \cos\left(\frac{\pi(x - X)}{L}\right)\right)\right]^2,$$

$$N_{\pm} = \left[\cosh^2(2\theta) \left(1 - \tanh(2\theta) \cos\left(\frac{2\pi x}{L}\right)\right) + \frac{1}{2} \sinh(4\theta) \cos\left(\frac{2\pi t_1}{L_{\text{eff}}}\right) \left(\cos\left(\frac{2\pi x}{L}\right) - \tanh(2\theta)\right)\right.$$

$$\left. \pm \sinh(2\theta) \sin\left(\frac{2\pi x}{L}\right) \sin\left(\frac{2\pi t_1}{L_{\text{eff}}}\right)\right]^2,$$

$$(3.14)$$

where the effective system size is defined as $L_{\text{eff}} = L \cosh 2\theta$. Thus, the leading order behaviors of these densities in the small ϵ expansion are $\mathcal{O}(1)$ and independent of time and the location of the local operator, while the next-to-leading order terms are $\mathcal{O}(\epsilon^2)$, and the insertion of the local operator contributes to these behaviors. The second order terms of energy densities for $i = 3, 4$ are periodic functions with t_0, and their periods are L For $i = 3, 4$, this small ϵ expansion becomes invalid at $t_0 = \pm(X - x) + nL$, where n are integers because the second order terms of energy densities diverges. This suggests that the local operator at x induces localized energies and they propagate to left and right at the speed of light When these local excitations reach X, the energy densities at X drastically grow.

3.3.2   SSD limit

Next, we explore the time dependence of the energy density after taking the SSD limit and then performing analytic continuation. Because the details are complicated, we relegate them to Appendix B. To simplify them and explore their properties, we take the small ϵ limit and closely look at the first and second order terms of the energy densities in this limit. In this

limit, the energy densities for four states are approximated by

$$\langle T_{ww}(w_X)\rangle_{i=1,\ldots,4} \approx \left(\frac{2\pi}{L}\right)^2 \left[-\frac{c}{24} + \epsilon^2 \mathcal{T}_{i=1,\ldots,4}^{\theta=\infty}\right], \langle T_{\overline{ww}}(\overline{w}_X)\rangle_{i=1,\ldots,4} \approx \left(\frac{2\pi}{L}\right)^2 \left[-\frac{c}{24} + \epsilon^2 \overline{\mathcal{T}}_{i=1,\ldots,4}^{\theta=\infty}\right],$$
(3.15)

where the functions, $\mathcal{T}_{i=1,\cdots,4}^{\theta=\infty}$ and $\overline{\mathcal{T}}_{i=1,\cdots,4}^{\theta=\infty}$, are defined as

$$\mathcal{T}_{i=1}^{\theta=\infty} = \frac{4 h_{\mathcal{O}} \pi^2 L^2}{\left[2\pi t_1 \sin\left[\frac{\pi X}{L}\right] \sin\left[\frac{\pi x}{L}\right] + L \sin\left[\frac{\pi (X-x)}{L}\right]\right]^4},$$

$$\overline{\mathcal{T}}_{i=1}^{\theta=\infty} = \frac{4 h_{\mathcal{O}} \pi^2 L^2}{\left[2\pi t_1 \sin\left[\frac{\pi X}{L}\right] \sin\left[\frac{\pi x}{L}\right] + L \sin\left[\frac{\pi (x-X)}{L}\right]\right]^4},$$

$$\mathcal{T}_{i=2}^{\theta=\infty} = \frac{h_{\mathcal{O}} \pi^2 \left[L^2 - 4\pi^2 t_1^2 \sin^2\left[\frac{\pi x}{L}\right] + 4\pi t_1 L \sin\left[\frac{\pi x}{L}\right]\cos\left[\frac{\pi x}{L}\right]\right]^2}{L^2 \left[2\pi t_1 \sin\left[\frac{\pi X}{L}\right]\sin\left[\frac{\pi x}{L}\right] + L\sin\left[\frac{\pi(X-x)}{L}\right]\right]^4},$$

$$\overline{\mathcal{T}}_{i=2}^{\theta=\infty} = \frac{h_{\mathcal{O}} \pi^2 \left[L^2 - 4\pi^2 t_1^2 \sin^2\left[\frac{\pi x}{L}\right] - 4\pi t_1 L \sin\left[\frac{\pi x}{L}\right]\cos\left[\frac{\pi x}{L}\right]\right]^2}{L^2 \left[2\pi t_1 \sin\left[\frac{\pi X}{L}\right]\sin\left[\frac{\pi x}{L}\right] + L\sin\left[\frac{\pi(x-X)}{L}\right]\right]^4},$$

(3.16)

$$\mathcal{T}_{i=3}^{\theta=\infty} = \frac{4\pi h_{\mathcal{O}} \sin^4\left[\frac{\pi x}{L}\right]}{L^2 \sin^4\left[\frac{\pi(t_0-x+X)}{L}\right]}, \quad \overline{\mathcal{T}}_{i=3}^{\theta=\infty} = \frac{4\pi h_{\mathcal{O}} \sin^4\left[\frac{\pi x}{L}\right]}{L^2 \sin^4\left[\frac{\pi(t_0+x-X)}{L}\right]},$$

$$\mathcal{T}_{i=4}^{\theta=\infty} = \frac{4\pi h_{\mathcal{O}} \sin^4\left[\frac{\pi(t_0-x)}{L}\right]}{L^2 \sin^4\left[\frac{\pi(t_0-x+X)}{L}\right]}, \quad \overline{\mathcal{T}}_{i=4}^{\theta=\infty} = \frac{4\pi h_{\mathcal{O}} \sin^4\left[\frac{\pi(t_0+x)}{L}\right]}{L^2 \sin^4\left[\frac{\pi(t_0+x-X)}{L}\right]}.$$

For $i = 1, 2$, unlike the Möbius time evolution, $\mathcal{T}_{i=1,2}^{\theta=\infty}$ and $\overline{\mathcal{T}}_{i=1,2}^{\theta=\infty}$ becomes non-periodic functions. Since the functions, $\mathcal{T}_{i=1,2}^{\theta=\infty}$ and $\overline{\mathcal{T}}_{i=1,2}^{\theta=\infty}$, diverge at $t_1 = \frac{L}{2\pi}\left[\cot\left(\frac{\pi X}{L}\right) - \cot\left(\frac{\pi x}{L}\right)\right]$ and $t_1 = \frac{-L}{2\pi}\left[\cot\left(\frac{\pi X}{L}\right) - \cot\left(\frac{\pi x}{L}\right)\right]$, this small ϵ expansion becomes invalid. One possible interpretation of this energy divergence is that the local operator at the spatial location x creates two local excitations called quasiparticles, and they propagate to left and right with velocities $v = \pm 2 \sin^2\left[\frac{\pi x}{L}\right]$. When this local excitations hit the point where we measure the energy densities, they grow drastically. For $i = 1$, the chiral and anti-chiral energy densities at $X = 0$ are independent of t_1. For $i = 2$, the energy densities at $X = 0$ depends on t_1, and for large t_1, the time dependence is approximated by

$$\langle T_{ww}(w_X)\rangle_2 = \langle T_{\overline{ww}}(\overline{w}_X)\rangle_2 \approx \left(\frac{2\pi}{L}\right)^2 \left[-\frac{c}{24} + \frac{16\pi^6 h_{\mathcal{O}} \epsilon^2 t_1^4}{L^6}\right].$$
(3.17)

Thus, in the late time regime, the energy is localized at the origin regardless of the insertion position of the local operator. This accumulation of energy around $X = 0$ can not be described by the propagation of quasiparticles with $v = \pm 2 \sin^2\left[\frac{\pi x}{L}\right]$ because the time for quasiparticles to arrive at the origin is infinite. Thus, this goes beyond the quasiparticle

18

picture. For the late time regime, in the spatial regions where the energy is not localized, the chiral and anti-chiral energy densities are independent of the insertion location of the local operator, and it is given by

$$\langle T_{ww}\left(w_X\right)\rangle_2 = \langle T_{\overline{ww}}\left(\overline{w}_X\right)\rangle_2 \approx \left(\frac{2\pi}{L}\right)^2 \left[-\frac{c}{24} + \frac{\pi^2 h_{\mathcal{O}}\epsilon^2}{L^2 \sin^4\left[\frac{\pi X}{L}\right]}\right]. \tag{3.18}$$

For $i = 3, 4$, $\mathcal{T}_{i=3,4}^{\theta=\infty}$ and $\overline{\mathcal{T}}_{i=3,4}^{\theta=\infty}$ are the periodic functions of t_0 with the period, L. The energy densities at X diverge at the times, $t_0 = \pm(x-X)+nL$. As in for $i = 1, 2$, their time dependence can be described by the quasiparticles that are created by the local operator which propagate to left and right at the speed of light. For $i = 4$, the t_0-dependence of numerators of $\mathcal{T}_{i=4}^{\theta=\infty}$ and $\overline{\mathcal{T}}_{i=4}^{\theta=\infty}$ exhibit the dynamical behavior that is not explained by this quasiparticle picture. For simplicity, focus on the chiral energy density in the middle time regime, when $L \gg t_0 \gg x$ and $L \gg t_0 \gg x - X$. In this time regime, the chiral energy density is approximated by

$$\langle T_{ww}\left(w_X\right)\rangle_4 \approx \left(\frac{2\pi}{L}\right)^2 \left[-\frac{c}{24} + \frac{4\pi\epsilon^2 h_{\mathcal{O}}}{L^2}\right]. \tag{3.19}$$

In the time regime where $L \gg t_0 \gg X - x$, the anti-chiral energy density is approximated by (3.19). This suggests that long after the local excitation has passed the spatial point X, the energy density can deviate from the vacuum one. The energy densities for $i = 3$ do not have such time regimes where the term at order $\mathcal{O}(\epsilon^2)$ is approximated by a constant. Thus, during the non-unitary time evolution, some properties of the energy densities go beyond the quasiparticle picture.

4 Entanglement entropy in Integrable Theories

In the following sections, we will explore the time dependence of a quantity that depends on the operator contents of the 2d CFT, namely the entanglement entropy. In this section, we focus on the time-dependent part of the entanglement entropy in 2d free bosons and rational CFTs (RCFTs). We collectively refer to these theories as integrable theories as opposed to the maximally chaotic holographic CFTs. Let us define the change in the n-th Rényi entanglement entropy as [74]

$$\Delta S_{A,i}^{(n)}(t_i) = \frac{1}{1-n} \log \frac{\mathrm{tr}_A(\rho_A)^n}{(\mathrm{tr}_A\rho_A)^n} - \frac{1}{1-n} \log \frac{\mathrm{tr}_A(\rho_A^{\mathrm{g.s.}})^n}{(\mathrm{tr}_A\rho_A^{\mathrm{g.s.}})^n} \tag{4.1}$$

where ρ_A and $\rho_A^{\mathrm{g.s.}}$ are the density matrices for the local operator excited state and the ground state respectively, and $t_i = t_1$ for $i = 1, 2$ and $t_i = t_0$ for $i = 3, 4$. This change, $\Delta S_{A,i}^{(n)}(t_i)$, is independent of the UV-cutoff because this is defined by subtracting the n-th Rényi entanglement entropy for the vacuum state. Then, in this section, we consider the change in the second Rényi entanglement entropy after the inhomogeneous and homogeneous

local operator quenches. The change in the entanglement entropy after a single local operator quench can be written in terms of a path integral over a n-sheeted Riemann surface with two copies of the local operator on each Riemann sheet [74, 26, 23, 24, 25, 75]

$$
\begin{aligned}
&\Delta S_{A,i}^{(n)}(t_i) \\
&= \frac{1}{1-n} \log \left[\frac{\left\langle \mathcal{O}^\dagger(w_1^{\text{New},i}, \overline{w}_1^{\text{New},i}) \mathcal{O}(w_2^{\text{New},i}, \overline{w}_2^{\text{New},i}) \dots \mathcal{O}^\dagger(w_{2n-1}^{\text{New},i}, \overline{w}_{2n-1}^{\text{New},i}) \mathcal{O}(w_{2n}^{\text{New},i}, \overline{w}_{2n}^{\text{New},i}) \right\rangle_{C^n}}{\left\langle \mathcal{O}^\dagger(w_\epsilon^{\text{New},i}, \overline{w}_\epsilon^{\text{New},i}) \mathcal{O}(w_{-\epsilon}^{\text{New},i}, \overline{w}_{-\epsilon}^{\text{New},i}) \right\rangle_C^n} \right]
\end{aligned}
$$
(4.2)

where

$$
w_1^{\text{New},i} = w_\epsilon^{\text{New},i}, \qquad w_2^{\text{New},i} = w_{-\epsilon}^{\text{New},i}
$$
(4.3)

where C and C^n are the cylinder and n-replicated cylinder and $w_{2j-1}^{\text{New},i}$ and $w_{2j}^{\text{New},i}$ are the corresponding coordinates of $w_1^{\text{New},i}$ and $w_2^{\text{New},i}$ on the jth sheet for $j = 1, \dots, n$. The same is true for the anti-holomorphic coordinates. The branch cut on each Riemann surface runs from $w = iX_2$ to $w = iX_1$ and from $\bar{w} = -iX_2$ to $\bar{w} = -iX_1$. We assume that the local operator is spinless with conformal dimension $h_{\mathcal{O}}$.

Perform a cylinder-to-plane conformal transformation $z = e^{\frac{2\pi w}{L}}$ and $\bar{z} = e^{\frac{2\pi \bar{w}}{L}}$. The branch cut is now given by an arc on the unit circle running from $z_2 = e^{i\frac{2\pi X_2}{L}}$ to $z_1 = e^{i\frac{2\pi X_1}{L}}$ and from $\bar{z}_2 = e^{-i\frac{2\pi X_2}{L}}$ to $\bar{z}_1 = e^{-i\frac{2\pi X_1}{L}}$. Next, we uniformize this Riemann surface with a suitable conformal transformation. To orient the branch cut along arbitrary directions, consider the conformal transformation

$$
\begin{aligned}
\zeta^n &= \frac{z - e^{i\frac{2\pi X_2}{L}}}{e^{i\frac{2\pi X_1}{L}} - z} e^{i\psi} = -e^{i\psi + i\frac{\pi(X_2-X_1)}{L}} \frac{\sinh \frac{\pi(w-iX_2)}{L}}{\sinh \frac{\pi(w-iX_1)}{L}}, \\
\overline{\zeta}^n &= \frac{\bar{z} - e^{-i\frac{2\pi X_2}{L}}}{e^{-i\frac{2\pi X_1}{L}} - \bar{z}} e^{-i\psi} = -e^{-i\psi + i\frac{\pi(X_1-X_2)}{L}} \frac{\sinh \frac{\pi(\bar{w}+iX_2)}{L}}{\sinh \frac{\pi(\bar{w}+iX_1)}{L}}
\end{aligned}
$$
(4.4)

where $\psi \in \mathbb{R}$ is an arbitrary parameter that allows us to orient the branch cut so that the branch cut is oriented along the rays with arguments $\psi - \frac{\pi(X_1-X_2)}{L}$ and $\frac{\pi(X_1-X_2)}{L} - \psi$ on the ζ^n and $\overline{\zeta}^n$ complex planes respectively. Note that it does not matter whether or not $X_2 < X_1$ or $X_1 < X_2$. In both cases, the branch cut lies along the same direction.

4.1 Second Rényi Entropy

For simplicity, set $n = 2$. The uniformized coordinates are related by $\zeta_1^{\text{New},i} = -\zeta_3^{\text{New},i}$ and $\zeta_2^{\text{New},i} = -\zeta_4^{\text{New},i}$ and $\overline{\zeta}_1^{\text{New},i} = -\overline{\zeta}_3^{\text{New},i}$ and $\overline{\zeta}_2^{\text{New},i} = -\overline{\zeta}_4^{\text{New},i}$. By performing a conformal transformation

$$
\eta = \frac{(Z - Z_1)(Z_3 - Z_4)}{(Z - Z_4)(Z_3 - Z_1)}, \qquad \overline{\eta} = \frac{(\overline{Z} - \overline{Z}_1)(\overline{Z}_3 - \overline{Z}_4)}{(\overline{Z} - \overline{Z}_4)(\overline{Z}_3 - \overline{Z}_1)},
$$
(4.5)

arbitrary four-point functions on the complex plane can be written as

$$\left\langle \mathcal{O}^\dagger(Z_1, \overline{Z}_1)\mathcal{O}(Z_2, \overline{Z}_2)\mathcal{O}^\dagger(Z_3, \overline{Z}_3)\mathcal{O}(Z_4, \overline{Z}_4)\right\rangle_{\mathbb{C}} \tag{4.6}$$
$$= \frac{1}{Z_{13}^{2h_\mathcal{O}} Z_{24}^{2h_\mathcal{O}}} \frac{1}{\overline{Z}_{13}^{2\overline{h}_\mathcal{O}} \overline{Z}_{24}^{2\overline{h}_\mathcal{O}}} \lim_{\eta_4, \overline{\eta}_4 \to \infty} \eta_4^{2h_\mathcal{O}} \overline{\eta}_4^{2\overline{h}_\mathcal{O}} \left\langle \mathcal{O}^\dagger(0)\mathcal{O}(\eta_2, \overline{\eta}_2)\mathcal{O}^\dagger(1)\mathcal{O}(\infty)\right\rangle_{\mathbb{C}}$$

where $\eta_2, \overline{\eta}_2$ are the cross-ratios and $Z_{ij} = Z_i - Z_j$. These cross ratios are defined as

$$\eta_2 = \frac{Z_{12} Z_{34}}{Z_{13} Z_{24}}, \qquad \overline{\eta}_2 = \frac{\overline{Z}_{12} \overline{Z}_{34}}{\overline{Z}_{13} \overline{Z}_{24}}. \tag{4.7}$$

Therefore, the ratio of correlation functions in (4.2) can be written as a function of the cross-ratio alone

$$\frac{\left\langle \mathcal{O}^\dagger(w_1^{\text{New},i}, \overline{w}_1^{\text{New},i})\mathcal{O}(w_2^{\text{New},i}, \overline{w}_2^{\text{New},i})\mathcal{O}^\dagger(w_3^{\text{New},i}, \overline{w}_3^{\text{New},i})\mathcal{O}(w_4^{\text{New},i}, \overline{w}_4^{\text{New},i})\right\rangle_{C^2}}{\left\langle \mathcal{O}^\dagger(w_\epsilon^{\text{New},i}, \overline{w}_\epsilon^{\text{New},i})\mathcal{O}(w_{-\epsilon}^{\text{New},i}, \overline{w}_{-\epsilon}^{\text{New},i})\right\rangle_C^2}$$
$$= [\eta_2(1 - \eta_2)\overline{\eta}_2(1 - \overline{\eta}_2)]^{2h_\mathcal{O}} \, G(\eta_2, \overline{\eta}_2) \tag{4.8}$$

where

$$G(x, \bar{x}) = \lim_{\eta, \overline{\eta} \to \infty} \eta^{2h_\mathcal{O}} \overline{\eta}^{2h_\mathcal{O}} \left\langle \mathcal{O}^\dagger(0)\mathcal{O}(x, \bar{x})\mathcal{O}^\dagger(1)\mathcal{O}(\infty)\right\rangle_{\mathbb{C}} \tag{4.9}$$

and the cross-ratio is

$$\eta_2 = \frac{(\zeta_1 - \zeta_2)(\zeta_3 - \zeta_4)}{(\zeta_1 - \zeta_3)(\zeta_2 - \zeta_4)}, \qquad \overline{\eta}_2 = \frac{(\overline{\zeta}_1 - \overline{\zeta}_2)(\overline{\zeta}_3 - \overline{\zeta}_4)}{(\overline{\zeta}_1 - \overline{\zeta}_3)(\overline{\zeta}_2 - \overline{\zeta}_4)} \tag{4.10}$$

These formulas (4.8), (4.9) and (4.10) hold for arbitrary choices of the branch cut direction ψ as one would expect. The change in the second Rényi entropy for a quench by the local operator $\mathcal{O}$ in any 2d CFT is

$$\Delta S_{A,i}^{(2)}(t_i) = -\log\left[\eta_2(1 - \eta_2)\overline{\eta}_2(1 - \overline{\eta}_2)\right]^{2h_\mathcal{O}} G(\eta_2, \overline{\eta}_2) \tag{4.11}$$

Free Boson

To obtain non-trivial entanglement dynamics under the local operator quench, we simply choose the local operator to be a sum of vertex operators [26, 23, 24]

$$\mathcal{O} = \frac{e^{\frac{i}{2}\phi} + e^{-\frac{i}{2}\phi}}{\sqrt{2}} \tag{4.12}$$

where ϕ is a $c = 1$ free boson. This local operator has conformal dimensions $h_\mathcal{O} = \overline{h}_\mathcal{O} = \frac{1}{8}$ and the four-point function (4.9) is

$$G(z, \bar{z}) = \frac{1 + |z| + |1 - z|}{2\sqrt{|z(1 - z)|}} \tag{4.13}$$

The change in entanglement entropy for the sum of vertex operator (4.12) is [26]

$$\Delta S_{A,i}^{(2)}(t_i) = \log \frac{2}{1 + |\eta_2| + |1 - \eta_2|}. \tag{4.14}$$

just as in [75]. As we will see later, when $\frac{\epsilon}{L} \to 0$, the cross ratios $\eta_2, \overline{\eta}_2 \to 0, 1$. For these four possibilities, the second Rényi entropy (4.14) to leading order in $\frac{\epsilon}{L}$ is

$$\Delta S_{A,i}^{(2)}(t_i) \xrightarrow{\epsilon/L \to 0} \begin{cases} 0, & \text{if} & \eta_2, \overline{\eta}_2 \to 0 & \text{or} & \eta_2, \overline{\eta}_2 \to 1 \\ \log 2, & \text{if} & \eta_2 \to 0, \overline{\eta}_2 \to 1 & \text{or} & \eta_2 \to 1, \overline{\eta}_2 \to 0 \end{cases} \tag{4.15}$$

General RCFTs

For general RCFTs, the four-point function can be written as a sum over intermediate primaries as [76, 25, 74]

$$G(z, \overline{z}) = \sum_b (C_{\mathcal{O}\mathcal{O}}^b)^2 F_{\mathcal{O}}(b|z) \overline{F}_{\mathcal{O}}(b|\overline{z}) \tag{4.16}$$

where b runs over the primaries and the conformal blocks are normalized so that $F_{\mathcal{O}}(b|z) = z^{h_b - 2h_{\mathcal{O}}}(1 + \mathcal{O}(z))$. By using a fusion transformation, the cross ratios of the conformal blocks can be changed as

$$F_{\mathcal{O}}(b|1 - z) = \sum_c F_{bc}[\mathcal{O}] F_{\mathcal{O}}(c|z) \tag{4.17}$$

For RCFTs,

$$F_{00}[\mathcal{O}] = \frac{1}{d_{\mathcal{O}}} \tag{4.18}$$

where 0 is the vacuum and $d_{\mathcal{O}}$ is the quantum dimension of the primary operator $\mathcal{O}$. When the cross ratios $\eta_2, \overline{\eta}_2 \to 0, 1$, applying the asymptotic form of the conformal blocks as well as the fusion transformation (4.17) and the crossing symmetry gives

$$\Delta S_{A,i}^{(2)}(t_i) \xrightarrow{\epsilon/L \to 0} \begin{cases} 0, & \text{if} & \eta_2, \overline{\eta}_2 \to 0 & \text{or} & \eta_2, \overline{\eta}_2 \to 1 \\ \log d_{\mathcal{O}}, & \text{if} & \eta_2 \to 0, \overline{\eta}_2 \to 1 & \text{or} & \eta_2 \to 1, \overline{\eta}_2 \to 0 \end{cases} \tag{4.19}$$

This is exactly the same behaviour as for the free boson (4.14), but with $\log d_{\mathcal{O}}$ instead of $\log 2$. Therefore, the results of the local operator quench in the RCFT can be obtained from that of the free boson by simply replacing $\log 2$ with $\log d_{\mathcal{O}}$.

Cross ratio

The cross ratio does not depend on the operator content of the 2d CFTs and is explicitly given by

$$\eta_2 = \frac{1}{2} \left[1 - \frac{\left(\zeta_{+\epsilon}^{\text{New},i} \right)^2 + \left(\zeta_{-\epsilon}^{\text{New},i} \right)^2}{2 \zeta_{+\epsilon}^{\text{New},i} \zeta_{-\epsilon}^{\text{New},i}} \right]. \tag{4.20}$$

The same expression holds for the anti-holomorphic components by replacing the holomorphic quantities with the anti-holomorphic quantities. These expressions (4.14) and (4.20) are valid for arbitrary directions of the uniformization branch cut ψ as expected. The only subtlety in the computation of the cross ratio (4.20) lies in the computation of the denominator. In what follows, let $\hat{\cdot}$ denote both holomorphic and anti-holomorphic coordinates and $\sigma = +1/-1$ for holomorphic/anti-holomorphic coordinates. For example, $\hat{\zeta}_{\rho\epsilon}$ denote both holomorphic and anti-holomorphic coordinates with $\rho = \pm 1$ indicating their Euclidean time positions. Assume that to second order in the small ϵ expansion, where $\delta = \frac{2\pi\epsilon}{L} \ll 1$, these coordinates take the form

$$\hat{\zeta}_{\rho\epsilon}^2 = \xi_0(t_i, L, x, X_1, X_2, \theta, \sigma)\left[1 + i\delta\rho\xi_1(t_i, L, x, X_1, X_2, \theta, \sigma) + \delta^2\xi_2(t_i, L, x, X_1, X_2, \theta, \sigma)\right] \tag{4.21}$$

where ξ_0, ξ_1, ξ_2 are arbitrary real functions that are independent of ρ and x is the spatial location of the local operator insertion. To first order in $\delta \ll 1$,

$$\hat{\zeta}_{\rho\epsilon}^2 = \xi_0(t_i, L, x, X_1, X_2, \theta, \sigma) + i\delta\rho\xi_0(t_i, L, x, X_1, X_2, \theta, \sigma)\xi_1(t_i, L, x, X_1, X_2, \theta, \sigma). \tag{4.22}$$

Assume that $\xi_0(t_i, L, x, X_1, X_2, \theta, \sigma), \xi_1(t_i, L, x, X_1, X_2, \theta, \sigma) \in \mathbb{R}$, are finite and

$$\xi_0(t_i, L, x, X_1, X_2, \theta, \sigma), \xi_1(t_i, L, x, X_1, X_2, \theta, \sigma) \neq 0. \tag{4.23}$$

This means that $\xi_0(t_i, L, x, X_1, X_2, \theta, \sigma)\xi_1(t_i, L, x, X_1, X_2, \theta, \sigma)$ is finite and non-zero. Therefore, to linear order in δ, $\hat{\zeta}_{\pm\epsilon}^2$ are two numbers that lie slightly off the positive or negative real axis on the complex $\zeta, \bar{\zeta}$ planes. Following [25], we choose the phase ψ in the uniformization map (4.4) such that the branch cut lies on the negative real axis on the complex $\zeta^n, \bar{\zeta}^n$ plane. If $\xi_0(t_i, L, x, X_1, X_2, \theta, \sigma) > 0$, then $\hat{\zeta}_{\rho\epsilon}^2$ lies slightly off the positive real axis for both $\rho = \pm 1$ and in the $\delta \to 0$,

$$\hat{\zeta}_{\rho\epsilon} = \sqrt{\xi_0}\sqrt{1 + i\delta\rho\xi_1 + \delta^2\xi_2} \tag{4.24}$$

so the denominator of the cross ratio (4.20) is

$$\hat{\zeta}_{+\epsilon}\hat{\zeta}_{-\epsilon} = \xi_0\left[1 + \frac{1}{2}\delta^2(\xi_1^2 + 2\xi_2)\right] \tag{4.25}$$

On the other hand, if $\xi_0(t_i, L, x, X_1, X_2, \theta, \sigma) < 0$, these coordinates $\hat{\zeta}_{+\epsilon}^2$ will lie slightly off the negative real axis where the branch cut is located. In order to take the $\delta \to 0$ limit while avoiding the branch cut, we can rotate them as such

$$\hat{\zeta}_{\rho_1\epsilon}^2 = e^{i\pi}\left(-\hat{\zeta}_{\rho_1\epsilon}^2\right), \qquad \hat{\zeta}_{\rho_2\epsilon}^2 = e^{-i\pi}\left(-\hat{\zeta}_{\rho_2\epsilon}^2\right) \tag{4.26}$$

where $(\rho_1, \rho_2) = (1, -1)$ or $(\rho_1, \rho_2) = (-1, 1)$ depending on the sign of $\xi_0\xi_1$. The function $-\hat{\zeta}_{\pm\epsilon}^2$ now lie slightly off the positive real axis and we can safely take the $\delta \to 0$ limit. The denominator in the cross ratio when $\xi_0 < 0$ is approximately given by

$$\hat{\zeta}_{+\epsilon}^2\hat{\zeta}_{-\epsilon}^2 = \sqrt{|\xi_0|\left[1 + i\delta\xi_1 + \delta^2\xi_2\right]}\sqrt{|\xi_0|\left[1 - i\delta\xi_1 + \delta^2\xi_2\right]} = |\xi_0|\left[1 + \frac{1}{2}\delta^2(\xi_1^2 + 2\xi_2)\right] \tag{4.27}$$

23

Therefore, for both sign of ξ_0, as long as $\xi_0 \neq 0$ and is finite,

$$\hat{\zeta}_{+\epsilon}\hat{\zeta}_{-\epsilon} = |\xi_0| \left[1 + \frac{1}{2}\delta^2(\xi_1^2 + 2\xi_2) \right] \tag{4.28}$$

Putting this back into the cross ratio (4.20), we find that to quadratic order in δ, the cross ratio is given by

$$\hat{\eta}_2 = \frac{1}{2} \left\{ 1 - \text{sgn}(\xi_0) \left[1 - \frac{1}{2}\delta^2\xi_1^2 \right] \right\} \tag{4.29}$$

which does not depend on ξ_2. Of course, we require that ξ_2 does not depend on $\rho = \pm 1$ and does not diverge and that both ξ_0, ξ_1 are finite and non-zero. It does not matter if ξ_2 vanishes or not.

Simple Example

The results for the change in the second Rényi entropy for these integrable theories for various choices of subsystems and two different local operator insertion positions are listed in Appendix C. Let us list the result for one such case here. Consider a subsystem that contains the origin as in case (a) and place the local operator at X_2^f. For Lorentzian time evolution with the SSD Hamiltonian, $i = 1, 2$, the cross ratio to second order in $\frac{\epsilon}{L}$ is

$$\hat{\eta}_2 = \frac{1}{2} \left\{ 1 - \text{sgn} \left[\frac{t_1 - \frac{\sigma L}{2\pi}\cot\frac{\pi X_2}{L}}{t_1 - \frac{\sigma L}{2\pi}\cot\frac{\pi X_1}{L}} \right] \left[1 - \left(\frac{\epsilon}{L}\right)^2 \times \text{positive number} \right] \right\} \tag{4.30}$$

so $\eta_2, \overline{\eta}_2 \to 0, 1$ as $\frac{\epsilon}{L} \to 0$ as mentioned earlier. The change in the second Rényi entropy for $i = 1, 2$ becomes

$$\Delta S_{A,i}^{(2)}(t_1) = \begin{cases} \log 2, & i = 1, 2, \frac{L}{2\pi}\cot\frac{\pi X_2}{L} < t_1 < \frac{L}{2\pi}|\cot\frac{\pi X_1}{L}| \\ 0 & i = 1, 2, 0 < t_1 < \frac{L}{2\pi}\cot\frac{\pi X_2}{L} \quad \text{and} \quad \frac{L}{2\pi}|\cot\frac{\pi X_1}{L}| < t_1 \end{cases} \tag{4.31}$$

in the free boson CFT and the $\log 2$ gets replaced with $\log d_{\mathcal{O}}$ for generic RCFTs. This is well-described by the quasiparticle picture which is detailed in the following subsection.

4.2 Quasiparticle Picture

It turns out that the behavior of the change in the second Rényi entropy is well-described by a quasiparticle picture. At the initial time $t_i = 0$, for $i = 0, 1$, a Bell pair of quasiparticles, one left-moving and the other right-moving, are created at the position of the local operator $\mathcal{O}$. These quasiparticles propagate with speed given by the envelope function $f(x)$ defined in (2.2).

For finite values of θ, a quasiparticle that begins at position x arrives at position X at time t_i given by

$$\tan\frac{\pi t_i}{L\cosh 2\theta} = \mu e^{2\theta} \frac{\tan\frac{\pi X}{L} - \tan\frac{\pi x}{L}}{1 + e^{4\theta}\tan\frac{\pi X}{L}\tan\frac{\pi x}{L}}, \tag{4.32}$$

where $\mu = +1/-1$ for right/left moving quasiparticles as found previously in [45, 65]. For the uniform Hamiltonian, setting $\theta = 0$ gives $X = (x + \mu t_0) \bmod L$ which is the trajectory for quasiparticles moving with uniform unit speed. Since we think of the local operators at x as the source of the quasiparticles and the endpoints of the subsystems X_1 and X_2 as the target X, by looking at the corresponding factors in the coordinates $\hat{\zeta}^n_{\rho\epsilon}$, we see that the holomorphic coordinates correspond to the left moving quasiparticles and the anti-holomorphic coordinates correspond to the right moving ones.

In the SSD limit, a quasiparticle that starts off at position x at $t_1 = 0$ winds up at position X at time t_1 that is determined by

$$\pm t_1 = \frac{L}{2\pi} \left(\cot \frac{\pi x}{L} - \cot \frac{\pi X}{L} \right) \tag{4.33}$$

where $+/-$ corresponds to right/left moving quasiparticles. The factor of $\cot \frac{\pi x}{L}$ diverges at X_1^f since the quasiparticles that start off at that position don't move. To get non-trivial entanglement dynamics, place the local operator at the other fixed point X_2^f.

The second Rényi entropy of a subsystem in the local operator excited state is the same as that of the vacuum state unless the subsystem contains exactly one member of the entangled bell pair of quasiparticles in which case the second Rényi entropy increases by an amount that is determined by the local operator $\mathcal{O}$.

4.3 Summary for integrable theories

While the calculation for the change in the second Rényi entropy for the local operator excited state in integrable theories is involved, the final result is simple and easy to understand. Therefore, we summarize the key physical result here and relegate the details of the calculation to Appendix C.

The entanglement entropy is described by a pair of bell pairs that are created at the location of the local operator insertion as first described in [25] with the qubits propagating with a speed given by the Möbius/SSD envelope function. When either member of the bell pair, but not both, is inside the subsystem, the second Rényi entropy increases by $\log 2$ for Hermitian sum of vertex operators (4.12) in the free boson theory and by $\log d_{\mathcal{O}}$ in general RCFTs for a primary $\mathcal{O}$.

The entanglement entropy is completely determined by the unitary time evolution operator and does not depend on the regulator Hamiltonian except for certain choices of x which causes the regulator to vanish. This is because the coordinates $\zeta^2_{\pm\epsilon}$ have a real part that at the leading $\mathcal{O}\left(\left(\frac{\epsilon}{L}\right)^0\right)$ order is given by the unitary operator while the imaginary part at the leading $\mathcal{O}\left(\left(\frac{\epsilon}{L}\right)\right)$ order is dependent on the regulator Hamiltonian. These coordinates therefore lie slightly off the real axis of the complex $\zeta^2, \bar{\zeta}^2$ planes with the real part determined by the unitary time evolution while the regulator Hamiltonian only serves to introduce a small separation between the two operators $\mathcal{O}$ and $\mathcal{O}^\dagger$. The jumps in the second Rényi entanglement entropy are determined by the location of the operators along the real axis and hence

only depend on the unitary time evolution. This also explains why swapping the order of the Lorentzian and Euclidean time evolution operators has no effect on the change in the second Rényi entropy to leading order in $\frac{\epsilon}{L}$ when $\Delta S_{A,i}^{(2)}(t_i)$ is finite for the three choices of subsystems (a), (b) and (c) considered in this paper, including the case where the interval $A = [0, X_1]$, $0 < X_1 < \frac{L}{2}$, ends on the fixed point X_1^f. Since the leading order term in $\frac{\epsilon}{L}$ in the coordinates and hence the cross ratios are independent of the ordering of the Lorentzian and Euclidean evolution, so is the change in the second Rényi entropy $\Delta S_{A,i}^{(2)}(t_i)$ to leading order. However, the order of the Lorentzian and Euclidean time evolution does affect the times at which $\Delta S_{A,i}^{(2)}(t_i)$ diverges which only occurs when the Euclidean time evolution is generated by the SSD Hamiltonian. When the local operator is inserted at X_1^f, $\Delta S_{A,3}^{(2)}(t_0)$ diverges for all t_0 while $\Delta S_{A,4}^{(2)}(t_0)$ diverges only for $t_0 = nL$ where $n \in \mathbb{Z}$. On the other hand, when the local operator is inserted at X_2^f, $\Delta S_{A,3}^{(2)}(t_0)$ remains finite for all t_0 while $\Delta S_{A,4}^{(2)}(t_0)$ diverges when $t_0 = \left(n + \frac{1}{2}\right) L$ where $n \in \mathbb{Z}$.

5 Entanglement entropy in two-dimensional Holographic CFTs (2d holographic CFTs)

Here, we explore the time dependence of $S_{A,i}$ during the Möbius/SSD time evolution. We begin by the Euclidean Rényi entanglement entropy in (2.17), and then map from the cylinder to the complex plane, $(z, \overline{z}) = (e^{\frac{2\pi w}{L}}, e^{\frac{2\pi \overline{w}}{L}})$. Then, $S_{A,i,E}^{(n)}$ is given by

$$S_{A,i,E}^{(n)} = \frac{1}{1-n} \log \left[\frac{\left\langle \mathcal{O}_n^\dagger(z_\epsilon^{\text{New},i}, \overline{z}_\epsilon^{\text{New},i}) \sigma_n(z_{X_1}, \overline{z}_{X_1}) \overline{\sigma}_n(z_{X_2}, \overline{z}_{X_2}) \mathcal{O}_n(z_{-\epsilon}^{\text{New},i}, \overline{z}_{-\epsilon}^{\text{New},i}) \right\rangle}{\left\langle \mathcal{O}^\dagger(z_\epsilon^{\text{New},i}, \overline{z}_\epsilon^{\text{New},i}) \mathcal{O}(z_{-\epsilon}^{\text{New},i}, \overline{z}_{-\epsilon}^{\text{New},i}) \right\rangle^n} \right] \tag{5.1}$$
$$- \frac{c(1+n)}{24n} \log \left[\prod_{i=1,2} \left| \frac{dz_{X_i}}{dw_{X_i}} \right| \right],$$

where $z_{\pm\epsilon}^{\text{New},i} = e^{\frac{2\pi w_{\pm\epsilon}^{\text{New},i}}{L}}$, $z_{X_{i=1,2}} = e^{\frac{2\pi w_{X_{i=1,2}}}{L}}$ and $\overline{z}$ is the complex conjugate of z. Furthermore, to simplify the form of $S_{A,i,E}^{(n)}$, we perform a conformal map,

$$\tilde{z}(z) = \frac{\left(z_\epsilon^{\text{New},i} - z\right)\left(z_{X_2} - z_{-\epsilon}^{\text{New},i}\right)}{\left(z - z_{-\epsilon}^{\text{New},i}\right)\left(z_\epsilon^{\text{New},i} - z_{X_2}\right)}, \quad \overline{\tilde{z}}(\overline{z}) = \frac{\left(\overline{z}_\epsilon^{\text{New},i} - \overline{z}\right)\left(\overline{z}_{X_2} - \overline{z}_{-\epsilon}^{\text{New},i}\right)}{\left(\overline{z} - \overline{z}_{-\epsilon}^{\text{New},i}\right)\left(\overline{z}_\epsilon^{\text{New},i} - \overline{z}_{X_2}\right)}. \tag{5.2}$$

Then, (5.1) reduces to the function of the cross ratios $(z_{c,i}, \overline{z}_{c,i})$,

$$S_{A,i,E}^{(n)} = \frac{1}{1-n} \log \left[|z_{X_1} - z_{X_2}|^{-4nh_n} |1 - z_{c,i}|^{4nh_n} G_n(z_{c,i}, \overline{z}_{c,i}) \right] - \frac{c(n+1)}{6n} \log \left(\frac{2\pi}{L} \right), \tag{5.3}$$

where $(z_{c,i}, \overline{z}_{c,i})$ are defined as

$$(z_{c,i}, \overline{z}_{c,i}) = \left(\frac{\left(z_{\epsilon}^{\text{New},i} - z_{X_1} \right) \left(z_{X_2} - z_{-\epsilon}^{\text{New},i} \right)}{\left(z_{X_1} - z_{-\epsilon}^{\text{New},i} \right) \left(z_{\epsilon}^{\text{New},i} - z_{X_2} \right)}, \frac{\left(\overline{z}_{\epsilon}^{\text{New},i} - \overline{z}_{X_1} \right) \left(\overline{z}_{X_2} - \overline{z}_{-\epsilon}^{\text{New},i} \right)}{\left(\overline{z}_{X_1} - \overline{z}_{-\epsilon}^{\text{New},i} \right) \left(\overline{z}_{\epsilon}^{\text{New},i} - \overline{z}_{X_2} \right)} \right). \tag{5.4}$$

Here, we assume that $z_{c,i}, \overline{z}_{c,i} \approx 1$, and then we perform the OPE at $z_{c,i}, \overline{z}_{c,i} \approx 1$. Subsequently, we closely look at the behavior of $\log G_n(z_{c,i}, \overline{z}_{c,i})$ at the leading order of the small n limit, where $n \approx 1$. The leading behavior of $\log G_n(z_{c,i}, \overline{z}_{c,i})$ reduces to

$$\log G_n(z_{c,i}, \overline{z}_{c,i}) \approx \frac{c(1-n)}{6} \log \left[\frac{z_{c,i}^{\frac{(1-\alpha_{\mathcal{O}})}{2}} \overline{z}_{c,i}^{\frac{(1-\overline{\alpha}_{\mathcal{O}})}{2}} (1 - z_{c,i}^{\alpha_{\mathcal{O}}})(1 - \overline{z}_{c,i}^{\overline{\alpha}_{\mathcal{O}}})}{\alpha_{\mathcal{O}} \overline{\alpha}_{\mathcal{O}}} \right], \tag{5.5}$$

where $\alpha_{\mathcal{O}} = \overline{\alpha}_{\mathcal{O}} = \sqrt{1 - 24 h_{\mathcal{O}}/c}$. Consequently, in the Von Neumann limit, $n \to 1$, (5.3) reduces to

$$\begin{aligned} S_{A,i,E} =& \frac{c}{6} \log \left[\frac{z_{c,i}^{\frac{1-\alpha_{\mathcal{O}}}{2}} \overline{z}_{c,i}^{\frac{1-\overline{\alpha}_{\mathcal{O}}}{2}} (1 - z_{c,i}^{\alpha_{\mathcal{O}}})(1 - \overline{z}_{c,i}^{\overline{\alpha}_{\mathcal{O}}})}{\alpha_{\mathcal{O}} \overline{\alpha}_{\mathcal{O}}} \right] \\ &+ \frac{c}{6} \log \left[|z_{X_1} - z_{X_2}|^2 \right] - \frac{c}{6} \log \left[|1 - z_{c,i}|^2 \right] - \frac{c}{3} \log \left(\frac{2\pi}{L} \right). \end{aligned} \tag{5.6}$$

Finally, take the analytic continuation, $\tau_1 = it_1$ and $\tau_0 = it_0$. We will explore the time evolution of $S_{A,i}$ in the three cases shown in Fig. 3 In this section, the insertions of local operator are at $x = X_{a=1,2}^f$. We will explore the characteristic properties of the dynamics for the state, $|\Psi\rangle_i$, by investigating the time dependence of entanglement entropy.

5.1   Möbius Hamiltonian

Here, we will investigate the time dependence of $S_{A,i}$ for finite θ. First, we will explore the time dependence of $S_{A,i}$ when the local operator is inserted at $x = X_1^f = 0$, and then we will explore the time dependence for the insertion at $x = X_2^f = L/2$ of the local operator.

5.1.1   When the local operator is inserted at $x = X_1^f = 0$.

Let us present the time dependence of the cross ratios for $i = 1 \sim 4$ when the local operator is inserted at $x = X_1^f = 0$. To explore the properties of dynamics irrelevant to the regulator as possible, we investigate the time dependence of the cross ratios and $S_{A,i}$ in the small ϵ expansion, $\frac{\epsilon}{L} \ll 1$. When the local operator is inserted at x, the small ϵ expansion of the cross ratios analytically-continued to the real time is approximated by

$$\begin{aligned} z_{c,i} &\approx 1 + i\epsilon f_i(T_i, x, \theta) \\ \overline{z}_{c,i} &\approx 1 + i\epsilon g_i(T_i, x, \theta), \end{aligned} \tag{5.7}$$

where $T_{i=1,2} = t_1$, $T_{i=3,4} = t_0$, and x denotes the insertion point of the local operator. For all the subsystems and the locations, considered in this paper, of the local operator, in the small ϵ limit, the next-to-leading terms of $z_{c,i}$ and $\overline{z}_{c,i}$ are $\mathcal{O}(\epsilon)$, and they are pure imaginary. We define $f_i(T_i, x, \theta)$ and $g_i(T_i, x, \theta)$ as the coefficient of $i\epsilon$ of $z_{c,i}$ and $\overline{z}_{c,i}$. The details of the cross ratios, when the local operator is inserted at X_1^f, are reported in Appendix D.1. In (5.7), the θ in $f_i(T_i, x, \theta)$ or $g_i(T_i, x, \theta)$ is a finite number. We use $f_i(T_i, x, \infty)$ or $g_i(T_i, x, \infty)$ to represent the limit as $\theta \to \infty$. We represent the time dependence of the cross ratio by the second order in the small ϵ limit. Define t_x by

$$t_x = \frac{L_{\text{eff}}}{\pi} \tan^{-1} \left[e^{2\theta} \tan \left(\frac{\pi x}{L} \right) \right]. \tag{5.8}$$

For $i = 1, 2$, $f_{i=1,2}(T_{i=1,2}, X_1^f, \theta)$ $(g_{i=1,2}(T_{i=1,2}, X_1^f, \theta))$ is positive in the time intervals, $nL_{\text{eff}} + t_{L-X_2} > t_1 > nL_{\text{eff}} + t_{L-X_1}$ $((n+1)L_{\text{eff}} + t_{X_2} > t_1 > nL_{\text{eff}} + t_{X_1})$, where n is an non-negative integer. It is negative in the time intervals, $(n+1)L_{\text{eff}} + t_{L-X_1} > t_1 > nL_{\text{eff}} + t_{L-X_2}$ $(nL_{\text{eff}} + t_{X_1} > t_1 > nL_{\text{eff}} + t_{X_2})$. Since the denominators of $f_{i=1,2}(T_{i=1,2}, X_1^f, \theta)$ $(g_{i=1,2}(T_{i=1,2}, X_1^f, \theta))$ vanishes around the times, $t_1 = nL_{\text{eff}} + t_{L-X_1}$ or $t_1 = nL_{\text{eff}} + t_{L-X_2}$ $(t_1 = nL_{\text{eff}} + t_{X_1}$ or $t_1 = nL_{\text{eff}} + t_{X_2})$, the small ϵ expansion in (5.7) breaks down. For $i = 3, 4$, $f_{i=3,4}(T_{i=1,2}, X_1^f, \theta)$ $(g_{i=3,4}(T_{i=1,2}, X_1^f, \theta))$ is positive in the time intervals, $nL - X_2 > t_0 > nL - X_1$ $((n+1)L + X_2 > t_0 > nL + X_1)$, while it is negative in the time intervals, $(n+1)L - X_1 > t_0 > nL - X_2$ $(nL + X_2 > t_0 > nL + X_1)$. Since $f_{i=1,2}(T_{i=1,2}, X_1^f, \theta)$ $(g_{i=1,2}(T_{i=1,2}, X_1^f, \theta))$ vanishes around the times $t_0 = nL - X_2$ or $t_0 = nL - X_1$ $(t_0 = nL + X_2$ or $t_0 = nL + X_1)$, the small ϵ expansion in (5.7) breaks down. As in [27], this suggests that we need to choose a different branch from that before the trajectory of the cross ratio encircles the origin,

$$z_{c,i} \to e^{\pm 2i\pi} z_{c,i}, \overline{z}_{c,i} \to e^{\pm 2i\pi} \overline{z}_{c,i}. \tag{5.9}$$

where $\pm$ is determined by how the trajectory encircles the origin. For example in the case of $z_{c,3}$, when $L - X_1 > t_0 > 0$, the location of $z_{c,3}$ is infinitesimally negative along the imaginary direction. Conversely, within the interval $L - X_2 > t_0 > L - X_1$, the location becomes infinitesimally positive. This suggests that around $t_0 = L - X_1$, the trajectory of $z_{c,3}$ encircles the origin clockwise, so that $z_{c,3} \to e^{-2i\pi} z_{c,3}$. The values of (5.6) depends on the branches, and the entanglement entropy in 2d holographic CFTs should be given by the geodesics length, [77, 78]. In this section, we assume that the trajectories of cross ratios respect causality, and we choose the branches such that the value of (5.6) is minimized. Thus, we determine the time dependence of $S_{A,i}$.

Before reporting the detailed time evolution of $S_{A,i}$, we will present the common behavior of $S_{A,i}$ for the Möbius case. The outlined time dependence of $S_{A,i}$ follows the propagation of the quasiparticles as in the integrable theories explained above. In other words, the local operator produces an entangled pair at its insertion point, and the quasiparticles of this pair propagate left and right at the velocity determined by the envelope function. The time dependence of $S_{A,i=1,2}$ $(S_{A,i=3,4})$ are given by the periodic functions of t_1 (t_0) with the period, L_{eff} (L). Unlike the integrable theories, the detailed time dependence of entanglement entropy

for $i = 1$ $(i = 3)$ is different from that for $i = 2$ $(i = 4)$. In other words, in the time intervals where the value of entanglement entropy is larger than that of the vacuum one, the value of $S_{A,i=1}$ $(S_{A,i=3})$ is different from that of $S_{A,i=2}$ $(S_{A,i=4})$. Therefore, the time dependence of $S_{A,i}$ in 2d CFTs depends on the time ordering of the Euclidean and real time evolution. Since we can see from the time dependence of $S_{A,i}$ for (a) that the characteristic behavior of entanglement dynamics for the Möbius case, we present $S_{A,i}$ only for (a) here, and report on that for (b) and (c) in Appendix E.1.1. The time dependence of $S_{A,i}$ is given by

$$S_{A,1} \approx \frac{c}{3} \log \left[\frac{L}{\pi} \sin \left(\frac{\pi (X_1 - X_2)}{L} \right) \right]$$

$$+ \begin{cases} 0 & t_{L-X_1} > t_1 > 0 \\ \frac{c}{6} \log \left[\frac{2 \sin[\pi \alpha_{\mathcal{O}}]}{\alpha_{\mathcal{O}}} \right] - \frac{c}{6} \log \left[\epsilon f_1(t_1, X_1^f, \theta) \right] & nL_{\text{eff}} + t_{1,+}^t > t_1 > nL_{\text{eff}} + t_{L-X_1} \\ \frac{c}{6} \log \left[\frac{2 \sin[\pi \alpha_{\mathcal{O}}]}{\alpha_{\mathcal{O}}} \right] - \frac{c}{6} \log \left[\epsilon g_1(t_1, X_1^f, \theta) \right] & nL_{\text{eff}} + t_{X_2} > t_1 > nL_{\text{eff}} + t_{1,+}^t \\ 0 & nL_{\text{eff}} + t_{L-X_2} > t_1 > nL_{\text{eff}} + t_{X_2} \\ \frac{c}{6} \log \left[\frac{2 \sin[\pi \alpha_{\mathcal{O}}]}{\alpha_{\mathcal{O}}} \right] - \frac{c}{6} \log \left[-\epsilon f_1(t_1, X_1^f, \theta) \right] & nL_{\text{eff}} + t_{1,-}^t > t_1 > nL_{\text{eff}} + t_{L-X_2} \\ \frac{c}{6} \log \left[\frac{2 \sin[\pi \alpha_{\mathcal{O}}]}{\alpha_{\mathcal{O}}} \right] - \frac{c}{6} \log \left[-\epsilon g_1(t_1, X_1^f, \theta) \right] & nL_{\text{eff}} + t_{X_1} > t_1 > nL_{\text{eff}} + t_{1,-}^t \\ 0 & (n+1)L_{\text{eff}} + t_{L-X_1} > t_1 > nL_{\text{eff}} + t_{X_1} \end{cases} ,$$

$$S_{A,2} \approx \frac{c}{3} \log \left[\frac{L}{\pi} \sin \left(\frac{\pi (X_1 - X_2)}{L} \right) \right]$$

$$+ \begin{cases} 0 & t_{L-X_1} > t_1 > 0 \\ \frac{c}{6} \log \left[\frac{2 \sin[\pi \alpha_{\mathcal{O}}]}{\alpha_{\mathcal{O}}} \right] - \frac{c}{6} \log \left[\epsilon f_2(t_1, X_1^f, \theta) \right] & nL_{\text{eff}} + t_{1,+}^t > t_1 > nL_{\text{eff}} + t_{L-X_1} \\ \frac{c}{6} \log \left[\frac{2 \sin[\pi \alpha_{\mathcal{O}}]}{\alpha_{\mathcal{O}}} \right] - \frac{c}{6} \log \left[\epsilon g_2(t_1, X_1^f, \theta) \right] & nL_{\text{eff}} + t_{X_2} > t_1 > nL_{\text{eff}} + t_{1,+}^t \\ 0 & nL_{\text{eff}} + t_{L-X_2} > t_1 > nL_{\text{eff}} + t_{X_2} \\ \frac{c}{6} \log \left[\frac{2 \sin[\pi \alpha_{\mathcal{O}}]}{\alpha_{\mathcal{O}}} \right] - \frac{c}{6} \log \left[-\epsilon f_2(t_1, X_1^f, \theta) \right] & nL_{\text{eff}} + t_{1,-}^t > t_1 > nL_{\text{eff}} + t_{L-X_2} \\ \frac{c}{6} \log \left[\frac{2 \sin[\pi \alpha_{\mathcal{O}}]}{\alpha_{\mathcal{O}}} \right] - \frac{c}{6} \log \left[-\epsilon g_2(t_1, X_1^f, \theta) \right] & nL_{\text{eff}} + t_{X_1} > t_1 > nL_{\text{eff}} + t_{1,-}^t \\ 0 & (n+1)L_{\text{eff}} + t_{L-X_1} > t_1 > nL_{\text{eff}} + t_{X_1} \end{cases} ,$$

$$S_{A,3} \approx \frac{c}{3} \log \left[\frac{L}{\pi} \sin \left(\frac{\pi (X_1 - X_2)}{L} \right) \right]$$

$$+ \begin{cases} 0 & L - X_1 > t_0 > 0 \\ \frac{c}{6} \log \left[\frac{2 \sin[\pi \alpha_{\mathcal{O}}]}{\alpha_{\mathcal{O}}} \right] - \frac{c}{6} \log \left[\epsilon f_3(t_0, X_1^f, \theta) \right] & nL + t_{0,+}^t > t_0 > (n+1)L - X_1 \\ \frac{c}{6} \log \left[\frac{2 \sin[\pi \alpha_{\mathcal{O}}]}{\alpha_{\mathcal{O}}} \right] - \frac{c}{6} \log \left[\epsilon g_3(t_0, X_1^f, \theta) \right] & nL + X_2 > t_0 > nL + t_{0,+}^t \\ 0 & (n+1)L - X_2 > t_0 > nL + X_2 \\ \frac{c}{6} \log \left[\frac{2 \sin[\pi \alpha_{\mathcal{O}}]}{\alpha_{\mathcal{O}}} \right] - \frac{c}{6} \log \left[-\epsilon f_3(t_0, X_1^f, \theta) \right] & nL + t_{0,-}^t > t_0 > (n+1)L - X_2 \\ \frac{c}{6} \log \left[\frac{2 \sin[\pi \alpha_{\mathcal{O}}]}{\alpha_{\mathcal{O}}} \right] - \frac{c}{6} \log \left[-\epsilon g_3(t_0, X_1^f, \theta) \right] & nL + X_1 > t_0 > nL + t_{0,-}^t \\ 0 & (n+2)L - X_1 > t_0 > nL + X_1 \end{cases} ,$$

$$S_{A,4} \approx \frac{c}{3} \log\left[\frac{L}{\pi} \sin\left(\frac{\pi(X_1 - X_2)}{L}\right)\right]$$

$$+ \begin{cases} 0 & L - X_1 > t_0 > 0 \\ \frac{c}{6} \log\left[\frac{2\sin[\pi\alpha_{\mathcal{O}}]}{\alpha_{\mathcal{O}}}\right] - \frac{c}{6} \log\left[\epsilon f_4(t_0, X_1^f, \theta)\right] & nL + t_{0,+}^t > t_0 > (n+1)L - X_1 \\ \frac{c}{6} \log\left[\frac{2\sin[\pi\alpha_{\mathcal{O}}]}{\alpha_{\mathcal{O}}}\right] - \frac{c}{6} \log\left[\epsilon g_4(t_0, X_1^f, \theta)\right] & nL + X_2 > t_0 > nL + t_{0,+}^t \\ 0 & (n+1)L - X_2 > t_0 > nL + X_2 \\ \frac{c}{6} \log\left[\frac{2\sin[\pi\alpha_{\mathcal{O}}]}{\alpha_{\mathcal{O}}}\right] - \frac{c}{6} \log\left[-\epsilon f_4(t_0, X_1^f, \theta)\right] & nL + t_{0,-}^t > t_0 > (n+1)L - X_2 \\ \frac{c}{6} \log\left[\frac{2\sin[\pi\alpha_{\mathcal{O}}]}{\alpha_{\mathcal{O}}}\right] - \frac{c}{6} \log\left[-\epsilon g_4(t_0, X_1^f, \theta)\right] & nL + X_1 > t_0 > nL + t_{0,-}^t \\ 0 & (n+2)L - X_1 > t_0 > nL + X_1 \end{cases} \quad (5.10)$$

Where n is an integer greater than or equal to 0 , and $t_{1,\pm}^t, t_{0,\pm}^t$ are positive. we define $t_{1,\pm}^t, t_{0,\pm}^t$ as follows:

$$t_{1,\pm}^t = \frac{L_{\text{eff}}}{\pi} \tan^{-1}\left[\pm\sqrt{e^{4\theta} \tan\frac{\pi(L - X_1)}{L} \tan\frac{\pi X_2}{L}}\right], \cos\left(\frac{\pi t_{0,\pm}^t}{L}\right) = \pm\sqrt{\frac{\prod_{i=1}^{2} \cos\left[\frac{\pi X_i}{L}\right]}{\cos\left[\frac{\pi(X_1 + X_2)}{L}\right]}}$$

$$(5.11)$$

We also studied the time dependence of $S_{A,i}$ when the local operator is inserted at $x = \frac{L}{2}$. However, the characteristic behavior of $S_{A,i}$ for the insertion at $x = \frac{L}{2}$ of the local operator is the same as that for $x = 0$. Therefore, we postpone $S_{A,i}$ for $x = \frac{L}{2}$ to Appendix E.1.2.

5.2 SSD limit

Now, let us consider the time dependence of $S_{A,i}$ in the SSD limit, $\theta \to \infty$. In this limit, L_{eff} will become infinite, while L will remain finite. This suggests that the time dependence of $S_{A,i=1,2}$ in the SSD limit may not be periodic, while for $i = 3, 4$ that may remain periodic.

5.2.1 When the insertion of $\mathcal{O}$ is at $x = X_1^f$

We consider the time evolution of S_A when the local operator $\mathcal{O}$ is the inserted at $x = X_1^f$. In this case, t_1-dependence of $S_{A,i=1,2}$ is given by

$$S_{A,1} = S_{A,2} = \frac{c}{3} \log\left[\frac{L}{\pi} \sin\left[\frac{\pi(X_1 - X_2)}{L}\right]\right]. \quad (5.12)$$

We can see from t_1-dependence of $S_{A,i=1,2}$ that the local operator at $x = X_1^f$ does not grow with time during the evolution induced by the SSD Hamiltonian. This is because the Hamiltonian density of H_{SSD} is zero at the origin, so that this evolution operator trivially acts on the local operator. For $|\Psi_3\rangle$, the cross ratios are exactly unity, so that $S_{A,i=3}$ becomes infinite. This is because the local operators inserted coincide with each other since H_{SSD} does

not play as the regulator. For $|\Psi_4\rangle$, the cross ratios are approximated by

$$z_{c,4} \approx 1 - \frac{4i\pi\epsilon \sin^2\left[\frac{\pi t_0}{L}\right] \sin\left[\frac{\pi(X_1-X_2)}{L}\right]}{L \prod_{i=1,2} \sin\left[\frac{\pi(t_0+X_i)}{L}\right]} + \mathcal{O}(\epsilon^2), \ \ \overline{z}_{c,4} \approx 1 + \frac{4i\pi\epsilon \sin^2\left[\frac{\pi t_0}{L}\right] \sin\left[\frac{\pi(X_1-X_2)}{L}\right]}{L \prod_{i=1,2} \sin\left[\frac{\pi(t_0-X_i)}{L}\right]} + \mathcal{O}(\epsilon^2),$$

(5.13)

where around $t_0 = t_{i=1,2,n,\pm}$, these expansions are invalid. The definition of $t_{i=1,2,n,\pm}$ are

$$t_{i=1,2,n,\pm} = nL \pm X_{i=1,2}, \tag{5.14}$$

where n is an integer number. The time dependence of the denominator of $z_{c,4}$ and $\overline{z}_{c,4}$ in this case is the same as that for Möbius case when the local operator is inserted at $x = X_1^f$. This suggests we may have the candidates, corresponding to the branches, of geodesics. The time dependence of entanglement entropy is determined by the minimal one of these candidates. Here, we report on the time dependence of $S_{A,4}$ for only (a) here, while that for (b) and (c) are presented in Appendix E.2.1. The time dependence of $S_{A,4}$ in (a) is determined by

$$S_{A,4} \approx \frac{c}{3} \log\left[\frac{L}{\pi} \sin\left(\frac{\pi(X_1-X_2)}{L}\right)\right]$$

$$+ \begin{cases} 0 & L - X_1 > t_0 > 0 \\ \frac{c}{6}\log\left[\frac{2\sin[\pi\alpha_{\mathcal{O}}]}{\alpha_{\mathcal{O}}}\right] - \frac{c}{6}\log\left[\epsilon f_4(t_0,X_1^f,\infty)\right] & nL + t_{0,+}^t > t_0 > (n+1)L - X_1 \\ \frac{c}{6}\log\left[\frac{2\sin[\pi\alpha_{\mathcal{O}}]}{\alpha_{\mathcal{O}}}\right] - \frac{c}{6}\log\left[\epsilon g_4(t_0,X_1^f,\infty)\right] & nL + X_2 > t_0 > nL + t_{0,+}^t \\ 0 & (n+1)L - X_2 > t_0 > nL + X_2 \\ \frac{c}{6}\log\left[\frac{2\sin[\pi\alpha_{\mathcal{O}}]}{\alpha_{\mathcal{O}}}\right] - \frac{c}{6}\log\left[-\epsilon f_4(t_0,X_1^f,\infty)\right] & nL + t_{0,-}^t > t_0 > (n+1)L - X_2 \\ \frac{c}{6}\log\left[\frac{2\sin[\pi\alpha_{\mathcal{O}}]}{\alpha_{\mathcal{O}}}\right] - \frac{c}{6}\log\left[-\epsilon g_4(t_0,X_1^f,\infty)\right] & nL + X_1 > t_0 > nL + t_{0,-}^t \\ 0 & (n+2)L - X_1 > t_0 > nL + X_1 \end{cases} \tag{5.15}$$

where the $t_{0,\pm}^t$ is given by (5.11).

Large L limit

Now, let us take the large L limit to check if the time dependence of $S_{A,4}$ is consistent with that in [27]. In this limit, $z_{c,4}$ and $\overline{z}_{c,4}$ are approximated by

$$z_{c,4} \approx 1 - \frac{4i\pi^2\epsilon(X_1-X_2)t_0^2}{L^2(t_0+X_1)(t_0+X_2)}, \overline{z}_{c,4} \approx 1 + \frac{4i\pi^2\epsilon(X_1-X_2)t_0^2}{L^2(t_0-X_1)(t_0-X_2)} \tag{5.16}$$

For simplicity, let us assume that $\frac{L}{2} > X_1 > X_2 > 0$. Consequently, the t_0-dependence of $S_{A,4}$ is given by

$$S_{A,4} \approx \begin{cases} \frac{c}{3}\log\left[(X_1-X_2)\right] & X_2 > t_0 \\ \frac{c}{6}\log\left[\frac{\sin(\pi\alpha_{\mathcal{O}})}{\pi\alpha_{\mathcal{O}}} \cdot \frac{L^2(X_1-t_0)(t_0-X_2)(X_1-X_2)}{2\pi\epsilon t_0^2}\right] & X_1 > t_0 > X_2 \\ \frac{c}{3}\log\left[(X_1-X_2)\right] & t_0 > X_1 \end{cases} \tag{5.17}$$

Thus, this is consistent with that in [27].

31

5.2.2 When the insertion of $\mathcal{O}$ is at $x = X_2^f$

Now, let us consider the case where the local operator is inserted at the other fixed point, $x = X_2^f = L/2$. To second order in the small ϵ expansion, the analytic-continued cross ratios are given by

$$z_{c,1} \approx 1 - \frac{2i\pi L\epsilon \sin\left(\frac{\pi(X_1-X_2)}{L}\right)}{\left(L\cos\left(\frac{\pi X_1}{L}\right) - 2\pi t_1 \sin\left(\frac{\pi X_1}{L}\right)\right)\left(L\cos\left(\frac{\pi X_2}{L}\right) - 2\pi t_1 \sin\left(\frac{\pi X_2}{L}\right)\right)} + \mathcal{O}(\epsilon^2),$$

$$\overline{z}_{c,1} \approx 1 + \frac{2i\pi L\epsilon \sin\left(\frac{\pi(X_1-X_2)}{L}\right)}{\left(2\pi t_1 \sin\left(\frac{\pi X_1}{L}\right) + L\cos\left(\frac{\pi X_1}{L}\right)\right)\left(2\pi t_1 \sin\left(\frac{\pi X_2}{L}\right) + L\cos\left(\frac{\pi X_2}{L}\right)\right)} + \mathcal{O}(\epsilon^2),$$

$$z_{c,2} \approx 1 - \frac{2i\pi\epsilon\left(L^2 + 4\pi^2 t_1^2\right)\sin\left[\frac{\pi(X_1-X_2)}{L}\right]}{L\left(L\cos\left(\frac{\pi X_1}{L}\right) - 2\pi t_1 \sin\left(\frac{\pi X_1}{L}\right)\right)\left(L\cos\left(\frac{\pi X_2}{L}\right) - 2\pi t_1 \sin\left(\frac{\pi X_2}{L}\right)\right)} + \mathcal{O}(\epsilon^2),$$

$$\overline{z}_{c,2} \approx 1 + \frac{2i\pi\epsilon\left(L^2 + 4\pi^2 t_1^2\right)\sin\left[\frac{\pi(X_1-X_2)}{L}\right]}{L\left(2\pi t_1 \sin\left(\frac{\pi X_1}{L}\right) + L\cos\left(\frac{\pi X_1}{L}\right)\right)\left(2\pi t_1 \sin\left(\frac{\pi X_2}{L}\right) + L\cos\left(\frac{\pi X_2}{L}\right)\right)} + \mathcal{O}(\epsilon^2),$$

$$z_{c,3} \approx 1 - \frac{4i\pi\epsilon \sin\left[\frac{\pi(X_1-X_2)}{L}\right]}{L\cos\left[\frac{\pi(t_0+X_1)}{L}\right]\cos\left[\frac{\pi(t_0+X_2)}{L}\right]} + \mathcal{O}(\epsilon^2), \quad \overline{z}_{c,3} \approx 1 + \frac{4i\pi\epsilon \sin\left[\frac{\pi(X_1-X_2)}{L}\right]}{L\cos\left[\frac{\pi(t_0-X_1)}{L}\right]\cos\left[\frac{\pi(t_0-X_2)}{L}\right]} + \mathcal{O}(\epsilon^2),$$

$$z_{c,4} \approx 1 - \frac{4i\pi\epsilon \cos^2\left(\frac{\pi t_0}{L}\right)\sin\left[\frac{\pi(X_1-X_2)}{L}\right]}{L\cos\left[\frac{\pi(t_0+X_1)}{L}\right]\cos\left[\frac{\pi(t_0+X_2)}{L}\right]} + \mathcal{O}(\epsilon^2), \quad \overline{z}_{c,4} \approx 1 + \frac{4i\pi \cos^2\left(\frac{\pi t_0}{L}\right)\sin\left[\frac{\pi(X_1-X_2)}{L}\right]}{L\cos\left[\frac{\pi(t_0-X_1)}{L}\right]\cos\left[\frac{\pi(t_0-X_2)}{L}\right]} + \mathcal{O}(\epsilon^2).$$

$$(5.18)$$

For $i = 1, 2$, define the characteristic time scales by

$$\tilde{t}_{i=1,2,\pm} = \frac{L}{2\pi}\tan\left[\frac{\pi}{L}\left(\frac{L}{2} \pm X_i\right)\right]. \tag{5.19}$$

The second order of cross ratios, $z_{c,i=1,2}$ ($\overline{z}_{c,i=1,2}$), is positive in the time interval, $\tilde{t}_{2,-} > t_1 > \tilde{t}_{1,-}$ ($\tilde{t}_{2,+} > t_1$ or $t_1 > \tilde{t}_{1,+}$), while it is negative in $\tilde{t}_{1,-} > t_1$ or $t_1 > \tilde{t}_{2,-}$ ($\tilde{t}_{1,+} > t_1 > \tilde{t}_{2,+}$). Around $t_1 = \tilde{t}_{i,-}$ ($t_1 = \tilde{t}_{i,+}$), the small ϵ expansion breaks down because the coefficient of ϵ^2 becomes drastically large. Thus, unlike the Möbius case, the cross ratios in the SSD limit do not periodically behave. For $i = 3, 4$, the time intervals determining the sign of the cross ratios and the times for the small ϵ expansion to be invalid are the same as those for the case of Möbius Hamiltonian. However, while during the unitary time evolution corresponding to $i = 3$, the value of $S_{A,i=3}$ is finite, during the non-unitary one corresponding to $i = 4$, $S_{A,i=4}$ diverges at $t_0 = L\cdot\left(\frac{1}{2} + n\right)$ because the cross ratios becomes unity for any ϵ. This suggests that $e^{-\epsilon H_{\text{SSD}}}$ does not work as a regulator at $x = X_2^f$. As in the Möbius case, the outlined time evolution of $S_{A,i}$ can be described by the quasiparticle picture. As explained in the Möbius case, the entangled pair is induced at the insertion point of the local operator, and then the quasiparticles of this pair moves to left and right at the velocity determined by the envelope

32

functions: for $i = 1, 2$ the velocity is $|2\sin^2\left(\frac{\pi x}{L}\right)|$; for $i = 3, 4$ the velocity is the speed of light. When only one of pair is in the subsystems considered, the entanglement between this pair contributes to $S_{A,i}$. Since we can see the properties of entanglement dynamics in the SSD limit from $S_{A,i}$ for (a), we only present it. The readers interested in (b) and (c) should look at Appendix E.2.2.

In the AdS/CFT correspondence, the time dependence of $S_{A,i}$ in (a) is given by

$$S_{A,1} \approx \frac{c}{3} \log \left[\frac{L}{\pi} \sin \left[\frac{\pi(X_1 - X_2)}{L} \right] \right]$$

$$+ \begin{cases} 0 & \tilde{t}_{2,-} > t_1 > 0 \\ \frac{c}{6} \log \left[\frac{2 \sin[\pi\alpha_{\mathcal{O}}]}{\alpha_{\mathcal{O}}} \right] - \frac{c}{6} \log \left[-\epsilon f_1(t_1, X_2^f, \infty) \right] & \tilde{t}_1^t > t_1 > \tilde{t}_{2,-} \\ \frac{c}{6} \log \left[\frac{2 \sin[\pi\alpha_{\mathcal{O}}]}{\alpha_{\mathcal{O}}} \right] - \frac{c}{6} \log \left[-\epsilon g_1(t_1, X_2^f, \infty) \right] & \tilde{t}_{1,+} > t_1 > \tilde{t}_1^t \\ 0 & t_1 > \tilde{t}_{1,+} \end{cases},$$

$$S_{A,2} \approx \frac{c}{3} \log \left[\frac{L}{\pi} \sin \left[\frac{\pi(X_1 - X_2)}{L} \right] \right]$$

$$+ \begin{cases} 0 & \tilde{t}_{2,-} > t_1 > 0 \\ \frac{c}{6} \log \left[\frac{2 \sin[\pi\alpha_{\mathcal{O}}]}{\alpha_{\mathcal{O}}} \right] - \frac{c}{6} \log \left[-\epsilon f_2(t_1, X_2^f, \infty) \right] & \tilde{t}_1^t > t_1 > \tilde{t}_{2,-} \\ \frac{c}{6} \log \left[\frac{2 \sin[\pi\alpha_{\mathcal{O}}]}{\alpha_{\mathcal{O}}} \right] - \frac{c}{6} \log \left[-\epsilon g_2(t_1, X_2^f, \infty) \right] & \tilde{t}_{1,+} > t_1 > \tilde{t}_1^t \\ 0 & t_1 > \tilde{t}_{1,+} \end{cases},$$

$$S_{A,3} \approx \frac{c}{3} \log \left[\frac{L}{\pi} \sin \left[\frac{\pi(X_1 - X_2)}{L} \right] \right]$$

$$+ \begin{cases} 0 & \frac{L}{2} - X_2 > t_0 > 0 \\ \frac{c}{6} \log \left[\frac{2 \sin[\pi\alpha_{\mathcal{O}}]}{\alpha_{\mathcal{O}}} \right] - \frac{c}{6} \log \left[-\epsilon f_3(t_0, X_2^f, \infty) \right] & nL + \tilde{t}_{0,+}^t > t_1 > \left(\frac{1}{2} + n \right) L - X_2 \\ \frac{c}{6} \log \left[\frac{2 \sin[\pi\alpha_{\mathcal{O}}]}{\alpha_{\mathcal{O}}} \right] - \frac{c}{6} \log \left[-\epsilon g_3(t_0, X_2^f, \infty) \right] & \left(n - \frac{1}{2} \right) L + X_1 > t_1 > nL + \tilde{t}_{0,+}^t \\ 0 & \left(n + \frac{3}{2} \right) L - X_1 > t_0 > \left(n - \frac{1}{2} \right) L + X_1 \\ \frac{c}{6} \log \left[\frac{2 \sin[\pi\alpha_{\mathcal{O}}]}{\alpha_{\mathcal{O}}} \right] - \frac{c}{6} \log \left[\epsilon f_3(t_0, X_2^f, \infty) \right] & nL + \tilde{t}_{0,-}^t > t_0 > \left(n + \frac{3}{2} \right) L - X_1 \\ \frac{c}{6} \log \left[\frac{2 \sin[\pi\alpha_{\mathcal{O}}]}{\alpha_{\mathcal{O}}} \right] - \frac{c}{6} \log \left[\epsilon g_3(t_0, X_2^f, \infty) \right] & \left(n + \frac{1}{2} \right) L + X_2 > t_0 > nL + \tilde{t}_{0,-}^t \\ 0 & \left(\frac{3}{2} + n \right) L - X_2 > t_0 > \left(\frac{1}{2} + n \right) L + X_2 \end{cases},$$

$$S_{A,4} \approx \frac{c}{3} \log \left[\frac{L}{\pi} \sin \left[\frac{\pi(X_1 - X_2)}{L} \right] \right]$$

$$+ \begin{cases} 0 & \frac{L}{2} - X_2 > t_0 > 0 \\ \frac{c}{6} \log \left[\frac{2 \sin[\pi\alpha_{\mathcal{O}}]}{\alpha_{\mathcal{O}}} \right] - \frac{c}{6} \log \left[-\epsilon f_4(t_0, X_2^f, \infty) \right] & nL + \tilde{t}_{0,+}^t > t_1 > \left(\frac{1}{2} + n \right) L - X_2 \\ \frac{c}{6} \log \left[\frac{2 \sin[\pi\alpha_{\mathcal{O}}]}{\alpha_{\mathcal{O}}} \right] - \frac{c}{6} \log \left[-\epsilon g_4(t_0, X_2^f, \infty) \right] & \left(n - \frac{1}{2} \right) L + X_1 > t_1 > nL + \tilde{t}_{0,+}^t \\ 0 & \left(n + \frac{3}{2} \right) L - X_1 > t_0 > \left(n - \frac{1}{2} \right) L + X_1 \\ \frac{c}{6} \log \left[\frac{2 \sin[\pi\alpha_{\mathcal{O}}]}{\alpha_{\mathcal{O}}} \right] - \frac{c}{6} \log \left[\epsilon f_4(t_0, X_2^f, \infty) \right] & nL + \tilde{t}_{0,-}^t > t_0 > \left(n + \frac{3}{2} \right) L - X_1 \\ \frac{c}{6} \log \left[\frac{2 \sin[\pi\alpha_{\mathcal{O}}]}{\alpha_{\mathcal{O}}} \right] - \frac{c}{6} \log \left[\epsilon g_4(t_0, X_2^f, \infty) \right] & \left(n + \frac{1}{2} \right) L + X_2 > t_0 > nL + \tilde{t}_{0,-}^t \\ 0 & \left(\frac{3}{2} + n \right) L - X_2 > t_0 > \left(\frac{1}{2} + n \right) L + X_2 \end{cases}.$$

(5.20)

where n is an integer greater than or equal to 0, and $\tilde{t}_{i,\pm}$ are positive. The characteristic

parameters are given by

$$\tilde{t}_1^t = \sqrt{\tilde{t}_{1,+}\tilde{t}_{2,-}}, \quad \cos\left(\frac{\pi \tilde{t}_{0,\pm}}{L}\right) = \pm\sqrt{\frac{-\prod_{i=1}^{2}\sin\left[\frac{\pi X_i}{L}\right]}{\cos\left[\frac{\pi(X_1+X_2)}{L}\right]}} \tag{5.21}$$

For general x, except for $x \neq 0$, the time dependence of $S_{A,i}$ is finite because the local operators inserted do not coincide with each other (See Appendix E.2.3 for the details of $S_{A,i}$).

5.3   Information survival

We close this section by exploring the contribution from the time ordering of the Euclidean and Lorentzian time evolution to the information scrambling. Let us assume that the time dependence of entanglement entropy follows the propagation of quasiparticles. During the evolution induced by the SSD Hamiltonian, the quasiparticles move to and then accumulate around $x = X_1^f$. Therefore, if the boundary of A is at $x = X_1^f$, the quantum entanglement of quasiparticles keeps contributing to the time dependence of S_A. To check whether or not the information of the local operator such as the dependence of S_A on the local operator conformal dimension survives at late times, we will explore the time dependence of $S_{A,i=1,2}$ in the SSD limit. We assume that the insertion point of the local operator is X_2^f, and take A to be

$$A = \left\{ x \middle| 0 \leq x \leq X_2 < \frac{L}{2} \right\}. \tag{5.22}$$

We closely look at the leading order of $S_{A,i=1,2}$ in the small ϵ limit. Then, the time dependence of $S_{A,i=1,2}$ in the SSD limit is given by

$$
\begin{aligned}
S_{A,i=1} &\approx \frac{c}{3}\log\left[\frac{L}{\pi}\sin\left(\frac{\pi X_1}{L}\right)\right] \\
&+ \begin{cases} 0 & \frac{L}{2\pi\tan\left(\frac{\pi X_1}{L}\right)} > t_1 > 0 \\ \frac{c}{6}\log\left[\frac{2\sin[\pi\alpha_{\mathcal{O}}]}{\alpha_{\mathcal{O}}}\right] + \frac{c}{6}\log\left[\frac{t_1 - \frac{L}{2\pi\tan\left(\frac{\pi X_1}{L}\right)}}{\epsilon}\right] & t_1 > \frac{L}{2\pi\tan\left(\frac{\pi X_1}{L}\right)} > 0 \end{cases}, \\[2mm]
S_{A,i=2} &\approx \frac{c}{3}\log\left[\frac{L}{\pi}\sin\left(\frac{\pi X_1}{L}\right)\right] \\
&+ \begin{cases} 0 & \frac{L}{2\pi\tan\left(\frac{\pi X_1}{L}\right)} > t_1 > 0 \\ \frac{c}{6}\log\left[\frac{2\sin[\pi\alpha_{\mathcal{O}}]}{\alpha_{\mathcal{O}}}\right] + \frac{c}{6}\log\left[\frac{L^2\left(t_1 - \frac{L}{2\pi\tan\left(\frac{\pi X_1}{L}\right)}\right)}{\epsilon\left(L^2+4\pi^2 t_1^2\right)}\right] & t_1 > \frac{L}{2\pi\tan\left(\frac{\pi X_1}{L}\right)} > 0 \end{cases},
\end{aligned}
\tag{5.23}
$$

Thus, as we expected, $S_{A,i=1,2}$ is not the vacuum entanglement entropy. Subsequently, we consider the time dependence of $S_{A,i=1,2}$ in the late time regime $t_1 \gg \frac{L}{2\pi\tan\left(\frac{\pi X_1}{L}\right)}, \frac{L}{2\pi}$. In this

late time regime, the time dependence of $S_{A,i=1}$ is approximately

$$S_{A,i=1} \approx \frac{c}{3} \log \left[\frac{L}{\pi} \sin \left(\frac{\pi X_1}{L} \right) \right] + \frac{c}{6} \log \left[\frac{2 \sin [\pi \alpha_{\mathcal{O}}]}{\alpha_{\mathcal{O}}} \right] + \frac{c}{6} \log \left[\frac{t_1}{\epsilon} \right], \qquad (5.24)$$

where since the last term of (5.24) grows logarithmically with t_1 and becomes larger than the term depending on $\alpha_{\mathcal{O}}$, the information of the local operator inserted is locally hidden by this logarithmic growth. Then, we consider the late-time dependence of $S_{A,i=2}$. In the late-time interval, $\frac{L^2}{\epsilon} \gg t_1 \gg \frac{L}{2\pi \tan \left(\frac{\pi X_1}{L} \right)}, \frac{L}{2\pi}$, the time dependence of $S_{A,i=2}$ is approximately

$$S_{A,i=2} \approx \frac{c}{3} \log \left[\frac{L}{\pi} \sin \left(\frac{\pi X_1}{L} \right) \right] + \frac{c}{6} \log \left[\frac{2 \sin [\pi \alpha_{\mathcal{O}}]}{\alpha_{\mathcal{O}}} \right] - \frac{c}{6} \log \left[\frac{4\pi^2 \epsilon t_1}{L^2} \right]. \qquad (5.25)$$

The last term of (5.25) contributes positively to $S_{A,i=2}$, while it deceases with t_1. Therefore, in this time interval, the dependence on $\alpha_{\mathcal{O}}$ of $S_{A,i=2}$ can still remain. In the very late-time regime, $t_1 > \frac{L^2}{\epsilon}$, the small ϵ expansion in (5.18) breaks down because the second order behavior of the cross ratios overcomes the leading one. By taking the late time limit, $t_1 \gg 1$, and then taking the small ϵ limit, let us explore the late time behavior of the cross ratios. In this limit, the leading order of the cross ratios is approximated by -1, so we cannot use the conformal block in (5.6). In the time regime, $\frac{L^2}{\epsilon} \gg t_1 \gg \frac{L}{2\pi \tan \left(\frac{\pi X_1}{L} \right)}, \frac{L}{2\pi}$, for $i = 1$, the information of the local operators is locally hidden, while $i = 2$, it cannot be hidden. This suggests that the initial state information for $i = 2$ survives longer than that for $i = 1$ during the SSD holographic time evolution. It would be interesting to explore the time dependence of $S_{A,i=2}$ in the very late-time region $t_1 \gg \frac{L^2}{\epsilon}$ to check whether or not the information of the local operator remains during the 2d holographic time evolution forever. We leave it as an open problem.

6   Discussions

In this paper, we explored the time dependence of the entanglement entropy for the excited states induced by the insertion of the local operators in 2d free, rational, and holographic CFTs. The time evolution considered is constructed of Euclidean and Lorentzian time evolution. For $i = 1, 3$, the systems undergo the Euclidean evolution first and then undergo the Lorentzian time evolution, while the order of the time evolution for $i = 2, 4$ is the opposite. Since the norm of the state for $i = 2, 4$ is not invariant under the real time evolution, the evolution for $i = 2, 4$ is non-unitary. Our main findings in this paper are threefold. The first one is about the Euclidean and Lorentzian time evolution induced by the SSD Hamiltonian. Since the Hamiltonian density of the SSD Hamiltonian at $x = X_1^f$ is zero, H_{SSD} is expected to commute with $\mathcal{O}(x = X_1^f)$. When the local operator is at $x = X_1^f$, for $i = 1, 2$, the entanglement entropy, energy density, and partition function do not depend on the times, while for $i = 3, 4$, they are divergent, as we expected. This suggests that in the continuum limit, the Euclidean and real time evolution of H_{SSD} does not play as the regulator and time

evolution operator at $x = X_1^f$, respectively.The second main result is that in free and rational CFTs, the time dependence of the entanglement entropy does not depend on the time ordering of the Euclidean and Lorentzian time evolution, while in the holographic CFTs, the ordering of these time evolutions with different signatures matters. The third one is about the local operator information survival for $i = 1, 2$. We considered the time dependence of the entanglement entropy when X_1^f is put on the boundary of the subsystems. In 2d holographic CFTs, during the unitary time evolution (for $i = 1$), in the late time regime, the entanglement entropy grows logarithmically in time, so that this logarithmic growth hides the dependence of the entanglement entropy on the conformal dimension. During the non-unitary time evolution (for $i = 2$), the dependence of the entanglement entropy on the local operator remains for a longer time than that for $i = 1$. However, we could not determine if for $i = 2$, the information about the local operator inserted remains forever. If we first take the late time limit, $t_1 \gg 1$, and subsequently take the small ϵ limit, then the cross ratios approaches to -1. Therefore, the approximation of the conformal blocks around $z, \overline{z} \approx 1$ is invalid. In this paper, we could not consider a situation where the quasiparticles contribute forever to the entanglement entropy during the evolution induced by the holographic CFT Hamiltonian because the inhomogeneous Hamiltonians are defined on a compact space. It would be interesting to explore if the information of the local operator inserted remains during a non-unitary process on a non-compact space that is more similar to the setup considered in [27, 23] . For example, it would be interesting to explore the system during the time evolution constructed out of the Euclidean evolution induced by the Rindler Hamiltonian and the real time evolution induced by the homogeneous time evolution.

Acknowledgements

A   Trajectory of the local operator

Here, we will explain how to compute the trajectories of the local operator and present the details.

A.1 How to compute the local operator trajectories

Here, we derive the transformation of the primary operator during the unitary and non-unitary time evolution. The Euclidean time evolution operators considered here are

$$U_{i,\epsilon}^E = \begin{cases} e^{-\tau_1 H_{\text{Möbius}}} e^{-\epsilon H_0} & \text{for } i = 1 \\ e^{-\epsilon H_0} e^{-\tau_1 H_{\text{Möbius}}} & \text{for } i = 2 \\ e^{-\tau_0 H_0} e^{-\epsilon H_{\text{Möbius}}} & \text{for } i = 3 \\ e^{-\epsilon H_{\text{Möbius}}} e^{-\tau_0 H_0} & \text{for } i = 4 \end{cases}, \quad \tilde{U}_{i,\epsilon}^E = \begin{cases} e^{-\epsilon H_0} e^{\tau_1 H_{\text{Möbius}}} & \text{for } i = 1 \\ e^{\tau_1 H_{\text{Möbius}}} e^{-\epsilon H_0} & \text{for } i = 2 \\ e^{-\epsilon H_{\text{Möbius}}} e^{\tau_0 H_0} & \text{for } i = 3 \\ e^{\tau_0 H_0} e^{-\epsilon H_{\text{Möbius}}} & \text{for } i = 4 \end{cases}. \tag{A.1}$$

First, we focus on H_0. In the complex coordinates, $(w, \overline{w})$, it is given by

$$H_0 = \frac{1}{2i\pi} \oint dw\, T(w) + \frac{1}{2i\pi} \oint d\overline{w}\, \overline{T}(\overline{w}) \tag{A.2}$$

Then, by performing the conformal transformation, $(z, \overline{z}) = (e^{\frac{2\pi w}{L}}, e^{\frac{2\pi \overline{w}}{L}})$, the energy densities transform as

$$T(w) = \left(\frac{dz}{dw}\right)^2 T(z) + \frac{c}{12}\{z; w\}, \quad \overline{T}(\overline{w}) = \left(\frac{d\overline{z}}{d\overline{w}}\right)^2 \overline{T}(\overline{z}) + \frac{c}{12}\{\overline{z}; \overline{w}\}, \tag{A.3}$$

where Schwarzian derivatives are defined as

$$\{z; w\} = \left(\frac{\frac{d^3 z}{dw^3}}{\frac{dz}{dw}}\right) - \frac{3}{2}\left(\frac{\frac{d^2 z}{dw^2}}{\frac{dz}{dw}}\right)^2, \quad \{\overline{z}; \overline{w}\} = \left(\frac{\frac{d^3 \overline{z}}{d\overline{w}^3}}{\frac{d\overline{z}}{d\overline{w}}}\right) - \frac{3}{2}\left(\frac{\frac{d^2 \overline{z}}{d\overline{w}^2}}{\frac{d\overline{z}}{d\overline{w}}}\right)^2. \tag{A.4}$$

Consequently, H_0 reduces to

$$H_0 = \frac{2\pi}{L} \cdot \left[\frac{1}{2i\pi} \oint dz\, z T(z) + \frac{1}{2i\pi} \oint d\overline{z}\, \overline{z}\, \overline{T}(\overline{z}) - \frac{c}{12}\right] = \frac{2\pi}{L}\left[L_0^z + \overline{L}_0^{\overline{z}} - \frac{c}{12}\right], \tag{A.5}$$

where the Virasoro generators are defined as

$$L_n^z = \frac{1}{2i\pi} \oint dz\, z^{n+1} T(z), \quad \overline{L}_n^{\overline{z}} = \frac{1}{2i\pi} \oint d\overline{z}\, \overline{z}^{n+1} \overline{T}(\overline{z}). \tag{A.6}$$

The transformation, induced by H_0, of the primary operator, $\mathcal{O}$, with the conformal factor $(h_{\mathcal{O}}, h_{\mathcal{O}})$ is given by

$$e^{aH_0} \mathcal{O}(z, \overline{z}) e^{-aH_0} = e^{\frac{2\pi a}{L}\left(L_0^z + \overline{L}_0^{\overline{z}}\right)} \mathcal{O}(z, \overline{z}) e^{-\frac{2\pi a}{L}\left(L_0^z + \overline{L}_0^{\overline{z}}\right)} = \lambda^{2h_{\mathcal{O}}} \mathcal{O}(\lambda z, \lambda \overline{z}), \tag{A.7}$$

where a is a real parameter, and λ is defined as

$$\lambda := e^{\frac{2\pi a}{L}}. \tag{A.8}$$

Define $(w_a^{\text{New}}, \overline{w}_a^{\text{New}})$ as

$$(e^{\frac{2\pi w_a^{\text{New}}}{L}}, e^{\frac{2\pi \overline{w}_a^{\text{New}}}{L}}) := (\lambda z, \lambda \overline{z}). \tag{A.9}$$

By using the conformal map, during the Euclidean time evolution induced by H_0, the transformation of the primary operator reduces to

$$e^{aH_0}\mathcal{O}(w,\overline{w})e^{-aH_0} = \left|\frac{dw_a^{\text{New}}}{dw}\right|^{2h_\mathcal{O}} \mathcal{O}(w_a^{\text{New}}, \overline{w}_a^{\text{New}}) \tag{A.10}$$

Next, we take a closer look at $H_{\text{Möbius}}$. Starting from the complex coordinates, $(w, \overline{w})$, it is written as

$$\begin{aligned} H_{\text{Möbius}} =& \frac{1}{2i\pi}\oint dw \left[T(w) - \frac{\tanh 2\theta}{2}\left(e^{\frac{2\pi w}{L}} + e^{\frac{-2\pi w}{L}}\right)T(w)\right] \\ &+ \frac{1}{2i\pi}\oint d\overline{w}\left[\overline{T}(\overline{w}) - \frac{\tanh 2\theta}{2}\left(e^{\frac{2\pi \overline{w}}{L}} + e^{\frac{-2\pi \overline{w}}{L}}\right)\overline{T}(\overline{w})\right]. \end{aligned} \tag{A.11}$$

We next map from $(w, \overline{w})$ to $(z, \overline{z})$ where the Hamiltonian is expressed as

$$\begin{aligned} H_{\text{Möbius}} =& \left(\frac{2\pi}{L}\right) \times \frac{1}{2i\pi}\oint dz\left[zT(z) - \frac{\tanh 2\theta}{2}(z^2 + 1)T(z)\right] \\ &+ \left(\frac{2\pi}{L}\right) \times \frac{1}{2i\pi}\oint d\overline{z}\left[\overline{z}\,\overline{T}(\overline{z}) - \frac{\tanh 2\theta}{2}(\overline{z}^2 + 1)\overline{T}(\overline{z})\right] - \frac{c}{12} \times \left(\frac{2\pi}{L}\right). \end{aligned} \tag{A.12}$$

Subsequently, we map $(z, \overline{z})$ to $(\tilde{z}, \overline{\tilde{z}}) = \left(\frac{-\cosh\theta z + \sinh\theta}{-\cosh\theta + \sinh\theta z}, \frac{-\cosh\theta\overline{z} + \sinh\theta}{-\cosh\theta + \sinh\theta\overline{z}}\right)$, and the Möbius Hamiltonian reduces to

$$\begin{aligned} H_{\text{Möbius}} &= \left(\frac{2\pi}{L}\right) \times \frac{1}{2i\pi}\left[\oint d\tilde{z}\,\tilde{z}T(\tilde{z}) + \oint d\overline{\tilde{z}}\,\overline{\tilde{z}}\,\overline{T}(\overline{\tilde{z}})\right] - \frac{c}{12} \times \left(\frac{2\pi}{L}\right) \\ &= \left(\frac{2\pi}{L_{\text{eff}}}\right) \times \left[L_0^{\tilde{z}} + L_0^{\overline{\tilde{z}}} - \frac{c}{12}\right], \end{aligned} \tag{A.13}$$

where the Virasoro generators on $(\tilde{z}, \overline{\tilde{z}})$ are defined as

$$L_n^{\tilde{z}} = \frac{1}{2i\pi}\oint d\tilde{z}\,\tilde{z}^{n+1}T(\tilde{z}), \quad \overline{L}_n^{\overline{\tilde{z}}} = \frac{1}{2i\pi}\oint d\overline{\tilde{z}}\,\overline{\tilde{z}}^{n+1}\overline{T}(\overline{\tilde{z}}). \tag{A.14}$$

Thus, the time evolution induced by $H_{\text{Möbius}}$ is equivalent to the evolution induced by the dilatation operator on $(\tilde{z}, \overline{\tilde{z}})$. Therefore, the transformation of the primary operator during the Möbius time evolution is given by

$$\mathcal{O}_{\text{H}}(\tilde{z}, \overline{\tilde{z}}, a) := e^{aH_{\text{Möbius}}}\mathcal{O}(\tilde{z}, \overline{\tilde{z}})e^{-aH_{\text{Möbius}}} = \lambda_{\text{eff}}^{2h_\mathcal{O}}\mathcal{O}(\lambda_{\text{eff}}\tilde{z}, \lambda_{\text{eff}}\overline{\tilde{z}}), \tag{A.15}$$

where L_{eff} is defined by replacing L of λ with L_{eff}. On a separate note, let us consider the Schrödinger equation of the local operator with respect to a. It is given by

$$\frac{d\mathcal{O}_{\text{H}}(\tilde{z}, \overline{\tilde{z}}, a)}{da} = \frac{2\pi}{L_{\text{eff}}}\left[2h_\mathcal{O}\mathcal{O}_{\text{H}}(\tilde{z}, \overline{\tilde{z}}, a) + \tilde{z}\partial_{\tilde{z}}\mathcal{O}_{\text{H}}(\tilde{z}, \overline{\tilde{z}}, a) + \overline{\tilde{z}}\partial_{\overline{\tilde{z}}}\mathcal{O}_{\text{H}}(\tilde{z}, \overline{\tilde{z}}, a)\right]. \tag{A.16}$$

This is equivalent to the transformation, induced by the dilation operator in $(\tilde{z}, \overline{\tilde{z}})$, of $\mathcal{O}_{\mathrm{H}}(\tilde{z}, \overline{\tilde{z}}, a)$,

$$\frac{d\mathcal{O}_{\mathrm{H}}(\tilde{z}, \overline{\tilde{z}}, a)}{da} = \left[H_{\mathrm{M\ddot{o}bius}}, \mathcal{O}_{\mathrm{H}}(\tilde{z}, \overline{\tilde{z}}, a) \right] = \left[\left(\frac{2\pi}{L_{\mathrm{eff}}} \right) \cdot \left[L_0^{\tilde{z}} + L_0^{\overline{\tilde{z}}} - \frac{c}{12} \right], \mathcal{O}_{\mathrm{H}}(\tilde{z}, \overline{\tilde{z}}, a) \right]. \quad (A.17)$$

Since the Möbius Hamiltonian is given by the linear combination of the Virasoro as in (2.4), $\mathcal{O}_{\mathrm{H}}(z, \overline{z}, a)$ should follow the Schrödinger equation in the complex coordinates, $(z, \overline{z})$,

$$\begin{aligned}
\frac{d\mathcal{O}_{\mathrm{H}}(z, \overline{z}, a)}{da} &= [H_{\mathrm{M\ddot{o}bius}}, \mathcal{O}_{\mathrm{H}}(z, \overline{z}, a)] \\
&= \frac{2\pi}{L} \left[L_0^z + \overline{L}_0^{\overline{z}} - \frac{\tanh 2\theta}{2} \left(L_1^z + L_{-1}^z + \overline{L}_1^{\overline{z}} + \overline{L}_{-1}^{\overline{z}} \right), \mathcal{O}_{\mathrm{H}}(z, \overline{z}, a) \right] \\
&= \frac{2\pi}{L_{\mathrm{eff}}} \left[h_{\mathcal{O}} \left(\cosh 2\theta - z \sinh 2\theta \right) \mathcal{O}_{\mathrm{H}}(z, \overline{z}, a) + \left(z \cosh 2\theta - \frac{\sinh 2\theta}{2}(1 + z^2) \right) \partial_z \mathcal{O}_{\mathrm{H}}(z, \overline{z}, a) \right] \\
&+ \frac{2\pi}{L_{\mathrm{eff}}} \left[h_{\mathcal{O}} \left(\cosh 2\theta - \overline{z} \sinh 2\theta \right) \mathcal{O}_{\mathrm{H}}(z, \overline{z}, a) + \left(\overline{z} \cosh 2\theta - \frac{\sinh 2\theta}{2}(1 + \overline{z}^2) \right) \partial_{\overline{z}} \mathcal{O}_{\mathrm{H}}(z, \overline{z}, a) \right].
\end{aligned}$$
$$(A.18)$$

By mapping from $(\tilde{z}, \overline{\tilde{z}})$ to $(z, \overline{z})$, the equation (A.17) reduces to (A.18). Thus, (A.18) is consistent with (A.17).

Now let us return to the main part of the analysis in this section. Define the complex coordinates $(w_{a,\mathrm{M\ddot{o}bius}}^{\mathrm{New}}, \overline{w}_{a,\mathrm{M\ddot{o}bius}}^{\mathrm{New}})$ as

$$(e^{\frac{2\pi w_{a,\mathrm{M\ddot{o}bius}}^{\mathrm{New}}}{L}}, e^{\frac{2\pi \overline{w}_{a,\mathrm{M\ddot{o}bius}}^{\mathrm{New}}}{L}}) := \left(\lambda_{\mathrm{eff}} \tilde{z}, \lambda_{\mathrm{eff}} \overline{\tilde{z}} \right). \quad (A.19)$$

Consequently, the transformation of the primary operator, $e^{aH_{\mathrm{M\ddot{o}bius}}} \mathcal{O}(w, \overline{w}) e^{-aH_{\mathrm{M\ddot{o}bius}}}$, is given by replacing w_a^{New} and $\overline{w}_a^{\mathrm{New}}$ of (A.10) with $w_{a,\mathrm{M\ddot{o}bius}}^{\mathrm{New}}$ and $\overline{w}_{a,\mathrm{M\ddot{o}bius}}^{\mathrm{New}}$,

$$e^{aH_{\mathrm{M\ddot{o}bius}}} \mathcal{O}(w, \overline{w}) e^{-aH_{\mathrm{M\ddot{o}bius}}} = \left| \frac{dw_{a,\mathrm{M\ddot{o}bius}}^{\mathrm{New}}}{dw} \right|^{2h_{\mathcal{O}}} \mathcal{O}(w_{a,\mathrm{M\ddot{o}bius}}^{\mathrm{New}}, \overline{w}_{a,\mathrm{M\ddot{o}bius}}^{\mathrm{New}}) \quad (A.20)$$

The transformation in (2.16) is given by the operation constructed of (A.10) and (A.20). For example, for $i = 1$ ($i = 3$), we perform the transformation, induced by H_0 ($H_{\mathrm{M\ddot{o}bius}}$), of the primary operator, and then we do the one induced by $H_{\mathrm{M\ddot{o}bius}}$ (H_0), while for $i = 2$ ($i = 4$), we do the one induced by $H_{\mathrm{M\ddot{o}bius}}$ (H_0), and then we do the one induced by H_0 ($H_{\mathrm{M\ddot{o}bius}}$).

A.2 The details of the trajectories

Here, we present the details of the local operator trajectories before the analytic continuation. They are given by

$$w^{\text{New},1}_{\pm\epsilon} = \frac{L}{2\pi} \log \left[\frac{\left[(1 - \hat{\lambda}_{-\tau_1}) \cosh 2\theta - (\hat{\lambda}_{-\tau_1} + 1) \right] \lambda_{\pm\epsilon} z + (\hat{\lambda}_{-\tau_1} - 1) \sinh 2\theta}{(1 - \hat{\lambda}_{-\tau_1}) \sinh 2\theta \lambda_{\pm\epsilon} z + (\hat{\lambda}_{-\tau_1} - 1) \cosh 2\theta - (\hat{\lambda}_{-\tau_1} + 1)} \right],$$

$$\overline{w}^{\text{New},1}_{\pm\epsilon} = \frac{L}{2\pi} \log \left[\frac{\left[(1 - \hat{\lambda}_{-\tau_1}) \cosh 2\theta - (\hat{\lambda}_{-\tau_1} + 1) \right] \lambda_{\pm\epsilon} \overline{z} + (\hat{\lambda}_{-\tau_1} - 1) \sinh 2\theta}{(1 - \hat{\lambda}_{-\tau_1}) \sinh 2\theta \lambda_{\pm\epsilon} \overline{z} + (\hat{\lambda}_{-\tau_1} - 1) \cosh 2\theta - (\hat{\lambda}_{-\tau_1} + 1)} \right],$$

$$w^{\text{New},2}_{\pm\epsilon} = \pm\epsilon + \frac{L}{2\pi} \log \left[\frac{\left[(1 - \hat{\lambda}_{-\tau_1}) \cosh 2\theta - (\hat{\lambda}_{-\tau_1} + 1) \right] z + (\hat{\lambda}_{-\tau_1} - 1) \sinh 2\theta}{(1 - \hat{\lambda}_{-\tau_1}) \sinh 2\theta z + (\hat{\lambda}_{-\tau_1} - 1) \cosh 2\theta - (\hat{\lambda}_{-\tau_1} + 1)} \right],$$

$$\overline{w}^{\text{New},2}_{\pm\epsilon} = \pm\epsilon + \frac{L}{2\pi} \log \left[\frac{\left[(1 - \hat{\lambda}_{-\tau_1}) \cosh 2\theta - (\hat{\lambda}_{-\tau_1} + 1) \right] \overline{z} + (\hat{\lambda}_{-\tau_1} - 1) \sinh 2\theta}{(1 - \hat{\lambda}_{-\tau_1}) \sinh 2\theta \overline{z} + (\hat{\lambda}_{-\tau_1} - 1) \cosh 2\theta - (\hat{\lambda}_{-\tau_1} + 1)} \right],$$

$$w^{\text{New},3}_{\pm\epsilon} = -\tau_0 + \frac{L}{2\pi} \log \left[\frac{\left[(1 - \hat{\lambda}_{\pm\epsilon}) \cosh 2\theta - (\hat{\lambda}_{\pm\epsilon} + 1) \right] z + (\hat{\lambda}_{\pm\epsilon} - 1) \sinh 2\theta}{(1 - \hat{\lambda}_{\pm\epsilon}) \sinh 2\theta z + (\hat{\lambda}_{\pm\epsilon} - 1) \cosh 2\theta - (\hat{\lambda}_{\pm\epsilon} + 1)} \right],$$

$$\overline{w}^{\text{New},3}_{\pm\epsilon} = -\tau_0 + \frac{L}{2\pi} \log \left[\frac{\left[(1 - \hat{\lambda}_{\pm\epsilon}) \cosh 2\theta - (\hat{\lambda}_{\pm\epsilon} + 1) \right] \overline{z} + (\hat{\lambda}_{\pm\epsilon} - 1) \sinh 2\theta}{(1 - \hat{\lambda}_{\pm\epsilon}) \sinh 2\theta \overline{z} + (\hat{\lambda}_{\pm\epsilon} - 1) \cosh 2\theta - (\hat{\lambda}_{\pm\epsilon} + 1)} \right],$$

$$w^{\text{New},4}_{\pm\epsilon} = \frac{L}{2\pi} \log \left[\frac{\left[(1 - \hat{\lambda}_{\pm\epsilon}) \cosh 2\theta - (\hat{\lambda}_{\pm\epsilon} + 1) \right] \lambda_{-\tau_0} z + (\hat{\lambda}_{\pm\epsilon} - 1) \sinh 2\theta}{(1 - \hat{\lambda}_{\pm\epsilon}) \sinh 2\theta \lambda_{-\tau_0} z + (\hat{\lambda}_{\pm\epsilon} - 1) \cosh 2\theta - (\hat{\lambda}_{\pm\epsilon} + 1)} \right],$$

$$\overline{w}^{\text{New},4}_{\pm\epsilon} = \frac{L}{2\pi} \log \left[\frac{\left[(1 - \hat{\lambda}_{\pm\epsilon}) \cosh 2\theta - (\hat{\lambda}_{\pm\epsilon} + 1) \right] \lambda_{-\tau_0} \overline{z} + (\hat{\lambda}_{\pm\epsilon} - 1) \sinh 2\theta}{(1 - \hat{\lambda}_{\pm\epsilon}) \sinh 2\theta \lambda_{-\tau_0} \overline{z} + (\hat{\lambda}_{\pm\epsilon} - 1) \cosh 2\theta - (\hat{\lambda}_{\pm\epsilon} + 1)} \right],$$

(A.21)

where z, $\overline{z}$, $\hat{\lambda}_{\pm\epsilon}$, $\hat{\lambda}_{-\tau_1}$, $\lambda_{\pm\epsilon}$, and $\lambda_{-\tau_0}$ are defined by

$$z = e^{i\frac{2\pi x}{L}}, \overline{z} = e^{-i\frac{2\pi x}{L}}, \hat{\lambda}_{\pm\epsilon} = \exp\left(\frac{\pm 2\pi\epsilon}{L \cosh 2\theta} \right), \hat{\lambda}_{-\tau_1} = \exp\left(\frac{-2\pi\tau_1}{L \cosh 2\theta} \right),$$

$$\lambda_{\pm\epsilon} = e^{\frac{\pm 2\pi\epsilon}{L}}, \lambda_{-\tau_0} = e^{\left(\frac{-2\pi\tau_0}{L} \right)}.$$

(A.22)

41

In SSD limit, $\theta \to \infty$, the trajectories of the local operators reduce to

$$
\begin{aligned}
w_{\pm\epsilon}^{\text{New},1} &= \frac{L}{2\pi} \log\left[\frac{\pi\tau_1\left(1 - e^{\frac{\pm 2\pi\epsilon}{L}} e^{\frac{2i\pi x}{L}}\right) + Le^{\frac{\pm 2\pi\epsilon}{L}} e^{\frac{2i\pi x}{L}}}{\pi\tau_1\left(1 - e^{\frac{\pm 2\pi\epsilon}{L}} e^{\frac{2i\pi x}{L}}\right) + L} \right], \\[2mm]
\overline{w}_{\pm\epsilon}^{\text{New},1} &= \frac{L}{2\pi} \log\left[\frac{\pi\tau_1\left(1 - e^{\frac{\pm 2\pi\epsilon}{L}} e^{\frac{-2i\pi x}{L}}\right) + Le^{\frac{\pm 2\pi\epsilon}{L}} e^{\frac{-2i\pi x}{L}}}{\pi\tau_1\left(1 - e^{\frac{\pm 2\pi\epsilon}{L}} e^{\frac{-2i\pi x}{L}}\right) + L} \right], \\[2mm]
w_{\pm\epsilon}^{\text{New},2} &= \pm\epsilon + \frac{L}{2\pi} \log\left[\frac{\pi\tau_1\left(1 - e^{\frac{2i\pi x}{L}}\right) + Le^{\frac{2i\pi x}{L}}}{\pi\tau_1\left(1 - e^{\frac{2i\pi x}{L}}\right) + L} \right], \\[2mm]
\overline{w}_{\pm\epsilon}^{\text{New},2} &= \pm\epsilon + \frac{L}{2\pi} \log\left[\frac{\pi\tau_1\left(1 - e^{\frac{-2i\pi x}{L}}\right) + Le^{\frac{-2i\pi x}{L}}}{\pi\tau_1\left(1 - e^{\frac{-2i\pi x}{L}}\right) + L} \right], \\[2mm]
w_{\pm\epsilon}^{\text{New},3} &= -\tau_0 + \frac{L}{2\pi} \log\left[\frac{\pm\pi\epsilon\left(1 - e^{\frac{2i\pi x}{L}}\right) + Le^{\frac{2i\pi x}{L}}}{\pm\pi\epsilon\left(1 - e^{\frac{2i\pi x}{L}}\right) + L} \right], \\[2mm]
\overline{w}_{\pm\epsilon}^{\text{New},3} &= -\tau_0 + \frac{L}{2\pi} \log\left[\frac{\pm\pi\epsilon\left(1 - e^{\frac{-2i\pi x}{L}}\right) + Le^{\frac{-2i\pi x}{L}}}{\pm\pi\epsilon\left(1 - e^{\frac{-2i\pi x}{L}}\right) + L} \right], \\[2mm]
w_{\pm\epsilon}^{\text{New},4} &= \frac{L}{2\pi} \log\left[\frac{\pm\pi\epsilon\left(1 - e^{\frac{-2\pi\tau_0}{L}} e^{\frac{2i\pi x}{L}}\right) + Le^{\frac{-2\pi\tau_0}{L}} e^{\frac{2i\pi x}{L}}}{\pm\pi\epsilon\left(1 - e^{\frac{-2\pi\tau_0}{L}} e^{\frac{2i\pi x}{L}}\right) + L} \right], \\[2mm]
\overline{w}_{\pm\epsilon}^{\text{New},4} &= \frac{L}{2\pi} \log\left[\frac{\pm\pi\epsilon\left(1 - e^{\frac{-2\pi\tau_0}{L}} e^{\frac{-2i\pi x}{L}}\right) + Le^{\frac{-2\pi\tau_0}{L}} e^{\frac{-2i\pi x}{L}}}{\pm\pi\epsilon\left(1 - e^{\frac{-2\pi\tau_0}{L}} e^{\frac{-2i\pi x}{L}}\right) + L} \right].
\end{aligned}
\tag{A.23}
$$

B The details of energy densities without taking the small ϵ limit

Here, without taking the small ϵ limit, we present the details of energy densities during Möbius/SSD time evolution.

B.1 Möbius evolution

First, we will closely look at the time dependence of the chiral and anti-chiral energy densities during the Möbius time evolution. After performing analytic continuations, $\tau_{i=0,1} = it_{0,1}$,

without the small ϵ expansion, they are determined by

$$\langle T_{ww}(w_X)\rangle_{i=1,\cdot,4} \approx \left(\frac{2\pi}{L}\right)^2 \left[-\frac{c}{24} + \mathcal{T}^{\theta}_{i=1,\cdot,4}\right], \quad \langle T_{\overline{w}\overline{w}}(\overline{w}_X)\rangle_{i=1,\cdot,4} \approx \left(\frac{2\pi}{L}\right)^2 \left[-\frac{c}{24} + \overline{\mathcal{T}}^{\theta}_{i=1,\cdot,4}\right],$$

(B.1)

where functions, $\mathcal{T}^{\theta}_{i=1,\cdots,4}$, $\overline{\mathcal{T}}^{\theta}_{i=1,\cdots,4}$, are defined as

$$\mathcal{T}^{\theta}_{i=1} = \left(\frac{1}{2}\sinh\left(\frac{2\pi\epsilon}{L}\right)\right)^2$$

$$\times \left(\frac{1}{\cos\left(\frac{\pi t_1}{L_{\text{eff}}}\right)\sin\left(\frac{\pi(x-X-i\epsilon)}{L}\right) - \sin\left(\frac{\pi t_1}{L_{\text{eff}}}\right)\left(\cosh(2\theta)\cos\left(\frac{\pi(x-X-i\epsilon)}{L}\right) - \sinh(2\theta)\cos\left(\frac{\pi(x+X-i\epsilon)}{L}\right)\right)}\right)^2$$

$$\times \left(\frac{1}{\cos\left(\frac{\pi t_1}{L_{\text{eff}}}\right)\sin\left(\frac{\pi(x-X+i\epsilon)}{L}\right) - \sin\left(\frac{\pi t_1}{L_{\text{eff}}}\right)\left(\cosh(2\theta)\cos\left(\frac{\pi(x-X+i\epsilon)}{L}\right) - \sinh(2\theta)\cos\left(\frac{\pi(x+X+i\epsilon)}{L}\right)\right)}\right)^2,$$

$$\overline{\mathcal{T}}^{\theta}_{i=1} = \left(\frac{1}{2}\sinh\left(\frac{2\pi\epsilon}{L}\right)\right)^2$$

$$\times \left(\frac{1}{\sin\left(\frac{\pi t_1}{L_{\text{eff}}}\right)\left(\cosh(2\theta)\cos\left(\frac{\pi(x-X-i\epsilon)}{L}\right) - \sinh(2\theta)\cos\left(\frac{\pi(x+X-i\epsilon)}{L}\right)\right) + \cos\left(\frac{\pi t_1}{L_{\text{eff}}}\right)\sin\left(\frac{\pi(x-X-i\epsilon)}{L}\right)}\right)^2$$

$$\times \left(\frac{1}{\sin\left(\frac{\pi t_1}{L_{\text{eff}}}\right)\left(\cosh(2\theta)\cos\left(\frac{\pi(x-X+i\epsilon)}{L}\right) - \sinh(2\theta)\cos\left(\frac{\pi(x+X+i\epsilon)}{L}\right)\right) + \cos\left(\frac{\pi t_1}{L_{\text{eff}}}\right)\sin\left(\frac{\pi(x-X+i\epsilon)}{L}\right)}\right)^2$$

$$\mathcal{T}^{\theta}_{i=2} = \left(\frac{1}{2}\sinh\left(\frac{2\pi\epsilon}{L}\right)\right)^2$$

$$\times \left(\sinh(2\theta)\sin\left(\frac{2\pi x}{L}\right)\sin\left(\frac{2\pi t_1}{L_{\text{eff}}}\right) + \sin^2\left(\frac{\pi t_1}{L_{\text{eff}}}\right)\left(\cosh(4\theta) - \sinh(4\theta)\cos\left(\frac{2\pi x}{L}\right)\right) + \cos^2\left(\frac{\pi t_1}{L_{\text{eff}}}\right)\right)^2$$

$$\times \left(\frac{1}{\cos\left(\frac{\pi t_1}{L_{\text{eff}}}\right)\sin\left(\frac{\pi(x-X-i\epsilon)}{L}\right) - \sin\left(\frac{\pi t_1}{L_{\text{eff}}}\right)\left(\cosh(2\theta)\cos\left(\frac{\pi(x-X-i\epsilon)}{L}\right) - \sinh(2\theta)\cos\left(\frac{\pi(x+X-i\epsilon)}{L}\right)\right)}\right)^2$$

$$\times \left(\frac{1}{\cos\left(\frac{\pi t_1}{L_{\text{eff}}}\right)\sin\left(\frac{\pi(x-X+i\epsilon)}{L}\right) - \sin\left(\frac{\pi t_1}{L_{\text{eff}}}\right)\left(\cosh(2\theta)\cos\left(\frac{\pi(x-X+i\epsilon)}{L}\right) - \sinh(2\theta)\cos\left(\frac{\pi(x+X+i\epsilon)}{L}\right)\right)}\right)^2,$$

$$\overline{\mathcal{T}}^{\theta}_{i=2} = \left(\frac{1}{2}\sinh\left(\frac{2\pi\epsilon}{L}\right)\right)^2$$

$$\left(-\sinh(2\theta)\sin\left(\frac{2\pi x}{L}\right)\sin\left(\frac{2\pi t_1}{L_{\text{eff}}}\right) + \sin^2\left(\frac{\pi t_1}{L_{\text{eff}}}\right)\left(\cosh(4\theta) - \sinh(4\theta)\cos\left(\frac{2\pi x}{L}\right)\right) + \cos^2\left(\frac{\pi t_1}{L_{\text{eff}}}\right)\right)^2$$

$$\times \left(\frac{1}{\sin\left(\frac{\pi t_1}{L_{\text{eff}}}\right)\left(\cosh(2\theta)\cos\left(\frac{\pi(x-X-i\epsilon)}{L}\right) - \sinh(2\theta)\cos\left(\frac{\pi(x+X-i\epsilon)}{L}\right)\right) + \cos\left(\frac{\pi t_1}{L_{\text{eff}}}\right)\sin\left(\frac{\pi(x-X-i\epsilon)}{L}\right)}\right)^2$$

$$\times \left(\frac{1}{\sin\left(\frac{\pi t_1}{L_{\text{eff}}}\right)\left(\cosh(2\theta)\cos\left(\frac{\pi(x-X+i\epsilon)}{L}\right) - \sinh(2\theta)\cos\left(\frac{\pi(x+X+i\epsilon)}{L}\right)\right) + \cos\left(\frac{\pi t_1}{L_{\text{eff}}}\right)\sin\left(\frac{\pi(x-X+i\epsilon)}{L}\right)}\right)^2$$

(B.2)

$$\mathcal{T}^{\theta}_{i=3} =$$

$$\left(\frac{\sinh\left(\frac{2\pi\epsilon}{L_{\text{eff}}}\right)\left(\sinh(2\theta)\cos\left(\frac{2\pi x}{L}\right) - \cosh(2\theta)\right)}{2\sinh^2\left(\frac{\pi\epsilon}{L_{\text{eff}}}\right)\left(\cosh(2\theta)\cos\left(\frac{\pi(t_0-x+X)}{L}\right) - \sinh(2\theta)\cos\left(\frac{\pi(t_0+x+X)}{L}\right)\right)2 + 2\cosh^2\left(\frac{\pi\epsilon}{L_{\text{eff}}}\right)\sin^2\left(\frac{\pi(t_0-x+X)}{L}\right)} \right)^2,$$

$$\overline{\mathcal{T}}^{\theta}_{i=3} =$$

$$\left(\frac{\sinh\left(\frac{2\pi\epsilon}{L_{\text{eff}}}\right)\left(\sinh(2\theta)\cos\left(\frac{2\pi x}{L}\right) - \cosh(2\theta)\right)}{2\sinh^2\left(\frac{\pi\epsilon}{L_{\text{eff}}}\right)\left(\cosh(2\theta)\cos\left(\frac{\pi(t_0+x-X)}{L}\right) - \sinh(2\theta)\cos\left(\frac{\pi(-t_0+x+X)}{L}\right)\right)2 + 2\cosh^2\left(\frac{\pi\epsilon}{L_{\text{eff}}}\right)\sin^2\left(\frac{\pi(t_0+x-X)}{L}\right)} \right)^2,$$

$$\mathcal{T}^{\theta}_{i=4} =$$

$$\left(\frac{\sinh\left(\frac{2\pi\epsilon}{L_{\text{eff}}}\right)\left(\sinh(2\theta)\cos\left(\frac{2\pi(t_0-x)}{L}\right) - \cosh(2\theta)\right)}{2\sinh^2\left(\frac{\pi\epsilon}{L_{\text{eff}}}\right)\left(\cosh(2\theta)\cos\left(\frac{\pi(t_0-x+X)}{L}\right) - \sinh(2\theta)\cos\left(\frac{\pi(t_0-x-X)}{L}\right)\right)2 + 2\cosh^2\left(\frac{\pi\epsilon}{L_{\text{eff}}}\right)\sin^2\left(\frac{\pi(t_0-x+X)}{L}\right)} \right)^2,$$

$$\overline{\mathcal{T}}^{\theta}_{i=4} =$$

$$\left(\frac{\sinh\left(\frac{2\pi\epsilon}{L_{\text{eff}}}\right)\left(\sinh(2\theta)\cos\left(\frac{2\pi(t_0+x)}{L}\right) - \cosh(2\theta)\right)}{2\sinh^2\left(\frac{\pi\epsilon}{L_{\text{eff}}}\right)\left(\cosh(2\theta)\cos\left(\frac{\pi(t_0+x-X)}{L}\right) - \sinh(2\theta)\cos\left(\frac{\pi(t_0+x+X)}{L}\right)\right)2 + 2\cosh^2\left(\frac{\pi\epsilon}{L_{\text{eff}}}\right)\sin^2\left(\frac{\pi(t_0+x-X)}{L}\right)} \right)^2,$$

$$\text{(B.3)}$$

where the effective system size is defined as $L_{\text{eff}} = L\cosh 2\theta$.

B.2 SSD evolution

The time evolution of the energy densities during the SSD evolution is given by

$$\langle T_{ww}(w_X)\rangle_1 = \left(\frac{2\pi}{L}\right)^2\left[-\frac{c}{24} + \frac{h_{\mathcal{O}}L^4\sinh^2\left[\frac{2\pi\epsilon}{L}\right]}{4\left[2\pi t_1\sin\left[\frac{\pi X}{L}\right]\sin\left[\frac{\pi(x-i\epsilon)}{L}\right] + L\sin\left[\frac{\pi((X-x)+i\epsilon)}{L}\right]\right]^2}\right.$$

$$\left.\times\frac{1}{\left[2\pi t_1\sin\left[\frac{\pi X}{L}\right]\sin\left[\frac{\pi(x+i\epsilon)}{L}\right] + L\sin\left[\frac{\pi((X-x)-i\epsilon)}{L}\right]\right]^2}\right],$$

$$\langle T_{\overline{ww}}(\overline{w}_X)\rangle_1 = \left(\frac{2\pi}{L}\right)^2\left[-\frac{c}{24} + \frac{h_{\mathcal{O}}L^4\sinh^2\left[\frac{2\pi\epsilon}{L}\right]}{4\left[2\pi t_1\sin\left[\frac{\pi X}{L}\right]\sin\left[\frac{\pi(x+i\epsilon)}{L}\right] - L\sin\left[\frac{\pi((X-x)-i\epsilon)}{L}\right]\right]^2}\right.$$

$$\left.\times\frac{1}{\left[2\pi t_1\sin\left[\frac{\pi X}{L}\right]\sin\left[\frac{\pi(x-i\epsilon)}{L}\right] - L\sin\left[\frac{\pi((X-x)+i\epsilon)}{L}\right]\right]^2}\right],$$

$$\langle T_{ww}(w_X)\rangle_2 = \left(\frac{2\pi}{L}\right)^2\left[-\frac{c}{24} + \frac{1}{\left[2\pi t_1\sin\left[\frac{\pi(X-i\epsilon)}{L}\right]\sin\left[\frac{\pi x}{L}\right] + L\sin\left[\frac{\pi((X-x)-i\epsilon)}{L}\right]\right]^2}\right.$$

$$\left.\times\frac{h_{\mathcal{O}}\sinh^2\left[\frac{2\pi\epsilon}{L}\right]\left[L^2 + 4\pi t_1 L\sin\left(\frac{\pi x}{L}\right)\cos\left(\frac{\pi x}{L}\right) + 4\pi^2 t_1^2\sin^2\left(\frac{\pi x}{L}\right)\right]^2}{\left[2\pi t_1\sin\left[\frac{\pi(X+i\epsilon)}{L}\right]\sin\left[\frac{\pi x}{L}\right] + L\sin\left[\frac{\pi((X-x)+i\epsilon)}{L}\right]\right]^2}\right],$$

$$\langle T_{\overline{ww}}(\overline{w}_X)\rangle_2 = \left(\frac{2\pi}{L}\right)^2\left[-\frac{c}{24} + \frac{1}{\left[2\pi t_1\sin\left[\frac{\pi(X+i\epsilon)}{L}\right]\sin\left[\frac{\pi x}{L}\right] - L\sin\left[\frac{\pi((X-x)+i\epsilon)}{L}\right]\right]^2}\right.$$

$$\left.\times\frac{h_{\mathcal{O}}\sinh^2\left[\frac{2\pi\epsilon}{L}\right]\left[L^2 - 4\pi t_1\sin\left(\frac{\pi x}{L}\right)\cos\left(\frac{\pi x}{L}\right) + 4\pi^2 t_1^2\sin^2\left(\frac{\pi x}{L}\right)\right]^2}{\left[2\pi t_1\sin\left[\frac{\pi(X-i\epsilon)}{L}\right]\sin\left[\frac{\pi x}{L}\right] - L\sin\left[\frac{\pi((X-x)-i\epsilon)}{L}\right]\right]^2}\right],$$

$$\langle T_{ww}(w_X)\rangle_3 = \left(\frac{2\pi}{L}\right)^2\left[-\frac{c}{24} + \frac{4h_{\mathcal{O}}\pi^2 L^2\epsilon^2\sin^2\left[\frac{4\pi x}{L}\right]}{\left[L^2\sin^2\left[\frac{\pi(t_0-x+X)}{L}\right] + 4\pi^2\epsilon^2\sin^2\left[\frac{\pi(t_0+X)}{L}\right]\sin^2\left[\frac{\pi x}{L}\right]\right]^2}\right],$$

$$\langle T_{\overline{ww}}(\overline{w}_X)\rangle_3 = \left(\frac{2\pi}{L}\right)^2\left[-\frac{c}{24} + \frac{4h_{\mathcal{O}}\pi^2 L^2\epsilon^2\sin^2\left[\frac{4\pi x}{L}\right]}{\left[L^2\sin^2\left[\frac{\pi(t_0+x-X)}{L}\right] + 4\pi^2\epsilon^2\sin^2\left[\frac{\pi(t_0-X)}{L}\right]\sin^2\left[\frac{\pi x}{L}\right]\right]^2}\right],$$

$$\langle T_{ww}(w_X)\rangle_4 = \left(\frac{2\pi}{L}\right)^2\left[-\frac{c}{24} + \frac{4h_{\mathcal{O}}\pi^2 L^2\epsilon^2\sin^2\left[\frac{\pi\pi(-x+t_0)}{L}\right]}{\left[L^2\sin^2\left[\frac{\pi(t_0-x+X)}{L}\right] + 4\pi^2\epsilon^2\sin^2\left[\frac{\pi(t_0-X)}{L}\right]\sin^2\left[\frac{\pi x}{L}\right]\right]^2}\right],$$

$$\langle T_{\overline{ww}}(\overline{w}_X)\rangle_4 = \left(\frac{2\pi}{L}\right)^2\left[-\frac{c}{24} + \frac{4h_{\mathcal{O}}\pi^2 L^2\epsilon^2\sin^4\left[\frac{\pi(x+t_0)}{L}\right]}{\left[L^2\sin^2\left[\frac{\pi(t_0+x-X)}{L}\right] + 4\pi^2\epsilon^2\sin^2\left[\frac{\pi(t_0+X)}{L}\right]\sin^2\left[\frac{\pi x}{L}\right]\right]^2}\right],$$

(B.4)

C Results for the Integrable Theories

As mentioned in Section 4.3, the calculation of the change in the second Rényi entropy in the integrable theories is involved so we collect the relevant techincal details and results in this appendix.

C.1 Möbius Case

Let hatted quantities stand for both holomorphic/anti-holomorphic quantities and let $\sigma = +1/-1$ for holomorphic/anti-holomorphic quantities respectively. Insert the local operator at position x. Set the phase $\psi = \pi + \frac{\pi(X_1 - X_2)}{L}$ to align the branch cut along the negative real axis in the ζ^n and $\bar{\zeta}^n$ planes. Then, perform the analytic continuation $\tau_1 \to it_1$ for $i = 1, 2$ and $\tau_0 \to it_0$ for $i = 3, 4$ and expand in powers of $\delta = \frac{2\pi\epsilon}{L}$ up to the second order to find:

$\underline{\mathbf{i = 1}}$:

$$
\hat{\zeta}^n_{\rho\epsilon}
$$

$$
= \frac{\sin \frac{\pi t_1}{L \cosh 2\theta} \left(\cos \frac{\pi(x+X_2)}{L} \tanh 2\theta - \cos \frac{\pi(x-X_2)}{L} \right) + \cos \frac{\pi t_1}{L \cosh 2\theta} \sin \frac{\pi\sigma(x-X_2)}{L} \operatorname{sech} 2\theta}{\sin \frac{\pi t_1}{L \cosh 2\theta} \left(\cos \frac{\pi(x+X_1)}{L} \tanh 2\theta - \cos \frac{\pi(x-X_1)}{L} \right) + \cos \frac{\pi t_1}{L \cosh 2\theta} \sin \frac{\pi\sigma(x-X_1)}{L} \operatorname{sech} 2\theta} \Bigg(1
$$

$$
+ \left(\frac{2\pi\epsilon}{L} \right) \frac{i\rho \sin \frac{\pi\sigma(X_1 - X_2)}{L} \operatorname{sech}^2 2\theta}{2 \left[\cos \frac{\pi t_1}{L \cosh 2\theta} \operatorname{sech} 2\theta \sin \frac{\pi\sigma(x-X_1)}{L} + \sin \frac{\pi t_1}{L \cosh 2\theta} \left(\cos \frac{\pi(x+X_1)}{L} \tanh 2\theta - \cos \frac{\pi(x-X_1)}{L} \right) \right]}
$$

$$
\times \frac{1}{\left[\cos \frac{\pi t_1}{L \cosh 2\theta} \operatorname{sech} 2\theta \sin \frac{\pi\sigma(x-X_2)}{L} + \sin \frac{\pi t_1}{L \cosh 2\theta} \left(\cos \frac{\pi(x+X_2)}{L} \tanh 2\theta - \cos \frac{\pi(x-X_2)}{L} \right) \right]}
$$

$$
- \left(\frac{\pi\epsilon}{L} \right)^2 \frac{\sin \frac{\pi\sigma(X_1 - X_2)}{L} \operatorname{sech}^2 2\theta}{\left[\cos \frac{\pi t_1}{L \cosh 2\theta} \operatorname{sech} 2\theta \sin \frac{\pi\sigma(x-X_1)}{L} + \sin \frac{\pi t_1}{L \cosh 2\theta} \left(\cos \frac{\pi(x+X_1)}{L} \tanh 2\theta - \cos \frac{\pi(x-X_1)}{L} \right) \right]^2}
$$

$$
\times \frac{\left[\cos \frac{\pi t_1}{L \cosh 2\theta} \operatorname{sech} 2\theta \cos \frac{\pi(x-X_1)}{L} + \sin \frac{\pi t_1}{L \cosh 2\theta} \left(\sin \frac{\pi\sigma(x-X_1)}{L} - \sin \frac{\pi\sigma(x+X_1)}{L} \tanh 2\theta \right) \right]}{\left[\cos \frac{\pi t_1}{L \cosh 2\theta} \operatorname{sech} 2\theta \sin \frac{\pi\sigma(x-X_2)}{L} + \sin \frac{\pi t_1}{L \cosh 2\theta} \left(\cos \frac{\pi(x+X_2)}{L} \tanh 2\theta - \cos \frac{\pi(x-X_2)}{L} \right) \right]} \Bigg)
$$

$$
\tag{C.1}
$$

i = 2 :

$$\hat{\zeta}^n_{\rho\epsilon}$$

$$= \frac{\sin\frac{\pi t_1}{L\cosh 2\theta}\left(\cos\frac{\pi(x+X_2)}{L}\tanh 2\theta - \cos\frac{\pi(x-X_2)}{L}\right) + \cos\frac{\pi t_1}{L\cosh 2\theta}\sin\frac{\pi\sigma(x-X_2)}{L}\operatorname{sech}2\theta}{\sin\frac{\pi t_1}{L\cosh 2\theta}\left(\cos\frac{\pi(x+X_1)}{L}\tanh 2\theta - \cos\frac{\pi(x-X_1)}{L}\right) + \cos\frac{\pi t_1}{L\cosh 2\theta}\sin\frac{\pi\sigma(x-X_1)}{L}\operatorname{sech}2\theta}\Bigg(1$$

$$+\left(\frac{2\pi\epsilon}{L}\right)\frac{i\rho\sin\frac{\pi\sigma(X_1-X_2)}{L}}{2\left[\cos\frac{\pi t_1}{L\cosh 2\theta}\operatorname{sech}2\theta\sin\frac{\pi\sigma(x-X_1)}{L} + \sin\frac{\pi t_1}{L\cosh 2\theta}\left(\cos\frac{\pi(x+X_1)}{L}\tanh 2\theta - \cos\frac{\pi(x-X_1)}{L}\right)\right]}$$

$$\times\left[\operatorname{sech}^2 2\theta\cos^2\frac{\pi t_1}{L\cosh 2\theta} + \sin^2\frac{\pi t_1}{L\cosh 2\theta}\left(1+\tanh^2 2\theta - 2\tanh 2\theta\cos\frac{2\pi x}{L}\right)\right.$$

$$+\sin\frac{2\pi t_1}{L\cosh 2\theta}\tanh 2\theta\operatorname{sech}2\theta\sin\frac{2\pi\sigma x}{L}\Bigg]$$

$$\times\frac{1}{\left[\cos\frac{\pi t_1}{L\cosh 2\theta}\operatorname{sech}2\theta\sin\frac{\pi\sigma(x-X_2)}{L} + \sin\frac{\pi t_1}{L\cosh 2\theta}\left(\cos\frac{\pi(x+X_2)}{L}\tanh 2\theta - \cos\frac{\pi(x-X_2)}{L}\right)\right]}$$

$$-\left(\frac{\pi\epsilon}{L}\right)^2\frac{\sin\frac{\pi\sigma(X_1-X_2)}{L}}{\left[\cos\frac{\pi t_1}{L\cosh 2\theta}\operatorname{sech}2\theta\sin\frac{\pi\sigma(x-X_2)}{L} + \sin\frac{\pi t_1}{L\cosh 2\theta}\left(\cos\frac{\pi(x+X_2)}{L}\tanh 2\theta - \cos\frac{\pi(x-X_2)}{L}\right)\right]}$$

$$\times\frac{\left[\cos\frac{\pi t_1}{L\cosh 2\theta}\operatorname{sech}2\theta\cos\frac{\pi(x-X_1)}{L} + \sin\frac{\pi t_1}{L\cosh 2\theta}\left(\sin\frac{\pi\sigma(x-X_1)}{L} + \sin\frac{\pi\sigma(x+X_1)}{L}\tanh 2\theta\right)\right]}{\left[\cos\frac{\pi t_1}{L\cosh 2\theta}\operatorname{sech}2\theta\sin\frac{\pi\sigma(x-X_1)}{L} + \sin\frac{\pi t_1}{L\cosh 2\theta}\left(\cos\frac{\pi(x+X_1)}{L}\tanh 2\theta - \cos\frac{\pi(x-X_1)}{L}\right)\right]^2}$$

$$\times\left[\operatorname{sech}^2 2\theta\cos^2\frac{\pi t_1}{L\cosh 2\theta} + \sin^2\frac{\pi t_1}{L\cosh 2\theta}\left(1+\tanh^2 2\theta - 2\tanh 2\theta\cos\frac{2\pi x}{L}\right)\right.$$

$$+\sin\frac{2\pi\sigma x}{L}\sin\frac{2\pi t_1}{L\cosh 2\theta}\tanh 2\theta\operatorname{sech}2\theta\Bigg] \tag{C.2}$$

i = 3 :

$$\hat{\zeta}^n_{\rho\epsilon}$$

$$= \frac{\sin\frac{\pi[t_0+\sigma(X_2-x)]}{L}}{\sin\frac{\pi[t_0+\sigma(X_1-x)]}{L}}\Bigg\{1 + \left(\frac{2\pi\epsilon}{L}\right)\frac{i\rho\sin\frac{\pi\sigma(X_1-X_2)}{L}\left(1-\cos\frac{2\pi x}{L}\tanh 2\theta\right)}{2\sin\frac{\pi[t_0+\sigma(X_1-x)]}{L}\sin\frac{\pi[t_0+\sigma(X_2-x)]}{L}}$$

$$+\left(\frac{2\pi\epsilon}{L}\right)^2\frac{\sin\frac{\pi\sigma(X_1-X_2)}{L}\left(1-\cos\frac{2\pi x}{L}\tanh 2\theta\right)\left[\cos\frac{\pi[t_0+\sigma(X_1-x)]}{L} - \cos\frac{\pi[t_0+\sigma(X_1+x)]}{L}\tanh 2\theta\right]}{4\sin^2\frac{\pi[t_0+\sigma(X_1-x)]}{L}\sin\frac{\pi[t_0+\sigma(X_2-x)]}{L}}\Bigg\} \tag{C.3}$$

<u>**i = 4 :**</u>

$$\hat{\zeta}_{\rho\epsilon}^{n}$$

$$=\frac{\sin\frac{\pi[t_0+\sigma(X_2-x)]}{L}}{\sin\frac{\pi[t_0+\sigma(X_1-x)]}{L}}\left\{1+\left(\frac{2\pi\epsilon}{L}\right)\frac{i\rho\sin\frac{\pi\sigma(X_1-X_2)}{L}\left(1-\cos\frac{2\pi(t_0-x\sigma)}{L}\tanh2\theta\right)}{2\sin\frac{\pi[t_0+\sigma(X_1-x)]}{L}\sin\frac{\pi[t_0+\sigma(X_2-x)]}{L}}+\left(\frac{\pi\epsilon}{L}\right)^2\right.$$

$$\left.\times\frac{\sin\frac{\pi\sigma(X_1-X_2)}{L}\left(1-\cos\frac{2\pi(t_0-\sigma x)}{L}\tanh2\theta\right)\left[\cos\frac{\pi[t_0+\sigma(X_1-x)]}{L}-\cos\frac{\pi[t_0-\sigma(X_1+x)]}{L}\tanh2\theta\right]}{\sin^2\frac{\pi[t_0+\sigma(X_1-x)]}{L}\sin\frac{\pi[t_0+\sigma(X_2-x)]}{L}}\right\}$$

$$\tag{C.4}$$

In these formulas, $\rho=\pm1$. Note that the signs always appear in the form $\rho\epsilon$, σx, σX_1 and σX_2 so the anti-holomorphic coordinates can be obtained from the holomorphic ones by simply flipping the signs $x\to-x$, $X_1\to-X_1$ and $X_2\to-X_2$. For finite values of θ, when $\sin\frac{\pi t_1}{L\cosh2\theta}\left(\cos\frac{\pi(x+X_j)}{L}\tanh2\theta-\cos\frac{\pi(x-X_j)}{L}\right)+\cos\frac{\pi t_1}{L\cosh2\theta}\sin\frac{\pi\sigma(x-X_j)}{L}\operatorname{sech}2\theta\neq0$ for $j=1,2$ and $i=1,2$, ξ_0,ξ_1 as defined in (4.21) are non-zero and finite and ξ_2 is finite. The envelope functions for $i=3$ and $i=4$, $1-\cos\frac{2\pi x}{L}\tanh2\theta$ and $1-\cos\frac{2\pi(t_0-\sigma x)}{L}\tanh2\theta$ respectively, are never zero for finite θ so for finite θ and $\frac{t_0+\sigma(X_j-x)}{L}\notin\mathbb{Z}$, $\xi_0,\xi_1\neq0$ and are finite while ξ_2 is finite. The cross ratios to second order in $\frac{\epsilon}{L}$ are

$$\hat{\eta}_2$$

$$=\begin{cases}
\frac{1}{2}\left(1-\operatorname{sgn}\left[\frac{\sin\frac{\pi t_1}{L\cosh2\theta}\left(\cos\frac{\pi(x+X_2)}{L}\tanh2\theta-\cos\frac{\pi(x-X_2)}{L}\right)+\cos\frac{\pi t_1}{L\cosh2\theta}\sin\frac{\pi\sigma(x-X_2)}{L}\operatorname{sech}2\theta}{\sin\frac{\pi t_1}{L\cosh2\theta}\left(\cos\frac{\pi(x+X_1)}{L}\tanh2\theta-\cos\frac{\pi(x-X_1)}{L}\right)+\cos\frac{\pi t_1}{L\cosh2\theta}\sin\frac{\pi\sigma(x-X_1)}{L}\operatorname{sech}2\theta}\right]\right. \\[4pt]
\left.\times\left[1-\left(\frac{\pi\epsilon}{L}\right)^2\frac{\sin^2\frac{\pi(X_1-X_2)}{L}\operatorname{sech}^4 2\theta}{2\left[\cos\frac{\pi t_1}{L\cosh2\theta}\operatorname{sech}2\theta\sin\frac{\pi\sigma(x-X_1)}{L}+\sin\frac{\pi t_1}{L\cosh2\theta}\left(\cos\frac{\pi(x+X_1)}{L}\tanh2\theta-\cos\frac{\pi(x-X_1)}{L}\right)\right]^2}\right.\right. \\[4pt]
\left.\left.\times\frac{1}{\left[\cos\frac{\pi t_1}{L\cosh2\theta}\operatorname{sech}2\theta\sin\frac{\pi\sigma(x-X_2)}{L}+\sin\frac{\pi t_1}{L\cosh2\theta}\left(\cos\frac{\pi(x+X_2)}{L}\tanh2\theta-\cos\frac{\pi(x-X_2)}{L}\right)\right]^2}\right]\right), & i=1 \\[10pt]
\frac{1}{2}\left(1-\operatorname{sgn}\left[\frac{\sin\frac{\pi t_1}{L\cosh2\theta}\left(\cos\frac{\pi(x+X_2)}{L}\tanh2\theta-\cos\frac{\pi(x-X_2)}{L}\right)+\cos\frac{\pi t_1}{L\cosh2\theta}\sin\frac{\pi\sigma(x-X_2)}{L}\operatorname{sech}2\theta}{\sin\frac{\pi t_1}{L\cosh2\theta}\left(\cos\frac{\pi(x+X_1)}{L}\tanh2\theta-\cos\frac{\pi(x-X_1)}{L}\right)+\cos\frac{\pi t_1}{L\cosh2\theta}\sin\frac{\pi\sigma(x-X_1)}{L}\operatorname{sech}2\theta}\right]\right. \\[4pt]
\times\left[1-\left(\frac{\pi\epsilon}{L}\right)^2\frac{\sin^2\frac{\pi(X_1-X_2)}{L}}{2\left[\cos\frac{\pi t_1}{L\cosh2\theta}\operatorname{sech}2\theta\sin\frac{\pi\sigma(x-X_1)}{L}+\sin\frac{\pi t_1}{L\cosh2\theta}\left(\cos\frac{\pi(x+X_1)}{L}\tanh2\theta-\cos\frac{\pi(x-X_1)}{L}\right)\right]^2}\right. \\[4pt]
\frac{1}{\left[\cos\frac{\pi t_1}{L\cosh2\theta}\operatorname{sech}2\theta\sin\frac{\pi\sigma(x-X_2)}{L}+\sin\frac{\pi t_1}{L\cosh2\theta}\left(\cos\frac{\pi(x+X_2)}{L}\tanh2\theta-\cos\frac{\pi(x-X_2)}{L}\right)\right]^2} \\[4pt]
\times\left\{\operatorname{sech}^2 2\theta\cos^2\frac{\pi t_1}{L\cosh2\theta}+\sin^2\frac{\pi t_1}{L\cosh2\theta}\left(1+\tanh^2 2\theta-2\tanh2\theta\cos\frac{2\pi x}{L}\right)\right. \\[4pt]
\left.\left.\left.+\sin\frac{2\pi\sigma x}{L}\sin\frac{2\pi t_1}{L\cosh2\theta}\tanh2\theta\operatorname{sech}2\theta\right\}^2\right]\right), & i=2 \\[10pt]
\frac{1}{2}\left\{1-\operatorname{sgn}\left[\frac{\sin\frac{\pi[t_0+\sigma(X_2-x)]}{L}}{\sin\frac{\pi[t_0+\sigma(X_1-x)]}{L}}\right]\left[1-\left(\frac{2\pi\epsilon}{L}\right)^2\frac{\sin^2\frac{\pi(X_1-X_2)}{L}\left(1-\cos\frac{2\pi x}{L}\tanh2\theta\right)^2}{8\sin^2\frac{\pi[t_0+\sigma(X_1-x)]}{L}\sin^2\frac{\pi[t_0+\sigma(X_2-x)]}{L}}\right]\right\}, & i=3 \\[10pt]
\frac{1}{2}\left\{1-\operatorname{sgn}\left[\frac{\sin\frac{\pi[t_0+\sigma(X_2-x)]}{L}}{\sin\frac{\pi[t_0+\sigma(X_1-x)]}{L}}\right]\left[1-\left(\frac{2\pi\epsilon}{L}\right)^2\frac{\sin^2\frac{\pi(X_1-X_2)}{L}\left(1-\cos\frac{2\pi(t_0-\sigma x)}{L}\tanh2\theta\right)^2}{8\sin^2\frac{\pi[t_0+\sigma(X_1-x)]}{L}\sin^2\frac{\pi[t_0+\sigma(X_2-x)]}{L}}\right]\right\}, & i=4.
\end{cases}$$

$$\tag{C.5}$$

Note that the cross ratios are periodic in time with period $L \cosh 2\theta$ for $i = 1, 2$ and L for $i = 3$ and they are completely symmetric under an exchange of X_1 and X_2. These cross ratios reduce to (C.18) in the SSD $\theta \to \infty$ limit.

C.1.1 Operator at X_1^f

In the $\frac{\epsilon}{L} \to 0$ limit, the cross ratios are approximately

$$
\hat{\eta}_2 = \begin{cases}
\frac{1}{2} \left\{ 1 - \mathrm{sgn} \left[\dfrac{\cos \frac{\pi X_2}{L} \tan \frac{\pi t_1}{L \cosh 2\theta} + \sigma e^{2\theta} \tan \frac{\pi X_2}{L}}{\cos \frac{\pi X_1}{L} \tan \frac{\pi t_1}{L \cosh 2\theta} + \sigma e^{2\theta} \tan \frac{\pi X_1}{L}} \right] \right. \\
\qquad \left. \times \left[1 - \left(\frac{\epsilon}{L}\right)^2 \times (\text{positive term}) \right] \right\}, & i = 1, 2, \cos \frac{\pi t_1}{L \cosh 2\theta} \neq 0 \\[2ex]
\frac{1}{2} \left\{ 1 - \mathrm{sgn} \left[\dfrac{\cos \frac{\pi X_2}{L}}{\cos \frac{\pi X_1}{L}} \right] \left[1 - \left(\frac{\epsilon}{L}\right)^2 \times (\text{positive term}) \right] \right\}, & i = 1, 2, \cos \frac{\pi t_1}{L \cosh 2\theta} = 0 \\[2ex]
\frac{1}{2} \left\{ 1 - \mathrm{sgn} \left[\dfrac{\sin \frac{\pi (t_0 + \sigma X_2)}{L}}{\sin \frac{\pi (t_0 + \sigma X_1)}{L}} \right] \left[1 - \left(\frac{\epsilon}{L}\right)^2 \times (\text{positive term}) \right] \right\}, & i = 3 \\[2ex]
\frac{1}{2} \left\{ 1 - \mathrm{sgn} \left[\dfrac{\sin \frac{\pi (t_0 + \sigma X_2)}{L}}{\sin \frac{\pi (t_0 + \sigma X_1)}{L}} \right] \right. \\
\qquad \left. \times \left[1 - \left(\frac{\epsilon}{L}\right)^2 \left(1 - \cos \frac{2\pi t_0}{L} \tanh 2\theta \right)^2 \times (\text{positive term}) \right] \right\}, & i = 4
\end{cases}
\tag{C.6}
$$

where we used the fact that $X_j \neq \frac{L}{2}$ for $i = 1, 2$.

Case (a)

Consider the interval $A = [0, X_2] \cup [X_1, L]$ with $0 < X_2 < \frac{L}{2} < X_1 < L$ and $X_2 > L - X_1 > 0$. The second Rényi entanglement entropy is

$$
\Delta S_{A,i}^{(2)}(t_i) = \begin{cases}
0, & i = 1, 2, m < \frac{t_1}{L \cosh 2\theta} < m - \frac{\tan^{-1}\left(e^{2\theta} \tan \frac{\pi X_1}{L}\right)}{\pi} \\[1.5ex]
\log 2, & i = 1, 2, m - \frac{\tan^{-1}\left(e^{2\theta} \tan \frac{\pi X_1}{L}\right)}{\pi} < \frac{t_1}{L \cosh 2\theta} < m + \frac{\tan^{-1}\left(e^{2\theta} \tan \frac{\pi X_2}{L}\right)}{\pi} \\[1.5ex]
0, & i = 1, 2, m + \frac{\tan^{-1}\left(e^{2\theta} \tan \frac{\pi X_2}{L}\right)}{\pi} < \frac{t_1}{L \cosh 2\theta} < m + 1 - \frac{\tan^{-1}\left(e^{2\theta} \tan \frac{\pi X_2}{L}\right)}{\pi} \\[1.5ex]
\log 2, & i = 1, 2, m + 1 - \frac{\tan^{-1}\left(e^{2\theta} \tan \frac{\pi X_2}{L}\right)}{\pi} < \frac{t_1}{L \cosh 2\theta} < m + 1 + \frac{\tan^{-1}\left(e^{2\theta} \tan \frac{\pi X_1}{L}\right)}{\pi} \\[1.5ex]
0, & i = 1, 2, m + 1 + \frac{\tan^{-1}\left(e^{2\theta} \tan \frac{\pi X_1}{L}\right)}{\pi} < \frac{t_1}{L \cosh 2\theta} < m + 1 \\[1.5ex]
0, & i = 3, 4, m < \frac{t_0}{L} < m + 1 - \frac{X_1}{L} \\[1ex]
\log 2, & i = 3, 4, m + 1 - \frac{X_1}{L} < \frac{t_0}{L} < m + \frac{X_2}{L} \\[1ex]
0, & i = 3, 4, m + \frac{X_2}{L} < \frac{t_0}{L} < m + 1 - \frac{X_2}{L} \\[1ex]
\log 2, & i = 3, 4, m + 1 - \frac{X_2}{L} < \frac{t_0}{L} < m + \frac{X_1}{L} \\[1ex]
0, & i = 3, 4, m + \frac{X_1}{L} < \frac{t_0}{L} < m + 1
\end{cases}
\tag{C.7}
$$

for non-negative integers m. The principal branch of the arctangent is chosen, i.e. $\tan^{-1}(x) \in (-\frac{\pi}{2}, \frac{\pi}{2})$. The $i = 1, 2$ results are fully explained by the Möbius quasiparticle picture with finite θ. Initially, $\Delta S_{A,1}^{(2)}(t_1) = 0$ because both quasiparticles are contained in subsystem A. At $\frac{t_1}{L \cosh 2\theta} = m - \frac{\tan^{-1}\left(e^{2\theta} \tan \frac{\pi X_1}{L}\right)}{\pi}$, the left-moving quasiparticle hits X_1 and exits subsystem A so the second Rényi entropy jumps to $\Delta S_{A,1}^{(2)}(t_1) = \log 2$. At $t_1 = L \cosh 2\theta \left[m + \frac{\tan^{-1}\left(e^{2\theta} \tan \frac{\pi X_2}{L}\right)}{\pi}\right]$, the right-moving quasiparticle hits X_2 and also exits the subsystem so the second Rényi entropy drops back down to $\Delta S_{A,1}^{(2)}(t_1) = 0$. At $t_1 = L \cosh 2\theta \left[m + 1 - \frac{\tan^{-1}\left(e^{2\theta} \tan \frac{\pi X_2}{L}\right)}{\pi}\right]$, the left-moving quasiparticle hits X_2 and re-enters the subsystem so the second Rényi entropy increases back up to $\Delta S_{A,1}^{(2)}(t_1) = \log 2$ until $t_1 = L \cosh 2\theta \left[m + 1 + \frac{\tan^{-1}\left(e^{2\theta} \tan \frac{\pi X_1}{L}\right)}{\pi}\right]$ when the right moving quasiparticle re-enters A so the second Rényi entropy drops back down to $\Delta S_{A,1}^{(2)}(t_1) = 0$. Setting $\theta = 0$ gives the obvious answer that generalizes the result in [25] but for a finite spatial system instead. Note that $\Delta S_{A,i}^{(2)}(t_1)$ for $i = 1, 2$ is continuous even when $\cos \frac{\pi t_1}{L \cosh 2\theta} = 0$ to leading order in $\frac{\epsilon}{L}$.

On the other hand, the $i = 3, 4$ case is explained by the uniform $\theta = 0$ quasiparticle picture.

Case (b)

Consider the interval $A = [X_2, X_1]$ with $X_1 > \frac{L}{2} > X_2 > 0$ and $\frac{L}{2} - X_2 > X_1 - \frac{L}{2}$. The second Rényi entanglement entropy is

$$\Delta S_{A,i}^{(2)}(t_i) = \begin{cases} 0, & i = 1, 2, m < \frac{t_1}{L \cosh 2\theta} < m + \frac{\tan^{-1}\left(e^{2\theta} \tan \frac{\pi X_2}{L}\right)}{\pi} \\ \log 2, & i = 1, 2, m + \frac{\tan^{-1}\left(e^{2\theta} \tan \frac{\pi X_2}{L}\right)}{\pi} < \frac{t_1}{L \cosh 2\theta} < m - \frac{\tan^{-1}\left(e^{2\theta} \tan \frac{\pi X_1}{L}\right)}{\pi} \\ 0, & i = 1, 2, m - \frac{\tan^{-1}\left(e^{2\theta} \tan \frac{\pi X_1}{L}\right)}{\pi} < \frac{t_1}{L \cosh 2\theta} < m + 1 + \frac{\tan^{-1}\left(e^{2\theta} \tan \frac{\pi X_1}{L}\right)}{\pi} \\ \log 2, & i = 1, 2, m + 1 + \frac{\tan^{-1}\left(e^{2\theta} \tan \frac{\pi X_1}{L}\right)}{\pi} < \frac{t_1}{L \cosh 2\theta} < m + 1 - \frac{\tan^{-1}\left(e^{2\theta} \tan \frac{\pi X_2}{L}\right)}{\pi} \\ 0, & i = 1, 2, m + 1 - \frac{\tan^{-1}\left(e^{2\theta} \tan \frac{\pi X_2}{L}\right)}{\pi} < \frac{t_1}{L \cosh 2\theta} < m + 1 \\ 0, & i = 3, 4, m < \frac{t_0}{L} < m + \frac{X_2}{L} \\ \log 2, & i = 3, 4, m + \frac{X_2}{L} < \frac{t_0}{L} < m + 1 - \frac{X_1}{L} \\ 0, & i = 3, 4, m + 1 - \frac{X_1}{L} < \frac{t_0}{L} < m + \frac{X_1}{L} \\ \log 2, & i = 3, 4, m + \frac{X_1}{L} < \frac{t_0}{L} < m + 1 - \frac{X_2}{L} \\ 0, & i = 3, 4, m + 1 - \frac{X_2}{L} < \frac{t_0}{L} < m + 1 \end{cases}$$

(C.8)

for non-negative integers m. The $i = 1, 2$ case is explained by the Möbius quasiparticle picture. Initially, both quasiparticles are outside of A so $\Delta S_{A,1}^{(2)}(t_1) = 0$. At $t_1 = L \cosh 2\theta \left[m + \frac{\tan^{-1}\left(e^{2\theta} \tan \frac{\pi X_2}{L}\right)}{\pi}\right]$, the right-moving quasiparticle hits X_2 and enters subsys-

tem A so the second Rényi entropy increases to $\Delta S_{A,1}^{(2)}(t_1) = \log 2$. The left-moving quasi-particle hits X_1 at $\frac{t_1}{L\cosh 2\theta} = m - \frac{\tan^{-1}\left(e^{2\theta}\tan\frac{\pi X_1}{L}\right)}{\pi}$ and also enters subsystem A so the second Rényi entropy drops back down to $\Delta S_{A,1}^{(2)}(t_1) = 0$. The right-moving quasiparticle subsequently arrives at X_1 at $\frac{t_1}{L\cosh 2\theta} = m + 1 + \frac{\tan^{-1}\left(e^{2\theta}\tan\frac{\pi X_1}{L}\right)}{\pi}$ and leaves subsystem A so the second Rényi entanglement entropy goes back up to $\Delta S_{A,1}^{(2)}(t_1) = \log 2$. Finally, at $t_1 = L\cosh 2\theta \left[m + 1 - \frac{\tan^{-1}\left(e^{2\theta}\tan\frac{\pi X_2}{L}\right)}{\pi}\right]$, the left-moving quasiparticle reaches X_2 and also leaves the subsystem so the second Rényi entropy drops back down to $\Delta S_{A,1}^{(2)}(t_1) = 0$. The change in the second Rényi entropy $\Delta S_{A,i}^{(2)}(t_1)$ for $i = 1, 2$ is continuous even when $\cos\frac{\pi t_1}{L\cosh 2\theta} = 0$ to leading order in $\frac{\epsilon}{L}$.

On the other hand, the $i = 3, 4$ case is described by the uniform $\theta = 0$ quasiparticle picture.

Case (c)

Consider the interval $A = [X_2, X_1]$ with $0 < X_2 < X_1 < \frac{L}{2}$. The second Rényi entanglement entropy is

$$
\Delta S_{A,i}^{(2)}(t_i) = \begin{cases}
0, & i = 1, 2, \, m < \frac{t_1}{L\cosh 2\theta} < m + \frac{\tan^{-1}\left(e^{2\theta}\tan\frac{\pi X_2}{L}\right)}{\pi} \\
\log 2, & i = 1, 2, \, m + \frac{\tan^{-1}\left(e^{2\theta}\tan\frac{\pi X_2}{L}\right)}{\pi} < \frac{t_1}{L\cosh 2\theta} < m + \frac{\tan^{-1}\left(e^{2\theta}\tan\frac{\pi X_1}{L}\right)}{\pi} \\
0, & i = 1, 2, \, m + \frac{\tan^{-1}\left(e^{2\theta}\tan\frac{\pi X_1}{L}\right)}{\pi} < \frac{t_1}{L\cosh 2\theta} < m + 1 - \frac{\tan^{-1}\left(e^{2\theta}\tan\frac{\pi X_1}{L}\right)}{\pi} \\
\log 2, & i = 1, 2, \, m + 1 - \frac{\tan^{-1}\left(e^{2\theta}\tan\frac{\pi X_1}{L}\right)}{\pi} < \frac{t_1}{L\cosh 2\theta} < m + 1 - \frac{\tan^{-1}\left(e^{2\theta}\tan\frac{\pi X_2}{L}\right)}{\pi} \\
0, & i = 1, 2, \, m + 1 - \frac{\tan^{-1}\left(e^{2\theta}\tan\frac{\pi X_2}{L}\right)}{\pi} < \frac{t_1}{L\cosh 2\theta} < m + 1 \\
0, & i = 3, 4, \, m < \frac{t_0}{L} < m + \frac{X_2}{L} \\
\log 2, & i = 3, 4, \, m + \frac{X_2}{L} < \frac{t_0}{L} < m + \frac{X_1}{L} \\
0, & i = 3, 4, \, m + \frac{X_1}{L} < \frac{t_0}{L} < m + 1 - \frac{X_1}{L} \\
\log 2, & i = 3, 4, \, m + 1 - \frac{X_1}{L} < \frac{t_0}{L} < m + 1 - \frac{X_2}{L} \\
0, & i = 3, 4, \, m + 1 - \frac{X_2}{L} < \frac{t_0}{L} < m + 1
\end{cases}
$$

$$\tag{C.9}$$

for non-negative integers m. The Möbius quasiparticle picture explains the $i = 1, 2$ cases. Initially, both quasiparticles are outside subsystem A so $\Delta S_{A,1}^{(2)}(t_1) = 0$. The right-moving quasiparticle arrives at X_2 and enters subsystem A at $t_1 = L\cosh 2\theta \left[m + \frac{\tan^{-1}\left(e^{2\theta}\tan\frac{\pi X_2}{L}\right)}{\pi}\right]$ so the second Rényi entanglement entropy increases to $\Delta S_{A,1}^{(2)}(t_1) = \log 2$. It then reaches X_1 at $\frac{t_1}{L\cosh 2\theta} = m + \frac{\tan^{-1}\left(e^{2\theta}\tan\frac{\pi X_1}{L}\right)}{\pi}$ at exits the subsystem A so the second Rényi entanglement entropy drops back down to $\Delta S_{A,1}^{(2)}(t_1) = 0$. Subsequently, the left-moving quasiparticle enters subsystem A through X_1 at $t_1 = L\cosh 2\theta \left[m + 1 - \frac{\tan^{-1}\left(e^{2\theta}\tan\frac{\pi X_1}{L}\right)}{\pi}\right]$

so the second Rényi entanglement entropy goes back up to $\Delta S_{A,1}^{(2)}(t_1) = \log 2$. Finally, at $t_1 = L \cosh 2\theta \left[m + 1 - \frac{\tan^{-1}\left(e^{2\theta} \tan \frac{\pi X_2}{L}\right)}{\pi} \right]$, the left-moving quasiparticle hits X_2 and exits subsystem A so the second Rényi entanglement entropy drops back down to $\Delta S_{A,1}^{(2)}(t_1) = 0$. As before, the change in the second Rényi entropy $\Delta S_{A,i}^{(2)}(t_1)$ for $i = 1, 2$ is continuous even when $\cos \frac{\pi t_1}{L \cosh 2\theta} = 0$ to leading order in $\frac{\epsilon}{L}$.

On the other hand, the $i = 3, 4$ case is described by the uniform $\theta = 0$ quasiparticle picture.

C.1.2 Operator at X_2^f

The trajectory of quasiparticles that begin at $x = \frac{L}{2}$ is given by sending $x \to \frac{L}{2}$ in (4.32) and can be rewritten as

$$
t_1 = L \cosh 2\theta \left[k - \frac{\mu \tan^{-1}\left(e^{-2\theta} \cot \frac{\pi X}{L}\right)}{\pi} \right] \tag{C.10}
$$

where $k \in \mathbb{Z}$ and $\mu = +1/-1$ for right/left moving quasiparticles.

When the local operator is placed at the second fixed point $x = X_2^f$, the cross ratio (C.5) simplifies to

$$
\hat{\eta}_2 = \begin{cases}
\frac{1}{2}\left\{ 1 - \text{sgn}\left[\frac{\tan \frac{\pi t_1}{L \cosh 2\theta} - \sigma e^{-2\theta} \cot \frac{\pi X_2}{L}}{\tan \frac{\pi t_1}{L \cosh 2\theta} - \sigma e^{-2\theta} \cot \frac{\pi X_1}{L}} \right] \right. \\
\left. \times \left[1 - \left(\frac{\epsilon}{L}\right)^2 \times \text{(positive term)} \right] \right\}, & i = 1, 2, \cos \frac{\pi t_1}{L \cosh 2\theta} \neq 0 \\[2mm]
\mathcal{O}\left(\left(\frac{\epsilon}{L}\right)^2 \right), & i = 1, 2, \cos \frac{\pi t_1}{L \cosh 2\theta} = 0 \\[2mm]
\frac{1}{2}\left\{ 1 - \text{sgn}\left[\frac{\cos \frac{\pi(t_0 + \sigma X_2)}{L}}{\cos \frac{\pi(t_0 + \sigma X_1)}{L}} \right] \left[1 - \left(\frac{\epsilon}{L}\right)^2 \times \text{positive number} \right] \right\}, & i = 3 \\[2mm]
\frac{1}{2}\left\{ 1 - \text{sgn}\left[\frac{\cos \frac{\pi(t_0 + \sigma X_2)}{L}}{\cos \frac{\pi(t_0 + \sigma X_1)}{L}} \right] \right. \\
\left. \times \left[1 - \left(\frac{\epsilon}{L}\right)^2 \left(1 + \cos \frac{2\pi t_0}{L} \tanh 2\theta\right)^2 \times \text{positive term} \right] \right\}, & i = 4
\end{cases} \tag{C.11}
$$

where we used the fact that $0 < X_2, X_1 < L$.

Case (a)

Consider the interval $A = [0, X_2] \cup [X_1, L]$ with $X_2 > L - X_1 > 0$. The second Rényi entanglement entropy is

$$\Delta S_{A,i}^{(2)}(t_i) = \begin{cases} 0, & i = 1, 2, m < \frac{t_1}{L \cosh 2\theta} < m + \frac{\tan^{-1}\left(e^{-2\theta} \cot \frac{\pi X_2}{L}\right)}{\pi} \\ \log 2, & i = 1, 2, m + \frac{\tan^{-1}\left(e^{-2\theta} \cot \frac{\pi X_2}{L}\right)}{\pi} < \frac{t_1}{L \cosh 2\theta} < m - \frac{\tan^{-1}\left(e^{-2\theta} \cot \frac{\pi X_1}{L}\right)}{\pi} \\ 0, & i = 1, 2, m - \frac{\tan^{-1}\left(e^{-2\theta} \cot \frac{\pi X_1}{L}\right)}{\pi} < \frac{t_1}{L \cosh 2\theta} < m + 1 + \frac{\tan^{-1}\left(e^{-2\theta} \cot \frac{\pi X_1}{L}\right)}{\pi} \\ \log 2, & i = 1, 2, m + 1 + \frac{\tan^{-1}\left(e^{-2\theta} \cot \frac{\pi X_1}{L}\right)}{\pi} < \frac{t_1}{L \cosh 2\theta} < m + 1 - \frac{\tan^{-1}\left(e^{-2\theta} \cot \frac{\pi X_2}{L}\right)}{\pi} \\ 0, & i = 1, 2, m + 1 - \frac{\tan^{-1}\left(e^{-2\theta} \cot \frac{\pi X_2}{L}\right)}{\pi} < \frac{t_1}{L \cosh 2\theta} < m + 1 \\ 0, & i = 3, 4, m < \frac{t_0}{L} < m + \frac{1}{2} - \frac{X_2}{L} \\ \log 2, & i = 3, 4, m + \frac{1}{2} - \frac{X_2}{L} < \frac{t_0}{L} < m + \frac{X_1}{L} - \frac{1}{2} \\ 0, & i = 3, 4, m + \frac{X_1}{L} - \frac{1}{2} < \frac{t_0}{L} < m + \frac{3}{2} - \frac{X_1}{L} \\ \log 2, & i = 3, 4, m + \frac{3}{2} - \frac{X_1}{L} < \frac{t_0}{L} < m + \frac{1}{2} + \frac{X_2}{L} \\ 0, & i = 3, 4, m + \frac{1}{2} + \frac{X_2}{L} < \frac{t_0}{L} < (m+1) \end{cases}$$

(C.12)

for non-negative integers m.

For $i = 1, 2$, the Rényi entropy is continuous at $t_1 = \frac{2k+1}{2} L \cosh 2\theta$ at leading order in $\frac{\epsilon}{L}$. Taking the $\theta = 0$ limit for $i = 1, 2$ gives the obvious generalization of the result in [25]. Initially, both quasiparticles are outside of A so $\Delta S_{A,1}^{(2)}(t_1) = 0$. At $t_1 = L \cosh 2\theta \left[m + \frac{\tan^{-1}\left(e^{-2\theta} \cot \frac{\pi X_2}{L}\right)}{\pi} \right]$, the left-moving quasiparticle hits X_2 and enters A so $\Delta S_{A,1}^{(2)}(t_1) = \log 2$. The right-moving quasiparticle hits X_1 at $\frac{t_1}{L \cosh 2\theta} = m - \frac{\tan^{-1}\left(e^{-2\theta} \cot \frac{\pi X_1}{L}\right)}{\pi}$ and enters A as well so the second Rényi entanglement entropy drops back down to $\Delta S_{A,1}^{(2)}(t_1) = 0$. At $t_1 = L \cosh 2\theta \left[m + 1 + \frac{\tan^{-1}\left(e^{-2\theta} \cot \frac{\pi X_1}{L}\right)}{\pi} \right]$, the left moving quasiparticle arrives at X_1 and exits subsystem A so the second Rényi entropy goes back up to $\Delta S_{A,1}^{(2)}(t_1) = \log 2$. The right moving quasiparticle also leaves the subsystem at $t_1 = L \cosh 2\theta \left[m + 1 - \frac{\tan^{-1}\left(e^{-2\theta} \cot \frac{\pi X_2}{L}\right)}{\pi} \right]$ so the second Rényi entanglement entropy returns to its original value of $\Delta S_{A,1}^{(2)}(t_1) = 0$. Note that the change in the second Rényi entropy $\Delta S_{A,i}^{(2)}(t_1)$ for $i = 1, 2$ is continuous even when $\cos \frac{\pi t_1}{L \cosh 2\theta} = 0$ to leading order in $\frac{\epsilon}{L}$.

On the other hand, the $i = 3, 4$ Rényi entropy is described by the uniform $\theta = 0$ quasiparticle picture.

Case (b)

Consider the interval $A = [X_2, X_1]$ with $X_1 > \frac{L}{2} > X_2 > 0$ and $\frac{L}{2} - X_2 > X_1 - \frac{L}{2}$. The second Rényi entanglement entropy is

$$\Delta S_{A,i}^{(2)}(t_i) = \begin{cases} 0, & i = 1, 2, m < \frac{t_1}{L \cosh 2\theta} < m - \frac{\tan^{-1}\left(e^{-2\theta} \cot \frac{\pi X_1}{L}\right)}{\pi} \\ \log 2, & i = 1, 2, m - \frac{\tan^{-1}\left(e^{-2\theta} \cot \frac{\pi X_1}{L}\right)}{\pi} < \frac{t_1}{L \cosh 2\theta} < m + \frac{\tan^{-1}\left(e^{-2\theta} \cot \frac{\pi X_2}{L}\right)}{\pi} \\ 0, & i = 1, 2, m + \frac{\tan^{-1}\left(e^{-2\theta} \cot \frac{\pi X_2}{L}\right)}{\pi} < \frac{t_1}{L \cosh 2\theta} < m + 1 - \frac{\tan^{-1}\left(e^{-2\theta} \cot \frac{\pi X_2}{L}\right)}{\pi} \\ \log 2, & i = 1, 2, m + 1 - \frac{\tan^{-1}\left(e^{-2\theta} \cot \frac{\pi X_2}{L}\right)}{\pi} < \frac{t_1}{L \cosh 2\theta} < m + 1 + \frac{\tan^{-1}\left(e^{-2\theta} \cot \frac{\pi X_1}{L}\right)}{\pi} \\ 0, & i = 1, 2, m + 1 + \frac{\tan^{-1}\left(e^{-2\theta} \cot \frac{\pi X_1}{L}\right)}{\pi} < \frac{t_1}{L \cosh 2\theta} < m + 1 \\ 0, & i = 3, 4, m < \frac{t_0}{L} < m + \frac{X_1}{L} - \frac{1}{2} \\ \log 2, & i = 3, 4, m + \frac{X_1}{L} - \frac{1}{2} < \frac{t_0}{L} < m + \frac{1}{2} - \frac{X_2}{L} \\ 0, & i = 3, 4, m + \frac{1}{2} - \frac{X_2}{L} < \frac{t_0}{L} < m + \frac{1}{2} + \frac{X_2}{L} \\ \log 2, & i = 3, 4, m + \frac{1}{2} + \frac{X_2}{L} < \frac{t_0}{L} < m + \frac{3}{2} - \frac{X_1}{L} \\ 0, & i = 3, 4, m + \frac{3}{2} - \frac{X_1}{L} < \frac{t_0}{L} < m + 1 \end{cases}$$

(C.13)

for non-negative integers m. For $i = 1, 2$, the Rényi entropy is continuous at $t_1 = \frac{2k+1}{2} L \cosh 2\theta$ for integer k at leading order in $\frac{\epsilon}{L}$. For $i = 1, 2$, the uniform $\theta = 0$ case gives the obvious sensible answer. For finite θ, both particles begin in subsystem A so $\Delta S_{A,1}^{(2)}(t_1) = 0$. The right moving quasiparticle reaches X_1 at $t_1 = L \cosh 2\theta \left[m - \frac{\tan^{-1}\left(e^{-2\theta} \cot \frac{\pi X_1}{L}\right)}{\pi}\right]$ and exits the subsystem A so the second Rényi entropy goes up to $\Delta S_{A,1}^{(2)}(t_1) = \log 2$. The left moving quasiparticle also exits the subsystem at $t_1 = L \cosh 2\theta \left[m + \frac{\tan^{-1}\left(e^{-2\theta} \cot \frac{\pi X_2}{L}\right)}{\pi}\right]$ so the second Rényi entropy drops back down to $\Delta S_{A,1}^{(2)}(t_1) = 0$. The right-moving quasiparticle subsequently re-enters subsystem A at $t_1 = L \cosh 2\theta \left[m + 1 - \frac{\tan^{-1}\left(e^{-2\theta} \cot \frac{\pi X_2}{L}\right)}{\pi}\right]$ so the second Rényi entropy goes back up to $\Delta S_{A,1}^{(2)}(t_1) = \log 2$. Finally, the left moving quasiparticle re-enters A at $\frac{t_1}{L \cosh 2\theta} = m + 1 + \frac{\tan^{-1}\left(e^{-2\theta} \cot \frac{\pi X_1}{L}\right)}{\pi}$ so the second Rényi entropy returns to $\Delta S_{A,1}^{(2)}(t_1) = 0$. As before, the change in the second Rényi entropy $\Delta S_{A,i}^{(2)}(t_1)$ for $i = 1, 2$ is continuous even when $\cos \frac{\pi t_1}{L \cosh 2\theta} = 0$ to leading order in $\frac{\epsilon}{L}$.

On the other hand, the $i = 3, 4$ cases are explained by the $\theta = 0$ uniform quasiparticle picture.

Case (c)

Consider the interval $A = [X_2, X_1]$ with $0 < X_2 < X_1 < \frac{L}{2}$. The second Rényi entanglement entropy is

$$\Delta S_{A,i}^{(2)}(t_i) = \begin{cases} 0, & i = 1, 2, m < \frac{t_1}{L\cosh 2\theta} < m + \frac{\tan^{-1}\left(e^{-2\theta}\cot\frac{\pi X_1}{L}\right)}{\pi} \\ \log 2, & i = 1, 2, m + \frac{\tan^{-1}\left(e^{-2\theta}\cot\frac{\pi X_1}{L}\right)}{\pi} < \frac{t_1}{L\cosh 2\theta} < m + \frac{\tan^{-1}\left(e^{-2\theta}\cot\frac{\pi X_2}{L}\right)}{\pi} \\ 0, & i = 1, 2, m + \frac{\tan^{-1}\left(e^{-2\theta}\cot\frac{\pi X_2}{L}\right)}{\pi} < \frac{t_1}{L\cosh 2\theta} < m + 1 - \frac{\tan^{-1}\left(e^{-2\theta}\cot\frac{\pi X_2}{L}\right)}{\pi} \\ \log 2, & i = 1, 2, m + 1 - \frac{\tan^{-1}\left(e^{-2\theta}\cot\frac{\pi X_2}{L}\right)}{\pi} < \frac{t_1}{L\cosh 2\theta} < m + 1 - \frac{\tan^{-1}\left(e^{-2\theta}\cot\frac{\pi X_1}{L}\right)}{\pi} \\ 0, & i = 1, 2, m + 1 - \frac{\tan^{-1}\left(e^{-2\theta}\cot\frac{\pi X_1}{L}\right)}{\pi} < \frac{t_1}{L\cosh 2\theta} < m + 1 \\ 0, & i = 3, 4, m < \frac{t_0}{L} < m + \frac{1}{2} - \frac{X_1}{L} \\ \log 2, & i = 3, 4, m + \frac{1}{2} - \frac{X_1}{L} < \frac{t_0}{L} < m + \frac{1}{2} - \frac{X_2}{L} \\ 0, & i = 3, 4, m + \frac{1}{2} - \frac{X_2}{L} < \frac{t_0}{L} < m + \frac{1}{2} + \frac{X_2}{L} \\ \log 2, & i = 3, 4, m + \frac{1}{2} + \frac{X_2}{L} < \frac{t_0}{L} < m + \frac{1}{2} + \frac{X_1}{L} \\ 0, & i = 3, 4, m + \frac{1}{2} + \frac{X_1}{L} < \frac{t_0}{L} < m + 1 \end{cases}$$

(C.14)

for non-negative integers m. For $i = 1, 2$, the Rényi entropy is continuous at $t_1 = \frac{2k+1}{2}L\cosh 2\theta$ for integer k at leading order in $\frac{\epsilon}{L}$. For $i = 1, 2$, the $\theta = 0$ case gives the sensible answer. For finite θ, initially, both quasiparticles are located outside A so $\Delta S_{A,1}^{(2)}(t_1) = 0$. At $t_1 = L\cosh 2\theta\left[m + \frac{\tan^{-1}\left(e^{-2\theta}\cot\frac{\pi X_1}{L}\right)}{\pi}\right]$, the left moving quasiparticle reaches X_1 and enters subsystem A so $\Delta S_{A,1}^{(2)}(t_1) = \log 2$. It then travels to X_2 at $t_1 = L\cosh 2\theta\left[m + \frac{\tan^{-1}\left(e^{-2\theta}\cot\frac{\pi X_2}{L}\right)}{\pi}\right]$ and exits the subsystem so the second Rényi entropy drops back down to $\Delta S_{A,1}^{(2)}(t_1) = 0$. The right moving quasiparticle arrives at X_2 at $t_1 = L\cosh 2\theta\left[m + 1 - \frac{\tan^{-1}\left(e^{-2\theta}\cot\frac{\pi X_2}{L}\right)}{\pi}\right]$ and enters subsystem A so the second Rényi entropy jumps to $\Delta S_{A,1}^{(2)}(t_1) = \log 2$. Finally, at $t_1 = L\cosh 2\theta\left[m + 1 - \frac{\tan^{-1}\left(e^{-2\theta}\cot\frac{\pi X_1}{L}\right)}{\pi}\right]$, the right moving quasiparticle reaches X_1 and exits the subsystem so the second Rényi entropy drops back down to $\Delta S_{A,1}^{(2)}(t_1) = 0$. As before, the change in the second Rényi entropy $\Delta S_{A,i}^{(2)}(t_1)$ for $i = 1, 2$ is continuous even when $\cos\frac{\pi t_1}{L\cosh 2\theta} = 0$ to leading order in $\frac{\epsilon}{L}$.

As usual, the $i = 3, 4$ cases are explained by the $\theta = 0$ uniform quasiparticle picture.

C.2 SSD Quench

Putting the $w^{\text{New,i}}, \overline{w}^{\text{New,i}}$ coordinates that correspond to SSD evolution into the uniformization map (4.4), aligning the branch cut of $\zeta^n, \overline{\zeta}^n$ along the negative real axis by setting $\psi = \pi + \frac{\pi(X_1 - X_2)}{L}$ and analytically continuing to real time $\tau_1 = it_1$ for $i = 1, 2$ and $\tau_0 = it_0$

for $i = 3, 4$, the coordinates on the n-sheeted Riemann surface to second order in $\frac{2\pi\epsilon}{L}$ are

$$\hat{\zeta}^n_{\rho\epsilon} = \begin{cases}
\frac{t_1 \sin\frac{\pi x}{L} \sin\frac{\pi X_2}{L} + \frac{L}{2\pi}\sin\frac{\pi\sigma(X_2-x)}{L}}{t_1 \sin\frac{\pi x}{L}\sin\frac{\pi X_1}{L} + \frac{L}{2\pi}\sin\frac{\pi\sigma(X_1-x)}{L}} \left\{ 1 \right. \\[2mm]
\quad + \left(\frac{2\pi\epsilon}{L}\right) \frac{i\rho L^2 \sin\frac{\pi\sigma(X_1-X_2)}{L}}{8\pi^2 \left[t_1 \sin\frac{\pi x}{L}\sin\frac{\pi X_1}{L} + \frac{L}{2\pi}\sin\frac{\pi\sigma(X_1-x)}{L}\right]\left[t_1 \sin\frac{\pi x}{L}\sin\frac{\pi X_2}{L} + \frac{L}{2\pi}\sin\frac{\pi\sigma(X_2-x)}{L}\right]} \\[2mm]
\quad \left. - \left(\frac{2\pi\epsilon}{L}\right)^2 \frac{L^2 \sin\frac{\pi\sigma(X_1-X_2)}{L}\left[t_1 \sin\frac{\pi\sigma X_1}{L}\cos\frac{\pi x}{L} - \frac{L}{2\pi}\cos\frac{\pi(x-X_1)}{L}\right]}{16\pi^2 \left[t_1 \sin\frac{\pi x}{L}\sin\frac{\pi X_1}{L} + \frac{L}{2\pi}\sin\frac{\pi\sigma(X_1-x)}{L}\right]^2 \left[t_1 \sin\frac{\pi x}{L}\sin\frac{\pi X_2}{L} + \frac{L}{2\pi}\sin\frac{\pi\sigma(X_2-x)}{L}\right]} \right\}, & i = 1 \\[6mm]

\frac{t_1 \sin\frac{\pi x}{L}\sin\frac{\pi X_2}{L} + \frac{L}{2\pi}\sin\frac{\pi\sigma(X_2-x)}{L}}{t_1 \sin\frac{\pi x}{L}\sin\frac{\pi X_1}{L} + \frac{L}{2\pi}\sin\frac{\pi\sigma(X_1-x)}{L}} \left\{ 1 \right. \\[2mm]
\quad + \left(\frac{2\pi\epsilon}{L}\right) \frac{i\rho \sin\frac{\pi\sigma(X_1-X_2)}{L}\left(L^2 + 4\pi^2 t_1^2 \sin^2\frac{\pi x}{L} + 2\pi t_1 L \sin\frac{2\pi x\sigma}{L}\right)}{8\pi^2 \left[t_1 \sin\frac{\pi x}{L}\sin\frac{\pi X_1}{L} + \frac{L}{2\pi}\sin\frac{\pi\sigma(X_1-x)}{L}\right]\left[t_1 \sin\frac{\pi x}{L}\sin\frac{\pi X_2}{L} + \frac{L}{2\pi}\sin\frac{\pi\sigma(X_2-x)}{L}\right]} \\[2mm]
\quad \left. + \left(\frac{2\pi\epsilon}{L}\right)^2 \frac{\sin\frac{\pi\sigma(X_1-X_2)}{L}\left[t_1 \sin\frac{\pi\sigma x}{L}\cos\frac{\pi X_1}{L} + \frac{L}{2\pi}\cos\frac{\pi(x-X_1)}{L}\right]\left(L^2 + 4\pi^2 t_1^2 \sin^2\frac{\pi x}{L} + 2\pi t_1 L \sin\frac{2\pi x\sigma}{L}\right)}{16\pi^2 \left[t_1 \sin\frac{\pi x}{L}\sin\frac{\pi X_1}{L} + \frac{L}{2\pi}\sin\frac{\pi\sigma(X_1-x)}{L}\right]^2 \left[t_1 \sin\frac{\pi x}{L}\sin\frac{\pi X_2}{L} + \frac{L}{2\pi}\sin\frac{\pi\sigma(X_2-x)}{L}\right]} \right\}, & i = 2 \\[6mm]

\frac{\sin\frac{\pi[t_0+\sigma(X_2-x)]}{L}}{\sin\frac{\pi[t_0+\sigma(X_1-x)]}{L}} \left\{ 1 - \left(\frac{2\pi\epsilon}{L}\right) \frac{i\rho \sin^2\frac{\pi x}{L}\sin\frac{\pi\sigma(X_1-X_2)}{L}}{\sin\frac{\pi[t_0+\sigma(X_1-x)]}{L}\sin\frac{\pi[t_0+\sigma(X_2-x)]}{L}} \right. \\[2mm]
\quad \left. + \left(\frac{2\pi\epsilon}{L}\right)^2 \frac{\sin^3\frac{\pi x\sigma}{L}\sin\frac{\pi\sigma(X_1-X_2)}{L}\sin\frac{\pi(t_0+\sigma X_1)}{L}}{\sin^2\frac{\pi[t_0+\sigma(X_1-x)]}{L}\sin\frac{\pi[t_0+\sigma(X_2-x)]}{L}} \right\}, & i = 3 \\[6mm]

\frac{\sin\frac{\pi[t_0+\sigma(X_2-x)]}{L}}{\sin\frac{\pi[t_0+\sigma(X_1-x)]}{L}} \left\{ 1 - \left(\frac{2\pi\epsilon}{L}\right) \frac{i\rho \sin^2\frac{\pi(t_0-\sigma x)}{L}\sin\frac{\pi\sigma(X_1-X_2)}{L}}{\sin\frac{\pi[t_0+\sigma(X_1-x)]}{L}\sin\frac{\pi[t_0+\sigma(X_2-x)]}{L}} \right. \\[2mm]
\quad \left. - \left(\frac{2\pi\epsilon}{L}\right)^2 \frac{\sin^3\frac{\pi(t_0-\sigma x)}{L}\sin\frac{\pi\sigma(X_1-X_2)}{L}\sin\frac{\pi\sigma X_1}{L}}{\sin^2\frac{\pi[t_0+\sigma(X_1-x)]}{L}\sin\frac{\pi[t_0+\sigma(X_2-x)]}{L}} \right\}, & i = 4
\end{cases}$$

$$\text{(C.15)}$$

where x is the position where the local operator was inserted. Taking the $\theta \to \infty$ limit of the Möbius coordinates (C.1,C.2,C.3,C.4) reproduces the SSD coordinates (C.15). When $x = 0$ for $i = 3$, the coordinates of the two local operators are

$$\hat{\zeta}_{\pm\epsilon} = \frac{\sin\frac{\pi(t_0+\sigma X_2)}{L}}{\sin\frac{\pi(t_0+\sigma X_1)}{L}} \tag{C.16}$$

which is equivalent to setting the regulator $\epsilon = 0$. The two local operators are coincident and hence the correlator is ill-defined. Naively, if

$$\frac{\sin\frac{\pi(t_0+\sigma X_2)}{L}}{\sin\frac{\pi(t_0+\sigma X_1)}{L}} < 0, \tag{C.17}$$

the coordinates of the two operators $\hat{\zeta}^2_{\pm\epsilon}$ sit on the branch cut on the negative real axis and the rotation that we have been doing would be ill-defined. Similarly, for $i = 4$, when $t_0 = \sigma x + nL$ for $n \in \mathbb{Z}$, the regulator ϵ drops out of the exact coordinates and the two operators become co-incident.

When $t_1 \sin \frac{\pi x}{L} \sin \frac{\pi X_j}{L} + \frac{L}{2\pi} \sin \frac{\pi \sigma (X_j - x)}{L} \neq 0$ for $j = 1, 2$ for $i = 1, 2$ and $x \neq 0$, $\frac{t_0 + \sigma(X_j - x)}{L} \notin \mathbb{Z}$ for $j = 1, 2$ for $i = 3$, and $\frac{t_0 - \sigma x}{L} \notin \mathbb{Z}$ and $\frac{t_0 + \sigma(X_j - x)}{L} \notin \mathbb{Z}$ for $j = 1, 2$ for $i = 4$, both ξ_0, ξ_1 as defined in (4.21) are non-zero and are finite and ξ_2 is finite so the cross ratios to second order in $\frac{\epsilon}{L}$ (4.29) are

$$
\hat{\eta}_2 = \begin{cases}
\frac{1}{2} \left\{ 1 - \text{sgn} \left[\frac{t_1 \sin \frac{\pi x}{L} \sin \frac{\pi X_2}{L} + \frac{L}{2\pi} \sin \frac{\pi \sigma(X_2 - x)}{L}}{t_1 \sin \frac{\pi x}{L} \sin \frac{\pi X_1}{L} + \frac{L}{2\pi} \sin \frac{\pi \sigma(X_1 - x)}{L}} \right] \left[1 \right. \right. \\
\left. \left. - \left(\frac{2\pi\epsilon}{L} \right)^2 \frac{L^4 \sin^2 \frac{\pi(X_1 - X_2)}{L}}{128\pi^4 \left[t_1 \sin \frac{\pi x}{L} \sin \frac{\pi X_1}{L} + \frac{L}{2\pi} \sin \frac{\pi\sigma(X_1 - x)}{L} \right]^2 \left[t_1 \sin \frac{\pi x}{L} \sin \frac{\pi X_2}{L} + \frac{L}{2\pi} \sin \frac{\pi\sigma(X_2 - x)}{L} \right]^2} \right] \right\}, & i = 1 \\[2em]
\frac{1}{2} \left\{ 1 - \text{sgn} \left[\frac{t_1 \sin \frac{\pi x}{L} \sin \frac{\pi X_2}{L} + \frac{L}{2\pi} \sin \frac{\pi \sigma(X_2 - x)}{L}}{t_1 \sin \frac{\pi x}{L} \sin \frac{\pi X_1}{L} + \frac{L}{2\pi} \sin \frac{\pi\sigma(X_1 - x)}{L}} \right] \left[1 \right. \right. \\
\left. \left. - \left(\frac{2\pi\epsilon}{L} \right)^2 \frac{\sin^2 \frac{\pi(X_1 - X_2)}{L} \left[L^2 + 4\pi^2 t_1^2 \sin^2 \frac{\pi x}{L} + 2\pi t_1 L \sin \frac{2\pi x \sigma}{L} \right]^2}{128\pi^4 \left[t_1 \sin \frac{\pi x}{L} \sin \frac{\pi X_1}{L} + \frac{L}{2\pi} \sin \frac{\pi\sigma(X_1 - x)}{L} \right]^2 \left[t_1 \sin \frac{\pi x}{L} \sin \frac{\pi X_2}{L} + \frac{L}{2\pi} \sin \frac{\pi\sigma(X_2 - x)}{L} \right]^2} \right] \right\}, & i = 2 \\[2em]
\frac{1}{2} \left\{ 1 - \text{sgn} \left[\frac{\sin \frac{\pi[t_0 + \sigma(X_2 - x)]}{L}}{\sin \frac{\pi[t_0 + \sigma(X_1 - x)]}{L}} \right] \left[1 - \left(\frac{2\pi\epsilon}{L} \right)^2 \frac{\sin^4 \frac{\pi x}{L} \sin^2 \frac{\pi(X_1 - X_2)}{L}}{2 \sin^2 \frac{\pi[t_0 + \sigma(X_1 - x)]}{L} \sin^2 \frac{\pi[t_0 + \sigma(X_2 - x)]}{L}} \right] \right\}, & i = 3 \\[2em]
\frac{1}{2} \left\{ 1 - \text{sgn} \left[\frac{\sin \frac{\pi[t_0 + \sigma(X_2 - x)]}{L}}{\sin \frac{\pi[t_0 + \sigma(X_1 - x)]}{L}} \right] \left[1 - \left(\frac{2\pi\epsilon}{L} \right)^2 \frac{\sin^4 \frac{\pi(t_0 - \sigma x)}{L} \sin^2 \frac{\pi(X_1 - X_2)}{L}}{2 \sin^2 \frac{\pi[t_0 + \sigma(X_1 - x)]}{L} \sin^2 \frac{\pi[t_0 + \sigma(X_2 - x)]}{L}} \right] \right\}, & i = 4
\end{cases}
$$
(C.18)

C.2.1 Operator at X_1^f

Setting $x = 0$ in (C.18) gives

$$
\hat{\eta}_2(x = 0) = \begin{cases}
\mathcal{O} \left(\frac{\epsilon^2}{L^2} \right), i = 1, 2, \forall t_1 > 0 \\[1em]
\frac{1}{2} \left\{ 1 - \text{sgn} \left[\frac{\sin \frac{\pi(t_0 + \sigma X_2)}{L}}{\sin \frac{\pi(t_0 + \sigma X_1)}{L}} \right] \left[1 - \left(\frac{\epsilon}{L} \right)^2 \sin^4 \frac{\pi t_0}{L} \times \text{positive number} \right] \right\}, i = 4
\end{cases}
$$
(C.19)

for $0 < X_1, X_2 < L$. The second order term in the cross ratio for the $i = 4$ case in (C.19) vanishes when $\frac{t_0}{L} \in \mathbb{Z}$. As explained previously, setting $x = 0$ for the $i = 3$ case as well as $t_0 = nL$ for $n \in \mathbb{Z}$ for $i = 4$ leads to correlators that are ill-defined because $w_\epsilon^{\text{New,i}} = w_{-\epsilon}^{\text{New,i}}$. That is, the operators become coincident and the cross ratios $\eta_2 = \bar{\eta}_2 = 0$ vanish identically to all orders in ϵ. The following results hold away from these special cases.

Contrast the $i = 4$ cross ratio with the corresponding Möbius cross ratio (C.6) where the regulator term does not vanish for finite θ for all time $t_0 \in \mathbb{R}$. The time-dependence of the cross ratio $\hat{\eta}_2$ is the same to $\mathcal{O} \left(\frac{\epsilon}{L} \right)$ as in the Möbius case so $\Delta S_{A,4}^{(2)}$ is the same for the Möbius case as it is for the SSD case with the exception that the correlation functions and hence the Rényi entropy remains well-defined even when $\frac{t_0}{L} \in \mathbb{Z}$ for the Möbius evolution. Note also that for $i = 4$, the cross ratio is periodic in time t_0 with period L.

Case (a)

The change in second Rényi entropy is

$$\Delta S^{(2)}_{A,i}(t_i) = \begin{cases} 0, & i = 1,2 \\ 0, & i = 4, mL < t_0 < mL + L - X_1 \\ \log 2, & i = 4, mL + L - X_1 < t_0 < mL + X_2 \\ 0, & i = 4, mL + X_2 < t_0 < mL + L - X_2 \\ \log 2, & i = 4, mL + L - X_2 < t_0 < mL + X_1 \\ 0, & i = 4, mL + X_1 < t_0 < (m+1)L \end{cases} \tag{C.20}$$

for non-negative integers m. Taking the SSD limit of (C.7) for $i = 1,2$ reproduces the corresponding result in (C.20). The $i = 4$ case is explained by the $\theta = 0$ uniform quasiparticle picture. Keep in mind that for $i = 4$, the local operator correlation function and hence the second Rényi entropy is ill-defined at $\frac{t_0}{L} \in \mathbb{Z}$.

Case (b)

The change in second Rényi entropy is

$$\Delta S^{(2)}_{A,i}(t_i) = \begin{cases} 0, & i = 1,2 \\ 0, & i = 4, mL < t_0 < mL + X_2 \\ \log 2, & i = 4, mL + X_2 < t_0 < mL + L - X_1 \\ 0, & i = 4, mL + L - X_1 < t_0 < mL + X_1 \\ \log 2, & i = 4, mL + X_1 < t_0 < mL + L - X_2 \\ 0, & i = 4, mL + L - X_2 < t_0 < (m+1)L \end{cases} \tag{C.21}$$

for non-negative integers m. Taking the $\theta \to \infty$ SSD limit in (C.8) reproduces the first line of (C.21). The $i = 4$ case is explained by the uniform $\theta = 0$ quasiparticle picture.

Case (c)

The change in second Rényi entropy is

$$\Delta S^{(2)}_{A,i}(t_i) = \begin{cases} 0, & i = 1,2 \\ 0, & i = 4, mL < t_0 < mL + X_2 \\ \log 2, & i = 4, mL + X_2 < t_0 < mL + X_1 \\ 0, & i = 4, mL + X_1 < t_0 < mL + L - X_1 \\ \log 2, & i = 4, mL + L - X_1 < t_0 < mL + L - X_2 \\ 0, & i = 4, mL + L - X_2 < t_0 < (m+1)L \end{cases} \tag{C.22}$$

for non-negative integers m. Taking the $\theta \to \infty$ SSD limit in (C.9) reproduces the first line of (C.22). As before, the $i = 4$ case is explained by the uniform $\theta = 0$ quasiparticle picture.

C.2.2 Operator at X_2^f

Setting $x = \frac{L}{2}$ in (C.18) gives

$$
\hat{\eta}_2\left(x = \frac{L}{2}\right)
$$

$$
= \begin{cases}
\frac{1}{2}\left\{1 - \mathrm{sgn}\left[\frac{t_1 - \frac{\sigma L}{2\pi}\cot\frac{\pi X_2}{L}}{t_1 - \frac{\sigma L}{2\pi}\cot\frac{\pi X_1}{L}}\right]\left[1 - \left(\frac{\epsilon}{L}\right)^2 \times \text{positive number}\right]\right\}, & i = 1, 2 \\[2ex]
\frac{1}{2}\left\{1 - \mathrm{sgn}\left[\frac{\cos\frac{\pi(t_0 + \sigma X_2)}{L}}{\cos\frac{\pi(t_0 + \sigma X_1)}{L}}\right]\left[1 - \left(\frac{\epsilon}{L}\right)^2 \times \text{positive number}\right]\right\}, & i = 3 \\[2ex]
\frac{1}{2}\left\{1 - \mathrm{sgn}\left[\frac{\cos\frac{\pi(t_0 + \sigma X_2)}{L}}{\cos\frac{\pi(t_0 + \sigma X_1)}{L}}\right]\left[1 - \left(\frac{\epsilon}{L}\right)^2 \cos^4\frac{\pi t_0}{L} \times \text{positive number}\right]\right\}, & i = 4
\end{cases}
\tag{C.23}
$$

where the cross ratio is periodic in time with $t_0 \sim t_0 + L$ for $i = 3$. The cross ratio for $i = 3$ is the same for both Möbius and SSD quenches so for $i = 3$, $\Delta S_{A,i}^{(2)}$ is the same for both Möbius and SSD when the local operator is inserted at $x = \frac{L}{2}$.

As before, when $t_0 = \frac{2k+1}{2}L$ for $k \in \mathbb{Z}$, the regulator term vanishes for the $i = 4$ case and the correlator and hence the second Rényi entropy is ill-defined since $w_\epsilon^{\mathrm{New},4} = w_{-\epsilon}^{\mathrm{New},4}$ which means that the operators become coincident and the cross ratios $\eta_2 = \bar{\eta}_2 = 0$ vanish identically to all orders in ϵ. The second Rényi entropy is ill-defined at these times for $i = 4$ for holographic CFTs as well. Contrast this with the Möbius case where the regulator term does not vanish for finite θ and the cross ratios are identical to those of the SSD quench for $\Delta S_{A,4}^{(2)}(t_0)$ with $x = \frac{L}{2}$ to order $\mathcal{O}\left(\frac{\epsilon}{L}\right)$ so the Rényi entropy is the same for both Möbius and SSD for $i = 4$ with the exception that the correlators and hence the Rényi entropy are well defined even at $t_0 = \frac{2k+1}{2}L$ for integers k in the Möbius quench.

Case (a)

The change in second Rényi entropy is

$$
\Delta S_{A,i}^{(2)}(t_i) = \begin{cases}
\log 2, & i = 1, 2, \frac{L}{2\pi}\cot\frac{\pi X_2}{L} < t_1 < \frac{L}{2\pi}|\cot\frac{\pi X_1}{L}| \\
0 & i = 1, 2, 0 < t_1 < \frac{L}{2\pi}\cot\frac{\pi X_2}{L} \quad \text{and} \quad \frac{L}{2\pi}|\cot\frac{\pi X_1}{L}| < t_1 \\
0, & i = 3, 4, mL < t_0 < mL + \frac{L}{2} - X_2 \\
\log 2, & i = 3, 4, mL + \frac{L}{2} - X_2 < t_0 < mL + X_1 - \frac{L}{2} \\
0, & i = 3, 4, mL + X_1 - \frac{L}{2} < t_0 < mL + \frac{3L}{2} - X_1 \\
\log 2, & i = 3, 4, mL + \frac{3L}{2} - X_1 < t_0 < mL + \frac{L}{2} + X_2 \\
0, & i = 3, 4, mL + \frac{L}{2} + X_2 < t_0 < (m+1)L
\end{cases}
\tag{C.24}
$$

for non-negative integers m. For $i = 1, 2$, both quasiparticles are initially outside the subsystem so $\Delta S_{A,1}^{(2)}(t_1) = 0$. The left-moving quasiparticle enters the subsystem at $\frac{L}{2\pi}\cot\frac{\pi X_2}{L}$ and $\Delta S_{A,1}^{(2)}(t_1)$ jumps to $\log 2$ before the right-moving quasiparticle also enters the subsystem at $\frac{L}{2\pi}|\cot\frac{\pi X_1}{L}|$ and $\Delta S_{A,1}^{(2)}(t_1)$ drops back down to 0. Taking the $\theta \to \infty$ SSD limit of (C.12), where only the $m = 0$ period matters, gives the $i = 1, 2$ result in (C.24).

The $i = 3, 4$ case is explained by the uniform $\theta = 0$ quasiparticle picture.

Case (b)

The change in second Rényi entropy is

$$\Delta S_{A,i}^{(2)}(t_i) = \begin{cases} \log 2, & i = 1, 2, \frac{L}{2\pi} |\cot \frac{\pi X_1}{L}| < t_1 < \frac{L}{2\pi} \cot \frac{\pi X_2}{L} \\ 0 & i = 1, 2, 0 < t_1 < \frac{L}{2\pi} |\cot \frac{\pi X_1}{L}| \quad \text{and} \quad \frac{L}{2\pi} \cot \frac{\pi X_2}{L} < t_1 \\ 0, & i = 3, 4, mL < t_0 < mL + X_1 - \frac{L}{2} \\ \log 2, & i = 3, 4, mL + X_1 - \frac{L}{2} < t_0 < mL + \frac{L}{2} - X_2 \\ 0, & i = 3, 4, mL + \frac{L}{2} - X_2 < t_0 < mL + \frac{L}{2} + X_2 \\ \log 2, & i = 3, 4, mL + \frac{L}{2} + X_2 < t_0 < mL + \frac{3L}{2} - X_1 \\ 0, & i = 3, 4, mL + \frac{3L}{2} - X_1 < t_0 < (m+1)L \end{cases} \tag{C.25}$$

for non-negative integers m. For $i = 1, 2$, both quasiparticles begin in subsystem A so $\Delta S_{A,1}^{(2)}(t_1) = 0$. At time $\frac{L}{2\pi} |\cot \frac{\pi X_1}{L}|$, the right-moving quasiparticle leaves subsystem A so $\Delta S_{A,1}^{(2)}(t_1)$ jumps to $\log 2$. Subsequently, the left-moving quasiparticle leaves the subsystem A at $\frac{L}{2\pi} \cot \frac{\pi X_2}{L}$ and $\Delta S_{A,1}^{(2)}(t_1)$ drops back down to 0. Taking the $\theta \to \infty$ SSD limit in (C.13) for $i = 1, 2$ reproduces the corresponding result in (C.25).

The uniform $\theta = 0$ quasiparticle picture fully explains the $i = 3, 4$ case.

Case (c)

The change in second Rényi entropy entropy is

$$\Delta S_{A,i}^{(2)}(t_i) = \begin{cases} \log 2, & i = 1, 2, \frac{L}{2\pi} \cot \frac{\pi X_1}{L} < t_1 < \frac{L}{2\pi} \cot \frac{\pi X_2}{L} \\ 0 & i = 1, 2, 0 < t_1 < \frac{L}{2\pi} \cot \frac{\pi X_1}{L} \quad \text{and} \quad \frac{L}{2\pi} \cot \frac{\pi X_2}{L} < t_1 \\ 0, & i = 3, 4, mL < t_0 < mL + \frac{L}{2} - X_1 \\ \log 2, & i = 3, 4, mL + \frac{L}{2} - X_1 < t_0 < mL + \frac{L}{2} - X_2 \\ 0, & i = 3, 4, mL + \frac{L}{2} - X_2 < t_0 < mL + \frac{L}{2} + X_2 \\ \log 2, & i = 3, 4, mL + \frac{L}{2} + X_2 < t_0 < mL + \frac{L}{2} + X_1 \\ 0, & i = 3, 4, mL + \frac{L}{2} + X_1 < t_0 < (m+1)L \end{cases} \tag{C.26}$$

for non-negative integers m. For $i = 1, 2$, both quasiparticles are initially outside subsystem A. The left-moving quasiparticle enters the subsystem at $\frac{L}{2\pi} \cot \frac{\pi X_1}{L}$, causing $\Delta S_{A,1}^{(2)}(t_1)$ to jump to $\log 2$ before exiting the subsystem at $\frac{L}{2\pi} \cot \frac{\pi X_2}{L}$ at which time $\Delta S_{A,1}^{(2)}(t_1)$ drops back down to 0. Taking the $\theta \to \infty$ SSD limit of (C.14) for $i = 1, 2$ reproduces the corresponding result in (C.26).

The $i = 3, 4$ case is explained by the uniform $\theta = 0$ quasiparticle picture.

C.2.3 Information survival in integrable theories

As we have seen in the previous subsections, when the time evolution operator is the SSD Hamiltonian, the late time second Rényi entropy for the local operator quenched state returns to the vacuum value as the subsystems are situated away from the fixed point X_1^f where the quasiparticles accumulate. To have a non-vacuum second Rényi entropy at late times, place the local operator at X_2^f and consider a subsystem $A = [X_2, X_1]$ where $X_2 = 0$ and $0 < X_1 < \frac{L}{2}$.

The coordinates are

$$
\hat{\zeta}_{\rho\epsilon}^n =
\begin{cases}
\dfrac{1}{\cos\frac{\pi X_1}{L} - \frac{2\pi t_1}{L}\sin\frac{\pi\sigma X_1}{L}}\left\{ 1 + \left(\frac{2\pi\epsilon}{L}\right) \dfrac{i\rho\sin\frac{\pi\sigma X_1}{L}}{2\left(\cos\frac{\pi X_1}{L} - \frac{2\pi t_1}{L}\sin\frac{\pi\sigma X_1}{L}\right)} \right. \\[4ex]
\left. - \left(\frac{2\pi\epsilon}{L}\right)^2 \dfrac{\sin^2\frac{\pi X_1}{L}}{4\left(\cos\frac{\pi X_1}{L} - \frac{2\pi t_1}{L}\sin\frac{\pi\sigma X_1}{L}\right)^2} \right\}, & i = 1 \\[6ex]
\dfrac{1}{\cos\frac{\pi X_1}{L} - \frac{2\pi t_1}{L}\sin\frac{\pi\sigma X_1}{L}}\left\{ 1 + \left(\frac{2\pi\epsilon}{L}\right) \dfrac{i\rho\sin\frac{\pi\sigma X_1}{L}\left(L^2 + 4\pi^2 t_1^2\right)}{2L^2\left(\cos\frac{\pi X_1}{L} - \frac{2\pi t_1}{L}\sin\frac{\pi\sigma X_1}{L}\right)} \right. \\[4ex]
\left. - \left(\frac{2\pi\epsilon}{L}\right)^2 \dfrac{\sin\frac{\pi\sigma X_1}{L}\left(\frac{2\pi t_1}{L}\cos\frac{\pi X_1}{L} + \sin\frac{\pi\sigma X_1}{L}\right)\left(L^2 + 4\pi^2 t_1^2\right)}{4L^2\left(\cos\frac{\pi X_1}{L} - \frac{2\pi t_1}{L}\sin\frac{\pi\sigma X_1}{L}\right)^2} \right\}, & i = 2 \\[6ex]
\dfrac{\cos\frac{\pi t_0}{L}}{\cos\frac{\pi(t_0 + \sigma X_1)}{L}}\left\{ 1 - \left(\frac{2\pi\epsilon}{L}\right) \dfrac{i\rho\sin\frac{\pi\sigma X_1}{L}}{\cos\frac{\pi(t_0 + \sigma X_1)}{L}\cos\frac{\pi t_0}{L}} \right. \\[4ex]
\left. - \left(\frac{2\pi\epsilon}{L}\right)^2 \dfrac{\sin\frac{\pi\sigma X_1}{L}\sin\frac{\pi(t_0 + \sigma X_1)}{L}}{\cos^2\frac{\pi(t_0 + \sigma X_1)}{L}\cos\frac{\pi t_0}{L}} \right\}, & i = 3 \\[6ex]
\dfrac{\cos\frac{\pi t_0}{L}}{\cos\frac{\pi(t_0 + \sigma X_1)}{L}}\left\{ 1 - \left(\frac{2\pi\epsilon}{L}\right) \dfrac{i\rho\sin\frac{\pi\sigma X_1}{L}\cos\frac{\pi t_0}{L}}{\cos\frac{\pi(t_0 + \sigma X_1)}{L}} \right. \\[4ex]
\left. - \left(\frac{2\pi\epsilon}{L}\right)^2 \dfrac{\sin^2\frac{\pi X_1}{L}\cos^2\frac{\pi t_0}{L}}{\cos^2\frac{\pi(t_0 + \sigma X_1)}{L}} \right\}, & i = 4
\end{cases}
\tag{C.27}
$$

These coordinates (C.27) can be obtained either by setting $X_2 = 0$ in (4.4) and then performing a Taylor expansion in $\frac{2\pi\epsilon}{L}$ or by sending $X_2 \to 0$ in the SSD coordinates (C.15). Since $0 < X_1 < \frac{L}{2}$, when $t_1 \neq \frac{L\sigma}{2\pi}\cot\frac{\pi X_1}{L}$, ξ_0, ξ_1 and ξ_2 as defined in (4.21) are finite and non-zero for $i = 1, 2$ while for $i = 3, 4$, when $\cos\frac{\pi t_0}{L}$, $\cos\frac{\pi(t_0 + \sigma X_1)}{L} \neq 0$, ξ_0 and ξ_1 are non-zero and finite while ξ_2 does not diverge. $t_1 = \frac{L\sigma}{2\pi}\cot\frac{\pi X_1}{L}$ for $i = 1, 2$ and $t_0 = (m + \frac{1}{2})L - \sigma X_1$ with integers m for $i = 3, 4$ correspond to the discontinuities in the second Rényi entropy anyway so away from these points the second Rényi entropy is well defined. When $t_0 = (m + \frac{1}{2})L$ for integers m, the change in the second Rényi entropy becomes ill-defined for $i = 3, 4$. Applying (4.29),

the cross ratios are

$$
\hat{\eta}_2 = \begin{cases}
\frac{1}{2}\left\{1 - \mathrm{sgn}\left[\cos\frac{\pi X_1}{L} - \frac{2\pi t_1}{L}\sin\frac{\pi\sigma X_1}{L}\right]\left[1 - \left(\frac{2\pi\epsilon}{L}\right)^2\frac{\sin^2\frac{\pi X_1}{L}}{8\left(\cos\frac{\pi X_1}{L} - \frac{2\pi t_1}{L}\sin\frac{\pi\sigma X_1}{L}\right)^2}\right]\right\}, & i = 1 \\[2em]
\frac{1}{2}\left\{1 - \mathrm{sgn}\left[\cos\frac{\pi X_1}{L} - \frac{2\pi t_1}{L}\sin\frac{\pi\sigma X_1}{L}\right]\left[1 - \left(\frac{2\pi\epsilon}{L}\right)^2\frac{\sin^2\frac{\pi X_1}{L}\left(L^2+4\pi^2 t_1^2\right)^2}{8L^4\left(\cos\frac{\pi X_1}{L} - \frac{2\pi t_1}{L}\sin\frac{\pi\sigma X_1}{L}\right)^2}\right]\right\}, & i = 2 \\[2em]
\frac{1}{2}\left\{1 - \mathrm{sgn}\left[\frac{\cos\frac{\pi t_0}{L}}{\cos\frac{\pi(t_0+\sigma X_1)}{L}}\right]\left[1 - \left(\frac{2\pi\epsilon}{L}\right)^2\frac{\sin^2\frac{\pi X_1}{L}}{2\cos^2\frac{\pi(t_0+\sigma X_1)}{L}\cos^2\frac{\pi t_0}{L}}\right]\right\}, & i = 3 \\[2em]
\frac{1}{2}\left\{1 - \mathrm{sgn}\left[\frac{\cos\frac{\pi t_0}{L}}{\cos\frac{\pi(t_0+\sigma X_1)}{L}}\right]\left[1 - \left(\frac{2\pi\epsilon}{L}\right)^2\frac{\sin^2\frac{\pi X_1}{L}\cos^2\frac{\pi t_0}{L}}{2\cos^2\frac{\pi(t_0+\sigma X_1)}{L}}\right]\right\}, & i = 4
\end{cases}
\tag{C.28}
$$

which can also be directly obtained by setting $X_2 = 0$, $x = \frac{L}{2}$ in (C.18) for all cases $i = 1, 2, 3, 4$. Since the cross ratios are periodic with $t_0 \sim t_0 + L$ for $i = 3, 4$, the corresponding change in second Rényi entropy will have the same periodicity as well. The change in the second Rényi entropy for the local operator (4.12) in the free boson theory is

$$
\Delta S_{A,i}^{(2)} = \begin{cases}
0, & i = 1, 2, 0 < t_1 < \frac{L}{2\pi}\cot\frac{\pi X_1}{L} \\
\log 2, & i = 1, 2, \frac{L}{2\pi}\cot\frac{\pi X_1}{L} < t_1 \\
0, & i = 3, 4, mL < t_0 < mL + \frac{L}{2} - X_1 \\
\log 2, & i = 3, 4, mL + \frac{L}{2} - X_1 < t_0 < mL + \frac{L}{2} + X_1 \\
0, & i = 3, 4, mL + \frac{L}{2} + X_1 < t_0 < (m+1)L
\end{cases}
\tag{C.29}
$$

for non-negative integers m. For $i = 1, 2$, the time $t_1 = \frac{L}{2\pi}\cot\frac{\pi X_1}{L}$ is the time it takes for a left moving quasiparticle starting at X_2^f to arrive at the rightmost boundary of the subsystem X_1. On the other hand, the $i = 3, 4$ cases are well-defined by the $\theta = 0$ quasiparticle picture. For $i = 4$, the Rényi is ill-defined for $t_0 = (k + \frac{1}{2})L$ for integers k. We get the same answer by sending $X_2 \to 0^+$ in (C.26) for all cases $i = 1, 2, 3, 4$.

D   The details of the cross ratios

Let us present the details of the cross ratio after we perform the analytic continuation to real time.

D.1 When the local operator is inserted at $x = X_1^f = 0$.

By the second order in the small ϵ expansion, the details of the cross ratios are given by

$$z_{c,1} \approx 1 - \frac{i2\pi\epsilon \sin\left[\frac{\pi(X_1-X_2)}{L}\right]}{Le^{-2\theta}\prod_{i=1,2}\left(\cosh\theta\sin\left[\frac{\pi(t_1+X_i\cosh 2\theta)}{L\cosh 2\theta}\right] - \sinh\theta\sin\left[\frac{\pi(t_1-X_i\cosh 2\theta)}{L\cosh 2\theta}\right]\right)} + \mathcal{O}(\epsilon^2),$$

$$\overline{z}_{c,1} \approx 1 + \frac{i2\pi\epsilon \sin\left[\frac{\pi(X_1-X_2)}{L}\right]}{Le^{-2\theta}\prod_{i=1,2}\left(\cosh\theta\sin\left[\frac{\pi(t_1-X_i\cosh 2\theta)}{L\cosh 2\theta}\right] - \sinh\theta\sin\left[\frac{\pi(t_1+X_i\cosh 2\theta)}{L\cosh 2\theta}\right]\right)} + \mathcal{O}(\epsilon^2),$$

$$z_{c,2} \approx 1 - \frac{i2\pi\epsilon \sin\left[\frac{\pi(X_1-X_2)}{L}\right]\left(e^{2\theta}\cos^2\left(\frac{\pi t_1}{L\cosh 2\theta}\right) + e^{-2\theta}\sin^2\left(\frac{\pi t_1}{L\cosh 2\theta}\right)\right)}{L\prod_{i=1,2}\left(\cosh\theta\sin\left[\frac{\pi(t_1+X_i\cosh 2\theta)}{L\cosh 2\theta}\right] - \sinh\theta\sin\left[\frac{\pi(t_1-X_i\cosh 2\theta)}{L\cosh 2\theta}\right]\right)} + \mathcal{O}(\epsilon^2),$$

$$\overline{z}_{c,2} \approx 1 + \frac{i2\pi\epsilon \sin\left[\frac{\pi(X_1-X_2)}{L}\right]\left(e^{2\theta}\cos^2\left(\frac{\pi t_1}{L\cosh 2\theta}\right) + e^{-2\theta}\sin^2\left(\frac{\pi t_1}{L\cosh 2\theta}\right)\right)}{L\prod_{i=1,2}\left(-\cosh\theta\sin\left[\frac{\pi(t_1-X_i\cosh 2\theta)}{L\cosh 2\theta}\right] + \sinh\theta\sin\left[\frac{\pi(t_1+X_i\cosh 2\theta)}{L\cosh 2\theta}\right]\right)} + \mathcal{O}(\epsilon^2),$$

$$z_{c,3} \approx 1 + \frac{2i\epsilon\pi(\tanh(2\theta)-1)\sin\left[\frac{\pi(X_1-X_2)}{L}\right]}{L\prod_{i=1,2}\sin\left[\frac{\pi(t_0+X_i)}{L}\right]} + \mathcal{O}(\epsilon^2),$$

$$\overline{z}_{c,3} \approx 1 - \frac{2i\epsilon\pi(\tanh(2\theta)-1)\sin\left[\frac{\pi(X_1-X_2)}{L}\right]}{L\prod_{i=1,2}\sin\left[\frac{\pi(t_0-X_i)}{L}\right]} + \mathcal{O}(\epsilon^2),$$

$$z_{c,4} \approx 1 + \frac{2i\pi\epsilon\sin\left[\frac{\pi(X_1-X_2)}{L}\right]\left(\cos\left(\frac{2\pi t_0}{L}\right)\tanh 2\theta - 1\right)}{L\prod_{i=1,2}\sin\left[\frac{\pi(t_0+X_i)}{L}\right]} + \mathcal{O}(\epsilon^2),$$

$$\overline{z}_{c,4} \approx 1 - \frac{2i\pi\epsilon\sin\left[\frac{\pi(X_1-X_2)}{L}\right]\left(\cos\left(\frac{2\pi t_0}{L}\right)\tanh 2\theta - 1\right)}{L\prod_{i=1,2}\sin\left[\frac{\pi(t_0-X_i)}{L}\right]} + \mathcal{O}(\epsilon^2),$$

$$\tag{D.1}$$

where around $t_1 = \frac{L\cosh 2\theta}{\pi}\tan^{-1}\left[\pm e^{2\theta}\tan\left(\frac{\pi X_i}{L}\right)\right] + nL\cosh 2\theta$, the small ϵ expansion of $z_{c,i=1,2}$ or $\overline{z}_{c,i=1,2}$ breaks down, while around $t_0 = nL \pm X_{i=1,2}$, that of $z_{c,i=3,4}$ or $\overline{z}_{c,i=3,4}$ breaks down. Here, we assume that $0 < \tan^{-1}\left[\pm e^{2\theta}\tan\left(\frac{\pi X_i}{L}\right)\right] < \pi$ and n is an integer greater than or equal to zero. Let us consider the time dependence of $S_{A,i}$ in cases, (a), (b), and (c).

D.2   When the local operator is inserted at $x = \frac{L}{2}$.

When the local operator is inserted at $x = \frac{L}{2}$, the small ϵ expansion of the cross ratios analytically-continued to real time is approximated by

$$z_{c,1} \approx 1 - \frac{2i\pi e^{-2\theta}\epsilon \sin\left[\frac{\pi(X_1 - X_2)}{L}\right]}{L\prod_{i=1,2}\left[\cos\left(\frac{\pi(X_i \cosh 2\theta + t_1)}{L \cosh 2\theta}\right)\cosh\theta - \cos\left(\frac{\pi(X_i \cosh 2\theta - t_1)}{L \cosh 2\theta}\right)\sinh\theta\right]} + \mathcal{O}(\epsilon^2),$$

$$\overline{z}_{c,1} \approx 1 + \frac{2i\pi e^{-2\theta}\epsilon \sin\left[\frac{\pi(X_1 - X_2)}{L}\right]}{L\prod_{i=1,2}\left[\cos\left(\frac{\pi(X_i \cosh 2\theta - t_1)}{L \cosh 2\theta}\right)\cosh\theta - \cos\left(\frac{\pi(X_i \cosh 2\theta + t_1)}{L \cosh 2\theta}\right)\sinh\theta\right]} + \mathcal{O}(\epsilon^2),$$

$$z_{c,2} \approx 1 - \frac{2i\pi\epsilon \sin\left[\frac{\pi(X_1 - X_2)}{L}\right]\left(\cosh 2\theta - \sinh 2\theta \cos\left(\frac{2\pi t_1}{L \cosh 2\theta}\right)\right)}{L\prod_{i=1,2}\left[\cos\left(\frac{\pi(X_i \cosh 2\theta + t_1)}{L \cosh 2\theta}\right)\cosh\theta - \cos\left(\frac{\pi(X_i \cosh 2\theta - t_1)}{L \cosh 2\theta}\right)\sinh\theta\right]} + \mathcal{O}(\epsilon^2),$$

$$\overline{z}_{c,2} \approx 1 + \frac{2i\pi\epsilon \sin\left[\frac{\pi(X_1 - X_2)}{L}\right]\left(\cosh 2\theta - \sinh 2\theta \cos\left(\frac{2\pi t_1}{L \cosh 2\theta}\right)\right)}{L\prod_{i=1,2}\left[\cos\left(\frac{\pi(X_i \cosh 2\theta - t_1)}{L \cosh 2\theta}\right)\cosh\theta - \cos\left(\frac{\pi(X_i \cosh 2\theta + t_1)}{L \cosh 2\theta}\right)\sinh\theta\right]} + \mathcal{O}(\epsilon^2),$$
$$\text{(D.2)}$$

$$z_{c,3} \approx 1 - i\frac{2\pi\epsilon(1 + \tanh 2\theta)\sin\left[\frac{\pi(X_1 - X_2)}{L}\right]}{L\prod_{i=1,2}\cos\left[\frac{\pi(t_0 + X_i)}{L}\right]} + \mathcal{O}(\epsilon^2),$$

$$\overline{z}_{c,3} \approx 1 + i\frac{2\pi\epsilon(1 + \tanh 2\theta)\sin\left[\frac{\pi(X_1 - X_2)}{L}\right]}{L\prod_{i=1,2}\cos\left[\frac{\pi(t_0 - X_i)}{L}\right]} + \mathcal{O}(\epsilon^2),$$

$$z_{c,4} \approx 1 - i\frac{2\pi\epsilon\left(1 + \cos\left(\frac{2\pi t_0}{L}\right)\tanh 2\theta\right)\sin\left[\frac{\pi(X_1 - X_2)}{L}\right]}{L\prod_{i=1,2}\cos\left[\frac{\pi(t_0 + X_i)}{L}\right]} + \mathcal{O}(\epsilon^2),$$

$$\overline{z}_{c,4} \approx 1 + i\frac{2\pi\epsilon\left(1 + \cos\left(\frac{2\pi t_0}{L}\right)\tanh 2\theta\right)\sin\left[\frac{\pi(X_1 - X_2)}{L}\right]}{L\prod_{i=1,2}\cos\left[\frac{\pi(t_0 - X_i)}{L}\right]} + \mathcal{O}(\epsilon^2),$$

where around $t_1 = \frac{L_{\text{eff}}}{\pi}\tan^{-1}\left[\pm e^{-2\theta}\cot\left(\frac{\pi X_i}{L}\right)\right] + nL_{\text{eff}}$, the small ϵ expansion of $z_{c,i=1,2}$, $\overline{z}_{c,i=1,2}$, breaks down, while around $t_0 = \pm X_i + L\left(\frac{1}{2} + n\right)$, the small ϵ expansion of $z_{c,i=3,4}$, $\overline{z}_{c,i=3,4}$ breaks down. Let us define the characteristic times, $0 < \hat{t} < L_{\text{eff}}$, as

$$\hat{t}_{\frac{L}{2} - X_2} = \frac{L_{\text{eff}}}{\pi}\tan^{-1}\left(e^{-2\theta}\tan\left[\frac{\pi}{L}\left(\frac{L}{2} - X_2\right)\right]\right), \quad \hat{t}_{\frac{L}{2} + X_2} = \frac{L_{\text{eff}}}{\pi}\tan^{-1}\left(e^{-2\theta}\tan\left[\frac{\pi}{L}\left(\frac{L}{2} + X_2\right)\right]\right),$$

$$\hat{t}_{X_1 - \frac{L}{2}} = \frac{L_{\text{eff}}}{\pi}\tan^{-1}\left(e^{-2\theta}\tan\left[\frac{\pi}{L}\left(X_1 - \frac{L}{2}\right)\right]\right), \quad \hat{t}_{\frac{3L}{2} - X_1} = \frac{L_{\text{eff}}}{\pi}\tan^{-1}\left(e^{-2\theta}\tan\left[\frac{\pi}{L}\left(\frac{3L}{2} - X_1\right)\right]\right),$$
$$\text{(D.3)}$$

where $L_{\text{eff}} > \hat{t}_{\frac{L}{2} + X_2} > \hat{t}_{\frac{3L}{2} - X_1} > \hat{t}_{X_1 - \frac{L}{2}} > \hat{t}_{\frac{L}{2} - X_2} > 0$.

D.3 When the local operator is inserted at general x.

To second order in the small ϵ expansion, the cross ratios are given by

$$z_{c,1} \approx \mathcal{O}(\epsilon^2)+$$

$$1 - \frac{2i\pi\epsilon \sin\left[\frac{\pi(X_1-X_2)}{L}\right]}{L\prod_{i=1,2}\left[\sin\left(\frac{\pi t_1}{L_{\text{eff}}}\right)\left(\cosh(2\theta)\cos\left(\frac{\pi(x-X_i)}{L}\right)-\sinh(2\theta)\cos\left(\frac{\pi(X_i+x)}{L}\right)\right)-\cos\left(\frac{\pi t_1}{L_{\text{eff}}}\right)\sin\left(\frac{\pi(x-X_i)}{L}\right)\right]},$$

$$\overline{z}_{c,1} \approx \mathcal{O}(\epsilon^2)+$$

$$1 + \frac{2i\pi\epsilon \sin\left[\frac{\pi(X_1-X_2)}{L}\right]}{L\prod_{i=1,2}\left[\sin\left(\frac{\pi t_1}{L_{\text{eff}}}\right)\left(\cosh(2\theta)\cos\left(\frac{\pi(x-X_i)}{L}\right)-\sinh(2\theta)\cos\left(\frac{\pi(X_i+x)}{L}\right)\right)+\cos\left(\frac{\pi t_1}{L_{\text{eff}}}\right)\sin\left(\frac{\pi(x-X_i)}{L}\right)\right]},$$

$$z_{c,2} \approx \mathcal{O}(\epsilon^2) + 1 - 2i\pi\epsilon \sin\left(\frac{\pi(X_1-X_2)}{L}\right)\left(\cos\left(\frac{\pi t_1}{L_{\text{eff}}}\right)-i\sin\left(\frac{\pi t_1}{L_{\text{eff}}}\right)\left(\cosh(2\theta)-\sinh(2\theta)e^{-\frac{2i\pi x}{L}}\right)\right)$$

$$\times \frac{\cos\left(\frac{\pi t_1}{L_{\text{eff}}}\right)-i\sin\left(\frac{\pi t_1}{L_{\text{eff}}}\right)\left(-\cosh(2\theta)+\sinh(2\theta)e^{\frac{2i\pi x}{L}}\right)}{L\prod_{i=1,2}\left[\sin\left(\frac{\pi t_1}{L_{\text{eff}}}\right)\left(\cosh(2\theta)\cos\left(\frac{\pi(x-X_i)}{L}\right)-\sinh(2\theta)\cos\left(\frac{\pi(X_i+x)}{L}\right)\right)-\cos\left(\frac{\pi t_1}{L_{\text{eff}}}\right)\sin\left(\frac{\pi(x-X_i)}{L}\right)\right]},$$

$$\overline{z}_{c,2} \approx \mathcal{O}(\epsilon^2) + 1 + 2i\pi\epsilon \sin\left(\frac{\pi(X_1-X_2)}{L}\right)\left(\cos\left(\frac{\pi t_1}{L_{\text{eff}}}\right)-i\sin\left(\frac{\pi t_1}{L_{\text{eff}}}\right)\left(\cosh(2\theta)-\sinh(2\theta)e^{\frac{2i\pi x}{L}}\right)\right)$$

$$\times \frac{\cos\left(\frac{\pi t_1}{L_{\text{eff}}}\right)-i\sin\left(\frac{\pi t_1}{L_{\text{eff}}}\right)\left(-\cosh(2\theta)+\sinh(2\theta)e^{-\frac{2i\pi x}{L}}\right)}{L\prod_{i=1,2}\left[\sin\left(\frac{\pi t_1}{L_{\text{eff}}}\right)\left(\cosh(2\theta)\cos\left(\frac{\pi(x-X_i)}{L}\right)-\sinh(2\theta)\cos\left(\frac{\pi(X_i+x)}{L}\right)\right)+\cos\left(\frac{\pi t_1}{L_{\text{eff}}}\right)\sin\left(\frac{\pi(x-X_i)}{L}\right)\right]},$$

$$z_{c,3} \approx 1 + \frac{2i\pi\epsilon \sin\left[\frac{\pi(X_1-X_2)}{L}\right]\left(\tanh(2\theta)\cos\left(\frac{2\pi x}{L}\right)-1\right)}{L\prod_{i=1,2}\sin\left[\frac{\pi(t_0-x+X_i)}{L}\right]} + \mathcal{O}(\epsilon^2),$$

$$\overline{z}_{c,3} \approx 1 - \frac{2i\pi\epsilon \sin\left[\frac{\pi(X_1-X_2)}{L}\right]\left(\tanh(2\theta)\cos\left(\frac{2\pi x}{L}\right)-1\right)}{L\prod_{i=1,2}\sin\left[\frac{\pi(t_0+x-X_i)}{L}\right]} + \mathcal{O}(\epsilon^2),$$

$$z_{c,4} \approx 1 + \frac{2i\pi\epsilon \sin\left[\frac{\pi(X_1-X_2)}{L}\right]\left(\tanh(2\theta)\cos\left(\frac{2\pi(t_0-x)}{L}\right)-1\right)}{L\prod_{i=1,2}\sin\left[\frac{\pi(t_0-x+X_i)}{L}\right]} + \mathcal{O}(\epsilon^2),$$

$$\overline{z}_{c,4} \approx 1 - \frac{2i\pi\epsilon \sin\left[\frac{\pi(X_1-X_2)}{L}\right]\left(\tanh(2\theta)\cos\left(\frac{2\pi(t_0+x)}{L}\right)-1\right)}{L\prod_{i=1,2}\sin\left[\frac{\pi(t_0+x-X_i)}{L}\right]} + \mathcal{O}(\epsilon^2),$$

$$\text{(D.4)}$$

where around $t_1 = \frac{L_{\text{eff}}}{\pi}\tan^{-1}\left[\left|\frac{\sin\left(\frac{\pi(x-X_i)}{L}\right)}{\cosh(2\theta)\cos\left(\frac{\pi(x-X_i)}{L}\right)-\sinh(2\theta)\cos\left(\frac{\pi(X_i+x)}{L}\right)}\right|\right] + nL_{\text{eff}}$, the small ϵ expansion of $z_{c,i=1,2}$, $\overline{z}_{c,i=1,2}$, breaks down, while around $t_0 = \pm(x-X_i)+nL$, the small ϵ expansion of $z_{c,i=3,4}$, $\overline{z}_{c,i=3,4}$ breaks down.

E   The time dependence of $S_{A,i}$ in 2d holographic CFTs

Here, we present the time dependence of $S_{A,i}$ for Möbius/SSD cases.

E.1   Möbius case

First, we report on the time dependence of $S_{A,i}$ for Möbius case. Here, we assume that the local operator is inserted at $x = 0, \frac{L}{2}$.

E.1.1 $x = X_1^f$

We present the time dependence of $S_{A,i}$ for the Möbius case when the local operator is inserted at $x = 0$. The subsystems considered here are (b) and (c).

For case (b), the time dependence of $S_{A,i}$ is given by

$$
S_{A,1} \approx \frac{c}{3} \log \left[\frac{L}{\pi} \sin \left(\frac{\pi (X_1 - X_2)}{L} \right) \right]
$$

$$
+ \begin{cases}
0 & t_{X_2} > t_1 > 0 \\
\frac{c}{6} \log \left[\frac{2 \sin[\pi \alpha_{\mathcal{O}}]}{\alpha_{\mathcal{O}}} \right] - \frac{c}{6} \log \left[-\epsilon g_1(t_1, X_1^f, \theta) \right] & nL_{\text{eff}} + t_{1,+}^t > t_1 > nL_{\text{eff}} + t_{X_2} \\
\frac{c}{6} \log \left[\frac{2 \sin[\pi \alpha_{\mathcal{O}}]}{\alpha_{\mathcal{O}}} \right] - \frac{c}{6} \log \left[-\epsilon f_1(t_1, X_1^f, \theta) \right] & nL_{\text{eff}} + t_{L-X_1} > t_1 > nL_{\text{eff}} + t_{1,+}^t \\
0 & nL_{\text{eff}} + t_{X_1} > t_1 > nL_{\text{eff}} + t_{L-X_1} \\
\frac{c}{6} \log \left[\frac{2 \sin[\pi \alpha_{\mathcal{O}}]}{\alpha_{\mathcal{O}}} \right] - \frac{c}{6} \log \left[\epsilon g_1(t_1, X_1^f, \theta) \right] & nL_{\text{eff}} + t_{1,-}^t > t_1 > nL_{\text{eff}} + t_{X_1} \\
\frac{c}{6} \log \left[\frac{2 \sin[\pi \alpha_{\mathcal{O}}]}{\alpha_{\mathcal{O}}} \right] - \frac{c}{6} \log \left[\epsilon f_1(t_1, X_1^f, \theta) \right] & nL_{\text{eff}} + t_{L-X_2} > t_1 > nL_{\text{eff}} + t_{1,-}^t \\
0 & (n+1)L_{\text{eff}} + t_{X_2} > t_1 > nL_{\text{eff}} + t_{L-X_2}
\end{cases} \quad ,
$$

$$S_{A,2} \approx \frac{c}{3} \log \left[\frac{L}{\pi} \sin \left(\frac{\pi (X_1 - X_2)}{L} \right) \right]$$

$$+ \begin{cases} 0 & t_{X_2} > t_1 > 0 \\ \frac{c}{6} \log \left[\frac{2 \sin[\pi \alpha_\mathcal{O}]}{\alpha_\mathcal{O}} \right] - \frac{c}{6} \log \left[-\epsilon g_2(t_1, X_1^f, \theta) \right] & nL_{\text{eff}} + t_{1,+}^t > t_1 > nL_{\text{eff}} + t_{X_2} \\ \frac{c}{6} \log \left[\frac{2 \sin[\pi \alpha_\mathcal{O}]}{\alpha_\mathcal{O}} \right] - \frac{c}{6} \log \left[-\epsilon f_2(t_1, X_1^f, \theta) \right] & nL_{\text{eff}} + t_{L-X_1} > t_1 > nL_{\text{eff}} + t_{1,+}^t \\ 0 & nL_{\text{eff}} + t_{X_1} > t_1 > nL_{\text{eff}} + t_{L-X_1} \\ \frac{c}{6} \log \left[\frac{2 \sin[\pi \alpha_\mathcal{O}]}{\alpha_\mathcal{O}} \right] - \frac{c}{6} \log \left[\epsilon g_2(t_1, X_1^f, \theta) \right] & nL_{\text{eff}} + t_{1,-}^t > t_1 > nL_{\text{eff}} + t_{X_1} \\ \frac{c}{6} \log \left[\frac{2 \sin[\pi \alpha_\mathcal{O}]}{\alpha_\mathcal{O}} \right] - \frac{c}{6} \log \left[\epsilon f_2(t_1, X_1^f, \theta) \right] & nL_{\text{eff}} + t_{L-X_2} > t_1 > nL_{\text{eff}} + t_{1,-}^t \\ 0 & (n+1)L_{\text{eff}} + t_{X_2} > t_1 > nL_{\text{eff}} + t_{L-X_2} \end{cases},$$

$$S_{A,3} \approx \frac{c}{3} \log \left[\frac{L}{\pi} \sin \left(\frac{\pi (X_1 - X_2)}{L} \right) \right]$$

$$+ \begin{cases} 0 & X_2 > t_0 > 0 \\ \frac{c}{6} \log \left[\frac{2 \sin[\pi \alpha_\mathcal{O}]}{\alpha_\mathcal{O}} \right] - \frac{c}{6} \log \left[-\epsilon g_3(t_0, X_1^f, \theta) \right] & nL + t_{0,+}^t > t_0 > nL + X_2 \\ \frac{c}{6} \log \left[\frac{2 \sin[\pi \alpha_\mathcal{O}]}{\alpha_\mathcal{O}} \right] - \frac{c}{6} \log \left[-\epsilon f_3(t_0, X_1^f, \theta) \right] & (n+1)L - X_1 > t_0 > nL + t_{0,+}^t \\ 0 & nL + X_1 > t_0 > (n+1)L - X_1 \\ \frac{c}{6} \log \left[\frac{2 \sin[\pi \alpha_\mathcal{O}]}{\alpha_\mathcal{O}} \right] - \frac{c}{6} \log \left[\epsilon g_3(t_0, X_1^f, \theta) \right] & nL + t_{0,-}^t > t_0 > nL + X_1 \\ \frac{c}{6} \log \left[\frac{2 \sin[\pi \alpha_\mathcal{O}]}{\alpha_\mathcal{O}} \right] - \frac{c}{6} \log \left[\epsilon f_3(t_0, X_1^f, \theta) \right] & (n+1)L - X_2 > t_0 > nL + t_{0,-}^t \\ 0 & (n+1)L + X_2 > t_0 > (n+1)L - X_2 \end{cases},$$

$$S_{A,4} \approx \frac{c}{3} \log \left[\frac{L}{\pi} \sin \left(\frac{\pi (X_1 - X_2)}{L} \right) \right]$$

$$+ \begin{cases} 0 & X_2 > t_0 > 0 \\ \frac{c}{6} \log \left[\frac{2 \sin[\pi \alpha_\mathcal{O}]}{\alpha_\mathcal{O}} \right] - \frac{c}{6} \log \left[-\epsilon g_4(t_0, X_1^f, \theta) \right] & nL + t_{0,+}^t > t_0 > nL + X_2 \\ \frac{c}{6} \log \left[\frac{2 \sin[\pi \alpha_\mathcal{O}]}{\alpha_\mathcal{O}} \right] - \frac{c}{6} \log \left[-\epsilon f_4(t_0, X_1^f, \theta) \right] & (n+1)L - X_1 > t_0 > nL + t_{0,+}^t \\ 0 & nL + X_1 > t_0 > (n+1)L - X_1 \\ \frac{c}{6} \log \left[\frac{2 \sin[\pi \alpha_\mathcal{O}]}{\alpha_\mathcal{O}} \right] - \frac{c}{6} \log \left[\epsilon g_4(t_0, X_1^f, \theta) \right] & nL + t_{0,-}^t > t_0 > nL + X_1 \\ \frac{c}{6} \log \left[\frac{2 \sin[\pi \alpha_\mathcal{O}]}{\alpha_\mathcal{O}} \right] - \frac{c}{6} \log \left[\epsilon f_4(t_0, X_1^f, \theta) \right] & (n+1)L - X_2 > t_0 > nL + t_{0,-}^t \\ 0 & (n+1)L + X_2 > t_0 > (n+1)L - X_2 \end{cases}.$$

$$(\text{E.1})$$

For case (c), the time dependence of $S_{A,i}$ is given by

$$S_{A,1} \approx \frac{c}{3} \log \left[\frac{L}{\pi} \sin \left(\frac{\pi (X_1 - X_2)}{L} \right) \right]$$

$$+ \begin{cases} 0 & t_{X_2} > t_1 > 0 \\ \frac{c}{6} \log \left[\frac{2 \sin[\pi \alpha_{\mathcal{O}}]}{\alpha_{\mathcal{O}}} \right] - \frac{c}{6} \log \left[-\epsilon g_1(t_1, X_1^f, \theta) \right] & nL_{\text{eff}} + t_{X_1} > t_1 > nL_{\text{eff}} + t_{X_2} \\ 0 & nL_{\text{eff}} + t_{L-X_1} > t_1 > nL_{\text{eff}} + t_{X_1} \\ \frac{c}{6} \log \left[\frac{2 \sin[\pi \alpha_{\mathcal{O}}]}{\alpha_{\mathcal{O}}} \right] - \frac{c}{6} \log \left[\epsilon f_1(t_1, X_1^f, \theta) \right] & nL_{\text{eff}} + t_{L-X_2} > t_1 > nL_{\text{eff}} + t_{L-X_1} \\ 0 & (n+1)L_{\text{eff}} + t_{X_2} > t_1 > nL_{\text{eff}} + t_{L-X_2} \end{cases} ,$$

$$S_{A,2} \approx \frac{c}{3} \log \left[\frac{L}{\pi} \sin \left(\frac{\pi (X_1 - X_2)}{L} \right) \right]$$

$$+ \begin{cases} 0 & t_{X_2} > t_1 > 0 \\ \frac{c}{6} \log \left[\frac{2 \sin[\pi \alpha_{\mathcal{O}}]}{\alpha_{\mathcal{O}}} \right] - \frac{c}{6} \log \left[-\epsilon g_2(t_1, X_1^f, \theta) \right] & nL_{\text{eff}} + t_{X_1} > t_1 > nL_{\text{eff}} + t_{X_2} \\ 0 & nL_{\text{eff}} + t_{L-X_1} > t_1 > nL_{\text{eff}} + t_{X_1} \\ \frac{c}{6} \log \left[\frac{2 \sin[\pi \alpha_{\mathcal{O}}]}{\alpha_{\mathcal{O}}} \right] - \frac{c}{6} \log \left[\epsilon f_2(t_1, X_1^f, \theta) \right] & nL_{\text{eff}} + t_{L-X_2} > t_1 > nL_{\text{eff}} + t_{L-X_1} \\ 0 & (n+1)L_{\text{eff}} + t_{X_2} > t_1 > nL_{\text{eff}} + t_{L-X_2} \end{cases} ,$$

$$S_{A,3} \approx \frac{c}{3} \log \left[\frac{L}{\pi} \sin \left(\frac{\pi (X_1 - X_2)}{L} \right) \right]$$

$$+ \begin{cases} 0 & X_2 > t_0 > 0 \\ \frac{c}{6} \log \left[\frac{2 \sin[\pi \alpha_{\mathcal{O}}]}{\alpha_{\mathcal{O}}} \right] - \frac{c}{6} \log \left[-\epsilon g_3(t_0, X_1^f, \theta) \right] & nL + X_1 > t_0 > nL + X_2 \\ 0 & (n+1)L - X_1 > t_0 > nL + X_1 \\ \frac{c}{6} \log \left[\frac{2 \sin[\pi \alpha_{\mathcal{O}}]}{\alpha_{\mathcal{O}}} \right] - \frac{c}{6} \log \left[\epsilon f_3(t_0, X_1^f, \theta) \right] & (n+1)L - X_2 > t_0 > (n+1)L - X_1 \\ 0 & (n+1)L + X_2 > t_0 > (n+1)L - X_2 \end{cases} ,$$

$$S_{A,4} \approx \frac{c}{3} \log \left[\frac{L}{\pi} \sin \left(\frac{\pi (X_1 - X_2)}{L} \right) \right]$$

$$+ \begin{cases} 0 & X_2 > t_0 > 0 \\ \frac{c}{6} \log \left[\frac{2 \sin[\pi \alpha_{\mathcal{O}}]}{\alpha_{\mathcal{O}}} \right] - \frac{c}{6} \log \left[-\epsilon g_4(t_0, X_1^f, \theta) \right] & nL + X_1 > t_0 > nL + X_2 \\ 0 & (n+1)L - X_1 > t_0 > nL + X_1 \\ \frac{c}{6} \log \left[\frac{2 \sin[\pi \alpha_{\mathcal{O}}]}{\alpha_{\mathcal{O}}} \right] - \frac{c}{6} \log \left[\epsilon f_4(t_0, X_1^f, \theta) \right] & (n+1)L - X_2 > t_0 > (n+1)L - X_1 \\ 0 & (n+1)L + X_2 > t_0 > (n+1)L - X_2 \end{cases} .$$

$$(E.2)$$

E.1.2 $\quad x = X_2^f$.

Next, we consider the time dependence of entanglement entropy for the states with the insertion at $x = \frac{L}{2}$ of the local operator. To second order in the small ϵ expansion, the cross ratios are approximately given by (5.7). The details of the cross ratios are reported in Appendix D.2. The time dependence of the cross ratios follows the propagation of quasiparticles.

Let us define $\hat{t}_x$ by

$$\hat{t}_x = \frac{L_{\text{eff}}}{\pi} \tan^{-1}\left[e^{-2\theta} \tan\left(\frac{\pi x}{L}\right)\right]. \tag{E.3}$$

The time dependence of cross ratios for $i = 3, 4$ with the insertion at $x = X_2^f$ of the local operator is similar to that with the insertion at $x = X_1^f$ of the local operator. Therefore, we present here the time dependence of the cross ratios for $i = 1, 2$. In the cases of (a) and (b) for $i = 1, 2$, $f_{i=1,2}(T_{i=1,2}, x = X_2^f, \theta)$ $(g_{i=1,2}(T_{i=1,2}, X_2^f, \theta))$ is positive in the time intervals, $(n + 1)L_{\text{eff}} + \hat{t}_{\frac{L}{2}-X_2} > t_1 > nL_{\text{eff}} + \hat{t}_{\frac{3}{2}L-X_1}$ $(nL_{\text{eff}} + \hat{t}_{\frac{L}{2}+X_2} > t_1 > nL_{\text{eff}} + \hat{t}_{X_1-\frac{L}{2}})$, where n is an integer, while it is negative in the time intervals, $nL_{\text{eff}} + \hat{t}_{\frac{3}{2}L-X_1} > t_1 > nL_{\text{eff}} + \hat{t}_{\frac{L}{2}-X_2}$ $((n + 1)L_{\text{eff}} + \hat{t}_{X_1-\frac{L}{2}} > t_1 > nL_{\text{eff}} + \hat{t}_{\frac{L}{2}+X_2})$.

In the case of (c), $f_{i=1,2}(T_{i=1,2}, X_2^f, \theta)$ $(g_{i=1,2}(T_{i=1,2}, X_2^f, \theta))$ is positive in the time intervals, $nL_{\text{eff}} + \hat{t}_{\frac{L}{2}-X_2} > t_1 > nL_{\text{eff}} + \hat{t}_{\frac{L}{2}-X_1}$ $((n + 1)L_{\text{eff}} + \hat{t}_{X_2+\frac{L}{2}} > t_1 > nL_{\text{eff}} + \hat{t}_{X_1+\frac{L}{2}})$, while it is negative in the time intervals, $(n+1)L_{\text{eff}} + t_{\frac{L}{2}-X_1} > t_1 > nL_{\text{eff}} + t_{\frac{L}{2}-X_2}$ $(nL_{\text{eff}} + \hat{t}_{\frac{L}{2}+X_1} > t_1 > nL_{\text{eff}} + \hat{t}_{\frac{L}{2}+X_2})$. Since the denominators of $z_{c,i}$ $(\overline{z}_{c,i})$ vanishes around the times, $t_1 = nL_{\text{eff}} + t_{X_1}$ or $t_1 = nL_{\text{eff}} + t_{X_2}$ $(t_1 = nL_{\text{eff}} + t_{L-X_1}$ or $t_1 = nL_{\text{eff}} + t_{L-X_2})$, the small ϵ expansion in (5.7) breaks down.

After choosing the branches correctly, the time dependence of entanglement entropy for (a), (b), and (c) is determined as follows. For case (a), the time dependence of $S_{A,i}$ is given

by

$$S_{A,1} \approx \frac{c}{3} \log \left[\frac{L}{\pi} \sin \left[\frac{\pi(X_1 - X_2)}{L} \right] \right]$$

$$+ \begin{cases} 0 & \hat{t}_{\frac{L}{2}-X_2} > t_1 > 0 \\ \frac{c}{6} \log \left[\frac{2\sin[\pi\alpha_\mathcal{O}]}{\alpha_\mathcal{O}} \right] - \frac{c}{6} \log \left[-\epsilon f_1(t_1, X_2^f, \theta) \right] & nL_{\text{eff}} + \hat{t}_{1,+}^t > t_1 > nL_{\text{eff}} + \hat{t}_{\frac{L}{2}-X_2} \\ \frac{c}{6} \log \left[\frac{2\sin[\pi\alpha_\mathcal{O}]}{\alpha_\mathcal{O}} \right] - \frac{c}{6} \log \left[-\epsilon g_1(t_1, X_2^f, \theta) \right] & nL_{\text{eff}} + \hat{t}_{X_1-\frac{L}{2}} > t_1 > nL_{\text{eff}} + \hat{t}_{1,+}^t \\ 0 & nL_{\text{eff}} + \hat{t}_{\frac{3}{2}L-X_1} > t_1 > nL_{\text{eff}} + \hat{t}_{X_1-\frac{L}{2}} \\ \frac{c}{6} \log \left[\frac{2\sin[\pi\alpha_\mathcal{O}]}{\alpha_\mathcal{O}} \right] - \frac{c}{6} \log \left[\epsilon f_1(t_1, X_2^f, \theta) \right] & nL_{\text{eff}} + \hat{t}_{1,-}^t > t_1 > nL_{\text{eff}} + \hat{t}_{\frac{3}{2}L-X_1} \\ \frac{c}{6} \log \left[\frac{2\sin[\pi\alpha_\mathcal{O}]}{\alpha_\mathcal{O}} \right] - \frac{c}{6} \log \left[\epsilon g_1(t_1, X_2^f, \theta) \right] & nL_{\text{eff}} + \hat{t}_{\frac{L}{2}+X_2} > t_1 > nL_{\text{eff}} + \hat{t}_{1,-}^t \\ 0 & (n+1)L_{\text{eff}} + \hat{t}_{\frac{L}{2}-X_2} > t_1 > nL_{\text{eff}} + \hat{t}_{\frac{L}{2}+X_2} \end{cases},$$

$$S_{A,2} \approx \frac{c}{3} \log \left[\frac{L}{\pi} \sin \left[\frac{\pi(X_1 - X_2)}{L} \right] \right]$$

$$+ \begin{cases} 0 & \hat{t}_{\frac{L}{2}-X_2} > t_1 > 0 \\ \frac{c}{6} \log \left[\frac{2\sin[\pi\alpha_\mathcal{O}]}{\alpha_\mathcal{O}} \right] - \frac{c}{6} \log \left[-\epsilon f_2(t_1, X_2^f, \theta) \right] & nL_{\text{eff}} + \hat{t}_{1,+}^t > t_1 > nL_{\text{eff}} + \hat{t}_{\frac{L}{2}-X_2} \\ \frac{c}{6} \log \left[\frac{2\sin[\pi\alpha_\mathcal{O}]}{\alpha_\mathcal{O}} \right] - \frac{c}{6} \log \left[-\epsilon g_2(t_1, X_2^f, \theta) \right] & nL_{\text{eff}} + \hat{t}_{X_1-\frac{L}{2}} > t_1 > nL_{\text{eff}} + \hat{t}_{1,+}^t \\ 0 & nL_{\text{eff}} + \hat{t}_{\frac{3}{2}L-X_1} > t_1 > nL_{\text{eff}} + \hat{t}_{X_1-\frac{L}{2}} \\ \frac{c}{6} \log \left[\frac{2\sin[\pi\alpha_\mathcal{O}]}{\alpha_\mathcal{O}} \right] - \frac{c}{6} \log \left[\epsilon f_2(t_1, X_2^f, \theta) \right] & nL_{\text{eff}} + \hat{t}_{1,-}^t > t_1 > nL_{\text{eff}} + \hat{t}_{\frac{3}{2}L-X_1} \\ \frac{c}{6} \log \left[\frac{2\sin[\pi\alpha_\mathcal{O}]}{\alpha_\mathcal{O}} \right] - \frac{c}{6} \log \left[\epsilon g_2(t_1, X_2^f, \theta) \right] & nL_{\text{eff}} + \hat{t}_{\frac{L}{2}+X_2} > t_1 > nL_{\text{eff}} + \hat{t}_{1,-}^t \\ 0 & (n+1)L_{\text{eff}} + \hat{t}_{\frac{L}{2}-X_2} > t_1 > nL_{\text{eff}} + \hat{t}_{\frac{L}{2}+X_2} \end{cases},$$

$$S_{A,3} \approx \frac{c}{3} \log \left[\frac{L}{\pi} \sin \left[\frac{\pi(X_1 - X_2)}{L} \right] \right]$$

$$+ \begin{cases} 0 & \frac{L}{2} - X_2 > t_0 > 0 \\ \frac{c}{6} \log \left[\frac{2\sin[\pi\alpha_\mathcal{O}]}{\alpha_\mathcal{O}} \right] - \frac{c}{6} \log \left[-\epsilon f_3(t_0, X_2^f, \theta) \right] & nL + \tilde{t}_{0,+}^t > t_1 > \left(n+\frac{1}{2}\right)L - X_2 \\ \frac{c}{6} \log \left[\frac{2\sin[\pi\alpha_\mathcal{O}]}{\alpha_\mathcal{O}} \right] - \frac{c}{6} \log \left[-\epsilon g_3(t_0, X_2^f, \theta) \right] & \left(n-\frac{1}{2}\right)L + X_1 > t_1 > nL + \tilde{t}_{0,+}^t \\ 0 & \left(n+\frac{3}{2}\right)L - X_1 > t_0 > \left(n-\frac{1}{2}\right)L + X_1 \\ \frac{c}{6} \log \left[\frac{2\sin[\pi\alpha_\mathcal{O}]}{\alpha_\mathcal{O}} \right] - \frac{c}{6} \log \left[\epsilon f_3(t_0, X_2^f, \theta) \right] & nL + \tilde{t}_{0,-}^t > t_0 > \left(n+\frac{3}{2}\right)L - X_1 \\ \frac{c}{6} \log \left[\frac{2\sin[\pi\alpha_\mathcal{O}]}{\alpha_\mathcal{O}} \right] - \frac{c}{6} \log \left[\epsilon g_3(t_0, X_2^f, \theta) \right] & \left(n+\frac{1}{2}\right)L + X_2 > t_0 > nL + \tilde{t}_{0,-}^t \\ 0 & \left(n+\frac{3}{2}\right)L - X_2 > t_0 > \left(n+\frac{1}{2}\right)L + X_2 \end{cases},$$

$$S_{A,4} \approx \frac{c}{3} \log\left[\frac{L}{\pi} \sin\left[\frac{\pi(X_1 - X_2)}{L} \right] \right]$$

$$+ \begin{cases} 0 & \frac{L}{2} - X_2 > t_0 > 0 \\ \frac{c}{6} \log\left[\frac{2\sin[\pi\alpha_\mathcal{O}]}{\alpha_\mathcal{O}} \right] - \frac{c}{6} \log\left[-\epsilon f_4(t_0, X_2^f, \theta) \right] & nL + \tilde{t}_{0,+}^t > t_1 > \left(n + \frac{1}{2}\right)L - X_2 \\ \frac{c}{6} \log\left[\frac{2\sin[\pi\alpha_\mathcal{O}]}{\alpha_\mathcal{O}} \right] - \frac{c}{6} \log\left[-\epsilon g_4(t_0, X_2^f, \theta) \right] & \left(n - \frac{1}{2}\right)L + X_1 > t_1 > nL + \tilde{t}_{0,+}^t \\ 0 & \left(n + \frac{3}{2}\right)L - X_1 > t_0 > \left(n - \frac{1}{2}\right)L + X_1 \\ \frac{c}{6} \log\left[\frac{2\sin[\pi\alpha_\mathcal{O}]}{\alpha_\mathcal{O}} \right] - \frac{c}{6} \log\left[\epsilon f_4(t_0, X_2^f, \theta) \right] & nL + \tilde{t}_{0,-}^t > t_0 > \left(n + \frac{3}{2}\right)L - X_1 \\ \frac{c}{6} \log\left[\frac{2\sin[\pi\alpha_\mathcal{O}]}{\alpha_\mathcal{O}} \right] - \frac{c}{6} \log\left[\epsilon g_4(t_0, X_2^f, \theta) \right] & \left(n + \frac{1}{2}\right)L + X_2 > t_0 > nL + \tilde{t}_{0,-}^t \\ 0 & \left(n + \frac{3}{2}\right)L - X_2 > t_0 > \left(n + \frac{1}{2}\right)L + X_2 \end{cases}$$

$$\text{(E.4)}$$

where n is an integer greater than or equal to 0, and $\hat{t}_{i,\pm}$ are positive. The characteristic parameters are given by

$$\hat{t}_{1,\pm}^t = \frac{L_{\text{eff}}}{\pi} \tan^{-1}\left[\pm \sqrt{ e^{-4\theta} \tan\left(\frac{\pi\left(X_1 - \frac{L}{2}\right)}{L} \right) \tan\left(\frac{\pi\left(\frac{L}{2} - X_2\right)}{L} \right) } \right],$$

$$\cos\left(\frac{\pi\tilde{t}_{0,\pm}^t}{L} \right) = \pm \sqrt{ \frac{-\prod_{i=1}^{2} \sin\left[\frac{\pi X_i}{L} \right]}{\cos\left[\frac{\pi(X_1 + X_2)}{L} \right]} }.$$

$$\text{(E.5)}$$

Note that the computation on $S_{A,4}$ breaks down at $t_0 = L\left(n + \frac{1}{2}\right)$ because $z_{c,4}$ and $\bar{z}_{c,4}$ exactly becomes unity. Since the Hamiltonian density at $x = X_1^f$ of H_{SSD} is zero, the damping factor, $e^{-\epsilon H_{\text{SSD}}}$, can not tame the high-energy mode there adequately. At $t_0 = L\left(n + \frac{1}{2}\right)$, the excitation created by the local operator at $x = X_2^f$ could arrive at $x = X_1^f$, so that $S_{A,4}$ becomes diverge. For case (b), the time dependence of $S_{A,i}$ is given by

$$S_{A,1} \approx \frac{c}{3} \log \left[\frac{L}{\pi} \sin \left[\frac{\pi(X_1 - X_2)}{L} \right] \right]$$

$$+ \begin{cases} 0 & \hat{t}_{X_1 - \frac{L}{2}} > t_1 > 0 \\ \frac{c}{6} \log \left[\frac{2\sin[\pi\alpha_\mathcal{O}]}{\alpha_\mathcal{O}} \right] - \frac{c}{6} \log \left[\epsilon g_1(t_1, X_2^f, \theta) \right] & nL_{\text{eff}} + \hat{t}_{1,+}^t > t_1 > nL_{\text{eff}} + \hat{t}_{X_1 - \frac{L}{2}} \\ \frac{c}{6} \log \left[\frac{2\sin[\pi\alpha_\mathcal{O}]}{\alpha_\mathcal{O}} \right] - \frac{c}{6} \log \left[\epsilon f_1(t_1, X_2^f, \theta) \right] & nL_{\text{eff}} + \hat{t}_{\frac{L}{2} - X_2} > t_1 > nL_{\text{eff}} + \hat{t}_{1,+}^t \\ 0 & nL_{\text{eff}} + \hat{t}_{\frac{L}{2} + X_2} > t_1 > nL_{\text{eff}} + \hat{t}_{\frac{L}{2} - X_2} \\ \frac{c}{6} \log \left[\frac{2\sin[\pi\alpha_\mathcal{O}]}{\alpha_\mathcal{O}} \right] - \frac{c}{6} \log \left[-\epsilon g_1(t_1, X_2^f, \theta) \right] & nL_{\text{eff}} + \hat{t}_{1,-}^t > t_1 > nL_{\text{eff}} + \hat{t}_{\frac{L}{2} + X_2} \\ \frac{c}{6} \log \left[\frac{2\sin[\pi\alpha_\mathcal{O}]}{\alpha_\mathcal{O}} \right] - \frac{c}{6} \log \left[-\epsilon f_1(t_1, X_2^f, \theta) \right] & nL_{\text{eff}} + \hat{t}_{\frac{3}{2}L - X_1} > t_1 > nL_{\text{eff}} + \hat{t}_{1,-}^t \\ 0 & (n+1)L_{\text{eff}} + \hat{t}_{X_1 - \frac{L}{2}} + > t_1 > nL_{\text{eff}} + \hat{t}_{\frac{3}{2}L - X_1} \end{cases} ,$$

$$S_{A,2} \approx \frac{c}{3} \log \left[\frac{L}{\pi} \sin \left[\frac{\pi(X_1 - X_2)}{L} \right] \right]$$

$$+ \begin{cases} 0 & \hat{t}_{X_1 - \frac{L}{2}} > t_1 > 0 \\ \frac{c}{6} \log \left[\frac{2\sin[\pi\alpha_\mathcal{O}]}{\alpha_\mathcal{O}} \right] - \frac{c}{6} \log \left[\epsilon g_2(t_1, X_2^f, \theta) \right] & nL_{\text{eff}} + \hat{t}_{1,+}^t > t_1 > nL_{\text{eff}} + \hat{t}_{X_1 - \frac{L}{2}} \\ \frac{c}{6} \log \left[\frac{2\sin[\pi\alpha_\mathcal{O}]}{\alpha_\mathcal{O}} \right] - \frac{c}{6} \log \left[\epsilon f_2(t_1, X_2^f, \theta) \right] & nL_{\text{eff}} + \hat{t}_{\frac{L}{2} - X_2} > t_1 > nL_{\text{eff}} + \hat{t}_{1,+}^t \\ 0 & nL_{\text{eff}} + \hat{t}_{\frac{L}{2} + X_2} > t_1 > nL_{\text{eff}} + \hat{t}_{\frac{L}{2} - X_2} \\ \frac{c}{6} \log \left[\frac{2\sin[\pi\alpha_\mathcal{O}]}{\alpha_\mathcal{O}} \right] - \frac{c}{6} \log \left[-\epsilon g_2(t_1, X_2^f, \theta) \right] & nL_{\text{eff}} + \hat{t}_{1,-}^t > t_1 > nL_{\text{eff}} + \hat{t}_{\frac{L}{2} + X_2} \\ \frac{c}{6} \log \left[\frac{2\sin[\pi\alpha_\mathcal{O}]}{\alpha_\mathcal{O}} \right] - \frac{c}{6} \log \left[-\epsilon f_2(t_1, X_2^f, \theta) \right] & nL_{\text{eff}} + \hat{t}_{\frac{3}{2}L - X_1} > t_1 > nL_{\text{eff}} + \hat{t}_{1,-}^t \\ 0 & (n+1)L_{\text{eff}} + \hat{t}_{X_1 - \frac{L}{2}} + > t_1 > nL_{\text{eff}} + \hat{t}_{\frac{3}{2}L - X_1} \end{cases} ,$$

$$S_{A,3} \approx \frac{c}{3} \log \left[\frac{L}{\pi} \sin \left[\frac{\pi(X_1 - X_2)}{L} \right] \right]$$

$$+ \begin{cases} 0 & X_1 - \frac{L}{2} > t_0 > 0 \\ \frac{c}{6} \log \left[\frac{2\sin[\pi\alpha_\mathcal{O}]}{\alpha_\mathcal{O}} \right] - \frac{c}{6} \log \left[\epsilon g_3(t_0, X_2^f, \theta) \right] & nL + \tilde{t}_{0,+}^t > t_0 > (n - \frac{1}{2})L + X_1 \\ \frac{c}{6} \log \left[\frac{2\sin[\pi\alpha_\mathcal{O}]}{\alpha_\mathcal{O}} \right] - \frac{c}{6} \log \left[\epsilon f_3(t_0, X_2^f, \theta) \right] & \left(n + \frac{1}{2}\right) L - X_2 > t_0 > nL + \tilde{t}_{0,+}^t \\ 0 & \left(n + \frac{1}{2}\right) L + X_2 > t_0 > \left(n + \frac{1}{2}\right) L - X_2 \\ \frac{c}{6} \log \left[\frac{2\sin[\pi\alpha_\mathcal{O}]}{\alpha_\mathcal{O}} \right] - \frac{c}{6} \log \left[-\epsilon g_3(t_0, X_2^f, \theta) \right] & nL + \tilde{t}_{0,-}^t > t_0 > \left(n + \frac{1}{2}\right) L + X_2 \\ \frac{c}{6} \log \left[\frac{2\sin[\pi\alpha_\mathcal{O}]}{\alpha_\mathcal{O}} \right] - \frac{c}{6} \log \left[-\epsilon f_3(t_0, X_2^f, \theta) \right] & \left(n + \frac{3}{2}\right) L - X_1 > t_0 > nL + \tilde{t}_{0,-}^t \\ 0 & (n + \frac{1}{2})L + X_1 > t_0 > \left(n + \frac{3}{2}\right) L - X_1 \end{cases} ,$$

$$S_{A,4} \approx \frac{c}{3} \log \left[\frac{L}{\pi} \sin \left[\frac{\pi(X_1 - X_2)}{L} \right] \right]$$

$$
+ \begin{cases}
0 & X_1 - \frac{L}{2} > t_0 > 0 \\
\frac{c}{6} \log \left[\frac{2\sin[\pi\alpha_{\mathcal{O}}]}{\alpha_{\mathcal{O}}} \right] - \frac{c}{6} \log \left[\epsilon g_4(t_0, X_2^f, \theta) \right] & nL + \tilde{t}_{0,+}^t > t_0 > (n - \frac{1}{2})L + X_1 \\
\frac{c}{6} \log \left[\frac{2\sin[\pi\alpha_{\mathcal{O}}]}{\alpha_{\mathcal{O}}} \right] - \frac{c}{6} \log \left[\epsilon f_4(t_0, X_2^f, \theta) \right] & \left(n + \frac{1}{2}\right) L - X_2 > t_0 > nL + \tilde{t}_{0,+}^t \\
0 & \left(n + \frac{1}{2}\right) L + X_2 > t_0 > \left(n + \frac{1}{2}\right) L - X_2 \,, \\
\frac{c}{6} \log \left[\frac{2\sin[\pi\alpha_{\mathcal{O}}]}{\alpha_{\mathcal{O}}} \right] - \frac{c}{6} \log \left[-\epsilon g_4(t_0, X_2^f, \theta) \right] & nL + \tilde{t}_{0,-}^t > t_0 > \left(n + \frac{1}{2}\right) L + X_2 \\
\frac{c}{6} \log \left[\frac{2\sin[\pi\alpha_{\mathcal{O}}]}{\alpha_{\mathcal{O}}} \right] - \frac{c}{6} \log \left[-\epsilon f_4(t_0, X_2^f, \theta) \right] & \left(n + \frac{3}{2}\right) L - X_1 > t_0 > nL + \tilde{t}_{0,-}^t \\
0 & (n + \frac{1}{2})L + X_1 > t_0 > \left(n + \frac{3}{2}\right) L - X_1
\end{cases}
$$

$$\text{(E.6)}$$

For case (c), the time dependence of $S_{A,i}$ is given by

$$S_{A,1} \approx \frac{c}{3} \log \left[\frac{L}{\pi} \sin \left[\frac{\pi(X_1 - X_2)}{L} \right] \right]$$

$$
+ \begin{cases}
0 & \hat{t}_{\frac{L}{2} - X_1} > t_1 > 0 \\
\frac{c}{6} \log \left[\frac{2\sin[\pi\alpha_{\mathcal{O}}]}{\alpha_{\mathcal{O}}} \right] - \frac{c}{6} \log \left[\epsilon f_1(t_1, X_2^f, \theta) \right] & nL_{\text{eff}} + \hat{t}_{\frac{L}{2} - X_2} > t_1 > nL_{\text{eff}} + \hat{t}_{\frac{L}{2} - X_1} \\
0 & nL_{\text{eff}} + \hat{t}_{\frac{L}{2} + X_2} > t_1 > nL_{\text{eff}} + \hat{t}_{\frac{L}{2} - X_2} \\
\frac{c}{6} \log \left[\frac{2\sin[\pi\alpha_{\mathcal{O}}]}{\alpha_{\mathcal{O}}} \right] - \frac{c}{6} \log \left[-\epsilon g_1(t_1, X_2^f, \theta) \right] & nL_{\text{eff}} + \hat{t}_{\frac{L}{2} + X_1} > t_1 > nL_{\text{eff}} + \hat{t}_{\frac{L}{2} + X_2} \\
0 & (n + 1)L_{\text{eff}} + \hat{t}_{\frac{L}{2} - X_1} > t_1 > nL_{\text{eff}} + \hat{t}_{\frac{L}{2} + X_1}
\end{cases} \,,
$$

$$S_{A,2} \approx \frac{c}{3} \log \left[\frac{L}{\pi} \sin \left[\frac{\pi(X_1 - X_2)}{L} \right] \right]$$

$$
+ \begin{cases}
0 & \hat{t}_{\frac{L}{2} - X_1} > t_1 > 0 \\
\frac{c}{6} \log \left[\frac{2\sin[\pi\alpha_{\mathcal{O}}]}{\alpha_{\mathcal{O}}} \right] - \frac{c}{6} \log \left[\epsilon f_2(t_1, X_2^f, \theta) \right] & nL_{\text{eff}} + \hat{t}_{\frac{L}{2} - X_2} > t_1 > nL_{\text{eff}} + \hat{t}_{\frac{L}{2} - X_1} \\
0 & nL_{\text{eff}} + \hat{t}_{\frac{L}{2} + X_2} > t_1 > nL_{\text{eff}} + \hat{t}_{\frac{L}{2} - X_2} \\
\frac{c}{6} \log \left[\frac{2\sin[\pi\alpha_{\mathcal{O}}]}{\alpha_{\mathcal{O}}} \right] - \frac{c}{6} \log \left[-\epsilon g_2(t_1, X_2^f, \theta) \right] & nL_{\text{eff}} + \hat{t}_{\frac{L}{2} + X_1} > t_1 > nL_{\text{eff}} + \hat{t}_{\frac{L}{2} + X_2} \\
0 & (n + 1)L_{\text{eff}} + \hat{t}_{\frac{L}{2} - X_1} > t_1 > nL_{\text{eff}} + \hat{t}_{\frac{L}{2} + X_1}
\end{cases} \,,
$$

$$S_{A,3} \approx \frac{c}{3} \log \left[\frac{L}{\pi} \sin \left[\frac{\pi(X_1 - X_2)}{L} \right] \right]$$

$$
+ \begin{cases}
0 & \frac{L}{2} - X_1 > t_1 > 0 \\
\frac{c}{6} \log \left[\frac{2\sin[\pi\alpha_{\mathcal{O}}]}{\alpha_{\mathcal{O}}} \right] - \frac{c}{6} \log \left[\epsilon f_3(t_0, X_2^f, \theta) \right] & (n + \frac{1}{2})L - X_2 > t_1 > (n + \frac{1}{2})L - X_1 \\
0 & (n + \frac{1}{2})L + X_2 > t_1 > (n + \frac{1}{2})L - X_2 \,, \\
\frac{c}{6} \log \left[\frac{2\sin[\pi\alpha_{\mathcal{O}}]}{\alpha_{\mathcal{O}}} \right] - \frac{c}{6} \log \left[-\epsilon g_3(t_0, X_2^f, \theta) \right] & (n + \frac{1}{2})L + X_1 > t_1 > (n + \frac{1}{2})L + X_2 \\
0 & (n + \frac{3}{2}) - X_1 > t_1 > (n + \frac{1}{2})L + X_1
\end{cases}
$$

73

$$S_{A,4} \approx \frac{c}{3} \log \left[\frac{L}{\pi} \sin \left[\frac{\pi(X_1 - X_2)}{L} \right] \right]$$

$$+ \begin{cases} 0 & \frac{L}{2} - X_1 > t_1 > 0 \\ \frac{c}{6} \log \left[\frac{2\sin[\pi\alpha_{\mathcal{O}}]}{\alpha_{\mathcal{O}}} \right] - \frac{c}{6} \log \left[\epsilon f_4(t_0, X_2^f, \theta) \right] & (n+\frac{1}{2})L - X_2 > t_1 > (n+\frac{1}{2})L - X_1 \\ 0 & (n+\frac{1}{2})L + X_2 > t_1 > (n+\frac{1}{2})L - X_2 \;, \\ \frac{c}{6} \log \left[\frac{2\sin[\pi\alpha_{\mathcal{O}}]}{\alpha_{\mathcal{O}}} \right] - \frac{c}{6} \log \left[-\epsilon g_4(t_0, X_2^f, \theta) \right] & (n+\frac{1}{2})L + X_1 > t_1 > (n+\frac{1}{2})L + X_2 \\ 0 & (n+\frac{3}{2}) - X_1 > t_1 > (n+\frac{1}{2})L + X_1 \end{cases}$$

$$\text{(E.7)}$$

The time dependence of $S_{A,i}$ is periodic with the periodicity L_{eff} for $i = 1, 2$ and L for $i = 3, 4$. The time dependence of $S_{A,i}$ follows the propagation of quasiparticles.

E.1.3 General x

The details of the small ϵ expansion of cross ratios in general x during the Möbius time evolution are reported in Appendix D.4 . Define $\grave{t}_y$ as

$$\grave{t}_y = \frac{L_{\text{eff}}}{\pi} \tan^{-1} \left[\left| \frac{\sin \left(\frac{\pi(x-y)}{L} \right)}{\cosh(2\theta) \cos \left(\frac{\pi(x-y)}{L} \right) - \sinh(2\theta) \cos \left(\frac{\pi(y+x)}{L} \right)} \right| \right] \quad \text{(E.8)}$$

For any given general x, X_1, X_2, where $0 < X_2 < X_1 < L$, when $i = 1, 2$ we observe several different behaviors when x is inserted in different regions on the circle. Then, we define some characteristic parameters:

$$\grave{t}_{1,\pm}^t = \frac{L_{\text{eff}}}{\pi} \tan^{-1} \left[\pm \sqrt{\frac{2L \sin \left(\frac{\pi(X_1 - x)}{L} \right) \sin \left(\frac{\pi(x - X_2)}{L} \right)}{\delta}} \right],$$

$$\cos \left(\frac{\pi \check{t}_{0,\pm}^t}{L} \right) = \pm \sqrt{\frac{\cos \left(\frac{\pi(2x - X_1 - X_2)}{L} \right) + \cos \left(\frac{\pi(X_1 - X_2)}{L} \right)}{2 \cos \left(\frac{\pi(2x - X_1 - X_2)}{L} \right)}}.$$

$$\text{(E.9)}$$

Here, δ is defined as

$$\delta =$$

$$2L \left(\sinh^2(2\theta) \cos \left(\frac{\pi(x + X_1)}{L} \right) \cos \left(\frac{\pi(x + X_2)}{L} \right) + \cosh^2(2\theta) \cos \left(\frac{\pi(x - X_1)}{L} \right) \cos \left(\frac{\pi(x - X_2)}{L} \right) \right)$$

$$- L \sinh(4\theta) \left(\cos \left(\frac{\pi(x + X_1)}{L} \right) \cos \left(\frac{\pi(x - X_2)}{L} \right) + \cos \left(\frac{\pi(x - X_1)}{L} \right) \cos \left(\frac{\pi(x + X_2)}{L} \right) \right)$$

$$\text{(E.10)}$$

Notice that in the general x case, even if we insert a local excitation in the middle of the interval $(X_1 - x = x - X_2 > 0)$ at $t = 0$, we still have $t_{X_2} \neq t_{X_1}$ in general.

We select four typical cases to consider the time-dependence of $S_{A,i}$ here (See Fig. 5):

$$
A = \begin{cases}
\begin{aligned}
&\{y \,|\, X_2 \leq y \leq X_1\}, \text{ where },\\
&\quad\begin{cases}
\text{when } i = 1,2,\\
X_2 < x < X_1, \grave{t}_{X_2} < \grave{t}_{X_1}, L_{\text{eff}} - \grave{t}_{X_1} > \grave{t}_{X_1} \text{ and } L_{\text{eff}} - \grave{t}_{X_2} > \grave{t}_{X_2}\\
\text{when } i = 3,4,\\
X_2 < x < X_1, |x - X_2| < |X_1 - x|, |L + x - X_1| > |X_1 - x|\\
\text{and } |L + x - X_2| > |X_2 - x|
\end{cases}\\
&\{y \,|\, X_2 \leq y \leq X_1\}, \text{ where },\\
&\quad\begin{cases}
\text{when } i = 1,2,\\
X_1 < x < L, \grave{t}_{X_1} < \grave{t}_{X_2}, L_{\text{eff}} - \grave{t}_{X_1} > \grave{t}_{X_1} \text{ and } L_{\text{eff}} - \grave{t}_{X_2} > \grave{t}_{X_2}\\
\text{when } i = 3,4,\\
X_1 < x < L, |X_1 - x| < |X_2 + L - x|, |L + x - X_1| > |X_1 - x|\\
\text{and } |L + x - X_2| > |X_2 - x|.
\end{cases}\\
&\{y \,|\, X_2 \leq y \leq X_1\}, \text{ where },\\
&\quad\begin{cases}
\text{when } i = 1,2,\\
0 < x < X_2, \grave{t}_{X_2} < \grave{t}_{X_1}, L_{\text{eff}} - \grave{t}_{X_1} > \grave{t}_{X_1} \text{ and } L_{\text{eff}} - \grave{t}_{X_2} > \grave{t}_{X_2}\\
\text{when } i = 3,4,\\
0 < x < X_2, |X_2 - x| < |X_1 - x|,\\
|L + x - X_1| > |X_1 - x| \text{ and } |L + x - X_2| > |X_2 - x|.
\end{cases}\\
&\{y \,|\, X_2 \leq y \leq X_1\}, \text{ where },\\
&\quad\begin{cases}
\text{when } i = 1,2 : \grave{t}_{X_2} = \grave{t}_{X_1} \text{ or } \grave{t}_{X_2} = L_{\text{eff}} - \grave{t}_{X_1}\\
\text{when } i = 3,4 : |x - X_2| = |X_1 - x| \text{ or } |X_2 + L - x| = |X_1 - x|
\end{cases}
\end{aligned}
\end{cases}
$$

$$\text{for (i)}$$
$$\text{for (ii)}$$
$$\text{for (iii)}$$
$$\text{for (iv)}$$
$$\text{(E.11)}$$
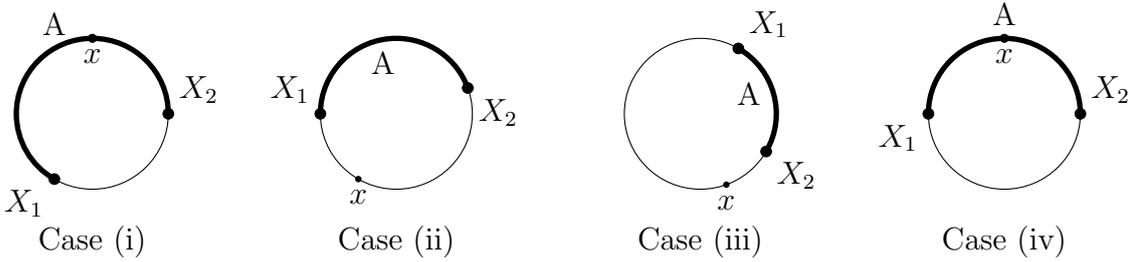
Figure 5: Four typical cases. The details of the subsystems illustrated here are in (E.11).

The time dependence of $S_{A,i}$ considered in the case of (i) is similar to inserting x at X_2^f , specifically case (a) for SSD cases, as shown in equation (5.20). The time-dependence of

$S_{A,i}$ is given by

$$S_{A,1} \approx \frac{c}{3} \log \left[\frac{L}{\pi} \sin \left[\frac{\pi(X_1 - X_2)}{L} \right] \right]$$

$$+ \begin{cases} 0 & \grave{t}_{X_2} > t_1 > 0 \\ \frac{c}{6} \log \left[\frac{2 \sin[\pi \alpha_{\mathcal{O}}]}{\alpha_{\mathcal{O}}} \right] - \frac{c}{6} \log \left[\epsilon \left| f_1(t_1, x, \theta) \right| \right] & nL_{\text{eff}} + \grave{t}_{0,+}^t > t_1 > nL_{\text{eff}} + \grave{t}_{X_2} \\ \frac{c}{6} \log \left[\frac{2 \sin[\pi \alpha_{\mathcal{O}}]}{\alpha_{\mathcal{O}}} \right] - \frac{c}{6} \log \left[\epsilon \left| g_1(t_1, x, \theta) \right| \right] & nL_{\text{eff}} + \grave{t}_{X_1} > t_1 > nL_{\text{eff}} + \grave{t}_{0,+}^t \\ 0 & (n+1)L_{\text{eff}} - \grave{t}_{X_1} > t_1 > nL_{\text{eff}} + \grave{t}_{X_1} \\ \frac{c}{6} \log \left[\frac{2 \sin[\pi \alpha_{\mathcal{O}}]}{\alpha_{\mathcal{O}}} \right] - \frac{c}{6} \log \left[\epsilon \left| f_1(t_1, x, \theta) \right| \right] & nL_{\text{eff}} + \grave{t}_{0,-}^t > t_1 > (n+1)L_{\text{eff}} - \grave{t}_{X_1} \\ \frac{c}{6} \log \left[\frac{2 \sin[\pi \alpha_{\mathcal{O}}]}{\alpha_{\mathcal{O}}} \right] - \frac{c}{6} \log \left[\epsilon \left| g_1(t_1, x, \theta) \right| \right] & (n+1)L_{\text{eff}} - \grave{t}_{X_2} > t_1 > nL_{\text{eff}} + \grave{t}_{0,-}^t \\ 0 & (n+1)L_{\text{eff}} + \grave{t}_{X_2} > t_1 > (n+1)L_{\text{eff}} - \grave{t}_{X_2} \end{cases},$$

$$S_{A,2} \approx \frac{c}{3} \log \left[\frac{L}{\pi} \sin \left[\frac{\pi(X_1 - X_2)}{L} \right] \right]$$

$$+ \begin{cases} 0 & \grave{t}_{X_2} > t_1 > 0 \\ \frac{c}{6} \log \left[\frac{2 \sin[\pi \alpha_{\mathcal{O}}]}{\alpha_{\mathcal{O}}} \right] - \frac{c}{6} \log \left[\epsilon \left| f_2(t_1, x, \theta) \right| \right] & nL_{\text{eff}} + \grave{t}_{0,+}^t > t_1 > nL_{\text{eff}} + \grave{t}_{X_2} \\ \frac{c}{6} \log \left[\frac{2 \sin[\pi \alpha_{\mathcal{O}}]}{\alpha_{\mathcal{O}}} \right] - \frac{c}{6} \log \left[\epsilon \left| g_2(t_1, x, \theta) \right| \right] & nL_{\text{eff}} + \grave{t}_{X_1} > t_1 > nL_{\text{eff}} + \grave{t}_{0,+}^t \\ 0 & (n+1)L_{\text{eff}} - \grave{t}_{X_1} > t_1 > nL_{\text{eff}} + \grave{t}_{X_1} \\ \frac{c}{6} \log \left[\frac{2 \sin[\pi \alpha_{\mathcal{O}}]}{\alpha_{\mathcal{O}}} \right] - \frac{c}{6} \log \left[\epsilon \left| f_2(t_1, x, \theta) \right| \right] & nL_{\text{eff}} + \grave{t}_{0,-}^t > t_1 > (n+1)L_{\text{eff}} - \grave{t}_{X_1} \\ \frac{c}{6} \log \left[\frac{2 \sin[\pi \alpha_{\mathcal{O}}]}{\alpha_{\mathcal{O}}} \right] - \frac{c}{6} \log \left[\epsilon \left| g_2(t_1, x, \theta) \right| \right] & (n+1)L_{\text{eff}} - \grave{t}_{X_2} > t_1 > nL_{\text{eff}} + \grave{t}_{0,-}^t \\ 0 & (n+1)L_{\text{eff}} + \grave{t}_{X_2} > t_1 > (n+1)L_{\text{eff}} - \grave{t}_{X_2} \end{cases},$$

$$S_{A,3} \approx \frac{c}{3} \log \left[\frac{L}{\pi} \sin \left[\frac{\pi(X_1 - X_2)}{L} \right] \right]$$

$$+ \begin{cases} 0 & x - X_2 > t_0 > 0 \\ \frac{c}{6} \log \left[\frac{2 \sin[\pi \alpha_{\mathcal{O}}]}{\alpha_{\mathcal{O}}} \right] - \frac{c}{6} \log \left[\epsilon \left| f_3(t_0, x, \theta) \right| \right] & nL + \breve{t}_{0,+}^t > t_0 > nL + x - X_2 \\ \frac{c}{6} \log \left[\frac{2 \sin[\pi \alpha_{\mathcal{O}}]}{\alpha_{\mathcal{O}}} \right] - \frac{c}{6} \log \left[\epsilon \left| g_3(t_0, x, \theta) \right| \right] & nL + X_1 - x > t_0 > nL + \breve{t}_{0,+}^t \\ 0 & (n+1)L + x - X_1 > t_0 > nL + X_1 - x \\ \frac{c}{6} \log \left[\frac{2 \sin[\pi \alpha_{\mathcal{O}}]}{\alpha_{\mathcal{O}}} \right] - \frac{c}{6} \log \left[\epsilon \left| f_3(t_0, x, \theta) \right| \right] & nL + \breve{t}_{0,-}^t > t_0 > (n+1)L + x - X_1 \\ \frac{c}{6} \log \left[\frac{2 \sin[\pi \alpha_{\mathcal{O}}]}{\alpha_{\mathcal{O}}} \right] - \frac{c}{6} \log \left[\epsilon \left| g_3(t_0, x, \theta) \right| \right] & (n+1)L + X_2 - x > t_0 > nL + \breve{t}_{0,-}^t \\ 0 & (n+1)L + x - X_2 > t_0 > (n+1)L + X_2 - x \end{cases},$$

$$S_{A,4} \approx \frac{c}{3} \log \left[\frac{L}{\pi} \sin \left[\frac{\pi(X_1 - X_2)}{L} \right] \right]$$

$$+ \begin{cases} 0 & x - X_2 > t_0 > 0 \\ \frac{c}{6} \log \left[\frac{2\sin[\pi\alpha_{\mathcal{O}}]}{\alpha_{\mathcal{O}}} \right] - \frac{c}{6} \log \left[\epsilon \left| f_4(t_0, x, \theta) \right| \right] & nL + \check{t}^t_{0,+} > t_0 > nL + x - X_2 \\ \frac{c}{6} \log \left[\frac{2\sin[\pi\alpha_{\mathcal{O}}]}{\alpha_{\mathcal{O}}} \right] - \frac{c}{6} \log \left[\epsilon \left| g_4(t_0, x, \theta) \right| \right] & nL + X_1 - x > t_0 > nL + \check{t}^t_{0,+} \\ 0 & (n+1)L + x - X_1 > t_0 > nL + X_1 - x \\ \frac{c}{6} \log \left[\frac{2\sin[\pi\alpha_{\mathcal{O}}]}{\alpha_{\mathcal{O}}} \right] - \frac{c}{6} \log \left[\epsilon \left| f_4(t_0, x, \theta) \right| \right] & nL + \check{t}^t_{0,-} > t_0 > (n+1)L + x - X_1 \\ \frac{c}{6} \log \left[\frac{2\sin[\pi\alpha_{\mathcal{O}}]}{\alpha_{\mathcal{O}}} \right] - \frac{c}{6} \log \left[\epsilon \left| g_4(t_0, x, \theta) \right| \right] & (n+1)L + X_2 - x > t_0 > nL + \check{t}^t_{0,-} \\ 0 & (n+1)L + x - X_2 > t_0 > (n+1)L + X_2 - x \end{cases}.$$

$$(E.12)$$

In the case of (ii), as in (5.10), the time dependence of $S_{A,i}$ is similar to that in the case (a) with $\theta \neq 0$ and the insertion of the local operator at X_1^f. The time-dependence of $S_{A,i}$ is given by

$$S_{A,1} \approx \frac{c}{3} \log \left[\frac{L}{\pi} \sin \left[\frac{\pi(X_1 - X_2)}{L} \right] \right]$$

$$+ \begin{cases} 0 & \grave{t}_{X_1} > t_1 > 0 \\ \frac{c}{6} \log \left[\frac{2\sin[\pi\alpha_{\mathcal{O}}]}{\alpha_{\mathcal{O}}} \right] - \frac{c}{6} \log \left[\epsilon \left| f_1(t_1, x, \theta) \right| \right] & nL_{\text{eff}} + \grave{t}^t_{0,+} > t_1 > nL_{\text{eff}} + \grave{t}_{X_1} \\ \frac{c}{6} \log \left[\frac{2\sin[\pi\alpha_{\mathcal{O}}]}{\alpha_{\mathcal{O}}} \right] - \frac{c}{6} \log \left[\epsilon \left| g_1(t_1, x, \theta) \right| \right] & nL_{\text{eff}} + \grave{t}_{X_2} > t_1 > nL_{\text{eff}} + \grave{t}^t_{0,+} \\ 0 & (n+1)L_{\text{eff}} - \grave{t}_{X_2} > t_1 > nL_{\text{eff}} + \grave{t}_{X_2} \\ \frac{c}{6} \log \left[\frac{2\sin[\pi\alpha_{\mathcal{O}}]}{\alpha_{\mathcal{O}}} \right] - \frac{c}{6} \log \left[\epsilon \left| f_1(t_1, x, \theta) \right| \right] & nL_{\text{eff}} + \grave{t}^t_{0,-} > t_1 > (n+1)L_{\text{eff}} - \grave{t}_{X_2} \\ \frac{c}{6} \log \left[\frac{2\sin[\pi\alpha_{\mathcal{O}}]}{\alpha_{\mathcal{O}}} \right] - \frac{c}{6} \log \left[\epsilon \left| g_1(t_1, x, \theta) \right| \right] & (n+1)L_{\text{eff}} - \grave{t}_{X_1} > t_1 > nL_{\text{eff}} + \grave{t}^t_{0,-} \\ 0 & (n+1)L_{\text{eff}} + \grave{t}_{X_1} > t_1 > (n+1)L_{\text{eff}} - \grave{t}_{X_1} \end{cases},$$

$$S_{A,2} \approx \frac{c}{3} \log \left[\frac{L}{\pi} \sin \left[\frac{\pi(X_1 - X_2)}{L} \right] \right]$$

$$+ \begin{cases} 0 & \grave{t}_{X_1} > t_1 > 0 \\ \frac{c}{6} \log \left[\frac{2\sin[\pi\alpha_{\mathcal{O}}]}{\alpha_{\mathcal{O}}} \right] - \frac{c}{6} \log \left[\epsilon \left| f_2(t_1, x, \theta) \right| \right] & nL_{\text{eff}} + \grave{t}^t_{0,+} > t_1 > nL_{\text{eff}} + \grave{t}_{X_1} \\ \frac{c}{6} \log \left[\frac{2\sin[\pi\alpha_{\mathcal{O}}]}{\alpha_{\mathcal{O}}} \right] - \frac{c}{6} \log \left[\epsilon \left| g_2(t_1, x, \theta) \right| \right] & nL_{\text{eff}} + \grave{t}_{X_2} > t_1 > nL_{\text{eff}} + \grave{t}^t_{0,+} \\ 0 & (n+1)L_{\text{eff}} - \grave{t}_{X_2} > t_1 > nL_{\text{eff}} + \grave{t}_{X_2} \\ \frac{c}{6} \log \left[\frac{2\sin[\pi\alpha_{\mathcal{O}}]}{\alpha_{\mathcal{O}}} \right] - \frac{c}{6} \log \left[\epsilon \left| f_2(t_1, x, \theta) \right| \right] & nL_{\text{eff}} + \grave{t}^t_{0,-} > t_1 > (n+1)L_{\text{eff}} - \grave{t}_{X_2} \\ \frac{c}{6} \log \left[\frac{2\sin[\pi\alpha_{\mathcal{O}}]}{\alpha_{\mathcal{O}}} \right] - \frac{c}{6} \log \left[\epsilon \left| g_2(t_1, x, \theta) \right| \right] & (n+1)L_{\text{eff}} - \grave{t}_{X_1} > t_1 > nL_{\text{eff}} + \grave{t}^t_{0,-} \\ 0 & (n+1)L_{\text{eff}} + \grave{t}_{X_1} > t_1 > (n+1)L_{\text{eff}} - \grave{t}_{X_1} \end{cases},$$

$$S_{A,3} \approx \frac{c}{3} \log \left[\frac{L}{\pi} \sin \left[\frac{\pi(X_1 - X_2)}{L} \right] \right]$$

$$+ \begin{cases} 0 & x - X_1 > t_0 > 0 \\ \frac{c}{6} \log \left[\frac{2\sin[\pi\alpha_\mathcal{O}]}{\alpha_\mathcal{O}} \right] - \frac{c}{6} \log \left[\epsilon \, |f_3(t_0, x, \theta)| \right] & nL + \check{t}^t_{0,+} > t_0 > nL + x - X_1 \\ \frac{c}{6} \log \left[\frac{2\sin[\pi\alpha_\mathcal{O}]}{\alpha_\mathcal{O}} \right] - \frac{c}{6} \log \left[\epsilon \, |g_3(t_0, x, \theta)| \right] & (n+1)L + X_2 - x > t_0 > nL + \check{t}^t_{0,+} \\ 0 & nL + x - X_2 > t_0 > (n+1)L + X_2 - x \\ \frac{c}{6} \log \left[\frac{2\sin[\pi\alpha_\mathcal{O}]}{\alpha_\mathcal{O}} \right] - \frac{c}{6} \log \left[\epsilon \, |f_3(t_0, x, \theta)| \right] & nL + \check{t}^t_{0,-} > t_0 > nL + x - X_2 \\ \frac{c}{6} \log \left[\frac{2\sin[\pi\alpha_\mathcal{O}]}{\alpha_\mathcal{O}} \right] - \frac{c}{6} \log \left[\epsilon \, |g_3(t_0, x, \theta)| \right] & (n+1)L + X_1 - x > t_0 > nL + \check{t}^t_{0,-} \\ 0 & (n+1)L + x - X_1 > t_0 > (n+1)L + X_1 - x \end{cases} ,$$

$$S_{A,4} \approx \frac{c}{3} \log \left[\frac{L}{\pi} \sin \left[\frac{\pi(X_1 - X_2)}{L} \right] \right]$$

$$+ \begin{cases} 0 & x - X_1 > t_0 > 0 \\ \frac{c}{6} \log \left[\frac{2\sin[\pi\alpha_\mathcal{O}]}{\alpha_\mathcal{O}} \right] - \frac{c}{6} \log \left[\epsilon \, |f_4(t_0, x, \theta)| \right] & nL + \check{t}^t_{0,+} > t_0 > nL + x - X_1 \\ \frac{c}{6} \log \left[\frac{2\sin[\pi\alpha_\mathcal{O}]}{\alpha_\mathcal{O}} \right] - \frac{c}{6} \log \left[\epsilon \, |g_4(t_0, x, \theta)| \right] & (n+1)L + X_2 - x > t_0 > nL + \check{t}^t_{0,+} \\ 0 & nL + x - X_2 > t_0 > (n+1)L + X_2 - x \\ \frac{c}{6} \log \left[\frac{2\sin[\pi\alpha_\mathcal{O}]}{\alpha_\mathcal{O}} \right] - \frac{c}{6} \log \left[\epsilon \, |f_4(t_0, x, \theta)| \right] & nL + \check{t}^t_{0,-} > t_0 > nL + x - X_2 \\ \frac{c}{6} \log \left[\frac{2\sin[\pi\alpha_\mathcal{O}]}{\alpha_\mathcal{O}} \right] - \frac{c}{6} \log \left[\epsilon \, |g_4(t_0, x, \theta)| \right] & (n+1)L + X_1 - x > t_0 > nL + \check{t}^t_{0,-} \\ 0 & (n+1)L + x - X_1 > t_0 > (n+1)L + X_1 - x \end{cases} .$$

(E.13)

As shown in equation (E.2), the time dependence of entanglement entropy in case (iii) is similar to that with $\theta \neq \infty$ and the insertion of the local operator at X_1^f, specifically case (c). The time-dependence of $S_{A,i}$ is given by

$$S_{A,1} \approx \frac{c}{3} \log \left[\frac{L}{\pi} \sin \left[\frac{\pi(X_1 - X_2)}{L} \right] \right]$$

$$+ \begin{cases} 0 & \dot{t}_{X_2} > t_1 > 0 \\ \frac{c}{6} \log \left[\frac{2 \sin[\pi \alpha_{\mathcal{O}}]}{\alpha_{\mathcal{O}}} \right] - \frac{c}{6} \log \left[\epsilon \, |g_1(t_1, x, \theta)| \right] & nL_{\text{eff}} + \dot{t}_{X_1} > t_1 > nL_{\text{eff}} + \dot{t}_{X_2} \\ 0 & (n+1)L_{\text{eff}} - \dot{t}_{X_1} > t_1 > nL_{\text{eff}} + \dot{t}_{X_1} \\ \frac{c}{6} \log \left[\frac{2 \sin[\pi \alpha_{\mathcal{O}}]}{\alpha_{\mathcal{O}}} \right] - \frac{c}{6} \log \left[\epsilon \, |f_1(t_1, x, \theta)| \right] & (n+1)L_{\text{eff}} - \dot{t}_{X_2} > t_1 > (n+1)L_{\text{eff}} - \dot{t}_{X_1} \\ 0 & (n+1)L_{\text{eff}} + \dot{t}_{X_2} > t_1 > (n+1)L_{\text{eff}} - \dot{t}_{X_2} \end{cases},$$

$$S_{A,2} \approx \frac{c}{3} \log \left[\frac{L}{\pi} \sin \left[\frac{\pi(X_1 - X_2)}{L} \right] \right]$$

$$+ \begin{cases} 0 & \dot{t}_{X_2} > t_1 > 0 \\ \frac{c}{6} \log \left[\frac{2 \sin[\pi \alpha_{\mathcal{O}}]}{\alpha_{\mathcal{O}}} \right] - \frac{c}{6} \log \left[\epsilon \, |g_2(t_1, x, \theta)| \right] & nL_{\text{eff}} + \dot{t}_{X_1} > t_1 > nL_{\text{eff}} + \dot{t}_{X_2} \\ 0 & (n+1)L_{\text{eff}} - \dot{t}_{X_1} > t_1 > nL_{\text{eff}} + \dot{t}_{X_1} \\ \frac{c}{6} \log \left[\frac{2 \sin[\pi \alpha_{\mathcal{O}}]}{\alpha_{\mathcal{O}}} \right] - \frac{c}{6} \log \left[\epsilon \, |f_2(t_1, x, \theta)| \right] & (n+1)L_{\text{eff}} - \dot{t}_{X_2} > t_1 > (n+1)L_{\text{eff}} - \dot{t}_{X_1} \\ 0 & (n+1)L_{\text{eff}} + \dot{t}_{X_2} > t_1 > (n+1)L_{\text{eff}} - \dot{t}_{X_2} \end{cases},$$

$$S_{A,3} \approx \frac{c}{3} \log \left[\frac{L}{\pi} \sin \left[\frac{\pi(X_1 - X_2)}{L} \right] \right]$$

$$+ \begin{cases} 0 & X_2 - x > t_0 > 0 \\ \frac{c}{6} \log \left[\frac{2 \sin[\pi \alpha_{\mathcal{O}}]}{\alpha_{\mathcal{O}}} \right] - \frac{c}{6} \log \left[\epsilon \, |g_3(t_0, x, \theta)| \right] & nL + X_1 - x > t_0 > nL + X_2 - x \\ 0 & (n+1)L + x - X_1 > t_0 > nL + X_1 - x \\ \frac{c}{6} \log \left[\frac{2 \sin[\pi \alpha_{\mathcal{O}}]}{\alpha_{\mathcal{O}}} \right] - \frac{c}{6} \log \left[\epsilon \, |f_3(t_0, x, \theta)| \right] & (n+1)L + x - X_2 > t_0 > (n+1)L + x - X_1 \\ 0 & (n+1)L + X_2 - x > t_0 > (n+1)L + x - X_2 \end{cases},$$

$$S_{A,4} \approx \frac{c}{3} \log \left[\frac{L}{\pi} \sin \left[\frac{\pi(X_1 - X_2)}{L} \right] \right]$$

$$+ \begin{cases} 0 & X_2 - x > t_0 > 0 \\ \frac{c}{6} \log \left[\frac{2 \sin[\pi \alpha_{\mathcal{O}}]}{\alpha_{\mathcal{O}}} \right] - \frac{c}{6} \log \left[\epsilon \, |g_4(t_0, x, \theta)| \right] & nL + X_1 - x > t_0 > nL + X_2 - x \\ 0 & (n+1)L + x - X_1 > t_0 > nL + X_1 - x \\ \frac{c}{6} \log \left[\frac{2 \sin[\pi \alpha_{\mathcal{O}}]}{\alpha_{\mathcal{O}}} \right] - \frac{c}{6} \log \left[\epsilon \, |f_4(t_0, x, \theta)| \right] & (n+1)L + x - X_2 > t_0 > (n+1)L + x - X_1 \\ 0 & (n+1)L + X_2 - x > t_0 > (n+1)L + x - X_2 \end{cases}.$$

$$(E.14)$$

In the case of (iv), the time-dependence of $S_{A,i}$ is given by

$$
\begin{aligned}
S_1 &\approx \frac{c}{3} \log \left[\frac{L}{\pi} \sin \left[\frac{\pi(X_1 - X_2)}{L} \right] \right] & t_1 > 0 \\
S_2 &\approx \frac{c}{3} \log \left[\frac{L}{\pi} \sin \left[\frac{\pi(X_1 - X_2)}{L} \right] \right] & t_1 > 0 \\
S_3 &\approx \frac{c}{3} \log \left[\frac{L}{\pi} \sin \left[\frac{\pi(X_1 - X_2)}{L} \right] \right] & t_0 > 0 \\
S_4 &\approx \frac{c}{3} \log \left[\frac{L}{\pi} \sin \left[\frac{\pi(X_1 - X_2)}{L} \right] \right] & t_0 > 0
\end{aligned}
\tag{E.15}
$$

where n is an integer greater than or equal to 0.

E.2 SSD case

Here we report on the time dependence of $S_{A,i}$ for (b) and (c) during the SSD time evolution when the local operator is inserted at $x = X_1^f$ or $x = X_2^f$.

E.2.1 $x = X_1^f$

Here, we assume that the local operator is inserted at X_1^f. Now, let us present the time dependence of $S_{A,i=4}$ for case (b). In this case, the time dependence of $S_{A,i=4}$ is determined by

$$
\begin{aligned}
S_{A,4} &\approx \frac{c}{3} \log \left[\frac{L}{\pi} \sin \left(\frac{\pi (X_1 - X_2)}{L} \right) \right] \\
&+ \begin{cases}
0 & X_2 > t_0 > 0 \\
\frac{c}{6} \log \left[\frac{2\sin[\pi\alpha_{\mathcal{O}}]}{\alpha_{\mathcal{O}}} \right] - \frac{c}{6} \log \left[-\epsilon g_4(t_0, X_1^f, \infty) \right] & nL + t_{0,+}^t > t_0 > nL + X_2 \\
\frac{c}{6} \log \left[\frac{2\sin[\pi\alpha_{\mathcal{O}}]}{\alpha_{\mathcal{O}}} \right] - \frac{c}{6} \log \left[-\epsilon f_4(t_0, X_1^f, \infty) \right] & (n+1)L - X_1 > t_0 > nL + t_{0,+}^t \\
0 & nL + X_1 > t_0 > (n+1)L - X_1 \\
\frac{c}{6} \log \left[\frac{2\sin[\pi\alpha_{\mathcal{O}}]}{\alpha_{\mathcal{O}}} \right] - \frac{c}{6} \log \left[\epsilon g_4(t_0, X_1^f, \infty) \right] & nL + t_{0,-}^t > t_0 > nL + X_1 \\
\frac{c}{6} \log \left[\frac{2\sin[\pi\alpha_{\mathcal{O}}]}{\alpha_{\mathcal{O}}} \right] - \frac{c}{6} \log \left[\epsilon f_4(t_0, X_1^f, \infty) \right] & (n+1)L - X_2 > t_0 > nL + t_{0,-}^t \\
0 & (n+1)L + X_2 > t_0 > (n+1)L - X_2
\end{cases}
\end{aligned}
\tag{E.16}
$$

Subsequently, we present the time dependence of $S_{A,i=4}$ for case (c). It is determined by

$$S_{A,4} \approx \frac{c}{3} \log \left[\frac{L}{\pi} \sin \left(\frac{\pi (X_1 - X_2)}{L} \right) \right]$$

$$+ \begin{cases} 0 & X_2 > t_0 > 0 \\ \frac{c}{6} \log \left[\frac{2 \sin[\pi \alpha_{\mathcal{O}}]}{\alpha_{\mathcal{O}}} \right] - \frac{c}{6} \log \left[-\epsilon g_4(t_0, X_1^f, \infty) \right] & nL + X_1 > t_0 > nL + X_2 \\ 0 & (n+1)L - X_1 > t_0 > nL + X_1 \\ \frac{c}{6} \log \left[\frac{2 \sin[\pi \alpha_{\mathcal{O}}]}{\alpha_{\mathcal{O}}} \right] - \frac{c}{6} \log \left[\epsilon f_4(t_0, X_1^f, \infty) \right] & (n+1)L - X_2 > t_0 > (n+1)L - X_1 \\ 0 & (n+1)L + X_2 > t_0 > (n+1)L - X_2 \end{cases}$$

$$\tag{E.17}$$

E.2.2 $\quad x = X_2^f$

Here, we assume that the local operator is inserted at X_2^f. Now, let us study the time dependence of $S_{A,i}$ as follows. The time dependence of $S_{A,i}$ in case (b) is given by

$$S_{A,1} \approx \frac{c}{3} \log \left[\frac{L}{\pi} \sin \left[\frac{\pi(X_1 - X_2)}{L} \right] \right]$$

$$+ \begin{cases} 0 & \tilde{t}_{1,+} > t_1 > 0 \\ \frac{c}{6} \log \left[\frac{2 \sin[\pi \alpha_{\mathcal{O}}]}{\alpha_{\mathcal{O}}} \right] - \frac{c}{6} \log \left[\epsilon g_1(t_1, X_2^f, \infty) \right] & \tilde{t}_1^t > t_1 > \tilde{t}_{1,+} \\ \frac{c}{6} \log \left[\frac{2 \sin[\pi \alpha_{\mathcal{O}}]}{\alpha_{\mathcal{O}}} \right] - \frac{c}{6} \log \left[\epsilon f_1(t_1, X_2^f, \infty) \right] & \tilde{t}_{2,-} > t_1 > \tilde{t}_1^t \\ 0 & t_1 > \tilde{t}_{2,-} \end{cases} ,$$

$$S_{A,2} \approx \frac{c}{3} \log \left[\frac{L}{\pi} \sin \left[\frac{\pi(X_1 - X_2)}{L} \right] \right]$$

$$+ \begin{cases} 0 & \tilde{t}_{1,+} > t_1 > 0 \\ \frac{c}{6} \log \left[\frac{2 \sin[\pi \alpha_{\mathcal{O}}]}{\alpha_{\mathcal{O}}} \right] - \frac{c}{6} \log \left[\epsilon g_2(t_1, X_2^f, \infty) \right] & \tilde{t}_1^t > t_1 > \tilde{t}_{1,+} \\ \frac{c}{6} \log \left[\frac{2 \sin[\pi \alpha_{\mathcal{O}}]}{\alpha_{\mathcal{O}}} \right] - \frac{c}{6} \log \left[\epsilon f_2(t_1, X_2^f, \infty) \right] & \tilde{t}_{2,-} > t_1 > \tilde{t}_1^t \\ 0 & t_1 > \tilde{t}_{2,-} \end{cases} ,$$

$$S_{A,3} \approx \frac{c}{3} \log\left[\frac{L}{\pi}\sin\left[\frac{\pi(X_1-X_2)}{L}\right]\right]$$

$$+\begin{cases} 0 & X_1 - \frac{L}{2} > t_0 > 0 \\ \frac{c}{6}\log\left[\frac{2\sin[\pi\alpha_{\mathcal{O}}]}{\alpha_{\mathcal{O}}}\right] - \frac{c}{6}\log\left[\epsilon g_3(t_0, X_2^f, \infty)\right] & nL + \tilde{t}_{0,+}^t > t_0 > \left(n-\frac{1}{2}\right)L + X_1 \\ \frac{c}{6}\log\left[\frac{2\sin[\pi\alpha_{\mathcal{O}}]}{\alpha_{\mathcal{O}}}\right] - \frac{c}{6}\log\left[\epsilon f_3(t_0, X_2^f, \infty)\right] & \left(n+\frac{1}{2}\right)L - X_2 > t_0 > nL + \tilde{t}_{0,+}^t \\ 0 & \left(\frac{1}{2}+n\right)L + X_2 > t_0 > \left(\frac{1}{2}+n\right)L - X_2 \,, \\ \frac{c}{6}\log\left[\frac{2\sin[\pi\alpha_{\mathcal{O}}]}{\alpha_{\mathcal{O}}}\right] - \frac{c}{6}\log\left[-\epsilon g_3(t_0, X_2^f, \infty)\right] & nL + \tilde{t}_{0,-}^t > t_0 > \left(\frac{1}{2}+n\right)L + X_2 \\ \frac{c}{6}\log\left[\frac{2\sin[\pi\alpha_{\mathcal{O}}]}{\alpha_{\mathcal{O}}}\right] - \frac{c}{6}\log\left[-\epsilon f_3(t_0, X_2^f, \infty)\right] & \left(\frac{3}{2}+n\right)L - X_1 > t_0 > nL + \tilde{t}_{0,-}^t \\ 0 & \left(\frac{1}{2}+n\right)L + X_1 > t_0 > \left(\frac{3}{2}+n\right)L - X_1 \end{cases}$$

$$S_{A,4} \approx \frac{c}{3} \log\left[\frac{L}{\pi}\sin\left[\frac{\pi(X_1-X_2)}{L}\right]\right]$$

$$+\begin{cases} 0 & X_1 - \frac{L}{2} > t_0 > 0 \\ \frac{c}{6}\log\left[\frac{2\sin[\pi\alpha_{\mathcal{O}}]}{\alpha_{\mathcal{O}}}\right] - \frac{c}{6}\log\left[\epsilon g_4(t_0, X_2^f, \infty)\right] & nL + \tilde{t}_{0,+}^t > t_0 > \left(n-\frac{1}{2}\right)L + X_1 \\ \frac{c}{6}\log\left[\frac{2\sin[\pi\alpha_{\mathcal{O}}]}{\alpha_{\mathcal{O}}}\right] - \frac{c}{6}\log\left[\epsilon f_4(t_0, X_2^f, \infty)\right] & \left(n+\frac{1}{2}\right)L - X_2 > t_0 > nL + \tilde{t}_{0,+}^t \\ 0 & \left(\frac{1}{2}+n\right)L + X_2 > t_0 > \left(\frac{1}{2}+n\right)L - X_2 \,, \\ \frac{c}{6}\log\left[\frac{2\sin[\pi\alpha_{\mathcal{O}}]}{\alpha_{\mathcal{O}}}\right] - \frac{c}{6}\log\left[-\epsilon g_4(t_0, X_2^f, \infty)\right] & nL + \tilde{t}_{0,-}^t > t_0 > \left(\frac{1}{2}+n\right)L + X_2 \\ \frac{c}{6}\log\left[\frac{2\sin[\pi\alpha_{\mathcal{O}}]}{\alpha_{\mathcal{O}}}\right] - \frac{c}{6}\log\left[-\epsilon f_4(t_0, X_2^f, \infty)\right] & \left(\frac{3}{2}+n\right)L - X_1 > t_0 > nL + \tilde{t}_{0,-}^t \\ 0 & \left(\frac{1}{2}+n\right)L + X_1 > t_0 > \left(\frac{3}{2}+n\right)L - X_1 \end{cases}$$

$$\text{(E.18)}$$

where n is a positive integer and t_0 is a positive number.

The time dependence of $S_{A,i}$ in case (c) is given by

$$S_{A,1} \approx \frac{c}{3} \log \left[\frac{L}{\pi} \sin \left[\frac{\pi(X_1 - X_2)}{L} \right] \right]$$

$$+ \begin{cases} 0 & t_{1,-} > t_1 > 0 \\ \frac{c}{6} \log \left[\frac{2\sin[\pi\alpha_{\mathcal{O}}]}{\alpha_{\mathcal{O}}} \right] - \frac{c}{6} \log \left[\epsilon f_1(t_1, X_2^f, \infty) \right] & t_{2,-} > t_1 > t_{1,-} \\ 0 & t_1 > t_{2,-} \end{cases} ,$$

$$S_{A,2} \approx \frac{c}{3} \log \left[\frac{L}{\pi} \sin \left[\frac{\pi(X_1 - X_2)}{L} \right] \right]$$

$$+ \begin{cases} 0 & t_{1,-} > t_1 > 0 \\ \frac{c}{6} \log \left[\frac{2\sin[\pi\alpha_{\mathcal{O}}]}{\alpha_{\mathcal{O}}} \right] - \frac{c}{6} \log \left[\epsilon f_2(t_1, X_2^f, \infty) \right] & t_{2,-} > t_1 > t_{1,-} \\ 0 & t_1 > t_{2,-} \end{cases} ,$$

$$S_{A,3} \approx \frac{c}{3} \log \left[\frac{L}{\pi} \sin \left[\frac{\pi(X_1 - X_2)}{L} \right] \right]$$

$$+ \begin{cases} 0 & \frac{L}{2} - X_1 > t_0 > 0 \\ \frac{c}{6} \log \left[\frac{2\sin[\pi\alpha_{\mathcal{O}}]}{\alpha_{\mathcal{O}}} \right] - \frac{c}{6} \log \left[\epsilon f_3(t_0, X_2^f, \infty) \right] & \left(\frac{1}{2} + n\right) L - X_2 > t_0 > \left(n + \frac{1}{2}\right) L - X_1 \\ 0 & \left(n + \frac{1}{2}\right) L + X_2 > t_0 > \left(n + \frac{1}{2}\right) L - X_2 \\ \frac{c}{6} \log \left[\frac{2\sin[\pi\alpha_{\mathcal{O}}]}{\alpha_{\mathcal{O}}} \right] - \frac{c}{6} \log \left[-\epsilon g_3(t_0, X_2^f, \infty) \right] & \left(\frac{1}{2} + n\right) L + X_1 > t_0 > \left(\frac{1}{2} + n\right) L + X_2 \\ 0 & \left(\frac{3}{2} + n\right) L - X_1 > t_0 > \left(\frac{1}{2} + n\right) L + X_1 \end{cases} ,$$

$$S_{A,4} \approx \frac{c}{3} \log \left[\frac{L}{\pi} \sin \left[\frac{\pi(X_1 - X_2)}{L} \right] \right]$$

$$+ \begin{cases} 0 & \frac{L}{2} - X_1 > t_0 > 0 \\ \frac{c}{6} \log \left[\frac{2\sin[\pi\alpha_{\mathcal{O}}]}{\alpha_{\mathcal{O}}} \right] - \frac{c}{6} \log \left[\epsilon f_4(t_0, X_2^f, \infty) \right] & \left(\frac{1}{2} + n\right) L - X_2 > t_0 > \left(n + \frac{1}{2}\right) L - X_1 \\ 0 & \left(n + \frac{1}{2}\right) L + X_2 > t_0 > \left(n + \frac{1}{2}\right) L - X_2 \\ \frac{c}{6} \log \left[\frac{2\sin[\pi\alpha_{\mathcal{O}}]}{\alpha_{\mathcal{O}}} \right] - \frac{c}{6} \log \left[-\epsilon g_4(t_0, X_2^f, \infty) \right] & \left(\frac{1}{2} + n\right) L + X_1 > t_0 > \left(\frac{1}{2} + n\right) L + X_2 \\ 0 & \left(\frac{3}{2} + n\right) L - X_1 > t_0 > \left(\frac{1}{2} + n\right) L + X_1 \end{cases}$$

$$\text{(E.19)}$$

E.2.3 General x

Here are the details of the small ϵ expansion of cross ratios for general x during the SSD time evolution:

$$z_{c,1} \approx 1 - \frac{2i\pi L\epsilon \sin\left[\frac{\pi(X_1-X_2)}{L}\right]}{\prod_{i=1,2}\left[L\sin\left(\frac{\pi(x-X_i)}{L}\right) - 2\pi t_1 \sin\left(\frac{\pi x}{L}\right)\sin\left(\frac{\pi X_i}{L}\right)\right]} + \mathcal{O}(\epsilon^2),$$

$$\overline{z}_{c,1} \approx 1 + \frac{2i\pi L\epsilon \sin\left[\frac{\pi(X_1-X_2)}{L}\right]}{\prod_{i=1,2}\left[L\sin\left(\frac{\pi(x-X_i)}{L}\right) + 2\pi t_1 \sin\left(\frac{\pi x}{L}\right)\sin\left(\frac{\pi X_i}{L}\right)\right]} + \mathcal{O}(\epsilon^2),$$

$$z_{c,2} \approx 1 - \frac{2i\pi\epsilon \sin\left[\frac{\pi(X_1-X_2)}{L}\right]\left[L^2 + 4\pi^2 t_1^2 \sin^2\left(\frac{\pi x}{L}\right) + 2\pi L t_1 \sin\left(\frac{2\pi x}{L}\right)\right]}{L\prod_{i=1,2}\left[L\sin\left(\frac{\pi(x-X_i)}{L}\right) - 2\pi t_1 \sin\left(\frac{\pi x}{L}\right)\sin\left(\frac{\pi X_i}{L}\right)\right]} + \mathcal{O}(\epsilon^2),$$

$$\overline{z}_{c,2} \approx 1 + \frac{2i\pi\epsilon \sin\left[\frac{\pi(X_1-X_2)}{L}\right]\left[L^2 + 4\pi^2 t_1^2 \sin^2\left(\frac{\pi x}{L}\right) - 2\pi L t_1 \sin\left(\frac{2\pi x}{L}\right)\right]}{L\prod_{i=1,2}\left[L\sin\left(\frac{\pi(x-X_i)}{L}\right) + 2\pi t_1 \sin\left(\frac{\pi x}{L}\right)\sin\left(\frac{\pi X_i}{L}\right)\right]} + \mathcal{O}(\epsilon^2),$$

$$z_{c,3} \approx 1 + \frac{2i\pi\epsilon \sin\left[\frac{\pi(X_1-X_2)}{L}\right]\left(\cos\left(\frac{2\pi x}{L}\right) - 1\right)}{L\prod_{i=1,2}\sin\left[\frac{\pi(t_0-x+X_i)}{L}\right]} + \mathcal{O}(\epsilon^2),$$

$$\overline{z}_{c,3} \approx 1 - \frac{2i\pi\epsilon \sin\left[\frac{\pi(X_1-X_2)}{L}\right]\left(\cos\left(\frac{2\pi x}{L}\right) - 1\right)}{L\prod_{i=1,2}\sin\left[\frac{\pi(t_0+x-X_i)}{L}\right]} + \mathcal{O}(\epsilon^2),$$

$$z_{c,4} \approx 1 + \frac{2i\pi\epsilon \sin\left[\frac{\pi(X_1-X_2)}{L}\right]\left(\cos\left(\frac{2\pi(t_0-x)}{L}\right) - 1\right)}{L\prod_{i=1,2}\sin\left[\frac{\pi(t_0-x+X_i)}{L}\right]} + \mathcal{O}(\epsilon^2),$$

$$\overline{z}_{c,4} \approx 1 - \frac{2i\pi\epsilon \sin\left[\frac{\pi(X_1-X_2)}{L}\right]\left(\cos\left(\frac{2\pi(t_0+x)}{L}\right) - 1\right)}{L\prod_{i=1,2}\sin\left[\frac{\pi(t_0+x-X_i)}{L}\right]} + \mathcal{O}(\epsilon^2),$$

(E.20)

Define $\check{t}_y$ as

$$\check{t}_y = \left|\frac{L\sin\left[\frac{\pi(y-x)}{L}\right]}{2\pi \sin\left(\frac{\pi x}{L}\right)\sin\left(\frac{\pi y}{L}\right)}\right|$$

(E.21)

One can easily check that for $0 < x < y_1 < y_2 < L$, we have $\check{t}_{y_1} < \check{t}_{y_2}$.

Around $t_1 = \check{t}_{X_i} + nL_{\text{eff}}$, the small ϵ expansion of $z_{c,i=1,2}$, $\overline{z}_{c,i=1,2}$, breaks down, while around $t_0 = \pm(x - X_i) + nL$, the small ϵ expansion of $z_{c,i=3,4}$, $\overline{z}_{c,i=3,4}$ breaks down. For any given x, X_1, X_2, where $0 < X_2 < X_1 < L$, when $i = 1, 2$ we observe several different behaviors as x is inserted in different regions on the circle. Here, we define the special point X_{spe} as the one satisfying $X_2 < X_{\text{spe}} < X_1$ which obeys the following equation for $i = 1, 2$,

$$\sin\left(\frac{\pi X_1}{L}\right)\sin\left[\frac{\pi(x_{\text{spe}} - X_2)}{L}\right] = \sin\left(\frac{\pi X_2}{L}\right)\sin\left[\frac{\pi(X_1 - x_{\text{spe}})}{L}\right].$$

(E.22)

The parameters are given by

$$\check{t}_1^t = \frac{\sqrt{L^2 \left(\cot\left(\frac{\pi x}{L}\right) - \cot\left(\frac{\pi X_1}{L}\right)\right)\left(\cot\left(\frac{\pi X_2}{L}\right) - \cot\left(\frac{\pi x}{L}\right)\right)}}{2\pi},$$

$$\cos\left(\frac{\pi \check{t}_{0,\pm}^t}{L}\right) = \sqrt{\pm \frac{\cos\left(\frac{\pi(2x - X_1 - X_2)}{L}\right) + \cos\left(\frac{\pi(X_1 - X_2)}{L}\right)}{2\cos\left(\frac{\pi(2x - X_1 - X_2)}{L}\right)}}.$$

(E.23)

In general, there exist five cases which correspond to the different behaviors of time-dependence of $S_{A,i}$ (See Fig. 6):

$$A = \begin{cases} \left\{y \,\middle|\, X_2 \le y \le X_1\right\}, & \text{where } 0 < x < X_2 & \text{for (I)} \\ \left\{y \,\middle|\, X_2 \le y \le X_1\right\}, & \text{where } X_2 < x < X_{spe} & \text{for (II)} \\ \left\{y \,\middle|\, X_2 \le y \le X_1\right\}, & \text{where } x = X_{spe} & \text{for (III)} \\ \left\{y \,\middle|\, X_2 \le y \le X_1\right\}, & \text{where } X_{spe} < x < X_1 & \text{for (IV)} \\ \left\{y \,\middle|\, X_2 \le y \le X_1\right\}, & \text{where } X_1 < x < L & \text{for (V)} \end{cases}$$

(E.24)
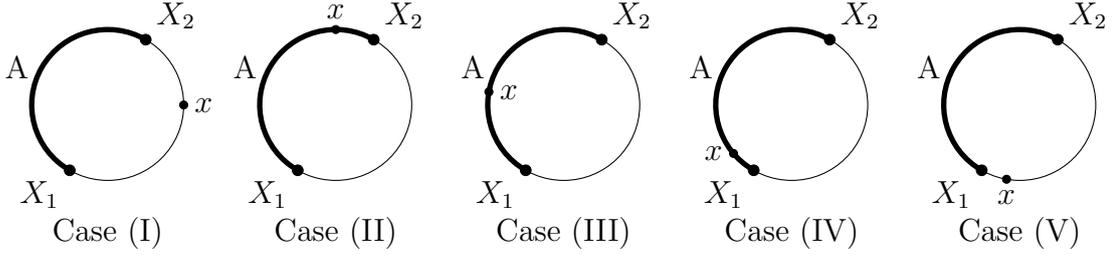
Figure 6: Five general cases. The details of subsystem illustrated here are reported in (E.24).

In the case of (I), the time dependence of $S_{A,i}$ is given by

$$S_1 \approx \frac{c}{3} \log\left[\frac{L}{\pi} \sin\left[\frac{\pi(X_1 - X_2)}{L}\right]\right]$$

$$+ \begin{cases} 0 & \check{t}_{X_2} > t_1 > 0 \\ \frac{c}{6} \log\left[\frac{2\sin[\pi\alpha_{\mathcal{O}}]}{\alpha_{\mathcal{O}}}\right] - \frac{c}{6} \log\left[\epsilon \,|g_1(t_1, x, \infty)|\right] & \check{t}_{X_1} > t_1 > \check{t}_{X_2} , \\ 0 & \check{t}_{X_1} \end{cases}$$

$$S_2 \approx \frac{c}{3} \log\left[\frac{L}{\pi} \sin\left[\frac{\pi(X_1 - X_2)}{L}\right]\right]$$

$$+ \begin{cases} 0 & \check{t}_{X_2} > t_1 > 0 \\ \frac{c}{6} \log\left[\frac{2\sin[\pi\alpha_{\mathcal{O}}]}{\alpha_{\mathcal{O}}}\right] - \frac{c}{6} \log\left[\epsilon \,|g_2(t_1, x, \infty)|\right] & \check{t}_{X_1} > t_1 > \check{t}_{X_2} , \\ 0 & t_1 > \check{t}_{X_1} \end{cases}$$

(E.25)

In the case of (II), the time dependence of $S_{A,i}$ is given by

$$S_1 \approx \frac{c}{3} \log\left[\frac{L}{\pi} \sin\left[\frac{\pi(X_1 - X_2)}{L}\right]\right]$$

$$+ \begin{cases} 0 & \check{t}_{X_2} > t_1 > 0 \\ \frac{c}{6} \log\left[\frac{2\sin[\pi\alpha_{\mathcal{O}}]}{\alpha_{\mathcal{O}}}\right] - \frac{c}{6} \log\left[\epsilon \left|f_1(t_1, x, \infty)\right|\right] & \check{t}_1^t > t_1 > \check{t}_{X_2} \\ \frac{c}{6} \log\left[\frac{2\sin[\pi\alpha_{\mathcal{O}}]}{\alpha_{\mathcal{O}}}\right] - \frac{c}{6} \log\left[\epsilon \left|g_1(t_1, x, \infty)\right|\right] & \check{t}_{X_1} > t_1 > \check{t}_1^t \\ 0 & t_1 > \check{t}_{X_1} \end{cases} ,$$

$$S_2 \approx \frac{c}{3} \log\left[\frac{L}{\pi} \sin\left[\frac{\pi(X_1 - X_2)}{L}\right]\right]$$

$$+ \begin{cases} 0 & \check{t}_{X_2} > t_1 > 0 \\ \frac{c}{6} \log\left[\frac{2\sin[\pi\alpha_{\mathcal{O}}]}{\alpha_{\mathcal{O}}}\right] - \frac{c}{6} \log\left[\epsilon \left|f_2(t_1, x, \infty)\right|\right] & \check{t}_1^t > t_1 > \check{t}_{X_2} \\ \frac{c}{6} \log\left[\frac{2\sin[\pi\alpha_{\mathcal{O}}]}{\alpha_{\mathcal{O}}}\right] - \frac{c}{6} \log\left[\epsilon \left|g_2(t_1, x, \infty)\right|\right] & \check{t}_{X_1} > t_1 > \check{t}_1^t \\ 0 & t_1 > \check{t}_{X_1} \end{cases} .$$

(E.26)

In the case of (III), the time dependence of $S_{A,i}$ is given by

$$S_1 \approx \frac{c}{3} \log\left[\frac{L}{\pi} \sin\left[\frac{\pi(X_1 - X_2)}{L}\right]\right] \quad t_1 > 0$$

$$S_2 \approx \frac{c}{3} \log\left[\frac{L}{\pi} \sin\left[\frac{\pi(X_1 - X_2)}{L}\right]\right] \quad t_1 > 0$$

(E.27)

In the case of (IV), the time dependence of $S_{A,i}$ is given by

$$S_1 \approx \frac{c}{3} \log\left[\frac{L}{\pi} \sin\left[\frac{\pi(X_1 - X_2)}{L}\right]\right]$$

$$+ \begin{cases} 0 & \check{t}_{X_1} > t_1 > 0 \\ \frac{c}{6} \log\left[\frac{2\sin[\pi\alpha_{\mathcal{O}}]}{\alpha_{\mathcal{O}}}\right] - \frac{c}{6} \log\left[\epsilon \left|g_1(t_1, x, \infty)\right|\right] & \check{t}_1^t > t_1 > \check{t}_{X_1} \\ \frac{c}{6} \log\left[\frac{2\sin[\pi\alpha_{\mathcal{O}}]}{\alpha_{\mathcal{O}}}\right] - \frac{c}{6} \log\left[\epsilon \left|f_1(t_1, x, \infty)\right|\right] & \check{t}_{X_2} > t_1 > \check{t}_1^t \\ 0 & t_1 > \check{t}_{X_2} \end{cases} ,$$

$$S_2 \approx \frac{c}{3} \log\left[\frac{L}{\pi} \sin\left[\frac{\pi(X_1 - X_2)}{L}\right]\right]$$

$$+ \begin{cases} 0 & \check{t}_{X_1} > t_1 > 0 \\ \frac{c}{6} \log\left[\frac{2\sin[\pi\alpha_{\mathcal{O}}]}{\alpha_{\mathcal{O}}}\right] - \frac{c}{6} \log\left[\epsilon \left|g_2(t_1, x, \infty)\right|\right] & \check{t}_1^t > t_1 > \check{t}_{X_1} \\ \frac{c}{6} \log\left[\frac{2\sin[\pi\alpha_{\mathcal{O}}]}{\alpha_{\mathcal{O}}}\right] - \frac{c}{6} \log\left[\epsilon \left|f_2(t_1, x, \infty)\right|\right] & \check{t}_{X_2} > t_1 > \check{t}_1^t \\ 0 & t_1 > \check{t}_{X_2} \end{cases} .$$

(E.28)

In the case of (V), the time dependence of $S_{A,i}$ is given by

$$S_1 \approx \frac{c}{3} \log \left[\frac{L}{\pi} \sin \left[\frac{\pi(X_1 - X_2)}{L} \right] \right]$$

$$+ \begin{cases} 0 & \check{t}_{X_1} > t_1 > 0 \\ \frac{c}{6} \log \left[\frac{2 \sin[\pi \alpha_{\mathcal{O}}]}{\alpha_{\mathcal{O}}} \right] - \frac{c}{6} \log \left[\epsilon \, |f_1(t_1, x, \infty)| \right] & \check{t}_{X_2} > t_1 > \check{t}_{X_1} \, , \\ 0 & t_1 > \check{t}_{X_2} \end{cases}$$

$$S_2 \approx \frac{c}{3} \log \left[\frac{L}{\pi} \sin \left[\frac{\pi(X_1 - X_2)}{L} \right] \right]$$

$$+ \begin{cases} 0 & \check{t}_{X_1} > t_1 > 0 \\ \frac{c}{6} \log \left[\frac{2 \sin[\pi \alpha_{\mathcal{O}}]}{\alpha_{\mathcal{O}}} \right] - \frac{c}{6} \log \left[\epsilon \, |f_2(t_1, x, \infty)| \right] & \check{t}_{X_2} > t_1 > \check{t}_{X_1} \, , \\ 0 & t_1 > \check{t}_{X_2} \end{cases}$$

(E.29)

For any given general x, X_1, X_2, where $0 < X_2 < X_1 < L$), for $i = 3, 4$, we select four typical cases, according to (E.11). As shown in equation (5.20), the time dependence of $S_{A,i}$ considered in the case of (i) is similar to that in case (a) with the insertion of the local

operator at X_2^f and $\theta = \infty$. The time dependence of $S_{A,i}$ is given by

$$S_{A,3} \approx \frac{c}{3} \log \left[\frac{L}{\pi} \sin \left[\frac{\pi(X_1 - X_2)}{L} \right] \right]$$

$$+ \begin{cases} 0 & x - X_2 > t_0 > 0 \\ \frac{c}{6} \log \left[\frac{2\sin[\pi\alpha_{\mathcal{O}}]}{\alpha_{\mathcal{O}}} \right] - \frac{c}{6} \log \left[\epsilon \, |f_3(t_0, x, \infty)| \right] & nL + \check{t}_{0,+}^t > t_0 > nL + x - X_2 \\ \frac{c}{6} \log \left[\frac{2\sin[\pi\alpha_{\mathcal{O}}]}{\alpha_{\mathcal{O}}} \right] - \frac{c}{6} \log \left[\epsilon \, |g_3(t_0, x, \infty)| \right] & nL + X_1 - x > t_0 > nL + \check{t}_{0,+}^t \\ 0 & (n+1)L + x - X_1 > t_0 > nL + X_1 - x \\ \frac{c}{6} \log \left[\frac{2\sin[\pi\alpha_{\mathcal{O}}]}{\alpha_{\mathcal{O}}} \right] - \frac{c}{6} \log \left[\epsilon \, |f_3(t_0, x, \infty)| \right] & nL + \check{t}_{0,-}^t > t_0 > (n+1)L + x - X_1 \\ \frac{c}{6} \log \left[\frac{2\sin[\pi\alpha_{\mathcal{O}}]}{\alpha_{\mathcal{O}}} \right] - \frac{c}{6} \log \left[\epsilon \, |g_3(t_0, x, \infty)| \right] & (n+1)L + X_2 - x > t_0 > nL + \check{t}_{0,-}^t \\ 0 & (n+1)L + x - X_2 > t_0 > (n+1)L + X_2 - x \end{cases} ,$$

$$S_{A,4} \approx \frac{c}{3} \log \left[\frac{L}{\pi} \sin \left[\frac{\pi(X_1 - X_2)}{L} \right] \right]$$

$$+ \begin{cases} 0 & x - X_2 > t_0 > 0 \\ \frac{c}{6} \log \left[\frac{2\sin[\pi\alpha_{\mathcal{O}}]}{\alpha_{\mathcal{O}}} \right] - \frac{c}{6} \log \left[\epsilon \, |f_4(t_0, x, \infty)| \right] & nL + \check{t}_{0,+}^t > t_0 > nL + x - X_2 \\ \frac{c}{6} \log \left[\frac{2\sin[\pi\alpha_{\mathcal{O}}]}{\alpha_{\mathcal{O}}} \right] - \frac{c}{6} \log \left[\epsilon \, |g_4(t_0, x, \infty)| \right] & nL + X_1 - x > t_0 > nL + \check{t}_{0,+}^t \\ 0 & (n+1)L + x - X_1 > t_0 > nL + X_1 - x \\ \frac{c}{6} \log \left[\frac{2\sin[\pi\alpha_{\mathcal{O}}]}{\alpha_{\mathcal{O}}} \right] - \frac{c}{6} \log \left[\epsilon \, |f_4(t_0, x, \infty)| \right] & nL + \check{t}_{0,-}^t > t_0 > (n+1)L + x - X_1 \\ \frac{c}{6} \log \left[\frac{2\sin[\pi\alpha_{\mathcal{O}}]}{\alpha_{\mathcal{O}}} \right] - \frac{c}{6} \log \left[\epsilon \, |g_4(t_0, x, \infty)| \right] & (n+1)L + X_2 - x > t_0 > nL + \check{t}_{0,-}^t \\ 0 & (n+1)L + x - X_2 > t_0 > (n+1)L + X_2 - x \end{cases} .$$

$$\tag{E.30}$$

In the case of (ii), the time dependence of $S_{A,i}$ is similar to case (a) when inserting x at X_1^f of the Möbius cases, as shown in equation (5.10). The time dependence of $S_{A,i}$ is given

by

$$S_{A,3} \approx \frac{c}{3} \log\left[\frac{L}{\pi} \sin\left[\frac{\pi(X_1 - X_2)}{L}\right]\right]$$

$$+ \begin{cases} 0 & x - X_1 > t_0 > 0 \\ \frac{c}{6} \log\left[\frac{2\sin[\pi\alpha_{\mathcal{O}}]}{\alpha_{\mathcal{O}}}\right] - \frac{c}{6} \log\left[\epsilon \,|f_3(t_0, x, \infty)|\right] & nL + \check{t}^t_{0,+} > t_0 > nL + x - X_1 \\ \frac{c}{6} \log\left[\frac{2\sin[\pi\alpha_{\mathcal{O}}]}{\alpha_{\mathcal{O}}}\right] - \frac{c}{6} \log\left[\epsilon \,|g_3(t_0, x, \infty)|\right] & (n+1)L + X_2 - x > t_0 > nL + \check{t}^t_{0,+} \\ 0 & nL + x - X_2 > t_0 > (n+1)L + X_2 - x \\ \frac{c}{6} \log\left[\frac{2\sin[\pi\alpha_{\mathcal{O}}]}{\alpha_{\mathcal{O}}}\right] - \frac{c}{6} \log\left[\epsilon \,|f_3(t_0, x, \infty)|\right] & nL + \check{t}^t_{0,-} > t_0 > nL + x - X_2 \\ \frac{c}{6} \log\left[\frac{2\sin[\pi\alpha_{\mathcal{O}}]}{\alpha_{\mathcal{O}}}\right] - \frac{c}{6} \log\left[\epsilon \,|g_3(t_0, x, \infty)|\right] & (n+1)L + X_1 - x > t_0 > nL + \check{t}^t_{0,-} \\ 0 & (n+1)L + x - X_1 > t_0 > (n+1)L + X_1 - x \end{cases},$$

$$S_{A,4} \approx \frac{c}{3} \log\left[\frac{L}{\pi} \sin\left[\frac{\pi(X_1 - X_2)}{L}\right]\right]$$

$$+ \begin{cases} 0 & x - X_1 > t_0 > 0 \\ \frac{c}{6} \log\left[\frac{2\sin[\pi\alpha_{\mathcal{O}}]}{\alpha_{\mathcal{O}}}\right] - \frac{c}{6} \log\left[\epsilon \,|f_4(t_0, x, \infty)|\right] & nL + \check{t}^t_{0,+} > t_0 > nL + x - X_1 \\ \frac{c}{6} \log\left[\frac{2\sin[\pi\alpha_{\mathcal{O}}]}{\alpha_{\mathcal{O}}}\right] - \frac{c}{6} \log\left[\epsilon \,|g_4(t_0, x, \infty)|\right] & (n+1)L + X_2 - x > t_0 > nL + \check{t}^t_{0,+} \\ 0 & nL + x - X_2 > t_0 > (n+1)L + X_2 - x \\ \frac{c}{6} \log\left[\frac{2\sin[\pi\alpha_{\mathcal{O}}]}{\alpha_{\mathcal{O}}}\right] - \frac{c}{6} \log\left[\epsilon \,|f_4(t_0, x, \infty)|\right] & nL + \check{t}^t_{0,-} > t_0 > nL + x - X_2 \\ \frac{c}{6} \log\left[\frac{2\sin[\pi\alpha_{\mathcal{O}}]}{\alpha_{\mathcal{O}}}\right] - \frac{c}{6} \log\left[\epsilon \,|g_4(t_0, x, \infty)|\right] & (n+1)L + X_1 - x > t_0 > nL + \check{t}^t_{0,-} \\ 0 & (n+1)L + x - X_1 > t_0 > (n+1)L + X_1 - x \end{cases}.$$

$$(\text{E}.31)$$

As shown in equation (E.2), the time dependence of entanglement entropy in case (iii) is similar to that with the insertion of the local operator at X_1^f and $\theta \neq \infty$, specifically case (c). The time dependence of $S_{A,i}$ is given by

$$S_{A,3} \approx \frac{c}{3} \log \left[\frac{L}{\pi} \sin \left[\frac{\pi(X_1 - X_2)}{L} \right] \right]$$

$$+ \begin{cases} 0 & X_2 - x > t_0 > 0 \\ \frac{c}{6} \log \left[\frac{2 \sin[\pi \alpha_{\mathcal{O}}]}{\alpha_{\mathcal{O}}} \right] - \frac{c}{6} \log \left[\epsilon \left| g_3(t_0, x, \infty) \right| \right] & nL + X_1 - x > t_0 > nL + X_2 - x \\ 0 & (n+1)L + x - X_1 > t_0 > nL + X_1 - x \\ \frac{c}{6} \log \left[\frac{2 \sin[\pi \alpha_{\mathcal{O}}]}{\alpha_{\mathcal{O}}} \right] - \frac{c}{6} \log \left[\epsilon \left| f_3(t_0, x, \infty) \right| \right] & (n+1)L + x - X_2 > t_0 > (n+1)L + x - X_1 \\ 0 & (n+1)L + X_2 - x > t_0 > (n+1)L + x - X_2 \end{cases},$$

$$S_{A,4} \approx \frac{c}{3} \log \left[\frac{L}{\pi} \sin \left[\frac{\pi(X_1 - X_2)}{L} \right] \right]$$

$$+ \begin{cases} 0 & X_2 - x > t_0 > 0 \\ \frac{c}{6} \log \left[\frac{2 \sin[\pi \alpha_{\mathcal{O}}]}{\alpha_{\mathcal{O}}} \right] - \frac{c}{6} \log \left[\epsilon \left| g_4(t_0, x, \infty) \right| \right] & nL + X_1 - x > t_0 > nL + X_2 - x \\ 0 & (n+1)L + x - X_1 > t_0 > nL + X_1 - x \\ \frac{c}{6} \log \left[\frac{2 \sin[\pi \alpha_{\mathcal{O}}]}{\alpha_{\mathcal{O}}} \right] - \frac{c}{6} \log \left[\epsilon \left| f_4(t_0, x, \infty) \right| \right] & (n+1)L + x - X_2 > t_0 > (n+1)L + x - X_1 \\ 0 & (n+1)L + X_2 - x > t_0 > (n+1)L + x - X_2 \end{cases}.$$

$$\text{(E.32)}$$

In the case of (iv), the time dependence of $S_{A,i}$ is given by

$$\begin{aligned} S_3 &\approx \frac{c}{3} \log \left[\frac{L}{\pi} \sin \left[\frac{\pi(X_1 - X_2)}{L} \right] \right] & t_0 > 0 \\ S_4 &\approx \frac{c}{3} \log \left[\frac{L}{\pi} \sin \left[\frac{\pi(X_1 - X_2)}{L} \right] \right] & t_0 > 0 \end{aligned} \qquad \text{(E.33)}$$

where n is an integer greater than or equal to 0.

References

[1] J. M. Deutsch, "Quantum statistical mechanics in a closed system," *Phys. Rev. A*, vol. 43, pp. 2046–2049, Feb 1991.

[2] M. Srednicki, "Chaos and quantum thermalization," *Phys. Rev. E*, vol. 50, pp. 888–901, Aug 1994.

[3] M. Rigol, V. Dunjko, and M. Olshanii, "Thermalization and its mechanism for generic isolated quantum systems," *Nature*, vol. 452, pp. 854–858, Apr. 2008.

[4] A. Polkovnikov, K. Sengupta, A. Silva, and M. Vengalattore, "Colloquium: Nonequilibrium dynamics of closed interacting quantum systems," *Reviews of Modern Physics*, vol. 83, pp. 863–883, July 2011.

[5] P. Calabrese and J. Cardy, "Evolution of entanglement entropy in one-dimensional systems," *Journal of Statistical Mechanics: Theory and Experiment*, vol. 4, p. 04010, Apr. 2005.

[6] K. A. Landsman, C. Figgatt, T. Schuster, N. M. Linke, B. Yoshida, N. Y. Yao, and C. Monroe, "Verified quantum information scrambling," *Nature*, vol. 567, pp. 61–65, Mar. 2019.

[7] M. K. Joshi, A. Elben, B. Vermersch, T. Brydges, C. Maier, P. Zoller, R. Blatt, and C. F. Roos, "Quantum Information Scrambling in a Trapped-Ion Quantum Simulator with Tunable Range Interactions," *Physical Review Letters*, vol. 124, p. 240505, June 2020.

[8] M. S. Blok, V. V. Ramasesh, T. Schuster, K. O'Brien, J. M. Kreikebaum, D. Dahlen, A. Morvan, B. Yoshida, N. Y. Yao, and I. Siddiqi, "Quantum Information Scrambling on a Superconducting Qutrit Processor," *Physical Review X*, vol. 11, p. 021010, Apr. 2021.

[9] B. Swingle, G. Bentsen, M. Schleier-Smith, and P. Hayden, "Measuring the scrambling of quantum information," *Physical Review A*, vol. 94, p. 040302, Oct. 2016.

[10] G. Zhu, M. Hafezi, and T. Grover, "Measurement of many-body chaos using a quantum clock," *Phys. Rev. A*, vol. 94, p. 062329, Dec 2016.

[11] N. Y. Yao, F. Grusdt, B. Swingle, M. D. Lukin, D. M. Stamper-Kurn, J. E. Moore, and E. A. Demler, "Interferometric Approach to Probing Fast Scrambling," *arXiv e-prints*, p. arXiv:1607.01801, July 2016.

[12] N. Yunger Halpern, "Jarzynski-like equality for the out-of-time-ordered correlator," *Physical Review A*, vol. 95, p. 012120, Jan. 2017.

[13] N. Yunger Halpern, B. Swingle, and J. Dressel, "Quasiprobability behind the out-of-time-ordered correlator," *Physical Review A*, vol. 97, p. 042105, Apr. 2018.

[14] M. Campisi and J. Goold, "Thermodynamics of quantum information scrambling," *Physical Review E*, vol. 95, p. 062127, June 2017.

[15] B. Yoshida and A. Kitaev, "Efficient decoding for the Hayden-Preskill protocol," *arXiv e-prints*, p. arXiv:1710.03363, Oct. 2017.

[16] M. Gärttner, J. G. Bohnet, A. Safavi-Naini, M. L. Wall, J. J. Bollinger, and A. M. Rey, "Measuring out-of-time-order correlations and multiple quantum spectra in a trapped-ion quantum magnet," *Nature Physics*, vol. 13, pp. 781–786, Aug. 2017.

[17] K. X. Wei, C. Ramanathan, and P. Cappellaro, "Exploring Localization in Nuclear Spin Chains," *arXiv e-prints*, p. arXiv:1612.05249, Dec. 2016.

[18] J. Li, R. Fan, H. Wang, B. Ye, B. Zeng, H. Zhai, X. Peng, and J. Du, "Measuring out-of-time-order correlators on a nuclear magnetic resonance quantum simulator," *Phys. Rev. X*, vol. 7, p. 031011, Jul 2017.

[19] E. J. Meier, J. Ang'ong'a, F. A. An, and B. Gadway, "Exploring quantum signatures of chaos on a Floquet synthetic lattice," *arXiv e-prints*, p. arXiv:1705.06714, May 2017.

[20] S. H. Shenker and D. Stanford, "Black holes and the butterfly effect," *JHEP*, vol. 03, p. 067, 2014.

[21] J. Maldacena, S. H. Shenker, and D. Stanford, "A bound on chaos," *JHEP*, vol. 08, p. 106, 2016.

[22] D. A. Roberts and D. Stanford, "Two-dimensional conformal field theory and the butterfly effect," *Physical Review Letters*, vol. 115, no. 13, p. 131603, 2015.

[23] P. Caputa, M. Nozaki, and T. Takayanagi, "Entanglement of Local Operators in large N CFTs," *arXiv e-prints*, p. arXiv:1405.5946, May 2014.

[24] M. Nozaki, "Notes on Quantum Entanglement of Local Operators," *JHEP*, vol. 10, p. 147, 2014.

[25] S. He, T. Numasawa, T. Takayanagi, and K. Watanabe, "Quantum dimension as entanglement entropy in two dimensional conformal field theories," *Phys. Rev. D*, vol. 90, no. 4, p. 041701, 2014.

[26] M. Nozaki, T. Numasawa, and T. Takayanagi, "Quantum Entanglement of Local Operators in Conformal Field Theories," *Phys. Rev. Lett.*, vol. 112, p. 111602, 2014.

[27] C. T. Asplund, A. Bernamonti, F. Galli, and T. Hartman, "Holographic entanglement entropy from 2d CFT: heavy states and local quenches," *Journal of High Energy Physics*, vol. 2, p. 171, Feb. 2015.

[28] Y. Kusuki and M. Miyaji, "Entanglement Entropy, OTOC and Bootstrap in 2D CFTs from Regge and Light Cone Limits of Multi-point Conformal Block," *JHEP*, vol. 08, p. 063, 2019.

[29] P. Caputa, J. Simón, A. Štikonas, T. Takayanagi, and K. Watanabe, "Scrambling time from local perturbations of the eternal BTZ black hole," *Journal of High Energy Physics*, vol. 8, p. 11, Aug. 2015.

[30] P. Caputa, J. Simón, A. Štikonas, and T. Takayanagi, "Quantum Entanglement of Localized Excited States at Finite Temperature," *JHEP*, vol. 01, p. 102, 2015.

[31] Y. Kusuki and M. Miyaji, "Entanglement Entropy after Double Excitation as an Interaction Measure," *Phys. Rev. Lett.*, vol. 124, no. 6, p. 061601, 2020.

[32] P. Caputa, T. Numasawa, T. Shimaji, T. Takayanagi, and Z. Wei, "Double Local Quenches in 2D CFTs and Gravitational Force," *JHEP*, vol. 09, p. 018, 2019.

[33] W.-z. Guo, S. He, and Z.-X. Luo, "Entanglement entropy in (1+1)d CFTs with multiple local excitations," *Journal of High Energy Physics*, vol. 2018, p. 154, May 2018.

[34] B. Chen, W.-Z. Guo, S. He, and J.-q. Wu, "Entanglement entropy for descendent local operators in 2d CFTs," *Journal of High Energy Physics*, vol. 2015, p. 173, Oct 2015.

[35] W.-Z. Guo and S. He, "Rényi entropy of locally excited states with thermal and boundary effect in 2d CFTs," *Journal of High Energy Physics*, vol. 2015, p. 99, Apr 2015.

[36] A. Gendiar, R. Krcmar, and T. Nishino, "Spherical deformation for one-dimensional quantum systems," *Progress of Theoretical Physics*, vol. 122, no. 4, pp. 953–967, 2009.

[37] A. Gendiar, R. Krcmar, and T. Nishino, "Spherical deformation for one-dimensional quantum systems," *Progress of Theoretical Physics*, vol. 123, no. 2, p. 393, 2010.

[38] T. Hikihara and T. Nishino, "Connecting distant ends of one-dimensional critical systems by a sine-square deformation," *Physical Review B*, vol. 83, Feb 2011.

[39] A. Gendiar, M. Daniška, Y. Lee, and T. Nishino, "Suppression of finite-size effects in one-dimensional correlated systems," *Physical Review A*, vol. 83, p. 052118, May 2011.

[40] K. Okunishi, "Sine-square deformation and möbius quantization of 2d conformal field theory," *Progress of Theoretical and Experimental Physics*, vol. 2016, p. 063A02, Jun 2016.

[41] X. Wen, S. Ryu, and A. W. W. Ludwig, "Evolution operators in conformal field theories and conformal mappings: Entanglement Hamiltonian, the sine-square deformation, and others," *Physical Review B*, vol. 93, p. 235119, June 2016.

[42] P. Caputa and I. MacCormack, "Geometry and Complexity of Path Integrals in Inhomogeneous CFTs," *JHEP*, vol. 01, p. 027, 2021. [Erratum: JHEP 09, 109 (2022)].

[43] X. Wen and J.-Q. Wu, "Quantum dynamics in sine-square deformed conformal field theory: Quench from uniform to nonuniform conformal field theory," *Phys. Rev. B*, vol. 97, p. 184309, May 2018.

[44] I. MacCormack, A. Liu, M. Nozaki, and S. Ryu, "Holographic duals of inhomogeneous systems: the rainbow chain and the sine-square deformation model," *Journal of Physics A Mathematical General*, vol. 52, p. 505401, Dec. 2019.

[45] K. Goto, M. Nozaki, K. Tamaoka, M. Tian Tan, and S. Ryu, "Non-Equilibrating a Black Hole with Inhomogeneous Quantum Quench," *arXiv e-prints*, p. arXiv:2112.14388, Dec. 2021.

[46] W. Berdanier, M. Kolodrubetz, R. Vasseur, and J. E. Moore, "Floquet dynamics of boundary-driven systems at criticality," *Phys. Rev. Lett.*, vol. 118, p. 260602, Jun 2017.

[47] X. Wen and J.-Q. Wu, "Floquet conformal field theory," *arXiv e-prints*, p. arXiv:1805.00031, Apr. 2018.

[48] R. Fan, Y. Gu, A. Vishwanath, and X. Wen, "Emergent Spatial Structure and Entanglement Localization in Floquet Conformal Field Theory," *Physical Review X*, vol. 10, p. 031036, July 2020.

[49] B. Han and X. Wen, "Classification of sL_2 deformed floquet conformal field theories," *Phys. Rev. B*, vol. 102, p. 205125, Nov 2020.

[50] X. Wen, R. Fan, A. Vishwanath, and Y. Gu, "Periodically, quasiperiodically, and randomly driven conformal field theories," *Physical Review Research*, vol. 3, p. 023044, Apr. 2021.

[51] R. Fan, Y. Gu, A. Vishwanath, and X. Wen, "Floquet conformal field theories with generally deformed Hamiltonians," *arXiv e-prints*, p. arXiv:2011.09491, Nov. 2020.

[52] X. Wen, Y. Gu, A. Vishwanath, and R. Fan, "Periodically, Quasi-periodically, and Randomly Driven Conformal Field Theories (II): Furstenberg's Theorem and Exceptions to Heating Phases," *arXiv e-prints*, p. arXiv:2109.10923, Sept. 2021.

[53] B. Lapierre and P. Moosavi, "Geometric approach to inhomogeneous floquet systems," *Phys. Rev. B*, vol. 103, p. 224303, Jun 2021.

[54] B. Lapierre, K. Choo, C. Tauber, A. Tiwari, T. Neupert, and R. Chitra, "Emergent black hole dynamics in critical floquet systems," *Phys. Rev. Res.*, vol. 2, p. 023085, Apr 2020.

[55] P. Moosavi, "Inhomogeneous conformal field theory out of equilibrium," *Annales Henri Poincaré*, Dec 2021.

[56] E. Langmann and P. Moosavi, "Diffusive heat waves in random conformal field theory," *Phys. Rev. Lett.*, vol. 122, p. 020201, Jan 2019.

[57] J. Dubail, J.-M. Stéphan, and P. Calabrese, "Emergence of curved light-cones in a class of inhomogeneous Luttinger liquids," *SciPost Phys.*, vol. 3, p. 019, 2017.

[58] A. Bernamonti, F. Galli, and D. Ge, "Boundary-induced transitions in Möbius quenches of holographic BCFT," *arXiv e-prints*, p. arXiv:2402.16555, Feb. 2024.

[59] M. P. Zaletel, A. M. Kaufman, D. M. Stamper-Kurn, and N. Y. Yao, "Preparation of Low Entropy Correlated Many-body States via Conformal Cooling Quenches," *arXiv e-prints*, p. arXiv:1611.04591, Nov. 2016.

[60] S. Roy, J. T. Chalker, I. V. Gornyi, and Y. Gefen, "Measurement-induced steering of quantum systems," *Physical Review Research*, vol. 2, p. 033347, Sept. 2020.

[61] T. Hartman and J. Maldacena, "Time evolution of entanglement entropy from black hole interiors," *Journal of High Energy Physics*, vol. 5, p. 14, May 2013.

[62] K. Agarwal, R. N. Bhatt, and S. L. Sondhi, "Fast Preparation of Critical Ground States Using Superluminal Fronts," *Physical Review Letters*, vol. 120, p. 210604, May 2018.

[63] P. Mitra, M. Ippoliti, R. N. Bhatt, S. L. Sondhi, and K. Agarwal, "Cooling arbitrary near-critical systems using hyperbolic quenches," *Physical Review B*, vol. 99, p. 104308, Mar. 2019.

[64] X. Wen, R. Fan, and A. Vishwanath, "Floquet's Refrigerator: Conformal Cooling in Driven Quantum Critical Systems," *arXiv e-prints*, p. arXiv:2211.00040, Oct. 2022.

[65] K. Goto, M. Nozaki, S. Ryu, K. Tamaoka, and M. Tian Tan, "Scrambling and Recovery of Quantum Information in Inhomogeneous Quenches in Two-dimensional Conformal Field Theories," *arXiv e-prints*, p. arXiv:2302.08009, Feb. 2023.

[66] M. Nozaki, K. Tamaoka, and M. Tian Tan, "Inhomogeneous quenches as state preparation in two-dimensional conformal field theories," *arXiv e-prints*, p. arXiv:2310.19376, Oct. 2023.

[67] K. Goto, T. Guo, T. Nosaka, M. Nozaki, S. Ryu, and K. Tamaoka, "Spatial deformation of many-body quantum chaotic systems and quantum information scrambling," *arXiv e-prints*, p. arXiv:2305.01019, May 2023.

[68] D. Das, S. R. Das, A. Kundu, and K. Sengupta, "Exactly Solvable Floquet Dynamics for Conformal Field Theories in Dimensions Greater than Two," 11 2023.

[69] J. Kudler-Flam, M. Nozaki, T. Numasawa, S. Ryu, and M. Tian Tan, "Bridging two quantum quench problems – local joining quantum quench and Möbius quench – and their holographic dual descriptions," *arXiv e-prints*, p. arXiv:2309.04665, Sept. 2023.

[70] X. Liu, A. McDonald, T. Numasawa, B. Lian, and S. Ryu, "Quantum Quenches of Conformal Field Theory with Open Boundary," 9 2023.

[71] P. Calabrese and J. Cardy, "Entanglement entropy and quantum field theory," *Journal of Statistical Mechanics: Theory and Experiment*, vol. 2004, p. P06002, Jun 2004.

[72] P. Calabrese and J. Cardy, "Entanglement entropy and conformal field theory," *Journal of Physics A: Mathematical and Theoretical*, vol. 42, p. 504005, Dec 2009.

[73] P. Calabrese and J. Cardy, "Entanglement entropy and quantum field theory," *Journal of Statistical Mechanics: Theory and Experiment*, vol. 6, p. 06002, June 2004.

[74] T. Numasawa, "Scattering effect on entanglement propagation in rcfts," *Journal of High Energy Physics*, vol. 2016, p. 61, Dec 2016.

[75] P. Caputa, J. Simón, A. Štikonas, and T. Takayanagi, "Quantum entanglement of localized excited states at finite temperature," *Journal of High Energy Physics*, vol. 2015, p. 102, Jan 2015.

[76] A. Belavin, A. Polyakov, and A. Zamolodchikov, "Infinite conformal symmetry in two-dimensional quantum field theory," *Nuclear Physics B*, vol. 241, no. 2, pp. 333–380, 1984.

[77] S. Ryu and T. Takayanagi, "Holographic Derivation of Entanglement Entropy from the anti de Sitter Space/Conformal Field Theory Correspondence," *Physical Review Letters*, vol. 96, p. 181602, May 2006.

[78] S. Ryu and T. Takayanagi, "Aspects of holographic entanglement entropy," *Journal of High Energy Physics*, vol. 8, p. 045, Aug. 2006.